# Junctional complexes and cell-cell signalling in zebrafish morphogenesis

David Barker

UCL

PhD

I, David Barker confirm that the work presented in this thesis is my own. Where information has been derived from other sources, I confirm that this has been indicated in the thesis.

## Abstract

Intercellular junctions are composed of tight, gap and adherens junctions and have been shown to play many roles in embryonic morphogenesis. I have been studying the role that ntercellular junctions play in zebrafish development. First I have studied the organisation of apical neuroepithelial junctions in the developing brain. By quantifying size and segmental patterning of the junctional arrangement in the hindbrain and elsewhere, I describe a distinct pattern of apical junctions in both boundary and non-boundary regions. This pattern appears to be in part regulated by the Notch signalling pathway since apical junction distribution is different in *hdac1*$^{-/-}$ zebrafish, which have deficient Notch-Delta signalling. Second I have established that boundary cells prevent the exchange of small molecular weight, gap junction permeable dyes between adjacent CNS compartments, suggesting that the compartments are separate developmental units. Third I have studied the role of gap junction mediated intercellular communication in the propagation of calcium waves and in the coordination of cell divisions in the zebrafish blastocyst. Calcium activity is cyclical, with cells producing a greater number of calcium transients and intercellular waves during cytokinesis than during interphase. In control conditions distinct waves of cell divisions spread across the embryo in an animal to vegetal progression. I show that both the calcium activity and cell division waves requires gap junction communication because pharmacological blockade of coupling reduces the frequency of calcium activity and disrupts cell division waves.

# *Table of Contents*

## *Table of figures*

## *List of abbreviations*

aa: Amino acid
AEF: Apical end foot/feet
AGA: 18 α-glycyrrhetinic acid
ap: Antero-Posterior
*ap:* *Apterous*
aPKC: Atypical Protein kinase C
ATP: Adenosine triphosphate
Cx: Connexin
Dfng: Drosophila Fringe
Dl: Delta
dv: Dorso-Ventral
EVL: Enveloping layer
F Actin: Filamentous Actin
FFA: Flufenamic acid
GFAP: Glial fibrillary acid protein
Hdac: Histone deacetylase
Her: Hairy/Enhancer of Split related
Hes: Hairy/Enhancer of Split
Hpf: Hours post fertilisation
IP3 Inositol trisphosphate
Lfng: Lunatic fringe
Mfng: Manic fringe
Mib: Mindbomb
N: Number of experiments
n: Number of observations
Par3: Partitioning-defective 3
PKC: Protein kinase C
rc: Rostro-Caudal
Rfng: Radical fringe
ROI: Region of interest
RPE: Retinal pigment Epithelium
Su(H): Suppressor of Hairless
VZ: Ventricular zone
Wg: Wingless
YSL: Yolk syncytial layer
ZLI: Zona limitans intrathalamica
ZO: Zonula Occludens

# Chapter 1: Introduction

This thesis is concerned with the epithelial organisation of the embryonic central nervous system, especially specialisations that occur at segment and compartment borders, and the possibility that cell-cell communication via gap junctions can pattern some aspects of early vertebrate development. This introduction will discuss each of these topics in turn.

## *Chapter 1.1: Developmental compartments and segments impose order on embryos*

During embryogenesis, an organism rapidly increases in complexity as cell numbers increase, cell types diversify and morphological changes create diverse tissues. It is of fundamental importance that developmental programs are instigated and maintained in the correct place, by the appropriate cells. An evolutionarily conserved strategy that ensures organs grow appropriately is to subdivide the organ into segments. This occurs in all multi cellular organisms with bilateral symmetry and an elongated anterior/posterior axis, from *C. elegans* to human, (Ingham and Martinez Arias, 1992; Kiecker and Lumsden, 2005). Segmentation is defined by these six attributes:

Gene expression: Developmentally important genes must be expressed in a unique combination within the segment

Integrity: Cells must remain in the segment (lineage restriction) and genes or cells from other segments must be excluded.

Boundaries: The edges of the segment must be specialised regions.

Morphology: The segment must be detectable by sight.

Metamerity: Segments must be a series of repeating units with the same basic plan, but with modification (if necessary) to ensure it develops into a unique structure.

Totality: In cross section, an entire segment is divided from adjacent segments.

A compartment is similar to a segment, but does not adhere so strictly to these six rules, especially morphology, metamerity and totality, however it is a lineage restricted zone with clear boundaries and borders of gene expression (Puelles and Rubenstein, 2003). Two of the first compartments to be defined were the dorsal and ventral compartments in the third instar *Drosophila* wing imaginal disc, which were originally found by lineage restriction (Garcia-Bellido et al., 1973). The lineage restricted zones aligned

with domains that became disrupted in animals with mutations in developmentally significant genes; e.g. the site of lineage restriction aligned exactly with the limit of *apterous (ap)* expression. *Ap* is a homeobox transcription factor necessary for wing and haltere development that is expressed in all dorsal cells and no ventral cells (Williams et al., 1993). At the interface between the dorsal and ventral compartments the wing margin forms (reviewed in Brower, 1985). Ablation of *ap* expression in a clone of cells within the dorsal compartment lead to the ectopic formation of a wing margin around the clone and the cells and the clone developed into a winglet (reviewed in Lawrence and Morata, 1994).

A compartment is therefore a discrete developmental unit, a functional zone within which a specific developmental program can be executed through expression of a unique combination of homeotic genes. The compartment has clear borders between it and adjacent compartments.

## Segmentation of the vertebrate brain

The developing vertebrate central nervous system can be divided into segmental compartments, defined by morphology and neuronal arrangement (Lumsden and Keynes, 1989).It is divided into 4 regions, the telencephalon, diencephalon, mesencephalon and rhombencephalon. Over the past two decades evidence has arisen to suggest that each of these large brain segments may be further subdivided into neuromeres. Many of these proposed neuromeres are demarcated by borders of gene expression, however many edges of gene expression, do not line up with morphological borders, do not impose lineage restriction on cells, or violate the definition of a segment in other ways (Kiecker and Lumsden, 2005; Larsen et al., 2001). Thus there has been considerable controversy over how many subdivisions there are (e.g. see Kiecker and Lumsden, 2005; Puelles and Rubenstein, 2003).

The segmentation of the hindbrain into rhombomeres is the best characterised and most widely accepted neuromeric division. The hindbrain consists of 7-8 rhombomeres, depending upon species, which are serially arranged from rostral to caudal (fig. 1.1A). During neurogenesis the topology of the hindbrain is wave-like, undulating with each rhombomere. Boundary regions bulge into the ventricular space, while the basal surface is indented (e.g. Hanneman et al., 1988; Lumsden and Keynes, 1989). Each rhombomere has the same basic morphology and population of proliferating cells and neurons and differences between rhombomeres appear to arise as modifications to a

basic plan, rather than each rhombomere obeying a unique developmental plan (Clarke et al., 1993).

The organisation of neurons is segmented. In chick embryos neurons coalesce into boundary regions (Lumsden and Keynes, 1989), while in zebrafish there is a large group of neurons in rhombomere centres and smaller groups in boundary regions (Trevarrow et al., 1990)(fig. 1.1B). Roots of the branchiomotor nerves exit the hindbrain in regular intervals, from r2, r4, r6 and r7 (fig. 1.1C). Odd numbered rhombomeres that lack a nerve root, project rostrally and exit the brain from the nearest nerve root (Lumsden and Keynes, 1989). The boundary neurons project axons contralaterally, creating a transient ladder pattern of axons (Trevarrow et al., 1990)(Fig.1.1.D). Segmental organisation extends to glial fibres in zebrafish hindbrain as they fasciculate into bundles adjacent to rhombomere boundaries (Trevarrow et al., 1990)(fig. 1.1B). Each rhombomere is a lineage restricted compartment, however this does not extend to the floor plate (Fraser et al., 1990). Thus to say the hindbrain is truly segmented, one would either have to not consider the floor plate part of the structure, or to relax the definition of a segment to allow for incomplete separation.

Segmental architecture in the hindbrain is brought about by differential expression of genes encoding transcription factors that control the identity of each segment. The first identified was *krox20*, expressed in r3 and r5 and with tight edges of expression that coincided perfectly with rhombomere boundaries (Wilkinson et al., 1989a). The limits of genes encoding homeobox transcription factors (*hox)* expression were subsequently found to also coincide with rhombomere boundaries. Segmental arrangement of the *hoxb (hox2)* gene group was first identified in mouse hindbrain, with expression of lower numbered *hoxb* genes generally extending further anterior than higher numbered genes (Wilkinson et al., 1989b) (fig. 1.1C). This expression is similar to that seen in insect segmentation (albeit in insects *hox* genes are confined to individual segments) and has since been confirmed to be conserved across vertebrates (Hueber and Lohmann, 2008; Ingham and Martinez Arias, 1992; Puelles and Rubenstein, 2003). Therefore the control of segmental identity through homeobox transcription factor expression appears to be a universal system used in embryogenesis.

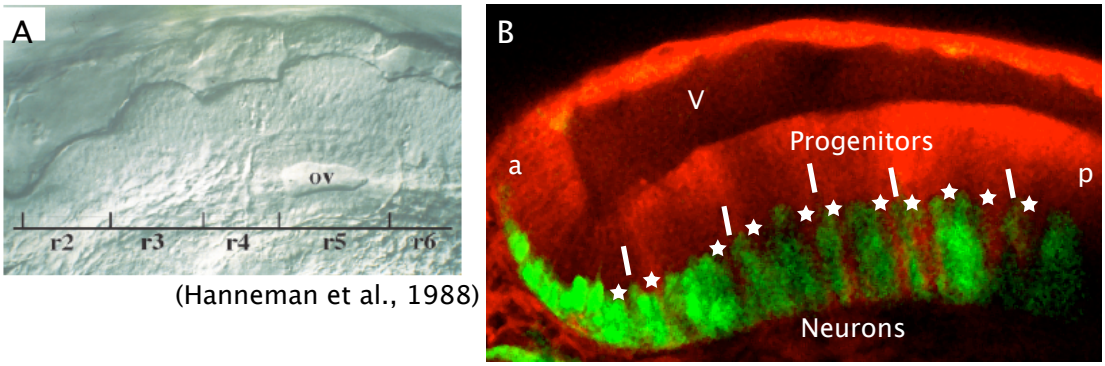


(Hanneman et al., 1988)

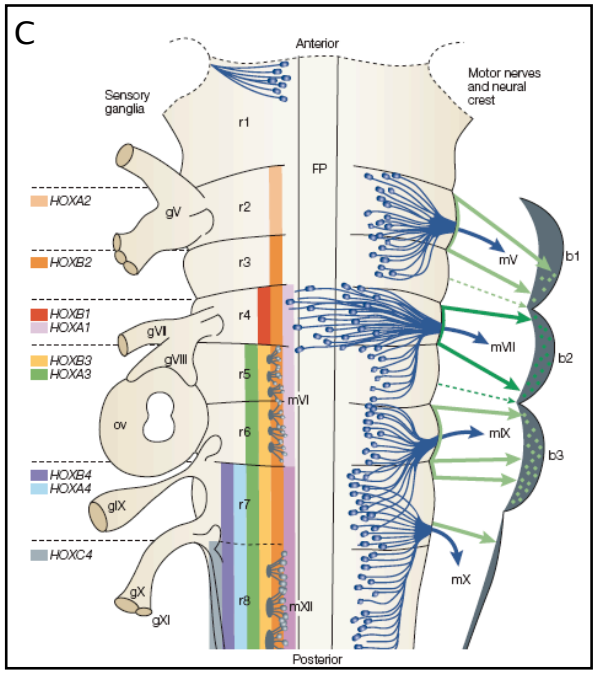


(Kiecker & Lumsden, 2005)

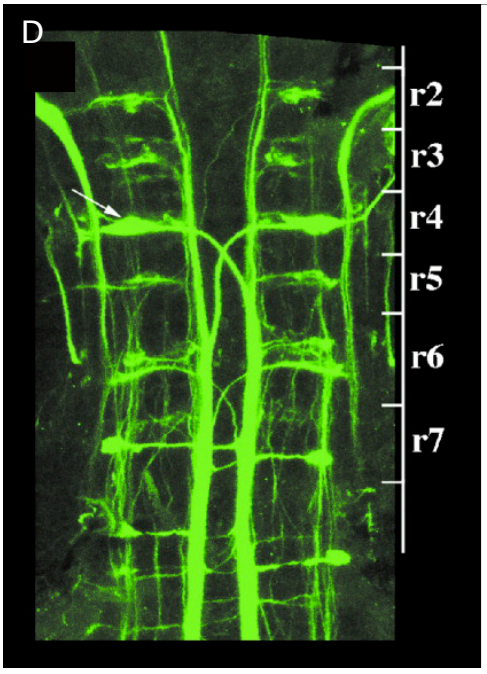


(Moens et al., 2002)

Fig. 1.1. Segmentation of the vertebrate hindbrain
A). Lateral view of a zerafish hindbrain demonstrating that rhombomeres are cleary visible by the undulating morphology of the neuroepithelium.
B). Lateral view of 24hpf Tg(HuC:GFP) zebafish hindbrain. Progenitors are labelled with calcein AM (red). Their glial fibres coalesce into glial curtains, which congragate adjacent to rhombomere boundaries. Neurons are clustered into groups. Larger groups occupy rhombomere centres and smaller groups lie in boundary regions, flanked on either side by the glial curtain.
C). Schematic of the avian hindbrain showing branchiomotor nerve roots exit the hindbrain from r2, r4, r6 and r7 in a repeating pattern. Neurons in odd numbered rhombomeres project into even numbered rhombomeres rostral to their location and exit through that root. Each rhombomere expresses a unique combination of hox genes, which give it its unique identity.
D). Dorsal view of a zebrafish hindbrain at 24hpf showing segmental position of commisural axonal projections in a ladder-like pattern.
Stars: glial curtain, lines: boundaries, v: IV ventricle, a: anterior, p: posterior

## *Chapter 1.2: CNS boundary cells are a unique cell type*

Cells that lie at the interface between adjacent rhombomeres assume characteristics that make them distinct from other cells in the compartment. These properties include altered cytoarchitecture, gene expression (including the expression of boundary specific markers), proliferation rate, neurogenic potential and they secrete molecules that pattern neighbouring rhombomeres (e.g. Amoyel et al., 2005; Cheng et al., 2004; Guthrie et al., 1991; Heyman et al., 1995; Heyman et al., 1993; Thisse, 2001).

### Boundary architecture differs from non-boundary architecture

Individual boundary cells have the same general morphology as cells in the centre of rhombomeres (Guthrie et al., 1991). They are bipolar; connecting to both pial and ventricular surfaces and have large nuclei. The reason for the bulges at the apical surface may be due to the observation that boundary cell nuclei sit close to the ventricular surface, rather than being randomly spread throughout the apico-basal extent of the hindbrain (Guthrie et al., 1991). The basal processes of the boundary cells converge, giving the boundary regions a fan shaped appearance when viewed in the sagital plane (Heyman et al., 1993). BrdU labelling of S-phase nuclei revealed that whilst in non-boundary regions S-phase nuclei were found close to the basal edge of the ventricular zone, they were found throughout the apico-basal axis in boundary regions. The proportion of S-phase cells was also greater in boundary regions than non-boundary regions indicating that boundary cells are held in S-phase for longer times than non-boundary cells. A count of dividing nuclei revealed fewer mitotic cells than non-boundary regions (Guthrie et al., 1991). Taken together, these observations suggest that cell cycles are slowed, and interkinetic nuclear migration decreased in boundary regions.

The volume of extracellular space is increased around the boundary cells, into which is secreted Chrondroitin Sulphate Proteoglycans (Guthrie et al., 1991; Lumsden and Keynes, 1989). There is more extracellular space on the basal side compared with the apical side of the VZ. This is due to boundary cell nuclei, in general, sitting closer to the apical end of the hindbrain, rather than being evenly distributed through the entire apico-basal thickness of the ventricular zone (Heyman et al., 1993). The function for this expansion of the extracellular space is not known, however it may serve to insulate one rhombomere from another, by reducing the amount of contact between the neighbouring cells and so reducing their abilities to interact.

Neuronal and axonal arrangements are transiently segmental in chick hindbrain in early to mid neurogenesis. There are more neurons in boundaries than non-boundaries in chick hindbrains, early in neurogenesis. This generates delta shaped marginal zones that extend far towards the apical surface of the hindbrain (Lumsden and Keynes, 1989). Neurons also cluster in boundary regions in zebrafish hindbrains, but there is a larger cluster in the centre of each rhombomere (Trevarrow et al., 1990). Axons transiently collect in rhombomere boundaries in chick and close to the boundaries in zebrafish (Lumsden and Keynes, 1989; Trevarrow et al., 1990). Ng-CAM, which preferentially labels fasciclulated axons is strongly expressed in rhombomere boundaries (Lumsden and Keynes, 1989).

## The segmental gene expression profile of rhombomere boundaries

In the zebrafish, boundary specific genetic markers can be detected by 14hpf, during neurulation (Amoyel et al., 2005; Cheng et al., 2004), approximately 8 hours before morphological boundaries can be seen (Kimmel et al., 1995). The early markers of zebrafish boundaries include sema3G (Cooke et al., 2005) *wnt1*, *radical fringe (rfng)* and *foxb1.2* (*mariposa*) (Amoyel et al., 2005; Cheng et al., 2004) and in zebrafish, each rhombomere boundary is two cells wide (Cheng et al., 2004). They also display a reduction in the expression of *deltaA, B* and *D*, proneural genes such as *ngn1*, *ashA* and *ashB*, and gap junction component *cx43.4* (Amoyel et al., 2005; Cheng et al., 2004; Thisse, 2001).

In the chick, *follistatin* is expressed only by boundary cells (Nittenberg et al., 1997). Up to HH stage 13 segment specific markers, such as *krox-20* and *hoxb-1*, are initially expressed up to rhombomere interfaces. Between stages 13 to 17, expression decreases and becomes absent from boundary cells (Heyman et al., 1995). Subsequent to this, Vimentin, a marker of radial glial identity becomes concentrated in boundary regions and along the basal surface of the neuroepithelium (Heyman et al., 1995). Expression of Pax6 is strong in boundary cells, but not in the centre of rhombomeres, in stage 20 chick and 24hpf zebrafish embryos (Heyman et al., 1995; Xu et al., 1995).

## *Chapter 1.3: Factors governing boundary formation*

Attempts to disrupt the formation of rhombomere boundaries or to eliminate them after their formation have revealed that boundary formation is a robust process in vertebrates. Chick boundaries have the ability to reform after surgical ablation (Guthrie and Lumsden, 1991) and zebrafish boundaries are resistant to genetic ablations that cause loss of boundaries in an analogous system, the dorso-ventral compartmentation of *Drosophila* wing discs (Cheng et al., 2004). Many manipulations that affected the formation of rhombomere boundaries in zebrafish also disrupted the segmental patterning of the hindbrain (Cooke et al., 2001; Waskiewicz et al., 2002), or alter cell fates. These experiments will be discussed.

### Boundaries reform after surgical ablation

Rhombomere boundary cells develop at the interfaces between rhombomeres that express different genes. It is the interaction between these two opposed domains that regulate the formation and maintenance of unique boundary cells. The mechanism behind boundary formation is robust and persists long after boundaries have formed since chick boundaries regenerate after surgical ablation (Guthrie and Lumsden, 1991). There is a pair-wise rule governing the generation of boundaries, since when a small piece of an odd numbered rhombomere was transplanted into an even rhombomere (or vice versa), a new boundary formed between the host and donor tissue (Guthrie and Lumsden, 1991). If an even numbered was transplanted into an even numbered rhombomere in a host chick embryo, the donor tissue integrated without creating a boundary. The same was true for odd numbered rhombomeres, except for rhombomere 7. Transplantation of r5 tissue into r7 resulted in the formation of the boundary between the donor and host tissue (Guthrie and Lumsden, 1991). As in normal boundaries, Chrondroitin sulphate proteoglycans accumulated in the interface between two experimentally juxtaposed segments, indicating that a boundary had formed between them (Heyman et al., 1995). Therefore there is some property of odd and even numbered rhombomeres that causes them to create boundaries at their interfaces.

## Genetic disruption of antero-posterior patterning eliminates rhombomere boundaries

Experimental manipulation of segmental genes in the hindbrain has been employed to uncover which instructions are necessary for boundary formation. There are numerous ways in which some or all rhombomere boundaries can be eliminated – for example: zebrafish lacking *pbx2* and *pbx4,* which encode transcription factors required for *hox* expression did not develop rhombomere boundaries. Loss of boundaries may have been secondary to antero-posterior patterning defects because the embryos entered a 'ground state' with the molecular identity of rhombomere 1. There was a corresponding drop in the number of cranial neurons that usually derive from r2-6 and a caudal expansion of *engrailed* expressing neurons that are found only in r1 in wild type fish (Waskiewicz et al., 2002). *Hoxb-1* was expressed during gastrula stages, but had disappeared by 18-20hpf, suggesting that segmental gene maintenance, rather than induction was disturbed (Waskiewicz et al., 2002).

Disrupted antero-posterior patterning may also be the cause for loss of rhombomere boundaries in *kreisler/valentino* mutants. *Kreisler/valentino* encodes a bzip transcription factor that, when mutated results in loss of boundaries in the caudal hindbrains of mice and zebrafish (Cooke et al., 2001; Frohman et al., 1993). *Kreisler,* the mouse homologue is expressed in the caudal hindbrain, extending up to the r4/5 boundary (Cordes and Barsh, 1994). *Kreisler* mutant mice lack morphological rhombomere boundaries caudal to the r3/4 boundary, however as with zebrafish lacking *pbx2* and *4* the effect is probably secondary to homeotic transformation of r5 and r6 and disruption to the patterning of r3 and 4 (Frohman et al., 1993). The phenotype in zebrafish *valentino* mutants was similar to *kreisler* mutant mice. They lacked r4/5 and r5/6 boundaries, however since homeotic transcription factor expression was disrupted in rhombomeres 3-7, boundary loss may have been secondary to defective specification of segmentation (Cooke et al., 2001).

These genetic manipulations show that boundaries are lost in regions where segments lose their identities and did so did not uncover which interactions at the interfaces of opposed segments cause boundaries to form.

## Loss of boundaries after Eph and Ephrin manipulation

Attempts to eliminate boundary formation without causing homeotic transformation of the hindbrain have provided evidence that Eph-Ephrin interactions at interrhombic interfaces are essential for boundary formation (Cooke et al., 2005; Nittenberg et al., 1997; Xu et al., 1995). Retinoic acid soaked beads were implanted into chick r4 after boundary formation which resulted in loss of boundaries caudal to the r3/4 boundary before *hoxb-1, hoxb-4* and *hoxa-2* gene expression changed (Nittenberg et al., 1997). Boundaries caudal to the r3/4 boundary could not be detected by morphology, extracellular space, axon accumulation or expression of boundary specific *follistatin* (Nittenberg et al., 1997). Before bead implantation, *krox-20* and *ephA4* (*cek8*) were expressed in r3 and r5. After bead implantation, but prior to the disappearance of boundaries, *krox-20* and *ephA4* expression was lost in r5 and *krox-20* expression was also lost from r3 (Nittenberg et al., 1997). This effect was developmentally significant because branchial motor neuron arrangement was disturbed in the retinoic acid treated embryos (Nittenberg et al., 1997).

The mechanism behind the loss of boundaries may have been the down regulation of *ephA4*, because zebrafish and *Xenopus* rhombomere boundaries require Eph-Ephrin interactions to form. EphA4 is expressed in the same pattern as in chick hindbrain (r3 and r5), while EphrinB2a has a complimentary expression pattern, in r2, r4 and r6 (Cooke et al., 2005; Xu et al., 1995). Injection of a truncated form of mouse or *Xenopus* EphA4 (Sek-1) into zebrafish or *Xenopus* embryos reduced expression of boundary markers and tight borders of *krox-20* expression were lost, indicating cells from different rhombomeres had not segregated (Xu et al., 1995). Morpholino (MO) knock down of EphA4 and EphrinB2a in combination in zebrafish more severely disrupted hindbrain boundary formation than knock down of EphA4 alone, as evidenced by extensive mixing of cells from different rhombomeres and a lack, or severe reduction of boundary specific *sema3G* mRNA from rhombomere boundaries (Cooke et al., 2005). This perturbation of boundary formation through disruption of Eph-Ephrin interaction had developmental consequences, since branchial motoneuron nuclei (abducens and trigeminal) became fused in double MO treated zebrafish (Cooke et al., 2005) and the segmental organisation of reticulospinal neurons was disturbed in zebrafish injected with truncated EphA4 (Xu et al., 1995). Thus, eliminating rhombomere boundaries disrupts the normal course of neuronal development (Cooke et al., 2005; Xu et al., 1995).

The mechanism behind Eph-Ephrin mediated sorting is at present unknown; however circumstantial evidence implicates modifications to intercellular junctions as a promising candidate. EphrinB1 can interact with Par6, part of the Par3-Par6-aPKC complex that establishes apico-basal polarity and dictates the location of tight junction formation in epithelia (Reviewed in Lee et al., 2008; Ohno, 2001). Disrupting the level of expression of EphrinB1 by over-expression or morpholino injection caused *Xenopus* blastocysts to dissociate and to lose tight and adherens junctions (Jones et al., 1998; Lee et al., 2008). Therefore it is possible that Eph-Ephrin interactions can modulate cellular adhesion during cell sorting to encourage misplaced cells to relocate into their correct segments.

## *Chapter 1.4: The Notch signalling pathway in boundary formation, hindbrain patterning and neurogenesis*

The Notch signalling pathway is an important determinant of cell fate and also in boundary formation that is conserved across the animal kingdom. In this section I will first describe the molecular pathway that make up the Notch signalling pathway, then describe how the Notch pathway affects boundary formation in flies and discuss if the same applies to vertebrates. Following this I will explain how Notch signalling affects neurogenesis in general and then how it affects patterning and neurogenesis in the zebrafish hindbrain.

### Molecular interactions in the Notch signalling pathway

The Notch signalling pathway is complex, and in 2005 there were in excess of 24 genes known to be involved in the pathway (Yoon and Gaiano, 2005). The pathway components fall into 5 categories: receptors, ligands, effectors, modulators and targets. Notch molecules are receptors and Delta, Serrate and Jagged are ligands. Delta is not secreted, therefore Notch signalling occurs between adjacent cells (fig. 1.2A) (Chitnis, 1995). Upon ligand binding, the Notch molecule is cleaved and the intracellular domain translocates to the nucleus where it modifies the cell's transcriptional output through binding to effectors. Suppressor of hairless (Su(H)) represses Notch target genes such as the bHLH *hairy* and *enhancer of split* genes (*hes* and *her g*enes), until bound by the intracellular domain of Notch. Upon Notch binding Su(H) the complex becomes a transcription activator and expresses *hes* and *her* genes(Bailey and Posakony, 1995). Like Su(H), Histone deacetylase 1 (Hdac-1) appears to be antagonistic towards Notch signalling. Without Notch activation Notch target genes are repressed by Hdac-1. Upon Notch activation target genes are derepressed after Notch binds to Su(H), which perhaps interacts with Hdac-1 to end its repression of Notch target genes (Cunliffe, 2004).

Once translated, Hes proteins then suppress the transcription of differentiation genes, including proneural genes *achaete-scute, neurogenin* and Notch ligand *delta,* ensuring the cell remains as a progenitor. Since Notch activation leads to reduced transcription of Notch ligands, a cell with activated Notch becomes less able to activate Notch in its neighbours. These then increase expression of proneural genes and *delta,* causing them to differentiate and inhibit differentiation in their neighbours. The pathway provides a mechanism by which groups of cells with the potential to differentiate compete with each other through lateral inhibition (Chitnis, 1995).

Modulators of Notch signalling either change the sensitivity of Notch to ligand binding, or change the ability of Delta/Serrate/Jagged to activate Notch. The *fringe* family modulate Notch function by glycosylating extracellular EGF repeats of the Notch receptor while it is in the Golgi apparatus (Bruckner et al., 2000; Moloney et al., 2000; Munro and Freeman, 2000) and make Notch more sensitive to Delta and less sensitive to Serrate or Jagged (Bruckner et al., 2000; Moloney et al., 2000; Panin et al., 1997). *Drosophila* posses only one *fringe* (*dfng*) while vertebrates have three*; manic* f*ringe* (*mfng*), *lunatic fringe* (*lfng*) and *radical fringe* (*rfng*) (Johnston et al., 1997).

In zebrafish the best characterised modulator of Delta is Mindbomb, an ubiquitin ligase that sequesters Delta away from the membrane and is essential for its ability to activate Notch (Itoh et al., 2003).

## The Notch pathway is required for dorso-ventral boundary formation in Drosophila wing disc

Spatial regulation of Notch activation in a developing tissue is achieved through spatial regulation of Notch pathway components. *Drosophila* imaginal wing discs have a characteristic Notch expression profile necessary for dorso-ventral boundary formation (fig. 1.2B). Notch is expressed throughout the wing disc and Notch ligands, Delta and Serrate are expressed in complimentary patterns; Serrate in the dorsal compartment and Delta in the ventral compartment (e.g. Micchelli and Blair, 1999). *Dfng* is expressed in dorsal cells within the wing imaginal discs and the edge of its expression marks the dorso-ventral boundary in the disc (Irvine and Wieschaus, 1994). The arrangement of *dfng,* Delta and Serrate generates heightened Notch activity at the boundary because Serrate only activates Notch in ventral cells at the edge of Serrate expression due to Dfng inhibition in the dorsal compartment. Likewise, Delta activates Notch in the Dfng expressing dorsal cells that lie at the edge of Delta expression (Irvine and Wieschaus, 1994; Moloney et al., 2000; Panin et al., 1997; Rauskolb et al., 1999). This results in w*ingless* (*wg),* an orthologue to vertebrate *wnt1,* to be expressed in a stripe along the dorsoventral border (de Celis and Garcia-Bellido, 1994; de Celis et al., 1996; Rulifson and Blair, 1995). Along with increased *wg* expression there are heightened levels of Actin and Myosin along the interface between dorsal and ventral cells (Major and Irvine, 2005; Major and Irvine, 2006).

Dorso-ventral boundary formation requires correct localisation of these molecules: Knockout of *notch* from the entire wing disc resulted in free mixing of dorsal and

ventral cells independently of Suppressor of Hairless, indicating that Notch signalling is required for boundary formation in a (canonical) transcription independent manner (Micchelli and Blair, 1999). Knockdown of *notch* or both *delta* and *serrate* prevented boundary expression of *wg.* Genetic disruption of *wg* itself failed to affect boundary formation, indicating that *wg* expression is an effect of rather than a cause of boundary formation (Micchelli and Blair, 1999).

The importance of *dfng* in dorso-ventral boundary formation and wing formation was discovered when mislocalisation of *dfng* by mutation resulted in disrupted wing growth and ectopic formation of wing margins (Irvine and Wieschaus, 1994). Miss-expression of *dfng,* so that the edge of its expression no longer coincided with the edge of expression of other dorsal genes (e.g. *apterous)* resulted in the stripe of *wg* expression and boundary formation, shifting to the new edge of *dfng* expression (Rauskolb et al., 1999). Thus *dfng* expression is required to form boundaries independent of dorsoventral patterning of wing disc cells.

In conclusion, the imaginal disc dorso-ventral boundary forms at the position where Notch activation is greatest. This heightened Notch activation is caused by spatial regulation of Notch ligands and modulators.

## Hindbrain expression of Notch pathway components and targets

It is possible to draw parallels between vertebrate brain compartmentation and the *Drosophila* wing disc because many Notch pathway components are expressed in strikingly similar patterns in some species, but not in others. *Notch* genes are expressed by all vertebrates, from humans to mice, *Xenopus* to zebrafish (e.g. Bierkamp and Campos-Ortega, 1993; Coffman et al., 1990; Lardelli and Lendahl, 1993; Larsson et al., 1994).

### Mammals

There are four mammalian *notch* genes (Yoon and Gaiano, 2005). *Notch* 1, 2 and 3 are found in the VZ of embryonic mouse hindbrain and they appear to be expressed continuously along the ap and dv axes, except for the floor plate (Lardelli et al., 1994). Similar expression patterns *of notch* genes were seen in rat (Weinmaster et al., 1991), Mouse *deltalike1*(Dll1) is expressed in the hindbrain as early as E8.5, however it is not clear if it is segmentally regulated (Bettenhausen et al., 1995; de la Pompa et al., 1997). In vertebrates there are 3 *fringes; manic* f*ringe* (*mfng*), *lunatic fringe* (*lfng*) and *radical fringe* (*rfng*). *Lfng* is expressed in the mouse ventricular zone, in rhombomeres 3 and 5

from presomitic stages (Johnston et al., 1997). There is confusion over the expression of *mfng* and *rfng*. One study claimed that *mfng* and *rfng* are expressed in the VZ, with *mfng* present in first in r3, followed by r5 then expansion into a wider hindbrain territory (Johnston et al., 1997) *Rfng* appeared to be expressed throughout the mouse CNS (Johnston et al., 1997). Another study could only detect *rfng* and *mfng* expression in differentiating and mature neurons (Cohen et al., 1997). *Wnt1* is strongly expressed in dorsal, posterior r2 and in two less intense lateral stripes from r2-r7 (Zervas et al., 2004), which bears little resemblance to imaginal wing disc expression, where heightened Notch activation at boundaries caused *wg* to be expressed within boundary cells (de Celis et al., 1996). However *hes1*, a Notch signalling target is strongly expressed in rhombomere boundaries suggesting heightened Notch activation in boundaries is evolutionarily conserved (Baek et al., 2006).

In conclusion it is difficult to compare mammalian Notch pathway component expression to the fly imaginal disc, due to a poor understanding of the hindbrain expression of many components.

**Chick and Xenopus**

*Notch* expression also appears uniform in chick (Myat et al., 1996) and *Xenopus* hindbrains (Coffman et al., 1990). In chick hindbrain *delta1* and *serrate1* are expressed in complimentary longitudinal stripes (Myat et al., 1996). This is also true of *delta1* expression in plate stage *Xenopus* embryos, where it is expressed in a spotty, salt-and-pepper pattern (Chitnis et al., 1995), however it is unclear if this pattern persists through neurogenesis. In accordance with *Xenopus delta1* expression, proneural genes, including *xash3* are expressed in longitudinal stripes with the same arrangement as *delta1* (Chitnis et al., 1995; Zimmerman et al., 1993). Therefore there does not appear to be much similarity between *Drosophila* wing discs and chick/*Xenopus* hindbrain with regard to Notch signalling at rhombomere boundaries.

**Zebrafish**

There are 5 genes encoding *notch* in zebrafish, which are *notch1a, 1b, 2, 3* and *notchlike* (Zfin.org). *Notch1a* and *1b* are expressed in the VZ of all rhombomeres and are more strongly expressed close to the midline, but are absent from the floor plate (Bierkamp and Campos-Ortega, 1993; Ke et al., 2008). Along the ap axis, rhombomere boundary cells express both *notch1a* and *notch1b* at lower levels than in the rest of the hindbrain, while *notch1a* and *notch1 b* expression in peri-boundary cells is strongest (Bierkamp and Campos-Ortega, 1993; Ke et al., 2008)(fig.1.2C). Like *notch1,* expression of *deltaA*

*deltaB* and *deltaD* is also enriched in peri-boundary regions, while boundary cells and the centre of rhombomeres do not express them (Cheng et al., 2004; Riley et al., 2004).Increased *delta* expression in peri-boundary regions is accompanied by expression of proneural genes such as *ngn1*, *ashA* and *ashB*, which are not expressed in the absolute centre of rhombomeres (Amoyel et al., 2005; Cheng et al., 2004).

The expression patterns of *lfng* and *rfng* are quite different in zebrafish compared with mice. Rather than r3 and r5, zebrafish *lfng* is present in r2 and r4 at neural rod stages (Nikolaou et al., 2009; Prince et al., 2001), then becomes localised to peri-boundary regions from 24hpf (Nikolaou et al., 2009). *Rfng* is expressed only in rhombomere boundary cells from 16hpf (Cheng et al., 2004). As in *Drosophila* wing discs, *wnt1, wnt3a, wnt3b, wnt8b* and *wnt10b* expression (orthologues to *wg*) are heightened at zebrafish rhombomere boundaries suggesting heightened Notch activation at boundaries (Amoyel et al., 2005; Riley et al., 2004). Based upon the expression of Notch pathway components in different vertebrate hindbrains it appears that Notch signalling may not serve the same roles. The expression of Notch components in the zebrafish hindbrain is highly reminiscent of the pattern in *Drosophila* wing discs and so one may assume that, as with flies, boundary formation is a Notch dependent process. In the next section I will discuss this possibility.

## Zebrafish boundaries are resistant to Notch pathway disruption

Unlike flies, the Notch signalling pathway is not entirely necessary for rhombomere boundary cell specification. Boundary markers *rfng* and *foxb1.2* were detected in prospective boundary cells at 16hpf in *mindbomb*$^{ta52b}$ zebrafish, which have severely reduced Notch signalling (Cheng et al., 2004). They were expressed at lower levels and in the case of *rfng*, not in all boundaries. Eventually precocious early neuronal production depletes the ventricular zone and so boundary cells are lost or severely disrupted by 24hpf, yet this could be an indirect effect of the lack of Notch signalling (Cheng et al., 2004). Notch activation does appear to encourage the boundary cell phenotype because cells induced to express a dominant active form of *notch* or of suppressor of hairless Su(H) preferentially sorted to rhombomere boundaries, while cells expressing dominant negative Su(H) sorted away from boundaries (Cheng et al., 2004).

As mentioned above, *fringe* determines the position of the dorso-ventral boundary in fly imaginal wing discs (Rauskolb et al., 1999). It is possible that *fringes* also play this role

in hindbrain boundary formation. The situation in vertebrates is complicated somewhat by the existence of 3 *fringe* family members. As with flies, *fringes* are required to maintain *wnt* expression at rhombomere boundaries since *wnt1* is absent from boundaries in zebrafish injected with *rfng* MO (Cheng et al., 2004). This was not the case in zebrafish injected with a morpholino against *lfng*, where boundary formation was normal (Nikolaou et al. 2009). This could be caused by redundancy in the *fringe* family or due to different potencies of each Fringe to modulate Notch activation (Johnston et al., 1997).

These studies show that Notch signalling is involved in boundary maintenance in the vertebrate hindbrain, but that it is not fully essential for boundaries to exist. Where Notch signalling is of fundamental importance is in the regulation of cell fate choices during neurogenesis.

## Notch-Delta signalling controls the rate of vertebrate neurogenesis

Neurogenesis is a prime example of how Notch-Delta interactions control the rate of differentiation of a pool of undifferentiated progenitor cells (fig. 1.2A). That Notch-Delta signalling controls neurogenesis was first uncovered in *Drosophila*, however a similar process occurs in vertebrate neurogenesis (Chitnis, 1995). The primary purpose of Notch signalling is to ensure that the progenitor pool is not exhausted by excessive differentiation into post mitotic neurons, through lateral inhibition (Chitnis, 1995). In situations where Notch signalling was reduced through mutation of the receptor, a subsequent over production of neurons at the expense of progenitors ensued (Coffman et al., 1993; de la Pompa et al., 1997; Lardelli et al., 1996). Conversely, expression of constitutively active Notch resulted in under-production of neurons and expansion of the progenitor pool (Chitnis et al., 1995; Kopan et al., 1994).

**Fig 1.2. The Notch signalling pathway in lateral inhibition, boundary formation and rhombomere patterning**

A). Diagram representing a simplified version of lateral inhibition between two hypothetical progenitor cells which are competing to differentiate into neurons. The left hand cell will differentiate and the right hand cell will remain as a progenitor. Both cells express Notch and Delta at their cell surfaces, however increased Notch expression and/or decreased Delta expression in the right hand cell has caused Notch activation to be greater in the right hand cell than the left hand cell. In the right hand cell, the activated intracellular domain of Notch translocates to the nucleus where it interacts with repressors of Notch target genes -Su(H) and Hdac-1. Su(H) and Hdac-1 then remove their inhibition of transcription of Notch target genes, including her and hes. Her and Hes then repress the expression of proneural genes and delta. Reduced cell surface Delta in the right hand cell renders it less able to activate Notch in its neighbour. The left hand cell has little Notch activation, so Su(H) and Hdac-1 prevent transcription of Notch target genes. Proneural genes ash, ngn and also delta are expressed. This encourages differentiation into a neuron and increased Delta expression at the cell membrane increases the cell's ability to inhibit differentiation in its neighbour, preventing over production of neurons. Modulators Mindbomb (Mib) and Fringe interact with Delta and Notch respectively. Mib is necessary for Delta to correctly activate Notch receptors, while Fringe increases the sensitivity of Notch to delta signalling.

B). Diagram of a Drosophila imaginal wing disc (adapted from (Kiecker and Lumsden, 2005). The spatial regulation of Notch pathway components determines the position of the dorso-ventral boundary. Notch is expressed ubiquitously. Serrate (SER), Fringe (Fng) and Apterous (AP) are expressed only in dorsal cells and Delta (DL) only in ventral cells. Fng prevents SER activation of Notch within the dorsal compartment, so only the ventral cells located at the edge of Fng expression activate Notch in response to SER. Likewise Fng causes increased Notch activation in response to DL only in dorsal cells that lie at the edge of DL expression. This creates a stripe of Notch activation and boundary development, which includes expression of wingless (WG) and actin.

C). Diagram showing the expression of Notch pathway components and targets in the zebrafish hindbrain. There are 3 populations of cells, based upon location. Boundary cells (purple) express *rfng, wnts* and lack deltas and proneural genes ash, ngn etc. Notch expression is lower in boundaries than peri boundaries, but the presence of positive Notch modulator rfng within the boundary and deltas in the peri-boundary regions causes high Notch activation in the boundary. F Actin (red) accumulates in the interface between adjacent rhombomeres. Peri-boundary regions contain a mixed population of progenitors (white) and differentiating neurons (black). Progenitors express Notches and GFAP. Immature neurons express Notches, Deltas, proneural genes (*ash, ngn* etc.) Therefore lateral inhibition is strong in this region. Central rhombomere cells also express gfap and express delta and notch at lower levels than in peri-boundary regions. *Lfng* is expressed in r2 and r4 at rod stages and in peri-boundary regions after ventricle opening and acts as a negative regulator of neurogenesis.

*ash: achaete/scute, ngn: neurogenin*, DL: Delta, mib: Mindbomb, Fng: Fringe, Su(H): Suppressor of Hairless, Hdac1: Histone Deacetlyase-1, *hes*: *Hairy/Enhancer of Split*, *her: Hes related*, AP: Apterous, WG: Wingless, SER: Serrate, DL: Delta, *lfng: lunatic fringe, rfng: radical fringe*

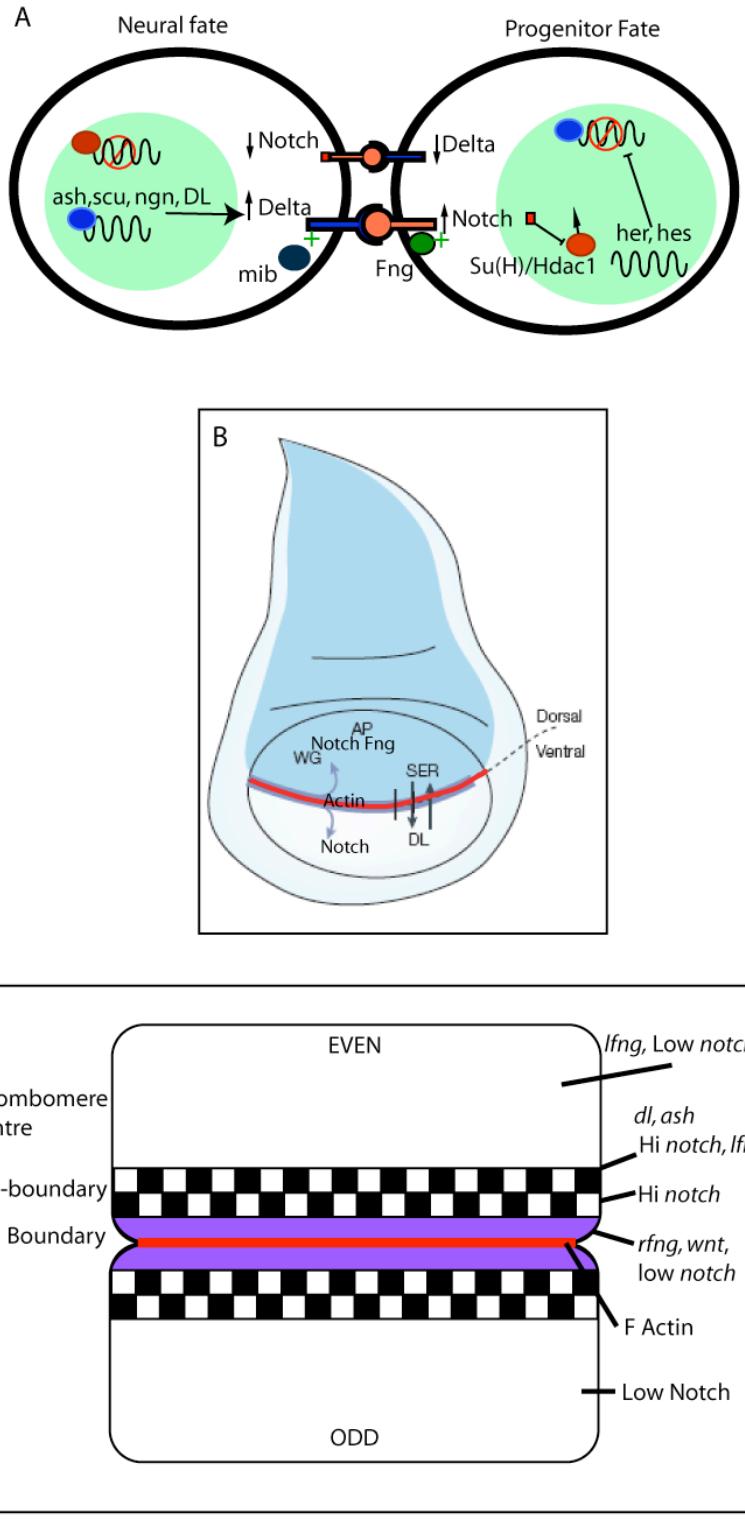


Fig 1.2. The Notch signalling pathway in lateral inhibition, boundary formation and rhombomere patterning

Manipulating Delta function also disrupted neurogenesis (e.g. Appel and Eisen, 1998; Chitnis et al., 1995; Henrique et al., 1997). Expression of dominant negative *delta* alleles in *Xenopus*, chick and zebrafish reduced Notch activation, and caused an over-production of primary neurons at the expense of progenitors that then caused later born neurons to be absent from the embryos (Appel and Eisen, 1998; Chitnis et al., 1995; Henrique et al., 1997). Over-expression of Delta, and hence increased Notch signalling had the opposite effect, reducing the production of neurons (Chitnis et al., 1995; Henrique et al., 1997). When small groups of cells were induced to over-express Delta, they differentiated, presumably because they were able to activate Notch signalling in their neighbours to a greater degree than their neighbours could activate it in them and so 'won' the lateral inhibition competition (Henrique et al., 1997). This finding demonstrated that a cell's fate decision is dependent upon not its expression of Delta, but on the expression of Delta in its neighbours and so clearly illustrates the process of lateral inhibition. Delta may not be an effector of differentiation, since within a group of *delta* over-expressing cells, those in the centre were inhibited from differentiating (Henrique et al., 1997). The classical model of lateral inhibition assumes that inhibition is produced by progenitor cells as they compete with each other to differentiate, however the expression of Deltas in the neuroepithelium suggests another situation: Studies have found delta in postmitotic immature neurons and in a low percentage (between 10-15%) of proliferating cells (Henrique et al., 1995; Henrique et al., 1997; Myat et al., 1996). Since most progenitors do not express Notch ligands they are incapable of inhibiting their neighbours until they complete their final division and become irreversibly fated to differentiate. Therefore Delta-Notch signalling is not reciprocal. Moreover it is a negative feedback mechanism between newly born neurons and the progenitor pool that ensures neurons are not over-produced (Henrique et al., 1997).

Disruption of Notch signalling modulators produces similar phenotypes as disrupting Delta or Notch. For example *mindbomb* zebrafish are so named because of excessive production of primary motor neurons at the expense of progenitors and later born neurons (Schier et al., 1996) a phenotype indicative of deficient Notch signalling (Itoh et al., 2003). In m*indbomb*$^{m178}$ mutants, excessive DeltaA is expressed at the cell surface, but this disrupts its ability to activate Notch in neighbouring cells (Itoh et al., 2003). Transplantation studies of *mindbomb* mutant cells into wildtype hosts or vice versa have shown that Mindbomb is required within cells expressing Delta, rather than

cells receiving Delta signalling because *mindbomb* cells in wildtype brains tend to remain as progenitors, while wildtype cells in *mindbomb* brains tend towards a neuronal fate (Itoh et al., 2003).

The *hdac-1* mutant has an opposite phenotype. As mentioned above *hdac-1* inhibits the transcription of Notch targets. Loss of function of Hdac-1 results in expansion of progenitors at the cost of neurons (Brunmeir et al., 2009; Cunliffe, 2004).

From these studies of manipulating either Notch or Delta function it is clear that the Notch signalling pathway mediates the choice between neuronal and progenitor fates.

## The Notch pathway patterns the hindbrain and controls neurogenesis in zebrafish.

I previously described (Chapter1.3) the hindbrain expression pattern of *notch*, *delta* and other components of the Notch signalling pathway. Segmental regulation of these genes produces a segmental pattern of neuronal production. In zebrafish, each rhombomere can be divided into three distinct regions; boundaries, peri-boundaries and rhombomere centres, based upon the expression of Notch pathway components and their neurogenic potential (e.g. see the expression patterns in Bierkamp and Campos-Ortega, 1993; Cheng et al., 2004) (fig. 1.4B). Heightened Notch activation at rhombomere boundaries suggests they have reduced neurogenic potential (Amoyel et al., 2005; Cheng et al., 2004). Peri-boundary cells, adjacent to boundaries contain a mixed population of cells; neuronal fated cells that express *deltaA, deltaD* and proneural genes (Cheng et al., 2004), and un-specified progenitor cells expressing heightened *notch* genes and GFAP expressing glial fibres (Cunliffe, 2004). The two populations are intermixed, illustrating that lateral inhibition underlies the cell fate choices made by peri-boundary cells. Within the centre of rhombomeres lie another population of cells that less strongly express proneural genes, *deltas* and *notches* indicating a lower neurogenic potential compared with peri-boundary regions (Bierkamp and Campos-Ortega, 1993; Cheng et al., 2004).

The patterning of individual rhombomeres is sensitive to disruption of Notch signalling. For example, elimination of *rfng* from boundary cells resulted in loss of *wnt1* expression in boundaries and expression of *wnt1* in the centre of rhombomeres instead (Cheng et al., 2004). The patterning of *mindbomb* hindbrains was severely disrupted. By 24hpf nearly all hindbrain expressed HuC and virtually none expressed *deltaD,* indicating that differentiation into primary (early) neurons was almost ubiquitous (Bingham et al., 2003). Hindbrain morphology was severely disrupted, with failed

ventricle opening and aberrant branchiomotor and commissural neuronal positioning (Bingham et al., 2003). Boundary markers, *hox* genes and *krox20* were initially expressed, indicating that segmental specification was not lost, however expression of these genes disappeared as the progenitor pool became exhausted (Bingham et al., 2003; Cheng et al., 2004).

Converse to *mindbomb* mutants, expression of dominant active Su(H) (increased Notch target output) reduced the expression of proneural markers and production of neurons (Cheng et al., 2004). A similar phenotype occurred in *histone deacetylase 1 (hdac-1)* mutants (Cunliffe, 2004; Golling et al., 2002). There was reduced expression of proneural genes *ash1b* and *ngn1* and a concomitant drop in the number of *HuC* and *isl1* expressing neurons. There was an increase in the expression of Notch target gene *her6*, and expansion of GFAP expressing glial fibres from peri-boundary regions into the entire rhombomere (Cunliffe, 2004). This mutant appeared to affect the segmental organisation of the hindbrain without disrupting the expression of segmental genes (e.g. *ephA4*), or preventing ventricle opening, however it is at present unclear if boundary cells are affected (Cunliffe, 2004).

Notch modulator *lfng* is co-expressed with cells expressing proneural genes in the peri-boundary region of zebrafish rhombomeres and is required to control the rate of neurogenesis (Nikolaou et al., 2009). Neurogenesis is increased in *lfng* MO injected zebrafish, however the spatial pattern of neurogenic markers was not disrupted, while peri-boundary Notch target gene expression was reduced in 40hpf embryos indicating that the normal patterning of neurons and progenitors was slightly disrupted (Nikolaou et al., 2009).

In conclusion, Notch pathway components are segmentally organised in the zebrafish hindbrain, which results in segmentally regulated neuronal production. Disruption to the Notch signalling pathway is capable of disrupting both the segmental organisation of Notch pathway components and of neuronal production.

## *Chapter 1.5: The function of rhombomere boundaries*

Many roles have been proposed for rhombomere boundaries, which include preventing intermingling of cells from neighbouring rhombomeres, preventing intercellular communication between rhombomeres, patterning the surrounding tissue and to provide guidance to extending axons. Three of these functions will be described in this section.

### Wnt secreted by boundaries patterns rhombomeres

*Wnt1, wnt3a, wnt3b, wnt8b* and *wnt10b* are strongly expressed in zebrafish rhombomere boundaries, resulting from heightened Notch activity there (Amoyel et al., 2005; Riley et al., 2004). Knockdown of *wnt1* caused a decrease in the expression of proneural genes including *ngn1, ashA, ashB* and *deltaA* and *deltaB*, which lead to reduced numbers of HuC expressing neurons at 24hpf (Amoyel et al. 2005). Therefore there appears to be a link between Notch signalling, Wnt signalling and neurogenesis. Correct boundary formation may also require Wnt1 because the expression of boundary markers also expands when *wnt1* is knocked down (Amoyel et al., 2005) and over expression of *wnt1* in *mindbomb* mutants partially rescued boundary marker expression (Riley et al., 2004). This suggests that secretion of Wnt1 from boundaries may both regulate neurogenesis through encouraging neuronal differentiation and also maintain tight control of boundary gene expression.

### Boundaries maintain rhombomere integrity

The two roles boundaries play discussed here; to maintain lineage restriction and to prevent ectopic gene induction both serve to maintain segment integrity. They maintain the exquisitely sharp borders of gene expression that are seen at the edge of segments. It appears that the brain utilises both of these strategies to maintain segmental integrity, however the degree to which each method is required to ensure correct segmentation is of considerable debate.

### 1. Interrhombic interfaces prevent cellular mixing between rhombomeres

Prevention of cells crossing compartment boundaries is important for establishment and maintenance of developmental domains. Compartments and segments are lineage restricted zones, meaning that a mother cell's progeny remain in the compartment. Clonally related cells can be identified by intracellular injection of cell impermeant dyes

such as rhodamine dextran, which remain in the progeny of the injected cell and do not enter unrelated cells. When prospective chick hindbrain cells were labelled with rhodamine dextran prior to the formation of morphological boundaries (neural plate stage), labelled cells were found in one or more rhombomeres. However if the injection was carried out subsequent to boundary formation (15 somites), clone members were restricted to a single rhombomere (Fraser et al., 1990). Separation of neighbouring cells is not perfect, roughly 5% of labelled cells crossed rhombomere boundaries (Birgbauer and Fraser, 1994). It is not clear which cell types could cross, since the clones were analysed at low resolution without the aid of cell specific antibodies, but the authors suggested that the crossing population consisted of both neurons and progenitors (Birgbauer and Fraser, 1994). Likewise, small numbers of cells expressing *krox 20*, or *ephA4* (Sek-1), which are markers of rhombomeres 3 and 5, have been detected in even-numbered rhombomeres in both mouse and chick, after boundary formation (Irving et al., 1996).

Whether neuroepithelial cells extensively mix in situations where boundaries are absent has been debated. In chick there was some mixing of cells from either side of the r4/5 boundary after it was ablated with retinoic acid, however the mixing was constrained to a few cell diameters from the interface between the two rhombomeres (Nittenberg et al., 1997). Therefore rhombomere boundaries are leaky barriers to cell mixing.

**Boundary specialisations that prevent cell mixing**

Specialisation of the boundary region creates the barrier to cells crossing. Increased levels of filamentous actin at zebrafish and chick rhombomere boundaries suggest that they generate a physical barrier, or a fence, to stop cells crossing from one rhombomere into another (Cooke and Moens, 2002; Guthrie et al., 1991). The time at which this fence is established in zebrafish has not been determined. An acto-myosin fence is employed in *Drosophila* imaginal discs to prevent mixing of dorsal and ventral cells in what may be a contractile mechanism that physically impairs cells from one compartment crossing into the other(Major and Irvine, 2005; Major and Irvine, 2006). Disruption of Notch signalling lead to both reduced actin expression at the boundary and intermingling of dorsal and ventral cells (Major and Irvine, 2005; Major and Irvine, 2006). To demonstrate that acto-myosin contractile machinery is directly required for dorso-ventral segregation, there was extensive mixing of dorsal and ventral cells in *zip* mutants which have deficient acto-myosin machinery, but intact Notch

signalling (Major and Irvine, 2006). Similar experiments have not currently been carried out in vertebrate CNS.

## 2. Boundaries prevent ectopic gene induction

Another conceivable mechanism to prevent ectopic segmental gene expression is to prevent inappropriate gene induction across boundaries. Implicit in this hypothesis is the assumption that neuroepithelial cells are competent to change their gene expression profiles. In chick embryos with the r3/r4 boundary ablated by RA application there was extensive expansion of *ephA4* expression from r3 into r4, which was too large to be explained by cell mixing alone (Nittenberg et al., 1997). It is therefore likely that boundary ablation allowed the *ephA4* inducing signal to expand into r4 cells, which were then induced to express *ephA4* ectopically.

In another study grafts of *engrailed2* (*en2*) expressing quail neuroepithelium into chick hindbrain, post boundary formation, induced *en2* expression in the host alar plate, but not medial regions of the hindbrain. The host tissue and the graft generated ectopic cerebellar structures, indicating a switch of identity to r1, which normally expresses *en2* (Martinez et al., 1995). The ability of the donor tissue to induce e*n2* in the host only occurred if there were no rhombomere boundaries between the donor and host tissue(Martinez et al., 1995). These experiments suggest that the hindbrain neuroepithelium is plastic and capable of changing fates and that ectopic gene induction is prevented by boundary cells.

Plasticity in *hox* gene expression has also been discovered. Grafting rostral segments into caudal regions, but not caudal segments into rostral positions caused re-patterning of the donor tissue (Grapin-Botton et al., 1995; Itasaki et al., 1996). For example, relocation of r3/4, into r7/8 before boundary formation resulted in re-specification of the donor tissue to r7/8, evidenced by *hoxb4* expression and neuronal development (Grapin-Botton et al., 1995). Transplantation of r5/6 into r7/8 induced *hoxb4* only in r6, with a sharp border of gene expression at the r5/6 boundary suggesting that the boundary within the graft inhibited *hoxb4* expansion into the grafted r5 (Grapin-Botton et al., 1995). In contrast to studies that found rhombomere boundaries prevent ectopic gene induction, plasticity persisted in rhombomere transpositions that were made after boundary formation, but this was after an extensive time delay (Itasaki et al., 1996).

Other transplantation studies could not detect plasticity in segmental identity. *Hoxb1* is normally expressed in r4 in stage 9 (6 somites) chick embryos. Excision of r4 and

replacement with r2, or vice versa, failed to induce changes in *hoxb1* expression in the grafted tissue. Also, the transposed segments generated cranial nerves as if they were in their original position (Guthrie et al., 1992). Similarly, grafts of r3 into r4 failed to elicit both expression of *hoxb1* and formation of the trigeminal nerve root in the transplanted tissue (Kuratani and Eichele, 1993).

The reason for these different findings was determined after exploring many permutations of transplants. There is an anterior to posterior gradient of competence to change, superimposed upon a posterior-to anterior gradient of a morphogen that induces *hox* gene expression (Itasaki et al., 1996). The morphogen is retinoic acid (RA), which has been shown to shift the fate of anterior brain structures to a posterior fate in a concentration dependent manner (Durston et al., 1989). Therefore, caudal to rostral grafts did not change, because the concentration and hence inductive ability of RA was weaker in more rostral positions; grafts of r2-r4 did not induce change because the r2 tissue was not competent to switch fate to r4 at the concentration of RA found in r4. Induction of *hox* gene expression in transplants with intact boundaries may have occurred because RA is secreted by the paraxial mesoderm and could have entered the transposed tissue through its lateral edge, bypassing the boundaries (Itasaki et al., 1996).

In conclusion rhombomere boundaries help to maintain borders of gene expression through both lineage restriction and prevention of ectopic gene induction, however lineage restriction is leaky and in certain contexts, rhombomere identity is robust. Therefore the vertebrate brain utilises more than one strategy to ensure gene expression domains are precise.

## *Chapter 1.6 Neuromeric theory: The controversy over anterior brain subdivisions*

Rhombomeres are unequivocally regarded as neuromeres. Other brain regions too have morphologies, gene expression profiles and lineage restriction domains that suggest they also contain neuromeres, but how many neuromeres they contain has been hotly debated. Some subdivisions are too short lived to be accepted as significant, while others lack properties that are essential requirements for them to be classed as separate segments. In the early 1990s the vertebrate forebrain was subdivided into 6 domains called prosomeres, three in the telencephalon, and that include the hypothalamus (P4-6) and 3 in the diencephalon (P1-3) based upon gene expression patterns and morphology (Puelles and Rubenstein, 1993; Rubenstein et al., 1994).

### Telencephalic subdivisions

The accuracy of the subdivision of the telencephalon into P4-6 is questionable. The hypothalamus is included in P5 along with the neocortex, despite the former being diencephalic and the latter being telencephalic (fig1.3A)(Puelles and Rubenstein, 1993; Rubenstein et al., 1994). Lineage restriction of progenitors within the chick hypothalamus, suggest that it is a compartment in its own right (Golden and Cepko, 1996). The model also did not take into account the lineage restriction between pallial (cortex) and subpallial (basal ganglia) telencephalon (Fishell et al., 1993), which are grouped together in P5 (Puelles and Rubenstein, 1993; Rubenstein et al., 1994). Little lineage restriction within the 3 telencephalic prosomeres has been found in chick embryos, but the experimenters examined post mitotic neurons and glia, rather than neuroepithelial cells (Szele and Cepko, 1998). Some neurons do not respect rhombomere boundaries, which are accepted to be neuromeres. For example there is a caudal migration of r4 derived facial neurons into r5 in mouse and zebrafish hindbrains (Higashijima et al., 2000; Studer et al., 1996). However, since lineage restriction is not complete in the anterior prosomeres, whether they are true compartments has been questioned and the prosomeric model has recently been modified to eliminate prosomeres 4-6 (Puelles and Rubenstein, 2003). Whilst some subdivisions of the telencephalon may be inaccurate, this does not mean that the neuromeric model is incorrect, but it may mean the model need further revising.

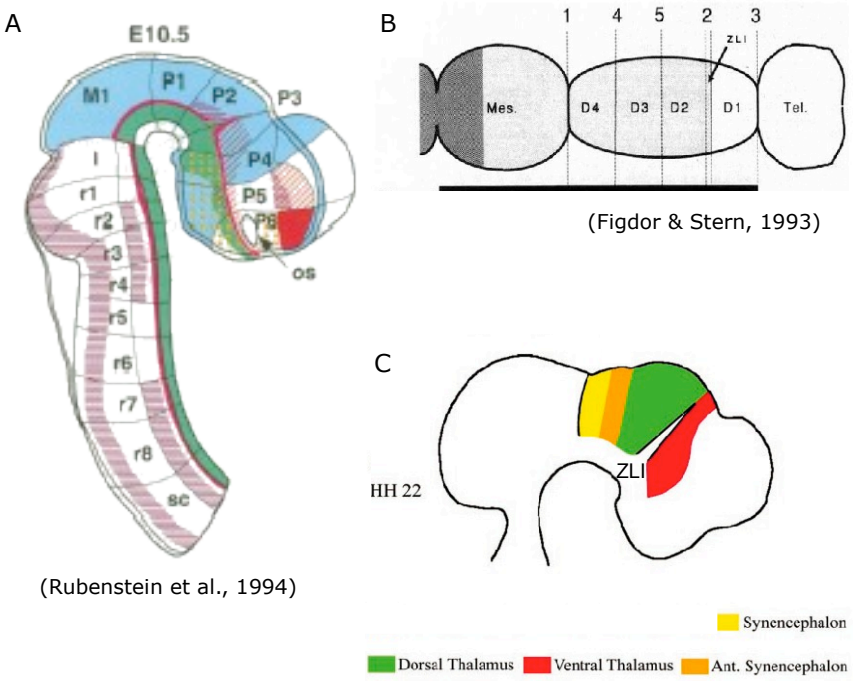


(Rubenstein et al., 1994)

(Figdor & Stern, 1993)

(Larson et al., 2001)

Fig. 1.3. The neuromeric theory of CNS segmentation
A). Diagramatic representation of an embryonic mouse brain at E10.5, subdivided into neuromeres; transverse segments based upon moprhology and gene expression domains. The hindbrain contains 8 rhombomeres (7 in zebrafish) with r1 rostral and r8 caudal.
Immediately rostral to the hindbrain is the isthmus (MHB), followed by the midbrain, which according the the theory has no subdivisions. The forebrain is divided into 6 prosomeres. P1-3 are predominantly diencehpalic, while P4-6 telencephalic. However the model does not account for brain curvature, so that diencephalic structures, such as the hypothalamus, are included in P5, which contains the neocortex.
B). The chick diencephalon was divided into 4 neuromeres, D1-4 by Figdor and Stern, with D1 the most rostral. The extra neuromere was produced by further subdividing P1 into rostral and caudal segments (Figdor & Stern, 1993)
C). Alternative division of the stage 22 chick diencephalon (not including the hypothalamus). It is divided into 5 domains: the ventral thalamus (P3, D1), ZLI, dorsal thalamus (P2,D2), anterior (P1,D3) and posterior synencephalon (P1, D4). Black lines mark where segment boundaries were found, therefore the dorsal thalamus and two halves of the synencephalon were not classed as true segments (Larson et al., 2001).

## Diencephalic subdivisions

The prosomeric model divides the diencephalon into three prosomeres, called (from anterior to posterior),

Anterior parencephalon / ventral thalamus / D1,

Posterior parencephalon / dorsal thalamus / D2 ,

Synencephalon / pretectum / D3

The chick synencephalon was then divided again into two, to create a total of 4 diencephalic domains, labelled D1-D4, with D1 the most anterior (fig. 1.3B) (Figdor and Stern, 1993). Each prosomere was defined morphologically by scanning electron microscopy, by alternating expression of Acetylcholinesterase and binding of PNA and by axon tracts that marked the outlines of each segment. As with rhombomere boundaries, each segment was as a lineage restricted unit (Figdor and Stern, 1993). Each neuromere became morphologically distinct at different developmental stages (Figdor and Stern, 1993). The division of the diencephalon into four neuromeres was then brought into dispute because further work could only confirm boundaries existed between D1/D2, which is the zona limitans intrathalamica (ZLI) and the diencephalon/midbrain boundary. Both boundaries shared significant numbers of properties with rhombomere boundaries, including boundary specific markers (vimentin, CSPGs NrCAM), apically positioned S-phase nuclei and lineage restriction (Larsen et al., 2001). The other proposed boundaries between diencephalic neuromeres did not possess enough attributes for a long enough period of time to be classed as such (Larsen et al., 2001) (fig. 1.3C). Therefore it is unclear at the present just how the diencephalon and telencephalon are subdivided into prosomeres, due to conflicting data.

## The ZLI: Boundary or Compartment?

It is widely accepted that the ZLI is a compartment border between the ventral and dorsal thalamus, however what is uncertain is if the ZLI is a boundary, or a compartment in its own right. It is a border of gene expression because D1 expresses d*lx2* and s*ix3* while D2 expresses *gbx2* and *irx3* (Kiecker and Lumsden, 2005; Larsen et al., 2001). It also patterns the surrounding thalamic tissue by secreting Shh (Scholpp et al., 2006). It strongly expresses *wnt8b* and *hes1*, both of which are also expressed in rhombomere boundaries (Baek et al., 2006; Garcia-Lopez et al., 2004). Therefore the ZLI has many properties in common with rhombomere boundaries.

The ZLI may also be a compartment in its own right, since basally it is wider than a standard boundary (Scholpp et al., 2006; Zeltser et al., 2001). Thalamic tissue on both sides of the ZLI expresses *lfng,* while the ZLI itself does not. In stage 12-13 chick diencephalon, the *lfng* free zone encompasses about 1/3 of the forebrain. The zone gradually shrinks down to a thin wedge at stage 19, when the ZLI proper can be detected by s*hh* expression (Zeltser et al., 2001). In this region, cells are lineage restricted from stage 14 onwards. When *lfn*g was ectopically induced in the ZLI by *in ovo* electroporation, the *lfng* expressing cells sorted out of the ZLI, indicating that ZLI cells have cell adhesion properties that make them immiscible with non ZLI cells (Zeltser et al., 2001).

Since the ZLI has properties of both boundary and compartment it cannot be concluded which it actually is.

## The midbrain-hindbrain boundary may be a lineage restricted compartment

There is also conflicting evidence regarding whether the midbrain hindbrain boundary (MHB) is a boundary, compartment or a mixture of the two. Time-lapse analysis of zebrafish embryos found a lineage restriction site at the caudal border of Otx expression, which is expressed in the midbrain, but not completely up to the morphological constriction of the MHB (Langenberg and Brand, 2005) (fig. 1.4). Accordingly, neurons derived from the Otx-2 expression domain in chick embryos also were constrained within the Otx-2 domain and did not extend fully to the morphological constriction (Millet et al., 1996). This was further supported in mouse studies that found lineage restriction between both midbrain and the isthmus (MHB) and between the cerebellum and isthmus (Zervas et al., 2004). These three studies suggest that the MHB/isthmus may be a lineage restricted compartment in its own right.

These results are controversial since other fate mapping studies have failed to find lineage restricted sites at the chick MHB (e.g. Jungbluth et al., 2001). Aggregation studies also do not support lineage restriction at the MHB: The majority of aggregates of chick r1 and mesencephalic tissue mix, suggesting they do not have different adhesive properties that may be necessary for lineage restriction (Jungbluth et al., 2001). The reason for the discrepancy between studies is not clear, however there may be developmental changes in lineage restriction, since in E8.5 mouse embryos the ventral side of the MHB is more permissive to cells crossing than the dorsal side, but at

E9.5 both dorsal and ventral MHB prevented cells from crossing (Zervas et al., 2004). Taken together these results suggest that the MHB may be a leaky boundary region between the midbrain and hindbrain and the presence of anterior and posterior borders suggest that it could actually be a compartment.

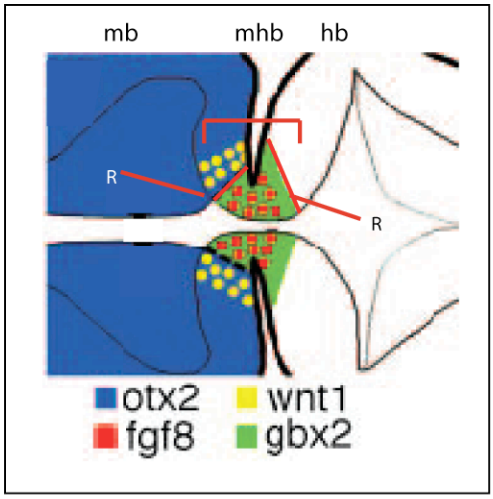


Fig. 1.4. The MHB may be a compartment
Schematic of the 24hpf zebrafish MHb in dorsal view. The midbrain expresses otx2 up to the proposed rostral edge of the MHB, which may be a lineage restriction site (R). Wnt 1 is expressed at the lineage restriction site. The MHB expresses Fgf8 and Gbx2. Fgf8 expression terminates at the border with the cerebellum (r1), but Gbx continues into the cerebellum. The edge of fgf8 expression may also be a lineage restriction site, suggesting that the MHB is a compartment, rather than a boundary.
mb: midbrain, hb: hindbrain, R: site of lineage restriction.

In conclusion, brain regions anterior to the hindbrain also appear to be subdivided into smaller compartments, however it is not clear how many compartments there are. This is due to some proposed neuromeres lacking properties that are essential for their definition as such, and some boundaries possessing characteristics that make them appear to be compartments too. An objective, simple method is required to probe the prospective boundaries that may help clarify where developmental borders are.

## *Chapter 1.7: The structure of the neuroepithelium*

The embryonic vertebrate central nervous system (CNS) is a polarised tissue. It has bilateral symmetry so that its apical side lies towards the midline and the basal side at the outer edge of the CNS. The CNS is organised into a tube that contains a central fluid filled cavity called the central canal in the spinal cord and ventricles 1-4 in the brain. The tissue is laminated, with proliferative cells located in the ventricular zone (VZ) and post mitotic cells, including neurons in the mantle zone, located at the basal edge of the neuroepithelium (fig. 1.1E). Progenitor cells are bipolar and span the entire apico-basal thickness of the VZ. They are attached to the ventricular and pial surfaces by expanded end feet (fig. 1.5A). Apical end feet of neighbouring progenitors are anchored by intercellular junctions (fig. 1.5B). The ventricular zone is pseudostratified since progenitor nuclei are arranged into what appears to be many layers. Nuclear position is linked to the cell cycle: Nuclei move through the VZ via a process of interkinetic nuclear migration so that mitoses occur at the ventricular surface, while DNA replication occurs at the basal limit of the VZ (Sauer and Chittenden, 1959).

Progenitors are called radial glia because they express glial cell markers, (e.g. glial fibrillary acid protein (GFAP) or astrocyte-specific glutamate transporter) (Levitt and Rakic, 1980; Shibata et al., 1997) and were originally believed to produce only astrocytes (Voigt, 1989). This was revised after lineage studies of radial glia both *in vitro* and *in vivo* discovered that neurons are also derived from radial glia (Malatesta et al., 2000; Noctor et al., 2001) and many seem to be produced by asymmetric cell division that produces one neuron (or a neuroblast that will divide again to produce 2 neurons) and one radial glial cell (e.g. Cai et al., 1997; Noctor et al., 2001). It is now known that radial glia can produce all cell types in the cerebral cortex (Williams and Price, 1995). The long basal processes of radial glia act as scaffolds for radially migrating neurons to move along towards the mantle zone (Rakic, 1972), with neurons primarily using clonally related glia as their guides (Noctor et al., 2001).

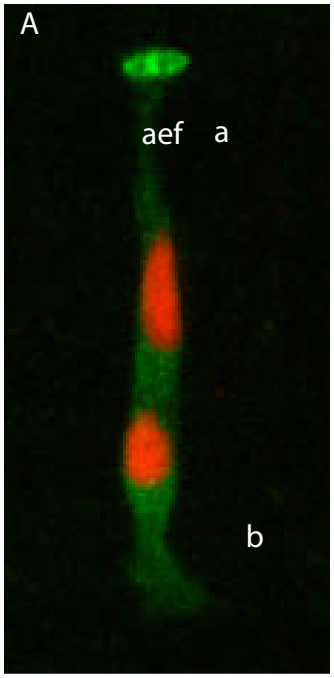


(Paula Alexandre)

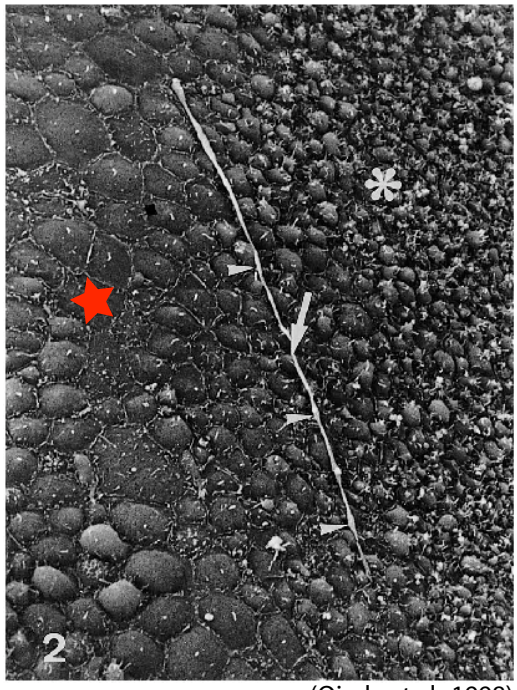


(Ojeda et al., 1998)

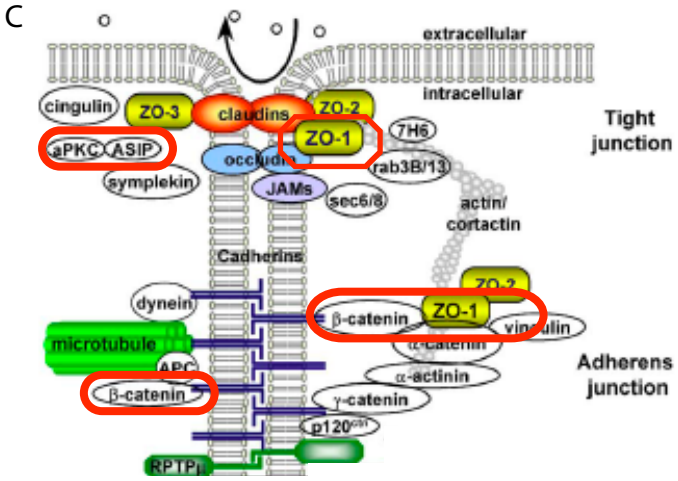


(Giepmans, 2004)

Fig. 1.5. Apical end feet and intercellular junctions in the neuroepithelium
A). Confocal micrograph of a pair of zebrafish neuroepithelial cells labelled with H2B-RFP and cytoplasmic GFP. Cells are bipolar and elongated along their apico-basal axes. Both apical and basal processes have enlarged end feet.
B). Scanning EM of embryonic chick hindbrain ventricular surface showing enlarged apical membranes at a rhombomere boundary (star). Disregard other annotation.
C). Proteins associated with tight and adherens junctions junctions. Pertinent proteins are outlined in red. Tight junctions are the most apical of intercellular junctions. ZO-1, aPKC and Par3 (ASIP) associate with tight junctions. Adherens junctions are located basal to tight junctions. B-Catenin and ZO-1 associate with adherens junctions.
a: apical, b: basal, rhb: rhombomere boundary, star: rhombomere boundary

Intercellular junctions maintain neuroepithelial polarity and determine cell fate

The polarity of all epithelia is maintained by the expression of intercellular junctions that separate the apical membrane from the basolateral membrane (fig. 1.5B). They are expressed in a ring by each epithelial cell and outline each cell's apical end foot (AEF). The function of the intercellular junctions is complex. They are adhesive, ensuring that neighbouring neuroepithelial cells remain attached; obstructive, preventing both the mixing of membrane bound structures between the apical and basolateral membranes and also paracellular movement of extracellular fluid between the ventricle/central canal and the basolateral extracellular space; and communicative, providing channels through which cells exchange small molecules and cytosol. There is also a growing body of evidence that cell fate determination is regulated by the expression of intercellular junctions. The four types of intercellular junctions are as follows:

- Tight junctions, which primarily act as barriers, but also have adhesive properties.
- Adherens junctions which serve to anchor neighbouring cells.
- Gap junctions are also adhesive, however they contain a central pore that allows the intercellular exchange of ions and small molecular weight compounds including second messengers and morphogens.
- Desmosomes which like adherens junctions serve to anchor adjacent cells to each other.

The composition and role of tight junctions and adherens junctions in neural development will be discussed below. Gap junctions will be explored in section 1.8, while desmosomes fall beyond the scope of this thesis.

**Tight Junctions**

Tight junctions are the apical-most of the intercellular junctions (fig. 1.5C). They create a water-tight seal between adjacent cells to prevent paracellular diffusion of the extracellular fluid and also inhibit passage of apical proteins to the basolateral membrane and vice-versa. Thus they maintain apico-basal polarity. Zonula Occludens 1 (ZO-1) was the first tight junction protein to be discovered (Stevenson et al., 1986). It is a membrane associated guanyulate kinase homologue (MAGUK) and is homologous to the *Drosophila* discs large protein (Willott et al., 1993). Immuno EM however revealed that ZO-1 is not an integral membrane protein, rather it exists in the junctional plaque adjacent to tight junctions and is therefore an accessory protein (Stevenson et al., 1986). Further work then expanded the ZO family to three members; ZO-1, ZO-2 and ZO-3 (Haskins et al., 1998; Jesaitis and Goodenough, 1994).

There are three categories of integral membrane proteins that bind neighbouring cells: Occludins, Claudins and Junctional adhesion molecules (JAM) (Furuse et al., 1998; Furuse et al., 1993; Martin-Padura et al., 1998). They may have redundant functions, since Occludin mutant epithelia still form tight junctions and ZOs still localise in the junctional plaques (Itoh et al., 1999). ZOs act as links between Occludin, Claudin and JAM to the actin cytoskeleton, therefore aiding in maintaining tight junctions and epithelial integrity (Bazzoni, 2003; Fanning et al., 1998; Furuse et al., 1994; Haskins et al., 1998; Itoh et al., 1999; Itoh et al., 2001; Wittchen et al., 1999). ZO-1 expression at intercellular junctions is required for epithelial integrity because truncation of ZO-1 to its PDZ motifs resulted in cytosolic localisation and induced epithelium to mesenchyme transition in Madin Darby canine kidney cells (Reichert et al., 2000). There is functional redundancy in the ZO family because mutant mouse epithelial cells lacking ZO-1 formed tight junctions through recruitment of cytoplasmic ZO-2 to tight junction plaques (Umeda et al., 2004).

Another polarity protein, Par3 forms a complex with Par6 and aPKC and this could potentially be the master complex that determines the location where tight junctions form and thus dictate how cell polarity is established (Reviewed in Ohno, 2001). The Par3-Par6-aPKC biochemically interacts with JAM, but not Claudin, so therefore JAM may re recruited to tight junctions by the complex, while ZO may be needed to tether Claudin to JAM in order for it to be transported to the site where tight junctions will form (Itoh et al., 2001).

**Adherens junctions**

Located slightly basal to tight junctions lie adherens junctions, which maintain adhesion between epithelial cells and direct correct localisation of tight junction components during epithelial development (Ohno, 2001) (fig. 1.5C). Cadherins are transmembrane molecules that form the adhesions between neighbouring cells, while α-catenin and β-catenin provide the link between Cadherins and the cytoskeleton (Gumbiner, 2005). Catenins are important for recruitment and/or maintenance of cadherin mediated cell-cell adhesion because adhesions in cultures lacking α-catenin were weaker and adhesion junctions less extensive than cultures with αcatenin (Shimoyama et al., 1992).

As well as promoting cell-cell adhesion through adhesion junctions, the catenins have signalling roles. Over-expressed β-catenin collected in the cytoplasm and caused ZO-1 expression levels to decrease and Wnt target expression to increase (Mann et al., 1999). β-catenin is a target of the Wnt-Tcf signalling pathway and is required for

transcriptional activation of Wnt target genes (Molenaar et al., 1996; Morin et al., 1997).

ZO-1 has been detected in the junctional plaque adjacent to adherens junctions in non-epithelial tissues such as cardiac muscle, which lack tight junctions (Itoh et al., 1993). Later work discovered that it can directly bind Cadherins, further demonstrating it is not simply a tight junction protein (Itoh et al., 1997). Whether ZO-1 localises to tight junctions or adherens junctions depends upon the degree to which the tissue is an epithelium. As mentioned above, cardiac muscle lacks tight junctions and ZO-1 is located at adherens junctions. Highly specialised epithelia such as the intestinal epithelial wall only have ZO-1 in tight junctions, despite containing adherens junctions as well. Intermediate epithelia, such as the liver contain ZO-1 in both adherens and tight junctions (Itoh et al., 1993).

## A potential role of intercellular junctions in neural cell fate

Recent work has suggested that rather than simply maintaining the structural integrity of the neuroepithelium, adherens junctions may actually be involved in determining whether a progenitor becomes a neuron, or remains as a progenitor (Rasin et al., 2007). In short, *in vivo* knockdown of E-cadherin or N-cadherin in a subset of cortical progenitors caused a loss of adherens junctions, delamination from the neuroepithelium, dispersal away from the VZ, and loss of radial glial morphology (Rasin et al., 2007). The authors of the study interpreted this as differentiation into neurons based upon the location of their cell bodies and their morphology (Rasin et al., 2007).

The Par3-Par6-aPKC complex too has been shown to control cell fate in a variety of organisms and tissues. Correct localisation of all 3 proteins is essential for correct adherens junction localisation in *Drosophila* neuroectoderm and for asymmetric division of *Drosophila* neuroblasts (Reviewed in Ohno, 2001).

## Apical organisation may be related to cell identity

The size and arrangement of apical end feet (AEF) at the ventricular surface of adult mouse cortex provides the information necessary to identify cell identity. Three cell types have AEF in the adult brain: two kinds of ependymal cells and sub-ventricular neural stem cells which divide and produce neurons. The AEF of stem cells were smaller than ependymal AEF and arranged into pinwheels, while ependymal cells were not (Mirzadeh et al., 2008).

Another example of the relationship between AEF arrangement and identity can be found in rhombomere boundaries. Scanning EM or phalloidin staining of the ventricular surface of chick hindbrain revealed that the apical membranes of boundary cells appeared larger in size than non-boundary cells (Guthrie et al., 1991). These observations suggest that apical organisation may be differentially regulated at segment boundaries and be related to cell identity. Currently the relationship between the structure of the neuroepithelium and segmentation is not well understood, however observations of differences in intercellular junctions at rhombomere boundaries have been made.

## Intercellular junctions at rhombomere boundaries

Electron micrographs of chick hindbrain show that junctional complexes in interrhombic interfaces extend less far basally than interfaces between non-boundary cells (Heyman et al., 1993; Ojeda and Piedra, 1998). This is in agreement with mRNA expression of the gap junction component *cx43.4*, which is down-regulated at zebrafish rhombomere boundaries (Thisse, 2001). Since intercellular junctions serve to attach cells and facilitate intercellular communication, a reduction in junctions at boundaries suggests that boundary cells are less tightly held together than cells in the centre of rhombomeres and that intercellular communication between rhombomeres may be decreased. Reduced intercellular communication at chick rhombomere boundaries has been observed (Martinez et al., 1992), the significance of which will be discussed in section 1.9. As mentioned above, boundary AEF are larger than non boundary AEF (Guthrie et al., 1991; Ojeda and Piedra, 1998). Whether this is also true in the zebrafish is not known and if this enlargement is mirrored by modified junctional arrangement remains to be determined. Filamentous actin, visualised by phalloidin staining was less concentrated at the ventricular surface of boundary cells when viewed in sagital section, while it was more strongly expressed in strips extending apically from the pial surface, whereas in non-boundary regions actin was only found at the apical and pial surfaces (Guthrie et al., 1991). In developmentally less mature zebrafish, where the IV ventricle had not yet opened, actin has been found in bands running through inter-rhombic interfaces (Cooke et al., 2001). The apico-basal location of this enrichment was not divulged. It will be interesting to learn when actin accumulates and how it is distributed in zebrafish embryos with open ventricles. At present there is little known about segmental regulation of other components of intercellular junctions, such as ZO-1, aPKC and Par3.

The expansion of AEF in rhombomere boundaries suggests that AEF size is in some way genetically controlled. The genetic pathway(s) that mediate the apical enlargement is currently not known. The Notch signalling pathway is a valid candidate because segmental patterning of rhombomeres and boundary cell formation and maintenance are partly dependent upon Notch signalling (Amoyel et al., 2005; Cheng et al., 2004; Micchelli and Blair, 1999). Manipulating Notch signalling could provide insight into how AEF size is regulated.

In conclusion the arrangement and expression of junctional proteins is modified in rhombomere boundaries, demonstrating that there is a relationship between epithelial organisation and brain sub-division. Understanding epithelial organisation may help to improve our knowledge of neural tube architecture, for instance modifications of the epithelial surface at rhombomere boundaries may be conserved between species and possibly between other CNS compartment boundaries. Therefore looking for boundary characteristics throughout the CNS may help to map out developmental domains and improve our understanding of brain compartmentation.

## *Chapter 1.8: Gap junction connectivity and calcium activity in neurogenesis*

Gap junctions are channels that allow the passage of ions and second messengers between cells. They are expressed throughout the embryo and adult and play important roles in generating and maintaining developmental compartments. In this next section I will outline their structure, expression and ability to create developmental groups of cells. In section 1.9, I will explain how neuromeric theory may require segmentally regulated gap junctional coupling in order for compartmentation to be effective.

### Gap junction structure

Gap junctions are the primary channels employed by the embryonic vertebrate CNS to electrically and chemically couple cells. They are predominantly located at the intercellular junctions of epithelial cells, in a slightly more basal position with respect to tight and adherens junctions (For a review, see Dermietzel, 1998; Giepmans, 2004). Gap junctions coalesce into plaques that vary in size. Some large plaques can contain over 1000 individual gap junctions channels. A single gap junction channel is composed to two docked connexons, which are transmembrane hexamers (fig. 1.6A). Connexon subunits are called connexins, which assemble into a barrel formation with a central pore region (Unwin and Zampighi, 1980). Connexons can also function as unopposed hemichannels which act as gated pores connecting a cell's cytoplasm to the extracellular space (reviewed in Evans et al., 2006). The channel created between the two opposed cells or a connexin hemichannel can be either in an open or closed conformation, depending upon the phosphorylation state of the channel proteins, intracellular pH or calcium ion concentration. For example, activation of protein kinase C (PKC) results in Connexin phosphorylation and a decrease in intercellular connectivity. This action is context dependent, because under certain conditions, PKC activation can actually increase gap junction communication (Reviewed in Houghton, 2005). There are at least 20 mammalian and 37 zebrafish connexins, which are named according to their predicted molecular weights. This nomenclature can create confusion because functionally equivalent connexins in different species may not have the same molecular weights and so have different names. For example, zebrafish Cx28.8 and Cx27.5 are orthologues of mammalian Cx25 and 26 respectively (Dermietzel et al., 2000; Eastman et al., 2006). A connexon may be homomeric (composed of 6 identical connexins), or heteromeric (composed of a mixture of connexins). Gap junctions can be composed of

two identical homomeric connexons (homotypic), or of two different connexons (heterotypic).

## Gap junction conductance depends upon subunit composition

The composition of connexons dictates their function, since gating properties and conductance differs between connexins (for an extensive summary of connexin diversity see Eastman et al., 2006). For example, mammalian Cx46 hemichannels expressed in *Xenopus* oocytes maintain an open conformation resulting in the oocyte swelling and eventual cell death, unless the cell is kept in a high external concentration of calcium. On the other hand it is possible to express mammalian Cx26 under normal conditions with no ill effects upon the oocyte (Saez et al., 2005). Mammalian Cx43 has a larger pore than Cx45 and so allows the passage of more current and also a greater number of small molecular weight dyes than Cx45 (Elfgang et al., 1995). Heteromeric channels too have different electrochemical properties than their constituent connexins, since a homotypic gap junction composed of rodent Cx32 is permeable to both cGMP and cAMP, while a heterotypic channel containing Cx32 and Cx26 subunits is less permeable to cAMP than cGMP (Bevans et al., 1998). Connexons vary in their affinity for each other. Mammalian Cx43 and Cx46 can create heterotypic gap junctions with many other connexins, while Cx40 only couples with itself (Dermietzel, 1998). Heteromeric gap junctions allow for asynchronous coupling, so that if cell A expresses connexons with less voltage sensitivity than cell B, the current passing through the heterotypic gap junction will be different depending upon whether cell A or cell B is depolarised (Dermietzel et al., 2000). Asymmetric gap junction coupling has been observed in the new born rat neocortex. Intracellular injection of a gap junction permeable dye into astrocytes often resulted in a labelled cluster of cells containing NeuN expressing neurons. However if a NeuN expressing neuron was targeted, astrocytes were not included in the cluster of labelled cells (Bittman et al., 2002). At this stage of development, rat neurons express Cx36, Cx26 and Cx43 in varying combinations, while astrocytes express Cx43 and Cx26. Thus their different expression of connexins may explain their asynchronous coupling (Bittman et al., 2002). The diversity of connexins and their different gating properties and conductance can be employed by the embryo to coordinate intercellular communication in a number of different ways.

## Connexin expression and coupling in the neuroepithelium

Connexins are expressed throughout the embryonic CNS. Cx26 is present at all levels of the rodent neocortex during early neurogenesis, but eventually becomes down-regulated (Nadarajah et al., 1997). Cx43 is prevalent throughout the life of all organisms studied (rat, human, mouse, zebrafish, carp, turtle) and is primarily found in undifferentiated cells and glial cells, however there is some evidence that it may also be present in at least some neurons, since it has been detected in amacrine cells of the zebrafish retina (Janssen-Bienhold et al., 1998; Nadarajah et al., 1997). During rodent neurogenesis, Cx43 is expressed only in the VZ, indicating that post-migratory cortical neurons do not express this Connexin, while Cx32 and Cx36 are expressed only in neurons (Bruzzone and Dermietzel, 2006; Elias et al., 2007; Nadarajah et al., 1997). As neurogenesis progresses there is a shift from expression of Cx26 towards Cx32 as progenitor cells progressively differentiate in to neurons and neurons mature (Nadarajah et al., 1997). In the zebrafish, Cx27.5 and Cx55.5 appear to be restricted to neuronal cells and Cx35 and Cx52.6 are only expressed in the retina. Cx55.5 and Cx52.6 have been localised to a subset of horizontal cells in the inner nuclear layer of the retina, suggesting a highly specialised function for these connexins (Dermietzel et al., 2000; McLachlan et al., 2003; Shields et al., 2007). Expression of a broad range of Connexins in the embryonic CNS suggests that coupling between cells is prevalent. This will be discussed below.

### Gap junction coupling between neural progenitors

Neural progenitors display dynamic patterns of gap junction connectivity. In embryonic rat cortex, clusters of up to 25 neural progenitors have been detected by dye injection. These clusters appeared as columns spanning the ventricular zone in a manner reminiscent of the cortical columns seen in the adult cortex (Bittman et al., 2002). Smaller clusters have also been detected in the VZ of the embryonic mouse cortex. The majority (84%) of clusters contained a single radial process and around 25 cells arranged into a column (Lo Turco and Kriegstein, 1991). Likewise intracellular injection of biocytin or Lucifer yellow into chick hindbrain neuroepithelial cells labelled approximately 20 cells (Martinez et al., 1992). BrdU incorporation experiments were carried out with different survival times in order to establish if gap junction coupling was regulated during the cell cycle. No mitotic cells were found in clusters, while proportionally fewer newly born cells were in clusters compared with the proportion of newly born cells in the population. Thus M and G1 phase cells are less likely to be coupled than at other stages in the cell cycle (Bittman et al., 1997). Blockade of gap

junctions with halothane or octanol dramatically reduced proliferation in E16 mouse cortical slices suggesting that progenitors must be coupled in order to coordinate their developmental programs (Bittman et al., 1997). Ventricular zone progenitors in slice or explant culture generate large calcium waves, which require connexins in order to be generated. However the evidence suggests that ATP release via connexin hemichannels is the wave initiation signal and since gap junction blockers also cause connexin hemichannels to close, calcium wave initiation may not occur through gap junctions (Weissman et al., 2004). It is still possible, however that propagation, rather than initiation of calcium waves requires gap junction function to some degree (Weissman et al., 2004).

**Gap junction coupling between neurons**

The neuronal communication compartment was discovered by gap junction permeable dye injection, electrophysiology and calcium imaging experiments. The extent to which neurons are coupled seems to vary as much due to which experimenter carried out the procedure and the technique employed as to the actual connectivity of the cells. The first evidence for neuronal connectivity came in 1983, through the injection of gap junction permeable dyes and electrical recordings from rat neocortex (Connors et al., 1983). Coupling was strongest from P1-4, with 70% of cortical neurons coupled in groups of 3-7 cells. The percentage of coupled cells in and the number of cells in each cluster decreased steadily until 20% of neurons were coupled in pairs at P14. Cluster size appeared to be far larger according to Peinado and colleagues, who labelled clusters of up to 90 neurons in P5 rats (Peinado et al., 1993). However this may have been the result of inadvertently injecting dye into more than a single cell, since experiments where the experimenters were sure they had targeted a single cell, resulted in clusters of 21-35 cells (Peinado et al., 1993). Despite differences in observed cluster size, the researchers agreed that clustering dramatically decreased as the cortex matured, until very few clusters were detected at P14 and none were found at P16 (Peinado et al., 1993). An alternative delivery system also produced similar findings. A gene gun was used to ballistically deliver gap junction permeable dyes into mouse cortical slices. At P0 32% of pyramidal neurons were coupled, while this number increased to 86% by P7 (Bittman et al., 2004). Taken together, these results suggest that coupling between cortical neurons is initially low, and then it increases from birth until the end of the first week after birth and finally decreases in the second week. This phenomenon has also been observed in ventral motoneurons in neonatal rat and *Xenopus* spinal cord (Chang

et al., 1999; Spitzer and Gu, 1997). In rat spinal cord, 74% of all cells are electrically coupled in the first two days before birth, while none are after P7. This change in coupling was accompanied by a down-regulation of Cx40 and Cx45, while treatment with halothane, an inhibitor of gap junction function blocked electrical coupling between spinal motoneurons (Chang et al., 1999).

Therefore in both the cortex and spinal cord gap neurons are organised into functional groups during circuit formation and maturation. Neurons coupled by gap junctions are coactive groups, because calcium imaging revealed columnar 50-120μm domains in the developing cortex that were abolished in the presence of gap junction inhibitors (Yuste et al., 1995; 1992) and *Xenopus* spinal motoneurons also group together in coactive clusters while they mature (Spitzer and Gu, 1997). It is important to note that neurons are coupled during synapse formation, suggesting that gap junction coupling is necessary for this process, but not afterwards. While the calcium imaging studies could not provide direct evidence for it, the data suggest that the cortical columns of synaptically connected neurons are generated from the coupled neurons (Yuste et al., 1995; 1992).

**Heterogeneous populations of coupled CNS cells**

Studies on cell-cell coupling have revealed that certain types of cells are able to form functional gap junction channels with cells of different types. For example the retinal pigment epithelium and the neuroblastic retina are heavily connected by gap junctions (Yuste et al., 1995; Yuste et al., 1992). Within the cortex, over 25% of all injected pyramidal neurons were coupled with GABAergic interneurons in P7 rats (Tibber et al., 2007). Perhaps more surprising was the discovery that pyramidal neurons and glia also can form gap junctions, since almost 60% of dye injected astrocytes were clustered with neurons, however very few astrocytes were labelled when pyramidal neurons were injected (Bittman et al., 2002). This result suggests that there is one-way traffic of metabolites and messengers from astrocytes into neurons.

In summary, both neurons and progenitors express Connexins that assemble into gap junctions during neurogenesis. Coupling through gap junctions is dynamic during development and changes in coupling reflect changes in expression of Connexins.

## Gap junction function during neurogenesis

Gap junctions appear to be necessary for embryonic CNS cells to proliferate at the correct rate. For example, an anti-Cx43 gel, when applied to the retina, resulted in decreased proliferation (Tibber et al., 2007). This agrees with experiments carried out on embryonic mouse cortex, where gap junction blockade with halothane or octanol significantly reduced the number of cells that incorporated BrdU (Bittman et al., 1997). The link between connexins and proliferation is made stronger by evidence that Cx43 is over-expressed in E18 albino rat retinas, which along with a lack of pigmentation also over-proliferate. Exogenous application of L-DOPA, the precursor to dopamine, both decreased Cx43 expression and mitosis (Tibber et al., 2007).
A channel independent role for Connexins in neurogenesis was recently discovered. Cx43 is expressed on radially migrating immature cortical neurons where they contact the processes of radial glia (Nadarajah et al., 1997). Genetic ablation of either Cx43 or Cx26 severely reduced the number of neurons that migrated from the ventricular zone to the cortical plate in embryonic rat cortex (Elias et al., 2007). The migration mechanism is independent of channel function since rescue of the migration phenotype was achieved through introduction of connexins capable of docking to form gap junctions, but unable to form functional channels. The mechanism appears to be cell-cell adhesion because control cultures of cortical neurons were more adhesive than cells with Cx43 knocked down. Therefore it appears that gap junctions are used by radially migrating neurons to adhere to the glial scaffold, allowing them to translocate towards the cortical plate (Elias et al., 2007).

## Calcium activity during neurogenesis involves gap junction mediated calcium waves and is required for proliferation, migration and differentiation

Calcium ions are one of the most ubiquitous second messengers in the body and they mediate a plethora of cellular events, from muscle contraction to cell division. During neural development, calcium signalling has been suggested to be important for numerous processes, including neuronal migration (Komuro and Rakic, 1996), cell division, proliferation (Weissman et al., 2004), neuronal differentiation (Gu and Spitzer, 1995), segmentation (Creton et al., 1998; Webb and Miller, 2003b), and neural induction (Leclerc et al., 2000; Moreau et al., 1994).

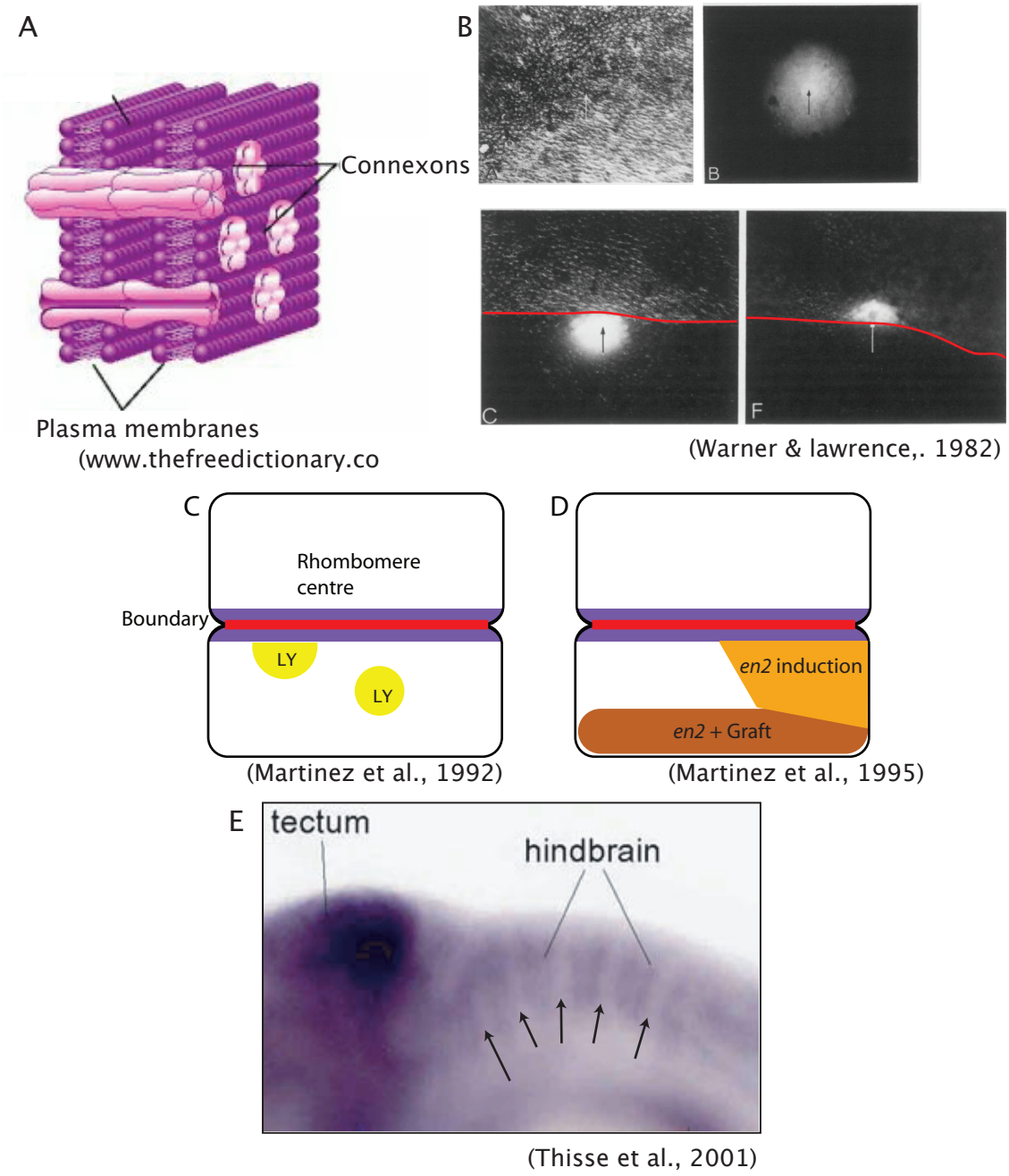


Fig. 1.6. Gap junction communication and developmental compartments
A). Schematic of gap junctions between two cells. Connexons, composed of 6 connexins, are expressed in the plasma membrane. Connexons in neighbouring cells dock. Their central pore allows the exchange of cytosol, ions and small molecular weight messengers.
B). Images of some of the first experiments to show restriction of intercellular communication between segments. *Oncopeltus* epidermal cells were injected with Lucifer yellow in the centre of a segment (top). Bright field image is to the left of the fluorescence image. Dye spread in a concentric pattern. Dye injected in to the edge of an Oncopeltus epidermal segment (bottom), did not cross the segment border.
C). Schematic of a chick hindbrain boundary. When Lucifer yellow (LY) is injected into rhombomere centres, circular patterns of intercellular dye transfer occur. When injected close to rhombomere boundaries, the dye does not cross into the neighbouring rhombomere.
D). Illustration of an *en2* expressing quail midbrain graft inducing *en2* expression in the host chick alar plate up to the rhombomere boundary, which prevents further induction.
F).Lateral view of a 24hpf zebrafish hindbrain. Anterior is left. *Cx43.4* mRNA is expressed in the hindbrain VZ, but absent from rhombomere boundaries (arrows).
LY: Lucifer yellow, *en2: engrailed 2*

Intercellular calcium waves require functional gap junctions and/or connexon hemichannels in order to be propagated through a tissue. For example neurons that produced calcium transients co-actively were coupled by gap junctions and gap junction blockade eliminated their connectivity (Yuste et al., 1995; 1992).

**Calcium activity in neural progenitors**

Both neurons and progenitors have been shown to spontaneously generate calcium transients and intercellular calcium waves during proliferation and differentiation in rodents, *Xenopus* and zebrafish (e.g. Gu and Spitzer, 1997; Owens and Kriegstein, 1998; Zimprich et al., 1998). Three patterns of calcium activity in the ventricular zone of embryonic rat cortical slices were reported: transients produced by individual cells, transients generated by pairs of daughter cells located at the ventricular surface and calcium waves that propagated through up to 35 cells at a velocity of 6-8μm/s (Owens et al., 2000; 1998; Weissman et al., 2004). The function of individual or paired transients was not elucidated, yet they may be analogous to the cytokinesis transients seen in early embryos (Fluck et al., 1991). Intercellular calcium waves appeared to be correlated with the rate of neuronal proliferation. The size of electronically stimulated calcium waves mirrored the rate at which neurons were generated between E14-E16. The signalling mechanism that was required for the propagation of calcium waves was determined to include ATP released by connexin hemichannels and IP3 gated ER stores of internal calcium (Weissman et al., 2004). Intercellular calcium waves dependent upon ATP and gap junctions or connexon hemichannels have also been observed in the chick (Pearson et al., 2004). Calcium waves have been observed in the retinal pigment epithelium (RPE), the neural retina and between the two tissues (Pearson et al., 2004; Pearson et al., 2005). Retinas with the RPE removed still produced calcium waves but to a lesser degree than retinas with the RPE intact (Pearson et al., 2004). The function of these ATP dependent calcium waves was to stimulate cell division and proliferation in the neural retina and cortical VZ (Lin et al., 2007; Pearson et al., 2005; Whitaker, 2008; 1990). In a study of mammalian retinal development VZ calcium waves were triggered by waves in the inner retina, providing the first evidence that neurons could communicate with neuronal progenitors via a retrograde signalling mechanism (Syed et al., 2004). This phenomenon suggests that a feedback mechanism between neurons and progenitors exists and implies that there is plasticity to the neurogenesis program, rather than a pre-ordained series of genetic events. Intercellular calcium activity is therefore an important process during neural development, however a caveat of these studies is the

possibility that tissue damage caused by dissecting the specimens may have resulted in calcium activity that does not occur in intact specimens. There is a body of evidence showing that physical damage to a tissue can induce calcium transients and waves (e.g. Gale et al., 2004; Sanderson et al., 1990). Carrying out similar experiments using the zebrafish may be instructive in uncovering if these calcium waves are produced *in vivo*, because of the transparency of the zebrafish embryo, coupled with its gestation occurring outside of the body of its mother, allows for non-invasive microscopy to be carried out. To study calcium activity, in single cells, during zebrafish neurogenesis fluorescent calcium indicators were injected mosaically into zebrafish embryos in an attempt to overcome their toxicity (Ashworth and Bolsover, 2002). A third of spinal cord neuronal precursors produced calcium transients at low frequency (4-5 transients/hour) (Ashworth and Bolsover, 2002). The mosaic labelling of progenitor cells precluded the detection of intercellular waves. To date intercellular calcium waves with a velocity that exceed 5μm/s have not been detected in intact zebrafish embryos, either because of sparse labelling techniques (Ashworth and Bolsover, 2002), or poor spatio-temporal resolution of the calcium imaging technique (Creton et al., 1998; Webb and Miller, 2003b).

**Calcium activity in neurons**

Neural tissue too requires calcium activity to develop normally. Studies of amphibians (*Xenopus* and salamander) suggest that Noggin based neural induction is dependent on transient increases in intracellular calcium in anterior dorsal cells during gastrulation. (Leclerc et al., 1997; Leclerc et al., 2000; Moreau et al., 1994). Noggin stimulates L-type calcium channels which then allow calcium ion influx from the extracellular space. Buffering calcium with BAPTA, or blocking L-type calcium channels caused a reduction in the expression of neural markers *zic3* and *Gemenin* (Leclerc et al., 2000).

To study calcium activity in neurons during zebrafish neurogenesis fluorescent calcium indicators were injected mosaically into zebrafish (Zimprich et al., 1998), showing that neurons generate spontaneous calcium transients *in vivo* (Ashworth and Bolsover, 2002; Ashworth et al., 2001; Zimprich et al., 1998), mirroring studies carried out in *Xenopus*, (Gu and Spitzer, 1997). Motoneurons must generate these transients in order to differentiate, since buffering calcium transients with BAPTA significantly reduced the number of axons generated by zebrafish spinal neurons (Ashworth et al., 2001). Inhibiting calcium transients also blocked the establishment of the GABA current and maturation of the potassium rectifying current in *Xenopus* spinal motoneurons,

signifying that they were not differentiating into mature motoneurons (Gu and Spitzer, 1997; Spitzer et al., 1995). Neurite extension is also dependent upon calcium activity. Calcium transients occur in growth cones and buffering calcium inhibits their outgrowth (Ashworth et al., 2001; Spitzer et al., 1995). A further requirement for intracellular calcium fluctuations in immature neurons was uncovered in radially migrating cerebellar granule cells. Whether or not a neuron was migrating was strongly correlated with the frequency of calcium transients. Furthermore, transient amplitude dictated migration velocity. Using various pharmacological interventions it was confirmed that the calcium transients do indeed dictate both whether a neuron migrates and its migration speed (Komuro and Rakic, 1996).

The signalling pathways involved in these cellular processes differ, which perhaps explains how a seemingly ubiquitous signal can be interpreted in many ways. Neuronal differentiation appears to occur independently of ryanodine activated calcium stores and classical voltage gated calcium channels; however removal of external calcium disrupted differentiation (Gu and Spitzer, 1997; Spitzer et al., 1995). These findings suggest that the source of calcium required for normal differentiation is from the extracellular space. In neuronal migration, on the other hand, both external calcium and ER calcium stores are important sources for the calcium ions that generate the transients required for cell movement (Komuro and Rakic, 1996).

To conclude, gap junctions are a diverse family of intercellular channels that are expressed in the developing CNS. Progenitors and neurons express gap junctions through which developmental signals, such as calcium ions, can pass. Calcium signalling is a developmentally significant process, required for progenitor proliferation, neuronal migration and differentiation. Therefore coupling and calcium signalling between progenitors and between neurons suggests their developmental programs are coordinated.

## *Chapter 1.9: Segmental regulation of gap junctions may maintain developmental compartments*

An evolutionally conserved property of developmental compartments is reduced gap junction connectivity between neighbouring compartments. This has been observed in a variety of organisms and tissues, including the epidermis of *Oncopeltus fasciatus (Warner and Lawrence, 1982)*, epithelium of blow fly maggots (Warner and Lawrence, 1982) and chick rhombomeres (Martinez et al., 1992) (fig. 1.6.B,C). During development, connexins are expressed in different combinations and at different levels, depending upon cell type and developmental stage. Since, as I mentioned above, connexins vary in their affinities for each other and in their gating and conductance, populations of functional related cells can form coupled groups while excluding cells from outside the group by selectively expressing a unique combination of Connexins. To illustrate: mature neurons are not coupled via gap junctions to the progenitors that produce them, however migrating immature neurons were found in clusters with radial glial cells (Bittman et al., 1997). On a similar note, calcium waves in rat cortical VZ never propagated into cortical plate neurons (Weissman et al., 2004). The significance of reducing gap junctional communication between compartments is currently unclear, but investigations into gap junction function during development have shown that signalling molecules with powerful morphogenetic and patterning abilities can be exchanged between cells via gap junctions. Some of these studies will be discussed below.

### Gap junctions in embryonic patterning

Studies of the requirement for gap junction communication in dorso-ventral patterning and the establishment of left-right asymmetry have provided evidence that morphogens are transferred through gap junctions.

#### Gap junctions in left-right patterning

Inhibition of gap junction communication in early *Xenopus* embryos using peptides raised against a 27kDa rat liver Connexin significantly reduced dye and current transfer between cells. Left-right patterning was disrupted in 63% of the treated embryos and loss of anterior brain structures occurred in 20% (usually from the left hand side), when the antibodies were injected into a single cell at the 8 cell stage (Warner et al., 1984). Heterotaxia of the heart, gut and gal bladder were also caused by disrupting gap

junction communication and this could be induced by artificially inducing increased gap junctional communication in the ventral half of the embryo, or decreased communication in the dorsal half (Levin and Mercola, 1998). A time window for this effect was determined to exist between the 16 cell stage (stage 5) and the end of epiboly (stage 12) (Levin and Mercola, 1998). Organ laterality also appears to be a gap junction dependent process in other vertebrates, because chick and rabbit embryos treated with gap junction inhibitors as late as 2-3 somites often expressed *nodal* ectopically on the right hand side of the lateral plate mesoderm (Levin and Mercola, 1999; Muders et al., 2006). Likewise *nodal* and *shh* expression in surgically manipulated chick embryos was altered in ways to suggest an anti-clockwise flow of a morphogen through gap junctions established left-right asymmetry (Levin and Mercola, 1999). It is relevant to compare these studies with thapsigargin treated zebrafish embryos, which raises cytosolic calcium levels by blocking ER calcium sequestering pumps. Laterality was disrupted in embryos treated with 0.5μM thapsigargin, while tail formation was perturbed in embryos immersed in 1μM thapsigargin. The defects were coincident with a loss of calcium transients and intercellular calcium waves (Creton, 2004; Kreiling et al., 2008; Wallingford et al., 2001); therefore intercellular calcium signalling via gap junctions may be required for laterality to be established normally.

**Gap junctions in dorso-ventral patterning**

Dorso-ventral patterning has also been suggested to require gap junction communication. For example morphogenesis of *Ilanassa obsoleta,* a marine mollusc is a gap junction dependent process. At the 24 cell stage, a single cell organises the embryo, instructing the formation of the dorso-ventral axis. Blockade of gap junction function at this stage prevented mitogen associated protein kinase activation, which is essential for the organiser to function. The result was disrupted dorso-ventral patterning (Nakamoto and Nagy, 2006). UV irradiation of 1 cell stage *Xenopus* embryos resulted in both reduced dye transfer between dorsal cells in the 32 cell stage embryo and loss of future dorsal structures (Nagajski et al., 1989). The converse experiment, where Lithium chloride was used to duplicate the body axis by converting the ventral side of the embryo to a dorsal fate, was also accompanied by an increase in intercellular communication between the usually relatively isolated ventral cells (Nagajski et al., 1989). This effect was then shown to be related to the Wnt signalling pathway. Over-expression of Wnt1 or Xwnt8 in *Xenopus* embryos caused an increase in functional gap

junctions in the ventral half of the embryo (assayed by Lucifer yellow injections) and ultimately to a duplication in the body axis (Olson et al., 1991).

In conclusion gap junctions are important components of developmental pathways, acting as conduits through which signals transfer between cells to coordinate and instruct development in large groups of connected cells.

## Gap junction expression and coupling is segmentally regulated in chick rhombomeres

I have described how gap junction communication can be employed to coordinate developmental processes within groups of cells or tissues. An implicit property of this form of communication is that cells which follow different developmental programs form separate communication groups. I will now discuss this knowledge of gap junctions in relation to the neuromeric model and suggest that rhombomeres and perhaps other embryonic CNS subdivisions use gap junctions to enforce their compartmentation. Ventricular zone cells are coupled via gap junctions, yet there is segmental regulation of this coupling. For example, intracellular injection of Lucifer yellow, a gap junction permeable dye, into a single chick hindbrain neuroepithelial cell resulted in a group of labelled cells (Martinez et al., 1992). If the injection site was the centre of a rhombomere, a round cluster of labelled cells resulted, with the injected cell at the centre (Martinez et al., 1992). However an injection at or near to a rhombomere boundary produced a D shaped cluster of cells (Martinez et al., 1992). Dye could diffuse into neighbouring cells on the same side of the rhombomere boundary, but could not cross the boundary into cells on the other side, while electrical coupling was not interrupted at rhombomere boundaries (Martinez et al., 1992). In a later experiment, grafts of *en2* expressing quail midbrain were placed in chick hindbrain. *En2* was induced in the alar plate of the host tissue up to rhombomere boundaries, but not beyond (Martinez et al., 1995). This study did not demonstrate that induction was via gap junctions, however it is tempting to speculate that it was, due to the similar pattern of dye coupling in the hindbrain.

### Decreased gap junction expression in boundaries may be the cause of decreased communication across rhombomere boundaries

One can envisage two strategies that could be employed to prevent communication between different rhombomeres; either for the populations to express different combinations of connexins that do not permit coupling between the populations (as

occurs with neurons not being coupled to progenitors), or for a connexin free zone to lie between the two rhombomeres. In the case of the hindbrain it appears that rhombomeres use the latter in order to prevent communication between adjacent segments. There is little evidence that suggests different connexins are expressed in different segments. Cx31 is expressed in rhombomeres 3 and 5 from E8-E11 (3 - 15 somites) in mouse embryos, under transcriptional control of Krox-20; while it is expressed in rhombomere 4 from E10.5-11.5 (Jungbluth et al., 2002). It is restricted to the lateral most quarters of r3 and r5 and to neural crest cells, while the r4 expression is restricted to a sub-population of cells in the ventral hindbrain and floor plate, which the authors of the study suggested were migrating vestibulo-acoustic efferent neurons (Jungbluth et al., 2002). *Cx43* expression in murine hindbrain progenitors is partially consistent with segmental regulation of gap junction communication. At E10.5 it is expressed in a continuous stripe from r2 back into the spinal cord, in a thinner lateral stripe from r3 to r6 and diffusely in r6 and r7 (Jungbluth et al., 2002). This is not the case in the zebrafish hindbrain, as *cx43* mRNA has only been detected in two transverse bands, one rostral to and the other caudal to the midbrain-hindbrain boundary. When GFP was driven by the mouse promoter for Cx43 in zebrafish, it was detected in the hindbrain during neurogenesis, suggesting that the regulation of Cx43 is different in teleost fish than in mammals (Chatterjee et al., 2005). The spatial pattern of expression, accompanied by the short duration of Cx31 expression and a lack of segmental *connexin* expression in the remaining rhombomeres, suggests that segmental expression of connexins is not the primary way communication is inhibited across rhombomere boundaries. However other members of the connexin family may be expressed in different spatial patterns that, in combination with Cx43 and Cx31 could ensure rhombomeres are developmental compartments.

There is evidence that a Connexin free zone exists between rhombomeres because *Cx43.4* mRNA expression is absent from zebrafish rhombomere boundaries (Thisse, 2001) (fig. 1.6D). This corresponds with EM data which shows intercellular junctions (which includes gap junctions) have a smaller apico-basal width in boundary regions than non boundary regions (Heyman et al., 1993). The mechanism behind creating this connexin free zone may be Eph-Ephrin interactions. Populations of cells expressing the same combination of Eph and Ephrins form functional gap junctions, while populations with different Ephs and Ephrins do not (Mellitzer et al., 1999) since Ephs and Ephrins are expressed in alternating patterns in the hindbrain, each interface between rhombomeres is therefore a site where altering populations of Ephs and Ephrins interact.

Since *Cx43*.4 mRNA is absent from boundaries, it is possible that bidirectional Eph-Ephrin signalling may potentially regulate gap junctions at the level of transcription, however there is currently no evidence to support this hypothesis.

The interaction between Ephrins and connexins has recently been suggested to be the underlying problem that causes craniofrontonasal syndrome in humans. In this X linked disease, the cranial bones do not successfully fuse together to form a continuous sheet of bone, which is called a calvarial defect. It is caused by a mutation in the *ephrin B1* gene and the syndrome occurs in female heterozygotes, while homozygotes and males possessing one single mutant *ephrin B1* gene to not have the defect. *Ephrin B1* heterozygous mice show random inactivation of each copy of the gene, thus a mosaic of e*phrin B1* expressing and non-expressing cranium cells exist. This heterogeneous population of cells caused repulsive rather than attractive interactions, down regulation of Cx43 and ultimately to calvarial defects. Experimental over-expression of Cx43 in heterozygous mice could partially rescue the phenotype (Davy et al., 2006). Zebrafish Cx43.4 is a functional orthologue to mammalian Cx45 and its down-regulation as a direct consequence of Eph-Ephrin mediated repulsion has not been demonstrated. However its absence from rhombomere boundaries, a site of repulsive Eph-Ephrin interactions suggests that it is. It will be interesting to learn if other CNS segments also inhibit intercellular communication in this fashion. It is first necessary to confirm if small molecular weight dyes behave in the same manner when injected into zebrafish hindbrains as in the chick, then the experiment can be repeated in other regions to test this possibility.

Since there appears to be segmental regulation of gap junction expression and connectivity the exchange of second messengers, such as calcium ions, through gap junctions should also be compartmentalised. Segmental regulation of calcium signalling within the embryonic CNS may have important developmental effects. At present there is little evidence for compartmentalised calcium activity during neurogenesis. Since VZ calcium waves require functional gap junction hemichannels (and possibly gap junctions) and *cx43* mRNA is not expressed in zebrafish rhombomere boundary cells (Thisse, 2001), calcium signalling may occur within individual rhombomeres but not between them. The rate of neuronal production could therefore be controlled separately in each rhombomere without interference from the activity within neighbouring rhombomeres.

## *Chapter 1.10: Calcium activity and gap junction connectivity in the blastocyst*

The blastula stage is the first developmental period when a requirement for intercellular communication becomes apparent and is therefore the simplest stage to study intercellular communication (Webb and Miller, 2003a). In the zebrafish, the blastula stage commences at the end of the 64 cell stage, where for the first time cells become completely cleaved following cell division. It lasts for 3-4 cell cycles, until the 512-1024 stage when the mid blastula transition begins and epiboly commences (Kane and Kimmel, 1993; Kimmel et al., 1995). At the 64 cell stage blastomeres sit in a group of cells that cover roughly half of the large yolk cell. They are arranged in an oblong, 8 cells long, 4 cells wide and 2 cells deep (fig. 1.7A). As blastomeres divide, the number of cell layers increases to produce a dome shaped cluster with radial symmetry (Kimmel et al., 1995).

During the blastula period two important developments occur: First, the outer layer of cells flatten as they develop into an epithelium called the enveloping layer (EVL), a transient structure that helps to maintain the integrity of the embryo before the epidermis proper is produced. Second, the cells adjacent to the yolk form the yolk syncytial layer (YSL) (Kimmel and Law, 1985a; Kimmel and Law, 1985b). The YSL develops in the $10^{th}$ cell cycle and is formed by the subset of blastomeres that lie at the margin of the blastocyst, in contact with the yolk. The marginal blastomeres flatten and do not cleave following nuclear division (Kimmel and Law, 1985b). The product is 3 identifiable populations of cells: the EVL, the YSL and deep blastomeres located between the other two groups. The EVL and deep blastomeres are not lineage restricted groups because fate mapping always produced a population of mixed deep and superficial cells (Kimmel and Law, 1985c). Likewise the progeny of marginal blastomeres include a mixture of cells in the YSL and deep blastomeres (Kimmel and Law, 1985b). Blastomeres are relatively immotile during the blastula stage as evidenced by a lack of motile structures called pseudopods and by lineage tracing experiments (Kane and Kimmel, 1993; Kimmel and Law, 1985c). Clones of an individual cell from the 32 or 63 cell stage remained tightly clustered throughout the blastula period and only dispersed once epiboly began during the MBT (Kimmel and Law, 1985c).

Cell divisions are metasynchronous during the blastula stage of zebrafish development (Kimmel et al., 1995), meaning they are closely, but not perfectly aligned. Blastomeres divide in a wave with those at the animal pole dividing first and marginal blastomeres divide last (Keller et al., 2008).

This relationship breaks down during the mid blastula period (MBT), when cell cycles lengthen but in no discernable pattern, so that the near synchrony of cell cycle timing is lost (Kane and Kimmel, 1993; Kimmel and Law, 1985a).

There is currently no explanation for the reason why blastomeres divide in this fashion in zebrafish. Gene expression is uniform, as is the concentration of intracellular calcium (Reviewed in Webb and Miller, 2006) and IP3 (Reinhard et al., 1995). Blastomeres are coupled by gap junctions (Reviewed in Houghton, 2005; Kimmel and Law, 1985a), so intercellular communication is possible at this stage, suggesting that calcium waves or other signalling molecules may propagate through blastomeres to organise their cell cycles.

## Mitotic waves in other developmental systems

The zebrafish blastocyst is not the only developmental system where waves of mitoses occur. A large number of mitotic domains in the *Drosophila* gastrula, arranged with bilateral symmetry have been observed. The number of cells within each domain varied, but in all, a 'trigger cell' initiated a wave of mitoses that propagated to the edges of the domain (Foe, 1989). There appeared to be developmental significance to these mitotic domains; first because the location of primordial larval structures corresponded to different mitotic domains and second, cells within each domain had morphologies in common with each other, but not with nearby cells outside of the domain (Foe, 1989).

A wave of mitoses that swept from posterior to anterior in the *Drosophila* eye imaginal disc during neural differentiation have also been observed. Anterior to the wave, cell cycles were random. The wave front appeared as an indentation, within which the cell cycles of all epithelial cells were synchronised to G1 phase. Posterior to the wave, cells either differentiated into neurons, or continued to proliferate for one more cell cycle (Thomas et al., 1994). Interfering with cell cycle progression in the eye disc also disrupted neuronal differentiation, suggesting that in some contexts, regulation of the cell cycle is an essential developmental requirement (Thomas et al., 1994).

Therefore it is possible that a group of cells that differentiate together coordinate their cell cycles and behaviour during the differentiation phase. This suggests that the near

synchrony of cell cycles in the zebrafish blastula may be important for ensuring the embryo executes its developmental program correctly.

## Gap junction expression during the blastula stage

The role that gap junctions play during the blastocyst stage of embryonic development is currently unclear. Functional gap junctions are expressed in blastulas of all vertebrates studied, including human, mouse, zebrafish and bovine embryos (Essner et al., 1996; Guthrie, 1984; Hardy et al., 1996; Lo and Gilula, 1979a; Lo and Gilula, 1979b; Wrenzycki et al., 1996). *Cx43.4* is expressed at low levels in the zebrafish blastula and when Cx43.4:GFP was expressed in blastocysts, gap junctions assembled at the interfaces between blastomeres, indicating that gap junction based intercellular signalling can occur at this stage of development (Essner et al., 1996). *Cx43* is also expressed in zebrafish at this developmental stage, however its expression is restricted to deep blastomeres (Chatterjee et al., 2005). Dye transfer experiments found that there is extensive coupling between blastomeres throughout the blastocyst stage and that coupling exists between the yolk and marginal blastomeres until the YSL is fully formed (Kimmel and Law, 1985a; Kimmel and Law, 1985b). This coupling is via both gap junctions and cytoplasmic bridges between incompletely cleaved cells initially, however the number of cells with cytoplasmic bridges decreases throughout the blastocyst stage (Kimmel and Law, 1985a). Thus it is possible that calcium waves or other organising factors propagate through zebrafish blastomeres via gap junctions.

In *Xenopus*, four connexins are known to be expressed in blastulas, which are Cx30, Cx38, Cx41 and Cx43 (Landesman et al., 2003). Nine connexin proteins are expressed in mouse blastocysts, which are Cx30, Cx31, Cx36, Cx43, Cx45, Cx57, Cx30.3, Cx31.1 and Cx40. The former 6 are expressed first at the 2-4 cell stage, while the latter 3 from the 8 cell stage (Becker et al., 1995; Davies et al., 1996). Few studies of human blastocysts have been carried out, but Cx43, Cx26, Cx32 and Cx45 have been detected from the 4 cell stage (Hardy et al., 1996). Cx43 expression is absent from IVF bovine embryos, but present in *in vivo* fertilised ones (Wrenzycki et al., 1996). In mouse embryos, gap junctions first become functional at the onset of compaction (blastocyst formation), which occurs towards the end of the third cell cycle. Connexins are expressed in mouse embryos prior to compaction, but do not form functional gap junctions. For example the phosphorylation state of Cx43 prohibited formation of functional gap junctions before compaction started at the 8 cell stage (Ogawa et al., 2000). This has been confirmed by electron microscopy, electrophysiological recordings

and gap junction permeable dye injection (Lo and Gilula, 1979a; Lo and Gilula, 1979b). Prior to this, sister cells are often interconnected by cytoplasmic bridges due to incomplete cleavage (Lo and Gilula, 1979b). Inner cell mass (ICM) cells (that grow to become the embryo proper) and trophoblast cells (which become the placenta) are initially heavily coupled. Coupling between the ICM and trophoblasts diminishes, followed by loss of trophoblast to trophoblast coupling, while regions within the ICM itself become selectively coupled (Lo and Gilula, 1979a; Lo and Gilula, 1979b).

## Dye transfer through gap junctions in early Xenopus embryos suggests dorso-ventral differences in connectivity

Evidence suggests that there may be a dorso ventral gradient of connectivity in early *Xenopus* embryos. Studies of intercellular dye transfer between the 16 cell stage and the early blastula have proved controversial though. Early studies discovered that cellular connectivity increased during this time period (Guthrie et al., 1988). At the 16-32 cell stages, cells in the dorsal half of the blastocyst were more likely to be interconnected than ventral cells when Lucifer yellow or fluorescein were injected, but both sides appeared equally connected when the smaller sized lead EDTA was injected instead (Guthrie et al., 1988; 1984). This finding suggested that there was ubiquitous expression of Connexins that form gap junctions with relatively small pores compared with dorsal expression of Connexins that form gap junctions with larger pores. The nature of intercellular connectivity became more complex at the 64 and 128 cell stages. No dorso-ventral differences were detected, but dye transfer was more common between the injected cell and its radial neighbours than to its lateral neighbours (Guthrie et al., 1988).

These findings were then countered by the suggestion that dorso-ventral differences in Lucifer yellow and fluorescein dye transfer were optical effects and actually no dye transfer occurred. Dye injected cells and their neighbours produced a lens effect whereby cells containing no dye appeared to be fluorescent. Pigmentation is stronger in the ventral half than in the dorsal half and so prevented the lens effect (Landesman et al., 2000). The authors of this study then provided evidence that gap junction coupling is even throughout the embryo because neurobiotin transfer was not dependent upon the injection location and that connectivity steadily increased from the 16 to 128 cell stage (Landesman et al., 2000).

While there is some credence to the claim that optical effects can make dye transfer appear to be more extensive than it truly is, the authors did not explain how anti connexin antibody injection can reduce the optical flare effect, since injection of such antibodies was shown to reduce both dye transfer and electrical connectivity between dorsal cells (Warner et al., 1984). The authors also claimed that Lucifer yellow did not transfer between cells after fixation and sectioning, which, by their own admission could have severely depleted the amount of dye remaining in the tissue after processing (Landesman et al., 2000). Therefore it is still possible that gap junctions exist that allow the passage of relatively large gap junction permeable dyes such as Lucifer yellow, but that optical effects may cause this dye transfer to appear more extensive than it actually is.

As mentioned in section 1.8, manipulation of gap junction expression to either increase gap junction communication in the ventral half or decrease connectivity in the dorsal half caused heterotaxia in *Xenopus* embryos (Levin and Mercola, 1998). The time window within which intervention could disrupt axial patterning was between the 16 cell stage and the end of gastrulation, so it is unclear whether this highlights a requirement for graded connectivity during the blastocyst stage of development, or during gastrulation, which follows. These studies have been discussed to highlight the fact that interpreting gap junction connectivity experiments is difficult and that caution is needed when doing so.

## Gap junction function in blastocysts

The presence of functional gap junction in blastocysts suggests they play important roles during this developmental stage, however studies of the function of gap junctions during the blastula stage have not provided much insight into the role or requirement for gap junction communication during the blastula stage of development (Reviewed in Houghton, 2005). The effect upon blastocyst development varied depending upon the technique employed to disrupt gap junction communication, which will be described in more detail below.

### Connexin mutants successfully complete the blastocyst stage

Individual *connexins* appear to be expendable for the blastula stage. Genetic ablation of Cx32, Cx43, Cx45, Cx36, Cx37, Cx40 Cx31, Cx30 and Cx46 did not significantly disrupt the blastula stage of mouse or zebrafish development (De Sousa et al., 1997; Gong et al., 1997; Guldenagel et al., 2001; Houghton, 2005; Houghton et al., 1999;

Iovine et al., 2005; Kumai et al., 2000; Nelles et al., 1996; Plum et al., 2001; Simon et al., 1997; Simon et al., 1998). Mice homozygous for *cx31.1*$^{-/-}$ are born in 30% lower proportions than predicted by Mendelian genetics and are reduced in size compared to their littermates. The developmental defect arises in the blastula, however placenta formation was the cause for this defect rather than defects in the embryo proper (Zheng-Fischhofer et al., 2007). Likewise placenta size is decreased in *cx31*$^{-/-}$ mice but no blastocyst defects were found (Plum et al., 2001).

Cx43 deficient mice blastomeres show severely reduced coupling when tested with Lucifer yellow or 6-carboxyfluorescein, however they appeared to develop normally during the blastula stage. Cx43 was not expressed in 30% of wild type gap junctions and intercellular exchange of 2´7´dichlorofluorescein in *cx43*$^{-/-}$ blastocysts revealed that functional gap junctions (probably Cx45) still existed in the mutant blastocysts (De Sousa et al., 1997). Therefore it is possible that the expression of remaining Connexins in the mutant blastocysts was sufficient to exchange the signals essential for blastocyst development, suggesting redundancy in Connexin function.

**Decompaction of mouse blastomeres suggests an adhesive role for gap junctions**

The experiments that produced the most informative results regarding gap junction function in mammalian blastocysts came from inhibiting communication in single blastomeres. Injection of gap junction blocking antibodies into a single mouse blastomere severely reduced both electrical and dye coupling. This blockade caused the injected cells to decompact and to be excluded from further development (Becker et al., 1995; Lee et al., 1987). A similar phenotype occurred in mice heterozygous for DDK, a severe, early lethal affliction with a 5-10% survival rate. Blastocyst at the 16 cell stage contained varying numbers of extruded cells, while dye transfer between blastomeres was significantly reduced (Buehr et al., 1987). The pH in heterozygous DDK blastocysts was lower than control embryos, which appeared to be the cause for decreased connectivity, because dye coupling was rescued by increasing pH (Buehr et al., 1987; Leclerc et al., 1994). Improving intercellular communication in this manner prevented blastomere extrusion, however long term survival was not rescued (Buehr et al., 1987). Manipulation of pH demonstrated that gap junction loss is a symptom, rather than cause of the DDK defect because artificially reducing pH in normal embryos reduced dye coupling junctions and caused blastomere decompaction (Buehr et al., 1987; Leclerc et al., 1994). The mechanism behind decompaction of the inhibited blastomeres may not simply be reduced communication because the size of gap junction

plaques were reduced in antibody injected blastomeres, DDK heterozygotes and pH reduced embryos. Gap junction localisation was reduced from large plaques distributed around the cortices of blastomeres to small puncta, indicating that gap junction assembly or maintenance was disturbed (Becker et al., 1995; Buehr et al., 1987; Leclerc et al., 1994; Lee et al., 1987). Gap junctions have been shown to promote cell-cell adhesion (Elias et al., 2007), so decompaction may have arisen from decreased adhesion, rather than reduced intercellular communication. Therefore there appears to be a correlation between cell health and gap junction connectivity.

A complimentary observation has been made in IVF human embryos. The majority of IVF human blastocysts harvested were abnormal, with vacuolated and bi-nucleated cells, which interestingly, displayed reduced gap junction labelling (Hardy et al., 1996). Compaction into blastocysts occurred asynchronously. Compacted, closely apposed blastomeres displayed strong labelling for Cx43, while Cx43 levels were lower between non-compacted, loosely apposed blastomeres (Hardy et al., 1996). Therefore these experiments suggest that gap junction assembly at intercellular interfaces is important for normal blastocyst development, however whether the requirement is for cell-cell adhesion, or intercellular communication is unclear.

**Unclear results following pan-embryonic gap junction inhibition**

Total inhibition of gap junctions in the whole blastocyst in *Xenopus* and mouse produced disparate results. When injected into 1 or 2 cell stage *Xenopus* embryos, peptides that block gap junction channels severely disrupted development and the embryos failed to reach gastrulation, which suggests that gap junctions are essential during the blastula stage (Warner, 1987). This was contradicted by blockade of gap junction communication in moue blastocysts with 18 α-glycyrrhetinic acid (AGA). Despite total blockade of gap junction channels blastocyst formation appeared to occur normally (Vance and Wiley, 1999). There were no differences in TUNEL staining, or measureable differences in metabolic rate (Houghton et al., 2002). However whether later development proceeded normally, or if the inhibited embryos were viable was not tested. This result needs to be interpreted with caution also because AGA is an indirect inhibitor of gap junction function, through activating protein kinases, G-proteins or transport ATPases that ultimately leads to altered phosphorylation (and therefore gating) of connexons (Houghton, 2005).

When blastomeres from normal and UV irradiated cleavage stage mouse embryos were aggregated, the normal cells proliferated at a faster rate than the irradiated cells during

the blastula stage. This advantage of the control cells was eliminated when gap junction communication was inhibited with AGA, suggesting that gap junction communication was reduced in the irradiated cells. This did not, however, have a significant effect upon development, since irradiated embryos completed the blastula stage successfully, indicating that gap junction communication does appear to improve blastomere proliferation, but is not essential for it (Vance and Wiley, 1999).

It is difficult to interpret the results obtained from pan-embryonic inhibition of gap junctions, since the requirement for gap junction communication appears to vary from absolute, to non-existent. Thus far, there is no evidence regarding an organisational role for gap junction communication in blastocysts from any species. Since cell cycles in the zebrafish blastocysts are spatio-temporally regulated, blastomeres may use gap junction communication to coordinate their cell cycles. This property of the zebrafish blastocyst could be used as a simple assay for the requirement for intercellular communication during the blastocyst stage of development.

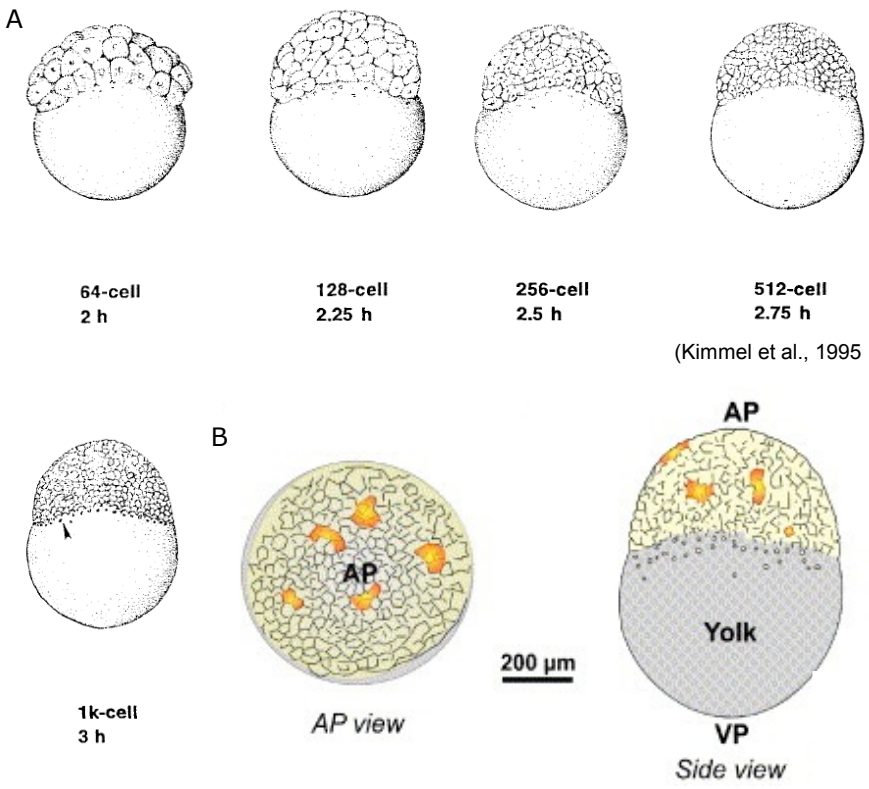


Fig. 1.7. The blastula stage of zebrafish development
A). The zebrafish blastula period begins at the end of the 64 cell stage, the fist stage where the embryo is no longer a monolayer. It lasts until the 1k cell stage, when the MBT commences and epiboly begins. The blastocyst consists of a group of embryonic cells clustered at the animal pole, attached to a spheroid, non-embryonic yolk cell. Initially it is close to spherical. With each division the mound of cells becomes larger until the blastocyst is ovoid in shape. Cell divisions occur in waves. Blastomeres at the peak of the animal pole divide first and those touching the yolk divide last.
B). Previous studies of calcium activity in zebrafish blastocysts have observed small, localised intercellular calcium waves spreading between up to 5 blastomeres with no spatial or temporal pattern.

## Calcium activity in blastocysts

Calcium ions are able to pass through gap junctions and have been shown to coordinate cellular processes in a variety of developmental contexts, therefore calcium signalling may be an important coordinator of cell behaviour in the blastocyst.

In mouse blastocysts, calcium activity is capable of altering the expression of developmentally significant genes (Webb and Miller, 2003a), therefore the mechanism is in place for calcium signalling to regulate the blastula stage. The role that calcium signalling plays in zebrafish blastocyst is not known. The majority of studies of calcium dynamics in early zebrafish development either did not record calcium signals beyond the first few cell cycles, or reported no patterns of activity in the blastocyst. Calcium spikes were found at a frequency of 1/min with aequorin as the calcium indicator (Creton et al., 1998). Calcium spikes and small waves consisting of around 5 cells were observed with nuclear localised calcium green dextran (fig. 1.7B)(Reinhard et al., 1995). These events were only seen in the outer cells of the blastocyst, which were converting to the EVL. These transients occurred after IP3 concentrations increased in the embryo, suggesting that they were dependent upon IP3 signalling for their production (Reinhard et al., 1995). No cell cycle dependent or pan-embryonic patterns of activity have been reported in the zebrafish blastocyst. This may in part be due to the choice of calcium indictor used in earlier studies. Poor spatial and temporal resolution when imaging aequorin rendered observing rapid, highly localised signals impossible (Creton et al., 1998). Reinhard and colleagues used a nuclear localized version of calcium green. During cytokinesis the nuclear envelope dissolves resulting in diffusion and dilution of the calcium indicator, making it impossible to record calcium activity throughout the cell cycle (Reinhard et al., 1995).

In *Xenopus* embryos there does appear to be a cyclical change in calcium concentrations. Measurement of calcium levels in the entire blastocyst with either calcium sensitive electrodes or aequorin revealed that calcium levels oscillate in a cell cycle dependent manner (Grandin and Charbonneau, 1991; Keating et al., 1994). This is surprising since aequorin injected zebrafish failed to reveal cyclical calcium activity (Creton et al., 1998). There is however debate over whether calcium levels are high before, during or after cleavage (Grandin and Charbonneau, 1991; Keating et al., 1994; Kubota et al., 1993).

Injection of individual *Xenopus* blastomeres with aequorin at the 64 cell stage showed that their oscillations differed subtly from the oscillation seen when the entire embryo

was imaged (Keating et al., 1994). This suggested that because blastomeres do not divide in a perfectly synchronous manner they do not oscillate in a perfectly synchronous manner either. The authors proposed that the calcium increase occurs in a wave; however a direct observation of calcium activity in all blastomeres individually is required to confirm if this is the case.

In summary, functional gap junctions are expressed in vertebrate blastocysts and gap junction communication does appear to mediate the rate of blastomere proliferation, while cell-cell adhesion also appears to require gap junctions. However understanding of the role they play in early development is currently quite unclear. The role that calcium signalling plays in the blastula stage is also currently unclear, however calcium activity may consist of small intercellular calcium waves and cyclical changes in calcium activity, or resting calcium levels. What yet has not been addressed is if gap junction communication and/or intercellular calcium activity organise and coordinate the cell division waves that occur during the zebrafish blastula stage. A study of the effect upon cell division waves and calcium signalling after interfering with gap junction communication, could provide useful insight into the role that gap junctions play in early development.

## *Experimental aims*

To investigate the relationship between epithelial arrangement and hindbrain segmentation in zebrafish embryos I observed the expression of ZO-1 and other junctional proteins, discovering that, like chick, zebrafish rhombomere boundary cells have enlarged apical end feet (AEF). I found a graded decrease in AEF size with increasing distance from rhombomere boundaries. To address if the Notch signalling pathway regulates AEF size distribution, I disrupted Notch signalling via *hdac-1* and *lfng* and analysed the arrangement of AEF in the hindbrain, finding that the Notch signalling pathway is involved in determining the patterning of the apical surface of the hindbrain. I then examined other CNS boundaries and proposed CNS boundaries to determine if boundary expansions of AEF were common, discovering boundary characteristics in other proposed compartment borders.

To assess if, like in chick, restricted dye transfer between rhombomeres occurs in the zebrafish, I examined intercellular communication within and between rhombomeres, confirming that zebrafish rhombomere boundaries have decreased gap junction communication. I then extended the technique to assess if reduced dye transfer between CNS compartments is conserved in more anterior regions. I discovered reduced dye connectivity between the dorsal and ventral thalamus, suggesting the ZLI is a barrier to intercellular communication.

To address if intercellular calcium waves are segmentally regulated by reduced gap junction connectivity at boundaries I recorded spontaneous calcium activity and attempted to induce calcium waves artificially. Neither spontaneous, nor induced calcium waves occurred, suggesting that the zebrafish hindbrain is not competent to produce intercellular calcium waves.

To attempt to assess the requirement for gap junction communication in zebrafish development, I studied the spatio-temporal pattern of cell division waves in the blastocyst, since this is the simplest developmental stage at which gap junction communication occurs. I discovered that gap junction function is a requirement for the coordination of division waves and for the generation of intercellular calcium waves, as well as the production of non-wave calcium activity. I also report that cyclical changes in calcium occur throughout the blastula stage, suggesting that calcium activity is cell-cycle dependent.

# Chapter 2: Materials and methods

## Embryo care

Wildtype and transgenic zebrafish (*Brachydanio rerio)*, embryos were reared at 28.5$^{o}$C, according to standard procedures (The Zebrafish Handbook). Embryos older than 24 hpf were administered 1-phenyl-2-thiourea in 10% Hank's saline (The Zebrafish Handbook) to prevent melanocyte differentiation. Embryos loaded with calcium indicators or expressing Kaede were reared in the dark to prevent photobleaching/conversion before experimentation.

Wildtype strains included AB Tubingen (UCL), King's College Wildtype (Kwt), and Shark Bait (SBwt). Transgenic lines used were Tg:(PGFP5.3), to visualise r3 and r5, (Picker et al., 2002), Tg:(HuC:GFP) to visualise neurons (Park et al., 2000) and Tg:(Shh:GFP) to visualise the ZLI (Ericson et al., 1995). One mutant line was used; *hdac*$^{-/-}$ (a gift from V. Cunliffe, Sheffield).

## Microinjection

Injections made at the 1-4 cell stage were carried out using a glass microelectrode, micromanipulator and Picospritzer (General Valve Corporation), under a dissecting microscope. All solutes were dissolved in Morpholino Buffer (5 mM HEPES (pH 7.5) and 0.2 mM KCl).

Masses injected were as follows: 200pg mRNA encoding Par3 GFP, 2ng Calcium Green dextran 10kD (C3713, Invitrogen$^{TM}$), 150pg mCherry mRNA, 200pg Kaede mRNA (Ando et al., 2002), 6ng *Lfng* MO, a kind gift from N. Nikolaou and D. Wilkinson, designed to block splicing between exon 1 and intron 1 (5'-ACCGTGTATACCTGTCGCATGTTTC-3') (Nikolaou et al. 2009), 0.5, 1 and 2 pmol ZO-1 MO (5'-TTTAATATCTTACTGTAGAAGTCCC-3'), designed to prevent splicing of the second exon and intron (Gene Tools).

## Pharmacological treatments

### Cell division blockade

To block cell division during neurogenesis, a cocktail of 100μM aphidicolin (Biomol) and 20mM hydroxyurea (Sigma) dissolved in 4% DMSO, was applied at tailbud stage until fixation at 30hpf.

**Gap Junction blockade**

Flufenamic acid (FFA)(F9005 Sigma™) was dissolved to 100mM in DMSO, then further diluted to 100µM in Embryo Medium (The Zebrafish Book). The pH of the solution was corrected back to 7.0 with weak NaOH. Blastocysts were placed in this solution for at least 30 min prior to imaging, since preliminary studies of calcium activity suggested that it took at least 20mins for the drug to take effect.

## Hindbrain AM dye loading

Embryos were reared to 24-30hpf. They were anaesthetised with tricaine/MS-222 (E102521 Sigma™), immobilised in 1.5% low melting point agarose (A9414 Sigma™) and a small piece of agarose was cut away to expose the injection site. Embryos were visualised with a long working distance compound microscope for injection.

Either 50µg Calcein AM (red-orange) (C34851, Invitrogen™), 50µg Fluo4 AM (F14201, Invitrogen™), or 50µg NP-EGTA AM (N6803, Invitrogen™) was dissolved in 2.5µl of 20% pluronic in DMSO (P-3000MP, Invitrogen™), then diluted to 100µl in Evans Solution (in mM): 134 NaCl, 2.9 KCl, 2.1 CaCl2, 1.2 MgCl2, 10 HEPES, 10 glucose.

A borosilicate glass micropipette connected to a picospritzer (General Valve Corporation) was used to inject the solution directly into the central lumen of the spinal cord, near to the midbrain-hindbrain boundary or directly into a rhombomere, depending upon experimental requirements. The injection consisted of 5-30 50ms pulses at 15psi. Embryos were left to recover in the dark at 28.5°C for at least 30mins, but usually over 1hr before imaging.

## Whole-mount immunocytochemistry

Embryos were fixed for 3h at room temperature or overnight at 4°C in Paraformaldehyde (4% w/v PFA in PBS, pH 7.3). After fixation they were rinsed 2x and washed 3 x 10mins in PBTr (Phosphate buffered saline, 0.5-0.8% Triton-X100) with gentle shaking. Then they were transferred to 50% methanol (MeOH) in PBTr, 3 x 5min washes in 100% MeOH and then placed at -20°C overnight to aid permiabilisation.

Embryos were rehydrated by 1 x 5mins wash in 50% MeOH in PBTr, then 3 x 5mins PBTr, then blocked in blocking solution (IB) for at least 1 hour at room temperature on a shaker (10% normal goat/horse/bovine serum (NGS), 1% DMSO, 0.5-0.8% Triton-X100 in PBS). They were then incubated in IB + primary antibody overnight at 4°C on shaker. Primary antibody concentrations: aPKC: 1:500 (Santa Cruz Biotechnology), GFP: 1:500 (Abcam), ZO-1: 1:500 (Invitrogen™: 339100), Acetylated Tubulin: 1:1000 (Sigma), ß-catenin: 1:2000 (Sigma).

Primary antibodies were removed and embryos rinsed 3x in PBTr, then washed at least 4 x 30min in PBTr with gentle shaking. Following this they were incubated in secondary antibody (Invitrogen), 1:500 in PBTr, overnight at 4°C with gentle shaking. Finally, embryos were rinsed 3x in PBS and washed at least 4 x 30min on shaker.

**F-actin labelling with Phalloidin**

F actin was labelled using alexa conjugated phalloidin (F432, Invitrogen™ ). Embryos were fixed for 3hrs or overnight in 4% PFA in PBS, washed 3 x 10 min in PBS then incubated overnight in 1:200 phalloidin in PBS. The following day they were washed 4 x 30 mins in PBS and stored in the dark until imaging.

## Dissection and mounting

When measuring apical end feet (AEF) at the ZLI or in hindbrains with small IV ventricles, it was not possible to accurately measure AEF sizes without dissection. To expose these occluded regions of the ventricular surface embryos were dissected in half. A 2% agarose floor was created in a small petri dish, then filled with 50% glycerol (Sigma™) in PBS. Embryos were placed in gradually increasing concentrations of glycerol over 30mins to allow them to equilibrate. An individual embryo was pinned in place using 0.020mm Tungsten wire (Advent Research Materials). Another piece of wire was used to make incisions through the epidermis along the midline of the head.

The wire was then pushed deeper into the head and used as a knife to cut the brain in half along the midline. The neural tube was severed with forceps and the halves of brain placed into a small drip of glycerol on a glass slide. Four small mounds of silicone grease were applied in a square around the embryo and a glass cover-slip placed onto them. The cover-slip was gently pressed down until it touched, but did not squash the embryo. Any air pockets under the cover-slip were removed by application of more glycerol solution at the edge of the cover-slip. The cover-slip was then sealed with nail varnish.

## Confocal microscopy

Embryos were mounted in low melting point agarose (A9414 Sigma$^{TM}$) for imaging. Live embryos were anaesthetised with tricaine/MS-222 (E102521 Sigma$^{TM}$). A Leica SP2 , SPE or SP5 confocal microscope (Leica GmBH Heidelberg, Germany) was used with a heated chamber set to 28.5$^{o}$C when live specimens were used.

### ZO-1 acquisition

To capture Z-stacks of ZO-1 immunofluorescence using a 40x or 63x long-working-distance water immersion objective, Z-spacing of 0.5 - 1µm was essential to capture fine detail and to allow for future rotations of the ventricular surface.

### Calcium imaging

In all experimental conditions the excitation wavelength was 488nm for calcium green dextran. Laser power was kept at the lowest possible level to reduce photobleaching. This drastically reduced the signal emitted from the calcium fluorophore. To compensate, the pinhole was expanded to 2.5-3.5 airy units.
For high resolution imaging of blastocysts and of 24-30hpf embryos, images were acquired with a 40x lens or 63x lens, with 512 x 512 resolution, at 3 Z-levels 10-15µm apart (blastocyst) or 7-8µm apart (24-30hpf), with 5s intervals, a scanning average of 2, at 400-600hz with bi-directional scanning activated for up to 4 hours.

In experiments where the entire animal surface of the blastocyst was imaged, speed rather than resolution was important. A 20x lens with zoom 1.7 was used. To improve the scan speed, the frame rate was increased to 700hz, resolution was decreased to 256 x 256 and no frame averaging was used. It was then possible to acquire 13 frames every 5 seconds, covering up to 200µm depth. Embryos younger than 10hpf were not dechorionated to avoid damaging them. This resulted in the embryos shifting within

their chorions during acquisition, so time-lapses were often stopped in order to reposition the embryo.

**Uncaging calcium from NP-EGTA**

A FRAP protocol was used in uncaging experiments. Embryos were imaged at 2.5s intervals and a single z level, with the 488nm laser line for up to 3 mins prior to uncaging. UV laser lines (405nM and 455 with the SP2 and 405 alone with the SP5) were used to lyse NP-EGTA within a defined Region Of Interest (ROI). Laser power was altered for different experiments. The microscope was set to 'zoom to ROI,' since not using this option failed to elicit uncaging. Post uncaging acquisition was as with pre-uncaging, but for up to 5 minutes.

**Cell division in Early Embryos**

The transgenic line Tg(H2B:GFP) was imaged at 1.5 or 2 min intervals with a 488nm laser. Z spacing was set to 10μm to ensure each nucleus was captured in at least 1 slice. Gap junction blockade was achieved by immersing the embryos in 100μM FFA pH 7 (F9005 Sigma$^{TM}$), 45 minutes prior to imaging. Embryos were kept in FFA for the duration of the experiment.

**Kaede Photo Conversion**

A Leica SP5 laser scanning microscope was used to photo-convert Kaede. Green and red fluorescence images were acquired before and after photoconversion using 488nm and 563nm laser lines. Conversion was carried out with a 405nm laser line targeted to a single cell. The microscope was set to 'zoom to ROI,' to enhance photoconversion.

## Analysis

### ZO-1 immunolabelling of apical end feet

Raw confocal data were exported to Image J (NIH. www.rsbweb.nih.gov/ij/) for analysis. Images were processed to improve visualisation of the apical end feet of the neuroepithelium. The skin and roof plate were deleted, then a median filter used to remove noise and improve contrast between the junctional domains and background fluorescence. In images with low contrast between the apical surface and deeper tissue (such as phalloidin), all structures except for the apical surface were deleted. Maximum projections were then created to visualise the ventricular surface.

In some parts of the brain the ventricular surface was at an angle when it was imaged, causing the apical end feet to be foreshortened. 3D models of each brain were created and the models rotated to correct the viewing angle. Up to 5 separate images were created from a single 3D model due to the topography of the ventricular surface.

Variations in fluorescence intensity made it impossible to directly measure apical end feet (AEF) sizes, so the flat images were printed and ZO-1 protein expression drawn over with a pen. These drawings were scanned and exported back to ImageJ.
The area of each AEF was then measured. The AEF were divided into transverse stripes one AEF thick. Boundary cells were put in one category, peri boundary in the next etc. The mean surface area of each group was then calculated.

In some cases the viewing angle was too steep for a rotation to accurately reproduce how the ventricular surface should have looked if flat. In these situations, the original projection was printed, drawn over, scanned and measured. The viewing angle was measured, then trigonometry used to compensate for foreshortening.

The most accurate equation to describe the end foot measurements was found by a process of elimination, in collaboration with Dr Eric Blanc. In the hindbrain an exponential curve best fit the data, while a line best fit the ZLI data.

Two exponential decay curves were calculated for each condition in the hindbrain. The first was the best fit for all data points. The second was formed from a bootstrap with 1000 permutations and replacement. Each permutation consisted of a subset of end foot area measurements taken at random from all measurements. A decay curve was fitted to each set and then the mean of this curve calculated.

**Calcein AM microinjection analysis**

Raw confocal data were exported to Image J (NIH. www.rsbweb.nih.gov/ij/) for analysis. Fluorescence intensity measurements were made by drawing a thick line over the boundary so that as many VZ cells were inside the line as possible. The average fluorescence intensity was then measured for each point along the length of the line (averaging the intensity along the dorso-ventral axis of the VZ) and exported to Microsoft™ Excel. To reduce the effect of noise fluctuations, intensity measurements were averaged over 30 pixels. To calculate the % change in fluorescence intensity per micron, the following equation was used:

$(I_{n+1} - I_n) / x$ pixels/um

Where I = fluorescence intensity, n = pixel number and x = the number of pixels per micron for the given image.

**Blastocyst calcium imaging analysis**

Raw data were exported and loaded into ImageJ.
For high resolution movies, a ROI was assigned to every cell at each of the 3 Z-levels. The ROI positions were adjusted whenever cells moved using a plugin developed by Daniel Ciantar (Cell and Developmental Biology, UCL) and the mean fluorescence intensity was recorded at each time point.

Low resolution, rapid movies were analysed differently. At each time point the mean fluorescence intensity was recorded from each square in a grid of 50 x 50 µm squares. Squares that did not, or only partially covered the embryo were not included in the analysis.

The data were then exported to Microsoft Excel for further analysis. Mean Fluorescence intensity was converted into % Intensity by the following equation: $(100*I_t/I_{max})$.

Integration of calcium activity over 30s periods was achieved by first creating an extended focus (maximum) projection of each time point by using the 'Grouped Zprojector' plugin (http://rsbweb.nih.gov/ij/plugins/group.html). Then increases in calcium activity at each time point were isolated by subtracting the image from 3 time points before. A running average of 6 time points (30s) was then created using the 'Running Z Projector' plugin (http://valelab.ucsf.edu/~nico/IJplugins/Running_ZProjector.html).

### *Thresholding*

Most individual calcium transients took approximately 4 timepoints to reach peak intensity from baseline levels, so % Intensity was converted into intensity change over 4 time points ($I_{t4} - I_{t1}$). Any intensity changes that exceeded a set threshold were counted as calcium transients. The threshold had to be determined separately for each time-lapse because of variability in signal-to-noise ratios. In each time-lapse, 5 cells were observed by eye and the number of transients they generated were counted. The threshold was adjusted to count the transients seen by eye and to discount intensity fluctuations caused by noise, or cell movement. In long time-lapses, the threshold was periodically changed to compensate for photobleaching or other changes in signal intensity. Time-lapses where the signal-to-noise ratio was too low to accurately separate transients from noise fluctuations were not analysed further.

### *Spike frequency histograms*

After thresholding the data were converted to binary, with time points where a cell exceeded threshold represented by 1s and all others represented as 0s. Particularly long or large amplitude calcium transients produced more than one time point with a score of 1. To correct for these false positives, the first time point was scored as 1 and subsequent time points adjusted to 0. The sum of transients at each time point was calculated to produce a spike frequency histogram.

### *Cell cycle analysis*

The earliest time point where a cell had indentations at the cleavage furrow was classed as time 0. In low resolution movies the onset of division was defined as the time point when the first cell in the division wave began to divide.

### *Calcium wave analysis*

To determine calcium wave frequency in high resolution movies, the binary data were studied to find coactive and sequentially active cells. Blastomeres were scored as being in a wave if they matched the following criteria:

1). Active cells were touching.

2). Activity occurred before fluorescence returned to baseline in neighbouring cells.

3). The pattern of activity followed a path: a line, sheet or spiral across the surface of the blastocyst.

**Data analysis 24-30 hpf embryos**

Calcium transients were detected by sight using ImageJ. ROIs were assigned to active cells to measure calcium fluorescence changes. Scarcity of calcium activity negated the need for sophisticated analysis methods.

**Uncaging NP-EGTA, analysis**

Raw data were exported and loaded into ImageJ.
Images were registered using the 'stackreg' plugin (Ecole polytechnique Federale De Lausanne, France). ROIS for different cells were defined and the mean fluorescence intensity of calcium green dextran was measured for each time point. The data were then exported to Excel. The average Intensity of the pre-bleach time-lapse was calculated and used as a baseline recording ($I^{base}$), then the raw intensity data were converted into % changes:

$$Change = 100 * \frac{(I^{t} - I^{base})}{I_{base}}$$

For comparison between experiments, the fluorescence change was normalised by dividing the fluorescence change in each cell by the change in the targeted cell.

**Kaede Photo Conversion analysis**

Fluorescence data were exported to ImageJ. Fluorescence intensity of the converted cell and nearby cells in the red channel was recorded before and after photouncaging and exported to Microsoft Excel. The change in fluorescence intensity was calculated and normalised by dividing the fluorescence change in each cell by the fluorescence change in the targeted cell.

## Division wave analysis

Data were exported to ImageJ for analysis. Dividing nuclei were marked in the first time point when two separate nuclei were visible. It was not possible to analyse the time-lapses as a projection, because of nuclei overlapping and occluding each other. Analysing individual slices was not appropriate either because when nuclei divided out of the plane of focus, only one daughter nucleus could be seen in some slices. So a partial projection technique was used. A maximum projection of 3 consecutive slices was created, which ensured that out of plane divisions could be detected. Many dividing

nuclei were found in more than one of these 3-slice projections. To eliminate double counts, the duplicated mark was erased from the deeper of the two projections. If a division was triple-counted, the upper and lower duplicated marks were erased. Once all dividing nuclei were marked, the fluorescence data were removed from the image. ImageJ ´particle analyser´ was then used to find the XYZT coordinates of each division mark.

Coordinates were exported to Microsoft Excel for further analysis. First a point of origin was established for each division wave. If a single cell divided first, Its coordinates were used as the point of origin. If there was more than one dividing cell in the first time point of the division wave, the mitotic pair with the greatest distance between daughter nuclei was chosen as the point of origin. If this was not possible to determine, the geometric midpoint between the dividing nuclei was calculated and used as the point of origin. The distance between subsequent divisions and the point of origin were calculated and the mean distance from the point of origin was determined for each time point.

## Western Blot protocol

### *Embryo preparation*

Ten 24hpf zebrafish embryos per experimental condition were dechorionated in Ginzberg solution (The Zebrafish Handbook). The yolks were removed and embryos transferred to a 1.5ml ependorf in 20µl Ginzberg. Added 40µl sample buffer, then vortexed for 30s and heated to 95°C for 10min. Subsequently the ependorf was rotated at 13,000 rpm for 20s, then frozen at –20°C.

### *Gel preparation and protein electrophoresis*

Poured 7% SDS page into a 1.5mm gel cast, then applied the stacking gel on top, with comb to create wells for Western samples. Once gel set, samples were placed in wells along with a Calibrated ladder. Gel was placed in a Biorad protein electrophoresis gel tank, which was filled with transfer buffer (20% MeOH, 25mM Tris, 190mM Glycine) and an ice block. The gel was run at 100V until the samples had passed through the stacking gel. Voltage was then increased to 150V for 1hr.

To make 7% SDS Page (10ml):

$H_2O$: 5ml, 1.5M Tris pH 8.8: 2.5ml, 10% SDS: 100µl, Acrylamide/Bis: 2.3ml, 10% APS: 100µl, Temed:10µl.

To make stacking Gel (5ml):

$H_20$:3.6ml, 1M Tris pH6.8: 625µl, 10% SDS: 50µl, Acrylamide/Bis: 670µl, 10% APS:50µl, Temed:5µl.

***Protein transfer***

Gel was removed and prepared for protein transfer. A stack of; sponge, 3 pieces of filter paper soaked in transfer buffer, transfer membrane, gel, 3 more pieces of filter paper and another sponge was made. This stack was placed in a Biorad protein electrophoresis tank for 1.5h at 100V.

***Protein labelling***

Transfer membranes were rinsed x2 in PBS + 0.1%Tween (PBTw), then blocked in 1% dry milk powder in PBTw for 1hr. Blots then left in primary antibody solution in sealed plastic pouches overnight with mild shaking at $4^oC$. Antibody concentration: αZO-1, 1:1000, αHSP90 1:1000. Blots were washed 4 x 15 min in PBTw, then incubated for 1hr with mild shaking in sealed plastic pouches containing HRP conjugated secondary antibodies in 0.5% milk in PBTw. Secondary vs. ZO-1, 1:1000, vs. HSP90 1:3000. Blots were then washed 4x15 min.

***Protein detection***

Mixed 2ml solution A with 50µl solution B of 'ECL Plus Western Blot Detection System' (Amersham) and applied the mixture to the blot. It was placed under a Camidoc luminescence detector to visualise protein bands.

# Chapter 3:
# Intercellular junctions are patterned in the neuroepithelium and can be used to detect compartment boundaries

## *Introduction*

The embryonic vertebrate hindbrain contains a series of neuronal nuclei and peripheral nerve roots that are segmentally organised (Kiecker and Lumsden, 2005). This pattern of neuronal arrangement appears to be the product of early segmentation of the hindbrain into compartments, called rhombomeres. Rhombomeres are defined by morphology, lineage restriction and homeobox transcription factor expression patterns (Fraser et al., 1990; Hunt and Krumlauf, 1991; Lumsden and Keynes, 1989). During neurogenesis the topology of the vertebrate hindbrain is wave-like, with boundary regions bulging into the ventricular space, while the centre of each rhombomere is indented (Guthrie et al., 1991; Lumsden and Keynes, 1989). During early neurogenesis in the avian hindbrain, there are more neurons in the mantle zone at rhombomere boundaries than non-boundaries and commissural axons transiently collect there (Lumsden and Keynes, 1989). A similar arrangement occurs in zebrafish hindbrains, except there is also a cluster of neurons in each rhombomere centre (Hanneman et al., 1988).

Hindbrain proliferating cells also have segmental organisation. At the interface between neighbouring rhombomeres a specialised cell type forms. Compared to cells in rhombomere centres boundary cells have altered gene expression profiles, cytoarchitecture, proliferation rates, neurogenic potential, increased extracellular space and they secrete molecules that pattern neighbouring rhombomeres (e.g. Amoyel et al., 2005; Cheng et al., 2004; Guthrie et al., 1991; Heyman et al., 1995; Heyman et al., 1993; Thisse, 2001). In zebrafish hindbrains, *in situ* hybridization for boundary markers suggests that each rhombomere contributes a single row of cells to its anterior and posterior boundaries, thus generating 2 rows of boundary cells per interrhombic interface (Cheng et al., 2004). Boundary specific genetic markers can be detected by 14hpf and include *sema3G*, *wnt1*, *radical fringe (rfng), foxb1.2* (*mariposa*), *follistatin,* Pax6 and Vimentin (Amoyel et al., 2005; Cheng et al., 2004; Cooke et al., 2005; Heyman et al., 1995; Nittenberg et al., 1997; Xu et al., 1995). In zebrafish, cells immediately adjacent to rhombomere boundaries also express a unique combination of

genes compared to boundary cells and rhombomere centres, including increased proneural gene expression, *deltaA,B,D* and higher levels of *notch1 and b* compared to other parts of rhombomeres (Bierkamp and Campos-Ortega, 1993; Cheng et al., 2004; Riley et al., 2004). Therefore each rhombomere appears to contain 3 subsets of cells: boundary, peri-boundary and central cells (fig. 1.2C).

Each rhombomere is a lineage restricted zone (Fraser et al., 1990), due to adhesive differences between cells in neighbouring rhombomeres (Wizenmann and Lumsden, 1997), that may be mediated by alternating expression of Eph and Ephrins in adjacent rhombomeres (Cooke et al., 2005; Mellitzer et al., 1999; Xu et al., 1995; Xu et al., 1999). Specialisation of the boundary region may further restrict cell mixing though construction of a physical barrier. Increased levels of Filamentous (F) Actin at rhombomere boundaries suggest that they generate a fence, to stop cells crossing from one rhombomere into another (Cooke and Moens, 2002; Guthrie et al., 1991), since Actin prevents cell mixing between dorsal and ventral compartments of the *Drosophila* wing disc (Major and Irvine, 2005; Major and Irvine, 2006). It is unclear if F Actin becomes enriched during boundary formation, or afterwards and so whether it plays roles in both segregation of rhombomeres and maintaining boundary integrity is not known.

The hindbrain neuroepithelium contains neural progenitors that are bipolar and span the apico-basal thickness of the ventricular zone (VZ). They are attached to the ventricular and pial surfaces by expanded end feet (fig. 1.5). A striking feature of chick rhombomere boundary cells is enlarged apical end feet (AEF) (Guthrie et al., 1991; Ojeda and Piedra, 1998). Whether boundary AEF are enlarged in other vertebrate hindbrains is not known. Apical end feet (AEF) are anchored to each other by a ring of intercellular junctions. Intercellular junctions are composed of tight junctions, adherens junctions, gap junctions and desmosomes.

Zonula Occludens 1 (ZO-1) was the first tight junction protein to be discovered (Stevenson et al., 1986). Biochemical studies of interactions revealed that ZOs link Occludin, Claudin and JAM to the actin cytoskeleton, therefore aiding in maintenance of tight junctions and hence epithelial structure (Bazzoni, 2003; Fanning et al., 1998; Furuse et al., 1994; Haskins et al., 1998; Itoh et al., 1999; Itoh et al., 2001; Wittchen et al., 1999). Adherens junctions are composed of Cadherins, the transmembrane molecules that through homophilic interactions anchor neighbouring cells. Accessory proteins α-catenin and β-catenin provide the link between Cadherins (Gumbiner, 2005).

ZO-1 also associates with adherens junctions in non-epithelial tissues and immature epithelia, through direct binding to Cadherins (Itoh et al., 1997; Itoh et al., 1993). Par3, a polarity protein, forms a complex with Par6 and aPKC and this could potentially be the master complex that determines the location where tight junctions and adherens junctions form, and thus dictate how cell polarity is established (Reviewed in Ohno, 2001).

There is a growing body of evidence that cell fate determination is regulated by the expression of intercellular junctions (Ohno, 2001; Rasin et al., 2007). For example the Par3-Par6-aPKC complex controls cell fate in a variety of organisms and tissues including *Drosophila* neural ectoderm and asymmetric division of the *C. elegans* zygote and of *Drosophila* neuroblasts (reviewed in Ohno, 2001). Secondly, *in vivo* knockdown of E-cadherin or N-cadherin in embryonic mouse cortex has suggested that rather than simply maintaining the structural integrity of the neuroepithelium, adherens junctions may regulate the choice between adopting a neuronal or progenitor fate (Rasin et al., 2007). There is also a correlation between apical end foot (AEF) size and cell identity. The AEF of adult neural stem cells are smaller than ependymal AEF and arranged into pinwheels, while ependymal cells are not (Mirzadeh et al., 2008). Therefore understanding the apical organisation of the neuroepithelium may provide useful information regarding the spatial regulation of neurogenesis.

Whether increased AEF size at boundaries is conserved in other vertebrates remains to be tested and there is little known about segmental regulation of other components of intercellular junctions, such as ZO-1, aPKC and Par3. I examined the expression of ZO-1, aPKC, β-catenin, Filamentous (F) actin and Par3 in zebrafish hindbrain, which allowed me to measure AEF sizes throughout the hindbrain. I discovered that not only are enlarged AEF conserved between chick and zebrafish rhombomere boundaries, but also that AEF sizes are arranged in a graded pattern throughout each rhombomere.

## *Results*

### The expression pattern of apical proteins in the hindbrain at 30hpf

The apical surface of the hindbrain is the floor of the IV ventricle and comprises the apical end feet (AEF) of neuroepithelial cells. In all epithelia, the apical surfaces of epithelial cells are anchored together by junction complexes, which can comprise tight junctions, gap junctions, adherens junctions and desmosomes. To understand the organisation of the apical surface of the zebrafish hindbrain, 30hpf zebrafish embryos were stained with antibodies against tight junction components Zonula occludens-1 (ZO-1); atypical protein kinase C (aPKC) and labelled with mRNA encoding Par3:GFP (von Trotha et al., 2006). Adherens junction accessory protein β-catenin, was labelled with antibodies and embryos were stained with phalloidin to detect filamentous actin.

I found these proteins were enriched near to the apical surface (fig. 3.1A-E). High magnification of the apical surface showed that all proteins occupy the junctional domain that separates the apical membrane from the basolateral membrane (fig. 3.1F-J). At lower magnification, a clear segmental arrangement of AEF was seen, suggesting enlarged AEF at rhombomere boundaries (fig. 3.1K-N). ZO-1 expression was restricted to the junctional domain (N=13). The interfaces between adjacent AEF appear linear, giving the protein expression a honeycomb appearance (fig. 3.1F,K).

APKC had a similar expression pattern to ZO-1, with some subtle differences (fig. 3.1B,G,L). It was not exclusively expressed in the junctional domain and may have expanded into the apical membrane, as its expression domain was larger and vertices less angular, than ZO-1 (fig. 3.1G).

Filamentous actin was strongly expressed at AEF junctions, and less strongly expressed along the apical and basolateral membranes (fig. 3.1C,H,M). The most striking feature of actin expression was that it appeared enriched at the interface between rhombomeres (fig. 3.1M). It was not enriched at boundaries in 14hpf embryos, but by 16hpf had accumulated in the boundaries (fig. 3.2A,B).

Fig. 3.1. Junctional proteins expressed at the apical membrane

A-E). Transverse sections of 24-30hpf zebrafish hindbrains showing expression of junctional proteins at the ventricular surface.

F-J). Projections of stacks of confocal micrographs acquired in dorsal view to visualise the ventricular surface in high detail.

K-N). Lower magnification projections of the ventricular surface in dorsal view. Rhombomere boundaries are clearly visible and marked with arrows.

A,F,K). ZO-1 expression is restricted to the apical surface of the neuroepithelium and outlines the apical end feet of progenitors.

B,G,L). APKC is also expressed in the apical end feet of neuroepithelial cells in a broader domain than ZO-1.

C,H,M). Filamentous Actin is enriched at the apical surface of the hindbrain and the boundary cells are further enriched.

D,I,J). Mosaic expression of Par3:GFP. It is also enriched at the apical surface and is co-expressed with ZO-1 (red).

E,N). ß-catenin expression is enriched at the ventricular surface of the neuroepithelium, however it is less restricted than the other proteins.

Scale bars: 5µm, 10µm, 20µm

Arrows: rhombomere boundaries, ml: midline, r: rostral, c: caudal

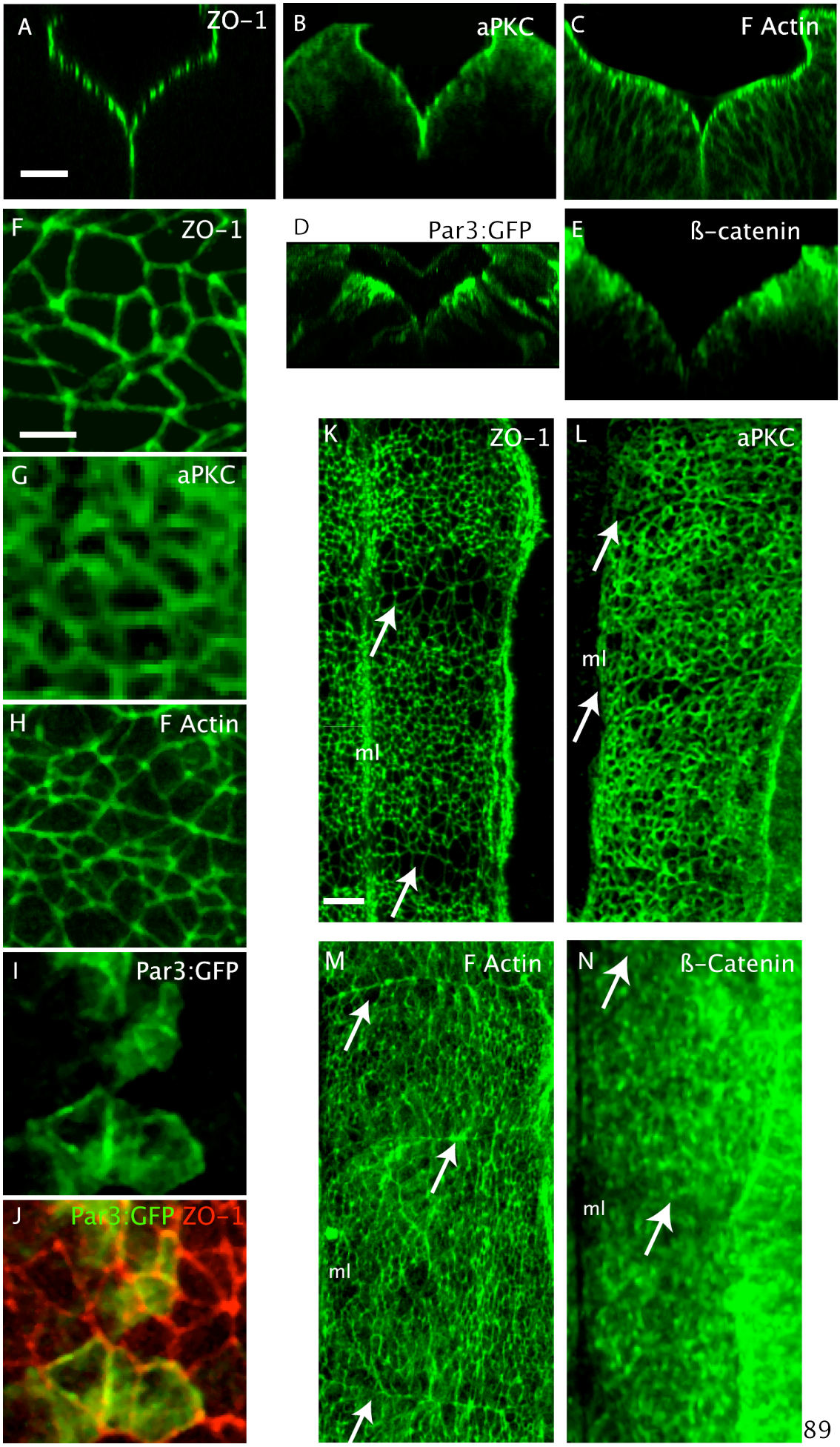
A
ZO-1
B
aPKC
C
F Actin
F
ZO-1
D
Par3:GFP
E
ß-catenin
G
aPKC
H
F Actin
I
Par3:GFP
J
Par3:GFP ZO-1
K
ZO-1
ml
L
aPKC
ml
M
F Actin
ml
N
ß-Catenin
ml

89

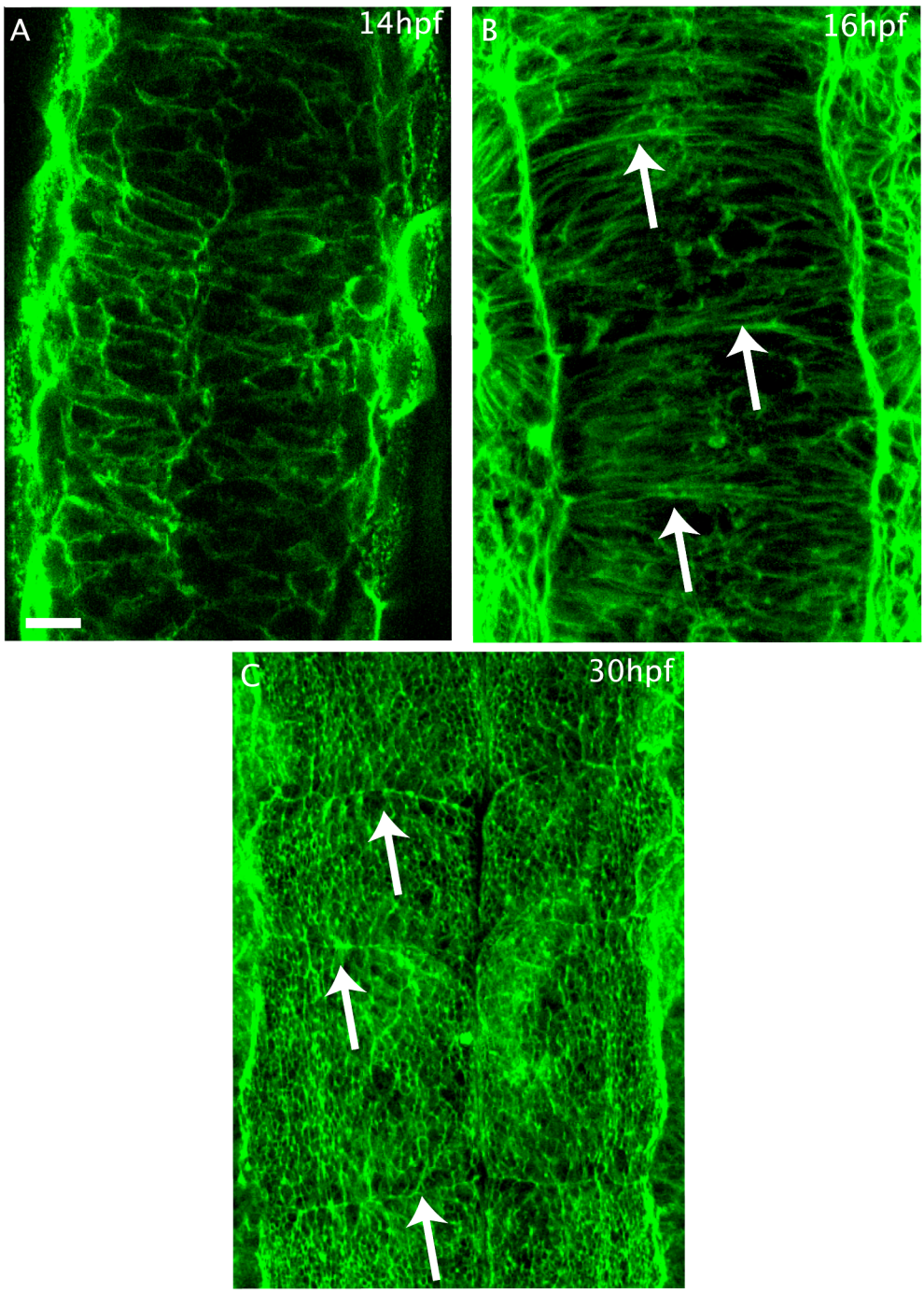


Fig. 3.2. Accumulation of Filamentous Actin during neurulation
A). Confocal slice of a 14hpf zebrafish hindbrain. F Actin is expressed in cell membranes, but does not appear accumulated at regular intervals, indicating it is not enriched at interrhombic interfaces.
B). Confocal slice of the dorsal hindbrain at16hpf. F Actin appears enriched at rhombomere boundaries.
C). Projection of the ventricular surface at 30hpf. F Actin is enriched at the ventricular surface and enriched further at rhombomere boundaries.
Scale bar: 20μm.
Arrows: rhombomere boundaries.

Par3:GFP is co-expressed with ZO-1 in the junction domain, which is again expected as it plays a role in the formation and maintenance of tight junctions (N=4). Its expression is not exclusive to the junctional domain though, as it was also found distributed around the baso-lateral and apical membranes, albeit at a lower intensity than within the apical junctions (fig. 3.1D,I,J). This could have been an artefact of injecting too great a quantity of mRNA encoding Par3:GFP, resulting in over-expression and miss-localisation. An anti-Par3 antibody was not available, however previous studies have shown endogenous Par3 expression to be restricted to the junctional domain in zebrafish neuroepithelium (Wei et al., 2004).

## Zonula Occludens 1 expression in junctions increases during neurulation

As mentioned in the above section, ZO-1 is expressed in the junctions between the apical end feet of neuroepithelial cells. In the teleost the neural tube forms by a process of cavitation. The neural plate converges and invaginates to form a neural rod, which then develops epithelial characteristics by localising apical components at the midline. Once an apical midline has formed, the two sides of the neural rod detach to form the neural tube (Geldmacher-Voss et al., 2003; Hong and Brewster, 2006; Tawk et al., 2007). To assess when the characteristic pattern of ZO-1 expression around apical end feet arises in zebrafish, embryos were immunostained for ZO-1 throughout neurulation.

I found that at tail bud (10hpf), ZO-1 protein was expressed in the interfaces between EVL cells (data not shown), however it was absent from the interfaces between neuroectodermal cells. Both ectoderm and EVL nuclei expressed ZO-1 (fig. 3.3). At 12 hpf a small number of sparsely distributed ZO-1 puncta were detected in ectoderm cells close to the prospective embryonic midline and nuclear localization of the protein persisted. Between 12 and 14 hpf the ZO-1 puncta at the prospective midline developed into latero-medial orientated stripes, while nuclear ZO-1 levels became less obvious than at 12hpf (fig. 3.3). Between 14 and 18 hpf the stripes of ZO-1 expression coalesced into a straight, continuous midline with some remaining medio-lateral orientated stripes (fig. 3.3). Between 28 and 24 hpf the IV ventricle opened. During this time period it became clear that ZO-1 expression was restricted to the intercellular junctions at the apical surface of the neuroepithelium. At 24 and 30hpf, ZO-1 appeared in a honeycomb network across the ventricular surface of the neuroepithelium, which outlined each cell's AEF (fig. 3.3).

In conclusion, ZO-1 protein expression in the prospective zebrafish brain increases during neurulation. It shifts from nuclear to apical and finally outlines the apical end feet of neuroepithelial cells when the ventricular system inflates.

## Apical end feet are distributed in a segmental and graded pattern

A striking feature of ZO-1 immunostained zebrafish hindbrain is a segmental organisation of apical end feet (fig. 3.1K, fig. 3.3, fig. 3.4A,B,C), which illustrates that the hindbrain is a series of repeating segmental units, called rhombomeres (Lumsden and Keynes, 1989). To analyse this segmental arrangement of apical end feet (AEF) I measured their size in zebrafish hindbrains at 30hpf. The average neuroepithelial AEF size was 5.7 ± 5.1$\mu m^2$, however sizes were highly varied, ranging from 0.2 - 46.9$\mu m^2$ (n = 3277 cells, N = 15 embryos. The largest end feet were located within rhombomere boundaries (n=15 boundaries), organised into two rows of AEF, one row belonging to the anterior rhombomere and the other to the posterior rhombomere (fig. 3.4A,B). The mean boundary cell apical surface size was 13.5 ± 8.9$\mu m^2$ (n=311), while non boundary cells were 4.9 ± 3.8$\mu m^2$ (n=2966), 35% of the size of boundary cells ($P<0.001$). Another striking feature of rhombomere boundaries was the linear arrangement of the two rows of boundary cells from the midline to the lateral edge of the hindbrain (fig. 3.4A). The majority (37/58) of rhombomere boundaries had a clear linear interface, but with minor interruptions, 2/58 were perfectly straight and the remaining 19/58 did not have a clear linear interface (N=11 embryos. Left and right boundaries were scored separately).

To assess if AEF sizes were also patterned in non-boundary regions, the hindbrain was divided into tiers along the anterior posterior axis, with boundary cells in one tier (red), peri-boundary cells in the next (blue), cells touching the peri-boundary cells in the third tier (green), etc. (fig. 3.4B). Up to 8 tiers of cells were measured for each rhombomere.

Fig. 3.3. ZO-1 accumulates at the CNS midline during neurulation and outlines apical end feet from the onset of ventricle opening

A). Projections of dorsal views of the zebrafish hindbrain from 10hpf to 30hpf, depicting ZO-1 accumulating at the midline, then lining the ventricular surface of the hindbrain. Prior to somitogenesis (10hpf), ZO-1 expression in the neural ectoderm is constrained to nuclei. At 12hpf, ZO-1 puncta can be detected close to the prospective midline. These puncta lengthen and thicken (14hpf), and then coalesce as the midline of the neural rod forms (14-18hpf). From 19hpf, the IV ventricle proceeds to open, with ZO-1 labelling the apical surface of the prospective neural tube. The two sides of the neural rod separate from the centre of rhombomeres before boundary regions (20hpf). At 22hpf the ventricle has opened fully, however it continues to inflate until the embryo reaches Prim-5 stage (24hpf). The ventricular surface appeared labelled in a honeycomb pattern, revealing the intercellular junctions between the apical end feet.

B) Transverse views from 14hpf to 22hpf. ZO-1 expression is scattered at 14hpf, then has coalesced at the midline by 18hpf. The IV ventricle is beginning to open at 19hpf and at 22hpf is fully open.

Scale bar: 25μm.

Lines mark the position of transverse sections, a: anterior, p: posterior, IV: fourth ventricle

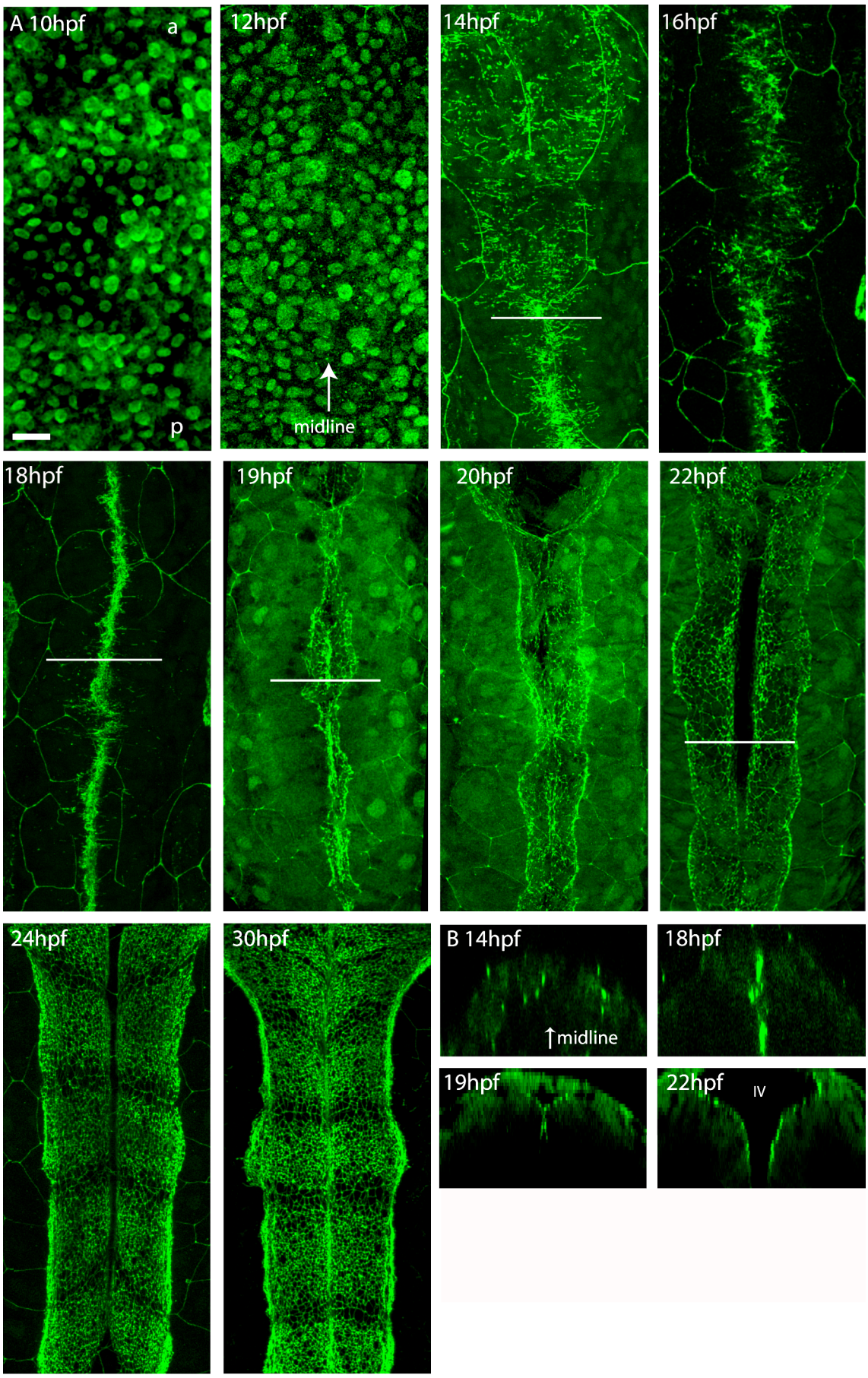
A 10hpf
a
p
12hpf
midline
14hpf
16hpf
18hpf
19hpf
20hpf
22hpf
24hpf
30hpf
B 14hpf
midline
18hpf
19hpf
22hpf
IV

Analysis revealed there was a graded change in apical surface area – the largest end feet were in boundary regions, and the smallest in the centre of the rhombomeres, with average AEF area just 3.5 ± 2.2µm$^2$ (n=250, fig. 3.4C, table 1). Boundary AEF were significantly larger than all other tiers (P<0.001, Tukey's test of honest significant difference) and peri boundary AEF, while smaller than the neighbouring boundary cells, were significantly larger than all other tiers (P<0.001, n=413). Tier 3 AEF were significantly larger than tiers 5-8 (P<0.01, n=472, 526, 436, 356 and 250 respectively), however the difference in size between tier 3 and tier 4 did not reach statistical significance (P>0.1, n=472, 513 respectively). Further towards the rhombomere centre, the differences in AEF sizes were small (a 1.3µm$^2$ decrease between tiers 4 and 8) and so did not reach significance because of variability within each tier (fig. 3.4C, table 1). Therefore, based upon AEF size there are 4 domains in the hindbrain consisting of boundary cells, peri-boundary cells and two sets in the centre of the rhombomere.

Two different statistical analyses were utilised to fit a curve to the AEF sizes. The first method included all measured AEF, while the second one was a bootstrap with 1000 permutations with replacement, which fit 1000 curves to subsets of the data, then found the mean of the curves (see methods for an explanation). In either case, an exponential decay curve best fit the data. The equation for the curve of best fit was either:

All end feet: End foot size = 26.5µm2 x e^(-1.1 x Tier number) + 4.13µm2 (Fig. 3.4C).

or

Bootstrap: End foot size =26.8µm2 x e^(-1.1 x Tier number) + 4.12µm2 (Fig. 3.4D).

The close agreement between these curves suggests that AEF sizes do indeed decrease in an exponential decay with increasing distance from rhombomere boundaries.

To conclude, ZO-1 accumulates at the apical surface of the neuroepithelium and F actin becomes concentrated at the interface between rhombomeres during neurulation. Following ventricle opening, components of tight and adherens junctions and F actin are expressed at the junctional belts that outline apical end feet. The distribution of apical end feet is graded. Boundary end feet are largest and rhombomere centre end feet are the smallest.

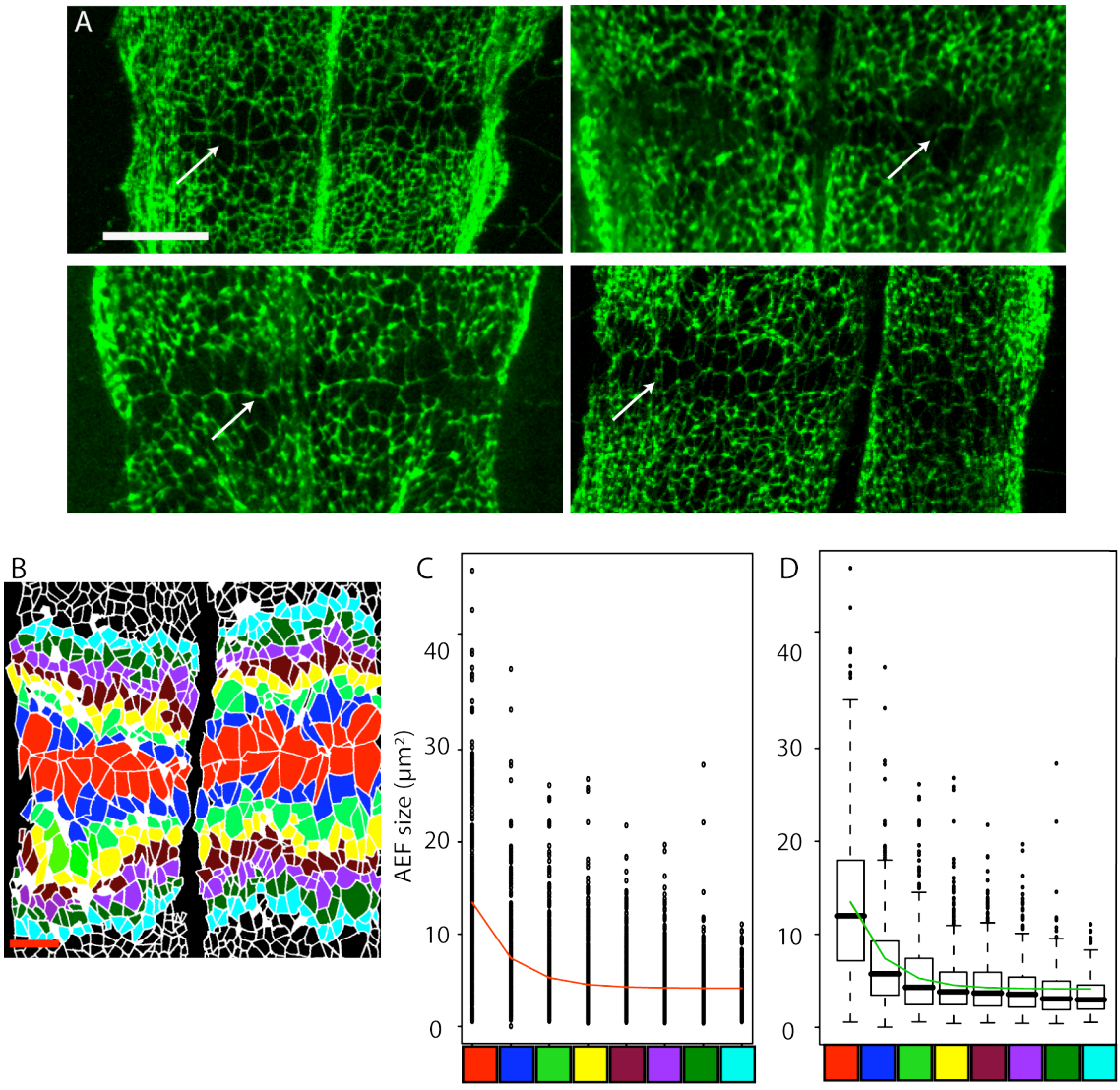


Fig. 3.4. AEF size distribution is graded along the anterior posterior axis of rhombomeres
A). Projections of the hindbrain ventricular surface.labelled against ZO-1. Two rows of cells occupying rhombomere boundaries (arrows) possess larger AEF than cells within the centre of rhombomeres. The interface between rhombomeres is linear from the midline to the lateral edge of the hindbrain.
B). The AEF were divided into tiers along the anterior posterior axis. Red AEF belong to boundary cells, blue to peri-boundary cells etc.
C). Plot of all AEF sizes by tier. The largest AEF occupy boundary regions and decrease in size in an exponential decay towards the centre of the rhombomere (Tukey's HSD test). The red curve represents the curve of best fit for the data, which is:

$$\text{End foot size} = 26.5\mu m^2 \times e^{\wedge(-1.05 \times \text{Tier number})} + 4.13\mu m^2$$

D). Removing outliers from the mean measurements by applying a Bootstrap with 1000 permutations produced a fitted curve with almost identical properties:

$$\text{End foot size} = 26.8\mu m^2 \times e^{\wedge(-1.05 \times \text{Tier number})} + 4.12\mu m^2$$

Scale bar: 20µm

# *Discussion*

## Patterning of the apical surface of the hindbrain neuroepithelium

By examining the expression pattern of ZO-1 protein in the embryonic zebrafish hindbrain I have discovered a novel characteristic of epithelial organisation. The expression of junctional bands clearly reveals boundary cells because they have enlarged AEF and a linear arrangement. ZO-1 immunostaining suggests each rhombomere contributes a single row of AEF to each boundary, so a boundary is comprised of two rows of cells, one from the anterior and one from the posterior rhombomere. Boundary specific genes, such as *rfng* are also expressed by two rows of cells, supporting this finding (Cheng et al., 2004). This characteristic arrangement was also seen in embryos labelled for aPKC and filamentous Actin expression and to a lesser extent β-catenin; however ZO-1 staining produced the most striking results. There was no observable difference in the intensity of ZO-1 staining between boundary junctions and non-boundary junctions despite the fact that EM studies of embryonic chick hindbrain found junctional complexes spanned a smaller apico-basal distance in boundaries than rhombomere centres (Heyman et al., 1993).

A surprising result was the discovery that the distribution of different sized AEF is graded through the entire rhombomere. There was an exponential decay in end foot size with the largest feet in boundary regions and smallest in the centre of rhombomeres. There were of course exceptions to this pattern as a small number of large AEF were scattered throughout the hindbrain and some boundary AEF were very small. Yet this study clearly demonstrates that not only are neuronal compartments delimited by the organisation of the epithelial surface, the cells residing within a compartment are also patterned. As well as boundary cells, apical organisation revealed a clear peri-boundary domain. This region has the highest neurogenic potential in the hindbrain (Amoyel et al., 2005; Cheng et al., 2004) and during early neurogenesis is composed of a mixture of GFAP expressing glial cells (Amoyel et al., 2005) and neural precursors that strongly express *deltaA* and *deltaD* (Cheng et al., 2004). It therefore has a unique expression profile compared with the rest of the rhombomere and since it can be identified by the size of the AEF of the cells within it, it further strengthens the prospect that epithelial organisation provides more information than simply the size of a cell's apical surface. The distribution of AEF sizes in the hindbrain suggests there are four regions, so there could be a further 2 sub-types alongside boundary and peri-boundary cells. It will be

interesting to see if there are any further differences in gene expression and neurogenic potential within the centre of rhombomeres that could confirm this hypothesis.

## Is there a developmental requirement for modified boundary apical end feet?

One possible reason for enlarged apical end feet at rhombomere boundaries is that the nuclei of rhombomere boundary cells are located close to the apical surface, creating the characteristic bulges seen along the ventricular surface (Guthrie et al., 1991). In the centre of rhombomeres an even distribution of nuclei throughout the apico-basal extent of the VZ allows more cells to be packed into a given volume of tissue. The cellular arrangement at boundaries leads to a lower density of neuroepithelial cells in boundaries than in non boundaries. This could require more apical surface per cell in boundary regions than non boundary regions. However it should be noted that mitotic cells possess minute AEF in embryonic mouse cortex (Rasin et al., 2007).

What causes or instructs boundary cells to become arranged in this way is less clear-cut. The marginal zone extends further towards the apical surface in boundary regions (Guthrie et al., 1991; Heyman et al., 1993), suggesting that boundary nuclei may be displaced by the growing population of neurons and axons there. However there is also increased extracellular space surrounding boundary cells (Heyman et al., 1993; Lumsden and Keynes, 1989), so the propensity for boundary cell nuclei to sit close to the apical surface and enlarged AEF cannot be explained simply by displacement. It is possible that the special arrangement of AEF at boundaries is important in maintaining segment integrity. The enlarged AEF at boundaries creates a large boundary zone which a neuroepithelial cell must cross in order to pass from one rhombomere to the next and so should reduce the chance of it happening. The position of boundary cells may also be stabilised by the large perimeter of their junctional domains. Likewise, reduced intercellular communication across boundaries (Martinez et al., 1992) would benefit from enlarged boundary cells and increased extracellular space, as this should provide a larger buffer zone than if boundary cells were tightly packed and evenly distributed.

## Interspecies differences in ZO-1 expression during neurulation

The dynamic ZO-1 expression pattern during zebrafish neurulation is different from other vertebrates. In the zebrafish ZO-1 expression is first detectable as small puncta in the neural ectoderm shortly after the tail bud stage, at the onset of neurulation. As neurulation proceeds it coalesces at the forming midline and then lines the ventricle as

the midline seam splits open. The same condensation of junctional proteins at the midline during neurulation has been described for aPKC, Par3 and β-catenin (Geldmacher-Voss et al., 2003; Hong and Brewster, 2006; Tawk et al., 2007). This is not the case in chick or mouse embryos where ZO-1 is expressed between neural plate cells at the onset of neurulation and persists throughout the process (Aaku-Saraste et al., 1996). This may be because the neural ectoderm is clearly epithelial from the plate stage in chick embryos (reviewed in Colas and Schoenwolf, 2001), while in zebrafish it does not become an epithelium until neurulation has almost completed (Geldmacher-Voss et al., 2003; Hong and Brewster, 2006; Tawk et al., 2007).

## Intercellular junctions expressed in the zebrafish neuroepithelium

To gain a better understanding of the structure and arrangement of junctional complexes in the zebrafish neuroepithelium, I examined the expression of ß-catenin, aPKC, Par3, Zonula Occludens 1 (ZO-1) and filamentous actin. ß-catenin associates with adherens junctions (Gumbiner, 2005); aPKC and Par3 with tight junctions (Ohno, 2001); ZO-1 can interact with tight junctions, gap junctions and adherens junctions (reviewed in Giepmans, 2004). All of these proteins and filamentous Actin are enriched at the apical surface of the hindbrain at 30hpf and are expressed in bands that outline the apical end foot of each cell indicating the presence of tight and adherens junctions at the apical surface of the hindbrain.

In chick embryos ZO-1 is expressed in intercellular junctions throughout neurulation, while Occludin, an essential tight junction component, is initially expressed at the neural plate stage, but its expression drops and is absent by the time of fusion of the roof plate. Disappearance of tight junctions also occurs in mouse embryos during neurulation. At the neural plate stage no diffusion of fluid from apical to lateral extracellular space can occur in mouse embryos, while later in neurulation fluid could pass from one location to the other (Aaku-Saraste et al., 1996). This result shows that the presence of ZO-1 does not automatically confirm the presence of tight junctions. It was not possible to perform an immunostain for Occludin to test if ZO-1 was expressed in tight junctions in the zebrafish neuroepithelium; however the co-expression of Par3-GFP and ZO-1 is consistent with the presence of tight junctions.

The subtly different labelling pattern produced by aPKC and ZO-1 is worth noting. The expression domain of aPKC was thicker than ZO-1 suggesting that the aPKC expression domain extends partly onto the apical surface. Apical aPKC has been described in

cultured epithelial cells so this result is not unexpected (Suzuki and Ohno, 2006). β-catenin was the least restricted protein of those labelled, since cellular morphology was difficult to visualise using the antibody we have in the Clarke laboratory. It is a component of adherens junctions, but also an important signalling molecule in pathways including canonical Wnt signalling, therefore a wider expression domain is not a surprise (Molenaar et al., 1996). These observations support the presence of both tight junctions and adherens junctions in the zebrafish hindbrain neuroepithelium during neurogenesis.

## An acto-myosin fence may contribute to segment integrity, but does not establish compartments

Filamentous actin is expressed throughout the neuroepithelium, but is enriched at the apical surface and strongly enriched at rhombomere boundaries. In *Drosophila* imaginal discs an acto-myosin fence prevents the mixing of dorsal and ventral compartments (Major and Irvine, 2005; Major and Irvine, 2006), so rhombomere boundaries could also use Actin to prevent mixing in this way. Elevated filamentous actin has been reported in rhombomere boundaries in zebrafish at 16hpf and chick at stage 17 (Cooke et al., 2001; Guthrie et al., 1991), however it was suggested that the time when actin is enriched in chick rhombomere boundaries is too late in development for an actin fence to play an important role in the segregation of cells before boundary formation, which begins at tail bud stage (Cooke et al., 2005). I examined filamentous actin expression at 14, 16 and at 30hpf. While enriched at rhombomere boundaries at the two later stages it was not enriched at the earlier time-point, therefore I can confirm that filamentous actin is not expressed early enough to be a major player in the earliest stages of boundary formation; yet it may play a role in maintenance of separation between cells from different rhombomeres after boundary formation.

# Chapter 4:

# The genetic control of apical end foot size

## *Introduction*

In the previous chapter I demonstrated that regulation of apical end foot size is segmental. Borders of gene expression contain boundary cells with larger apical end feet (AEF) than non-boundary cells. Mean apical end foot size decreases in a graded manner away from boundaries. This observation prompts the question: what mechanism instructs the neuroepithelium to become patterned in this manner?

It is possible that AEF size reflects cellular identity. For example the AEF of adult neural stem cells are smaller than ependymal AEF (Mirzadeh et al., 2008). Therefore if cell identity affects AEF size, then signalling pathways involved in cell fate specification should also affect AEF size. The Notch signalling pathway is an important determinant of cell fate (Chitnis, 1995) and in boundary formation (Micchelli and Blair, 1999), that may be conserved across the animal kingdom. Manipulating the function of Notch pathway components to increase or decrease Notch signalling results in over or under-production of neurons respectively (e.g. Appel and Eisen, 1998; Chitnis et al., 1995; Henrique et al., 1997). Also, knockout of *notch* from the *Drosophila* imaginal wing disc prevents dorso-ventral boundary formation (Micchelli and Blair, 1999). Boundary cell development is partially dependent upon the Notch signalling pathway in zebrafish, however boundary gene expression is still induced in embryos with total elimination of Notch activation, such as *mindbomb,* but is lost when precocious differentiation exhausts the progenitor pool (Cheng et al., 2004).

Within zebrafish rhombomeres there are three known domains based upon expression of Notch pathway components: boundary, peri-boundary and rhombomere centre. This differential expression leads to different neurogenic potential in the three regions. Rhombomere boundaries express *wnt1*, *wnt3a, wnt8b,* and *wnt10,* and *radical fringe (rfng)* (Amoyel et al., 2005; Cheng et al., 2004; Riley et al., 2004). There is also reduced expression of *notch1a, notch1b, lunatic fringe (lfng)* (from 24hpf onwards) and proneural genes compared with the centre of rhombomeres (Bierkamp and Campos-Ortega, 1993; Cheng et al., 2004; Ke et al., 2008; Nikolaou et al., 2009). This expression pattern is similar to the dorso-ventral boundary in *Drosophila* imaginal wing disc (e.g. Micchelli and Blair, 1999) and indicates heightened Notch activity in

rhombomere boundary cells (fig. 1.2B). *Hes1*, a Notch target gene and repressor of proneural genes is strongly expressed in mouse rhombomere boundaries (Baek et al., 2006) demonstrating that heightened Notch at boundaries is evolutionally conserved.

Peri-boundary cells contain a mixed population of cells fated to differentiate into neurons, that express proneural genes *ngn1*, *ashA* and *ashB, notch1a* and *b,* Notch ligands *deltaA*, *B* and *D* and Notch modulator *lunatic fringe (lfng) (Amoyel et al., 2005; Cheng et al., 2004; Nikolaou et al., 2009)*; and un-specified progenitors that express GFAP, *notch1a* and *notch1b* (Bierkamp and Campos-Ortega, 1993; Cunliffe, 2004; Ke et al., 2008). The two populations are mixed, illustrating that lateral inhibition underlies the cell fate choices made by peri-boundary cells. Within the centre of rhombomeres lie another population of cells that express GFAP (Trevarrow et al., 1990) and less strongly express proneural genes, *deltas* and *notches* indicating a lower neurogenic potential compared with peri-boundary regions (Bierkamp and Campos-Ortega, 1993; Cheng et al., 2004).

Based on the segmental regulation of Notch pathway components and the segmental organisation of apical end feet in the hindbrain, it is reasonable to predict that interfering with neurogenesis by manipulating the Notch signalling pathway may also alter the graded organisation of apical end feet. Total knock-down of Notch function in severe *mindbomb* mutants, results in excessive production of primary neurons and depletion of the progenitor pool (Itoh et al., 2003), along with failed ventricle opening (Bingham et al., 2003). Therefore less severe interventions are required to examine the arrangement of AEF at the ventricular surface in embryos with reduced Notch signalling. This can be achieved through manipulating Notch modulators.

The *fringe* family of Notch modulators, glycosylate Notch receptors and make them more sensitive to Delta and less sensitive to Serrate or Jagged (Bruckner et al., 2000; Moloney et al., 2000; Panin et al., 1997). *Drosophila fng (dfng)* is required to form boundaries independent of dorsoventral patterning of wing disc cells (Rauskolb et al., 1999) and mislocalisation of *dfng* by mutation resulted in disrupted wing growth and ectopic formation of wing margins (Irvine and Wieschaus, 1994). Prior to ventricle opening *Lfng is expressed* throughout r2 and 4 (Prince et al., 2001) and after ventricle opening *Lfng is* expressed in neural progenitors in peri-boundary domains (Nikolaou et al., 2009), therefore its expression is consistent with a role in boundary formation and/or neurogenesis. Segmentation is not significantly disrupted in zebrafish injected with a morpholino against *lfng*, possibly due to compensation from other members of the

*fringe* family. Notch activation is, however reduced as neurons are overproduced (Nikolaou et al., 2009).

Histone deacetylase 1 (Hdac-1) is a negative regulator of Notch signalling (Cunliffe, 2004; Golling et al., 2002). *Hdac-1*$^{-/-}$ fish have a phenotype reminiscent of Notch over-activation, since proneural genes *ash1b* and *ngn1* are expressed at lower levels and the number of HuC and Isl1 expressing neurons drops. Notch target genes, for example *her6* are up-regulated and GFAP expressing glial fibres spread throughout each rhombomere instead of being concentrated in peri-boundary regions (Cunliffe, 2004). Segmental identity genes, such as *ephA4* are expressed normally; therefore this mutant appears to affect the segmental organisation of the hindbrain without disrupting the expression of segmental genes (Cunliffe, 2004).

In conclusion manipulating the Notch signalling pathway results in changes in cell fate and adversely affects boundary formation. It is currently not known if Notch pathway manipulation results in changes to the arrangement of intercellular junctions in the hindbrain. I disrupted Notch signalling via *hdac-1* and *lfng* and analysed the arrangement of apical end feet in the hindbrain, discovering that the Notch signalling pathway controls apical surface area of neuroepithelial cells.

# *Results*

## Hdac-1 is involved in determining apical end foot size and patterning

The Notch signalling pathway is an essential requirement for the formation and maintenance of the dorso-ventral compartment boundary in *Drosophila* imaginal wing discs (de Celis and Garcia-Bellido, 1994; de Celis et al., 1996; Rulifson and Blair, 1995). Histone deacetylase 1 (*hdac*-1) is a transcriptional repressor of notch target genes, since in *Hdac-1* mutant zebrafish, Notch target genes become up-regulated throughout the hindbrain. For example *her6* expression increases. This is mirrored by a decrease in the number of neurons. (Cunliffe, 2004) (fig. 4.1D-G). To determine if *hdac-1* and therefore probably Notch signalling is required to pattern AEF, I carried out an analysis of AEF distribution in the *hdac-1* mutant.

At 30 hpf *hdac1*$^{-/-}$ zebrafish were immunolabelled with the human ZO-1 antibody. I found that the gross morphology of the hindbrain ventricular surface was similar to wt; however in some cases the IV ventricle was closer to a cylindrical rather than chalice shape, due to the roof plate not expanding. However this did not prevent measurement of AEF sizes (fig. 4.1A,B). As in wt fish, rhombomere boundary cells appeared larger than non-boundary cells and the linear interfaces between boundary cells from adjacent rhombomeres were also still clearly visible. In fact, in 5/5 animals analysed, the interface between neighbouring rhombomeres appeared to be more linear than wt boundaries. All 22 boundaries appeared linear and 14/22 boundaries were perfectly straight, which only occurred in 2 wildtype boundaries (n=58). Division of AEF in each rhombomere into tiers produced up to 9 groups, one more than the 8 tiers in wt fish. Measurement of AEF areas in *hdac1*$^{-/-}$ hindbrains revealed that, as in wt fish the peri-boundary end feet were considerably smaller than boundary end feet (fig. 4.1J,K). Boundary AEF were $11.3 \pm 7.7\mu m^2$ (n=275, 11 boundaries, 5 embryos), 87% larger than peri-boundary cells, which were $6.0 \pm 3.9\mu m^2$ in size ($P<0.001$, n= 255). There was a 13% difference in AEF size between peri-boundary and tier 3 AEF (average size= 5.9, n= 323), however depending upon the statistical test this difference may or may not be significantly different. A T-test with Welch correction (which accounts for uneven population variances) gave a P value of 0.05, while Tukeys HSD test, (which is a more stringent test that compensates for the large number of tests that were carried out) gave a P value of 0.2. Peri-boundary cells, when compared with tiers 4-9 also produced ambiguous results. They were significantly larger than the other tiers using a t-test with

Welch correction (P<0.05 in all cases), however were not using Tukey's HSD (P>0.06 in all cases). Therefore there is little difference between the size of AEF in peri-boundary cells compared with other tiers in *hdac*$^{-/-}$ rhombomeres and so are too similar to each other to be classed as a different group with certainty. Neither test could find a statistical difference between AEF sizes from tier 3 to tier 8, suggesting that these tiers contain a homogenous group of AEF sizes (n=323, 335, 326, 329, 297 and 96 respectively). Fitting an exponential decay curve to the *hdac-1*$^{-/-}$ data set produced a curve with the following equation:

$$\text{AEF size} = 36.9\text{um}^2 \times e^{\wedge(-1.8 \times \text{tier number})} + 6.2\text{um}^2$$

The shape of this curve is remarkably different from the wildtype equation (P = 0.02). Most notably, the slope of the curve is almost 0 from tier 3 to 9, which illustrates the lack of any difference between the average AEF sizes between these groups.

When compared with wild type AEF, some notable differences were found: the average AEF size was 6.6 ± 4.8µm2, which was 16% larger than wt (P<0.001 Student's t test, wt: n=3277, *hdac-1*$^{-/-}$: n=2536). Remarkably *hdac-1*$^{-/-}$ boundary AEF were 17% smaller than wt boundary AEF (P<0.05 wt: n=311, *hdac-1*$^{-/-}$: n=275), while non-boundary cells were 24% larger than their wt counterparts (P<0.001 student's t test wt: n=2966, *hdac-1*$^{-/-}$: n=2261). There was no difference, however, between the size of *hdac-1*$^{-/-}$ peri-boundary cells and wt peri-boundary cells (P>0.5 T Test with Welch correction, P>0.99 Tukey's HSD. wt: n=413, *hdac-1*$^{-/-}$: n=255). These observations suggest that *hdac-1*$^{-/-}$ mutant hindbrain neuroepithelial AEF sizes are shifted towards the peri-boundary size. Boundary AEF were still the largest, but smaller than wt boundary AEF, while tiers 3-8 were larger than wt AEF and similar in size to peri boundary AEF, which did not change (table 1).

Fig. 4.1. Disrupting the Notch signalling pathway affects apical end foot patterning

A-C). Projections of ZO-1 stained 30hpf wt (A), *hdac-1*$^{-/-}$ (B) and *lfng* MO injected (C) hindbrains. Boundaries (arrows) form in all 3 situations. In *hdac-1*$^{-/-}$ boundaries are straighter than in wt or *lfng* knockdown.

D-I). Wt, *hdac-1*$^{-/-}$ and *lfng* MO injected hindbrains stained for Hu to label neurons (D,E,F,I) and GFAP to label glial fibres, which are found in peri boundary regions in wt. (G,H). Neuronal number is depleted and glial fibre distribution expanded in *hdac-1*$^{-/-}$ (E,H)(Cunliffe et al., 2004), while neuronal number increased in *lfng* MO fish (F), but close examination on neuronal arrangement shows their segmental organsisation is not significantly disrupted (I).

J-L). The AEF were divided into tiers along the anterior posterior axis. *Hdac-1*$^{-/-}$ have an extra tier, while *lfng* knockdown fish have one fewer. Exponential decay curves were fitted to AEF measurements. Wt and *lfng* knockdown curves are not statistically different, while the *hdac-1* curve is different from both with 0 slope from tiers 3-9.

Scale bar: 25µm

ml: midline

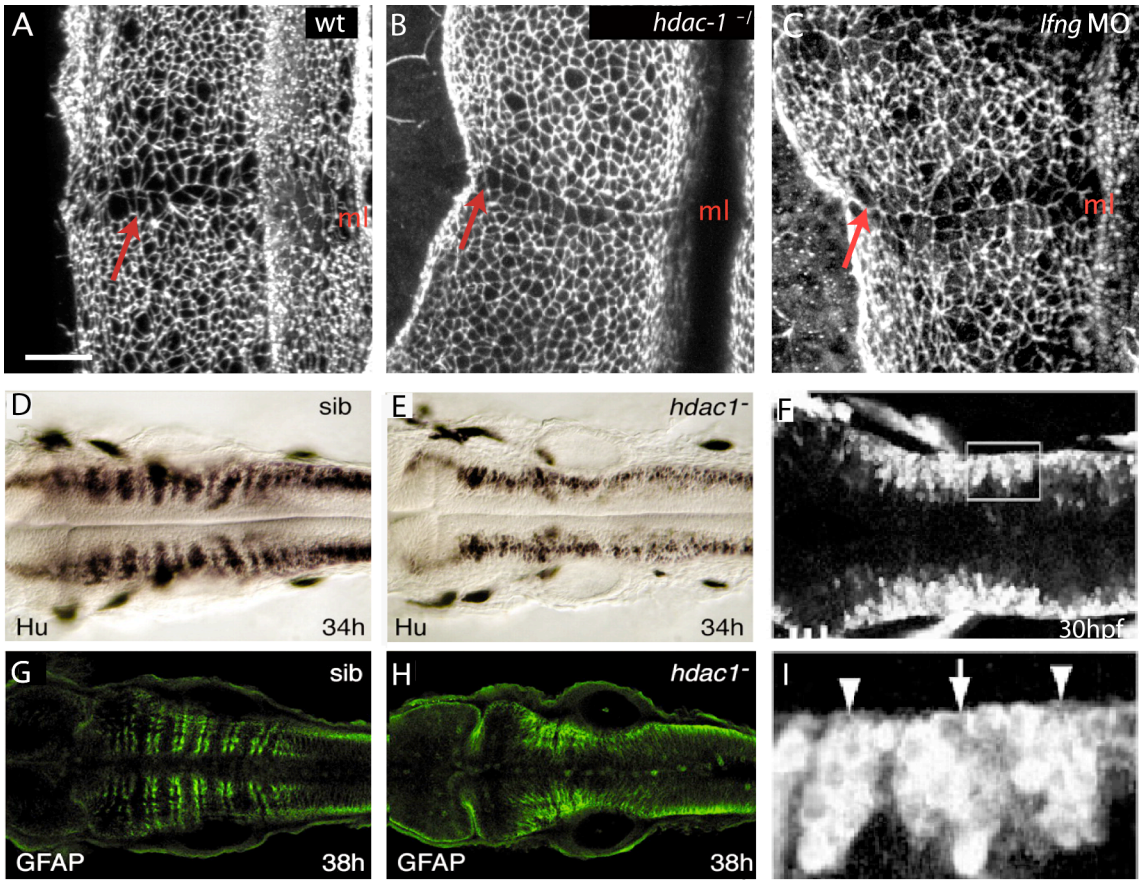


Cunliffe et al., 2004) (Nikolaou et al., 2(

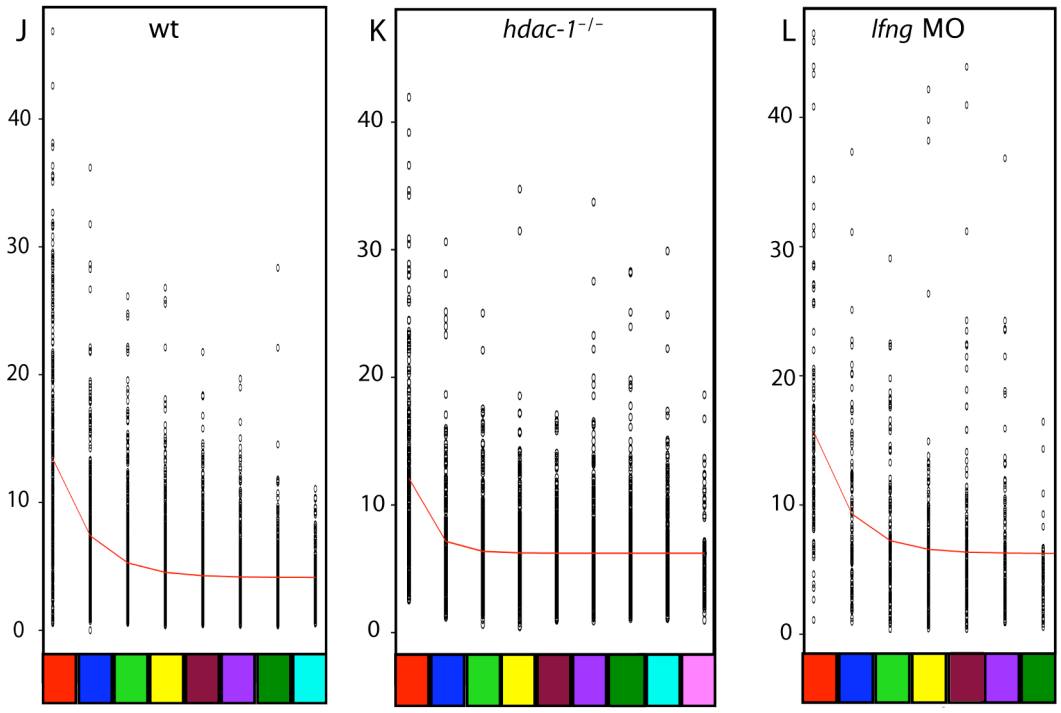


Fig. 4.1. Disrupting the Notch signalling pathway affects apical end foot patterning

## *Lfng* regulates AEF size but not patterning

*Lfng* is a glycosyltransferase that modulates Notch signalling (Moloney et al., 2000) and its fly orthologue is essential for dorsoventral compartmentation of the imaginal wing disc (Irvine and Wieschaus, 1994). *Lfng* is expressed in rhombomeres 2 and 4 in the zebrafish hindbrain (Prince et al., 2001). Zebrafish injected with a morpholino against *lfng* have a mild phenotype characterised by an over-production of neurons at the expense of progenitors, without significantly disrupting the patterning of the hindbrain during early neurogenesis (fig. 4.1F,I) (Nikolaou et al., 2009). ZO-1 immunolabelling and AEF measurements were carried out to determine if boundary cells and/or the graded distribution of AEF sizes were disrupted in embryos lacking *lfng*. The gross morphology of the hindbrain in *lfng* knockdown embryos was similar to wildtype. The IV ventricle opened, albeit to a lesser degree than in wildtype embryos, and there was a clear segmental patterning of AEF sizes reminiscent of the arrangement in wildtype, suggesting that *lfng* is not required for epithelial patterning. Linear interfaces persisted, with 7/9 linear with minor interruptions, 1/9 perfectly straight and 1 without clear linearity (N=3 embryos, left and right boundaries scored separately, fig. 4.1C).

Detailed analysis of *lfng* knockdown zebrafish revealed that AEF were larger than wildtype embryos. Average AEF size was 8.16 ± 6.1 μm2, 43% larger than wt AEF (P<.001 wt: n=3277, *lfng* MO: n=852 cells, 6 boundaries, 3 embryos, fig. 4.1L). This increase in size correlated with a reduction in the number of tiers from 8 to 7 (table 1). Comparison of individual tiers with their wildtype equivalents revealed that tiers 2 (peri-boundary), to 6 (n=109, 323, 335, 326, 329 respectively) were larger in zebrafish with *lfng* knocked down, while tiers 1 (boundary), and 7 were not significantly different (Tukey's HSD, n=115, 55. fig. 4.1L). As in wt fish, AEF size decreased exponentially with distance from the rhombomere boundaries. This decrease is best represented by the decay curve:

$$\text{AEF size} = 29\mu m^2 \times e^{\wedge(-1.12 \times \text{tier number})} + 6.2\mu m^2$$

The shape of this curve is quite similar to the decay curve that was fitted to the wildtype data and not statistically different (P = 0.78), which suggests that the arrangement of AEF in *lfng* knockdown zebrafish hindbrains is similar to wild type fish. Thus it suggests that *lfng* function is not required for controlling the fine patterning of the neuroepithelium, but that it does have a general affect of the size of AEF.

## Differences in proliferation rates do not affect the graded pattern of hindbrain AEF

Previous studies have suggested that rhombomere boundary cells have different cell cycle kinetics in comparison with non-boundary cells (Guthrie et al., 1991b). It is well documented that there is minimal growth during the first 24 hours of zebrafish development, as cell size halves during mitosis during this period. Therefore it was necessary to determine if large boundary AEF were simply a product of these cells dividing at a slow rate and thus remaining larger than the faster proliferating non-boundary cells. Inhibiting mitosis during neurulation and neurogenesis tested this possibility. Cell division was inhibited with a cocktail of aphidicolin (100µM) and hydroxyurea (20mM), which has an efficiency of >70% (Clarke lab, unpublished data). Drugs were applied at tailbud (the onset of hindbrain segmentation and 10 hours prior to ventricle opening), until 30hpf. Embryos were fixed at 30hpf and immunostained for ZO-1 expression (fig. 4.2A,B).

I found that average AEF in division-blocked embryos was 13.0 ±11.0µm$^2$ 129% larger than control embryos (P<0.001 wt: n=3277, div block: n =1039 cells, 16 boundaries, 8 embryos (fig. 4.2C). This large increase in the average AEF size across the same surface area of apical surface resulted in fewer tiers; up to 6 in division blocked embryos, rather than 8 in control embryos and the AEF in each of these six tiers were larger than their wt equivalents (P=0, Tukey's HSD). This large increase in AEF size did not greatly affect the distribution of AEF sizes though the hindbrain. The largest AEF were located in rhombomere boundaries, at 24.2±16.9µm2 (n=184). These AEF were 87% larger than non-boundary cells, which were 10.6±7.2µm2 =3277 (n =855). The graded distribution of end foot size was remarkably similar to wt embryos (table 1). The exponential decay curve that best fits the data set is:

AEF size = 51.5µm$^2$ x e ^ $^{(-1.18 \text{ x tier number})}$ + 8.4µm$^2$ (fig. 4.2 D,E).

As in embryos with knockdown of *lfng*, the shape of this decay curve is similar to the decay curve fitted to control AEF sizes (P =0.5). The differences in the curve are caused by a general increase in AEF size, rather than a change in their fine patterning. This result indicates that the graded distribution of apical end foot size is not caused by a slowed rate of cell division in rhombomere boundary cells and that there must be another mechanism by which this organisation is generated.

**Table 1: Distribution of AEF sizes within 30hpf rhombomeres**

| | Apical End Foot Size ($um^2$) | | | |
|---|---|---|---|---|
| | WT | Div Block | Hdac-$1^{-/-}$ | LFNG MO |
| Boundary | 13.5 | 24.2 | 11.3 | 15.7 |
| Peri-boundary | 7.0 | 13.0 | 6.8 | 9.1 |
| Tier 3 | 5.6 | 10.2 | 5.9 | 7.5 |
| Tier 4 | 4.8 | 8.9 | 5.9 | 6.2 |
| Tier 5 | 4.5 | 7.4 | 6.1 | 7.2 |
| Tier 6 | 4.2 | 7.8 | 6.0 | 6.4 |
| Tier 7 | 3.7 | | 6.1 | 4.6 |
| Tier 8 | 3.5 | | 5.7 | |
| Tier 9 | | | 5.3 | |

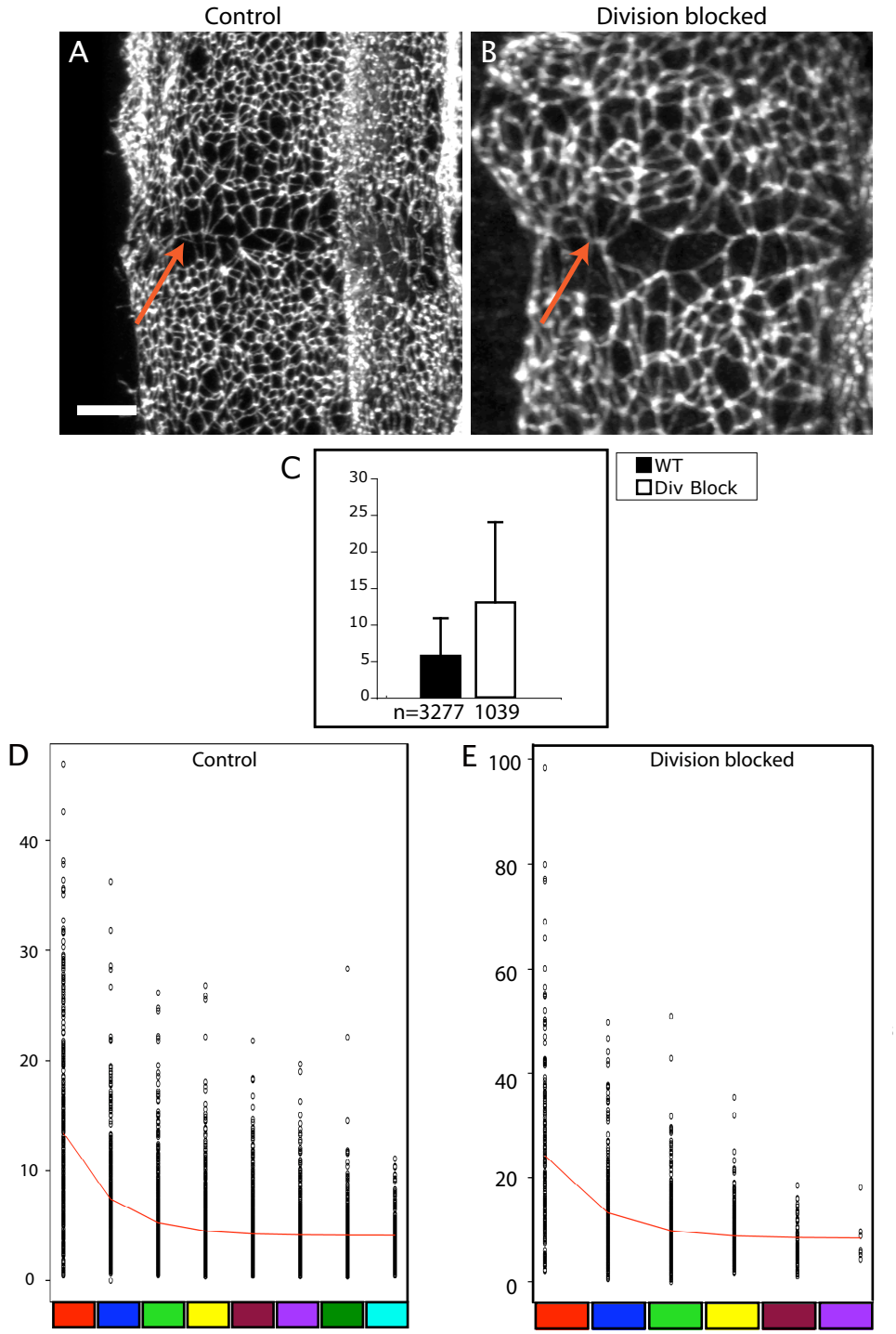


AEF size = 26.5µm2 x e^(-1.1 x Tier) + 4.13µm2
N= 3277 cells, 15 boundaries, 7 embryos

AEF size = 51.5µm2 x e ^ (-1.18 x tier) + 8.4µm2
N= 1039 cells, 16 boundaries, 8 embryos

Fig. 4.2. Cell division block increases AEF size without affecting their graded distribution
A). Projection of wt hindbrain ventricular surface labelled with ZO-1 showing a rhombomere boundary (arrow).
B). When division was blocked at tail bud stage until 30hpf with aphidicolin and hydroxyurea, all AEF were increased in size compared with control embros. Boundary AEF appear larger than non boundary AEF.
C). AEF size comparison shows division blocked AEF are 2.3x larger than wt AEF.
D,E). The AEF were divided into tiers along the anterior posterior axis. Wt had 8 tiers, division blocked 6. Exponential decay curves fit to AEF sizes. The curve is similar in both conditions suggesting that the graded pattern of AEF size persists in division blocked embryos.
Scale: 25µm

## Redundancy in function of the ZO protein family

The reason why AEF sizes in the hindbrain are patterned in a graded manner may be due to the organisation of the junctional domains between the apices of neuroepithelial cells. The Zona Occludens family has been shown the be an important mediator of tight junction, adherens junction and gap junction assembly and maintenance (Bazzoni, 2003; Fanning et al., 1998; Furuse et al., 1994; Haskins et al., 1998; Itoh et al., 1999; Itoh et al., 2001; Wittchen et al., 1999), thus it is possible that they may play a role in creating the graded difference in apical end foot size in the hindbrain during development. In an attempt to test this hypothesis, a splice blocking morpholino against the second intron in ZO-1.1 (Ensemble sequence: ENSDARG00000059419) was designed and injected into zebrafish zygotes.

Irrespective of the dose of morpholino injected, ZO immunoreactivity persisted (fig. 4.3A,B). At 0.5pmol, ZO expression appeared unaffected in 30hpf embryos, which displayed a wt phenotype (fig. 4.3B). Western blot analysis using the human anti ZO-1 antibody produced 3 bands: 205, 140 and 160 Kda from control embryos. The 205Kda band was not detected after injection of 0.5pmol morpholino, however the two smaller bands were still present (fig. 4.3C). Online bioinformatics tools were used in an attempt to elucidate which proteins produced these three bands. The amino acid sequence of the 300 amino acid peptide used to generate the human anti ZO-1 antibody was BLASTed against the zebrafish genome. The sequence aligned with the predicted sequences of ZO-1.1 (93% of 256 aas), ZO-1.2 (91% of 266 residues) (ENDSARG00000062597) and ZO-2.1 (64.7% of 224 residues) (ENDSARG00000063309), suggesting that the three bands detected by Western blot correspond to these three proteins and that the 205 Kda band, absent in the 0.5pmol injected embryos, was ZO-1.1 (fig. 4.3D).
To date it is not possible to confirm whether this is the case because zebrafish ZO-1.1, 1.2 and 2.1 have not been cloned. Based upon their predicted amino acid sequences their molecular weights were calculated to be 185, 170 and 125 Kda respectively. This discrepancy between predicted molecular weights and the sizes of the bands detected by Western blot will only be explained once the ZO family of genes has successfully been cloned.

What can be concluded is that ZO-1.1 is not essential for normal development, since knocking down the expression of this protein does not produce a phenotype. The protein that remains detectable by immunohistochemistry using the human anti ZO-1 antibody

appears to be sufficient for neural tube formation, ventricle opening and also for the differences in AEF size distribution within the hindbrain.

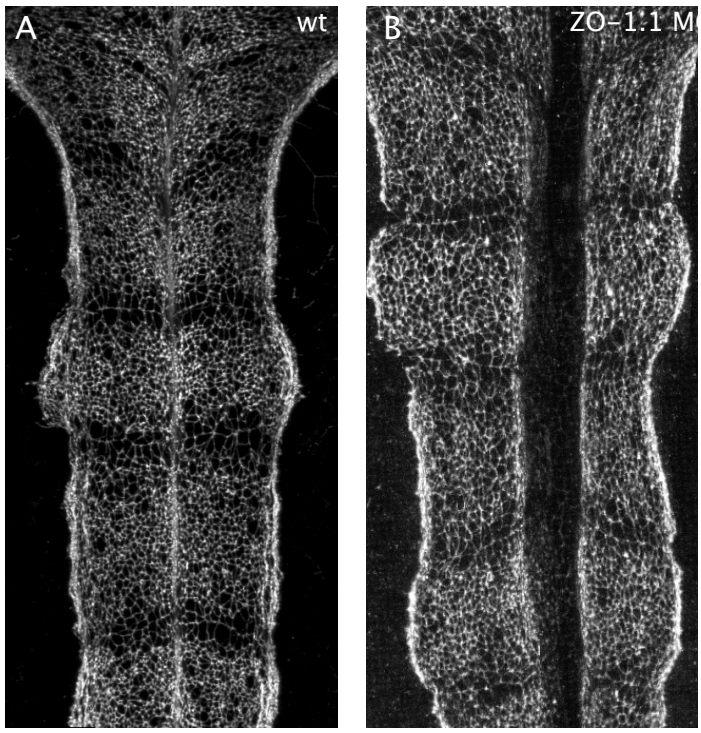


C

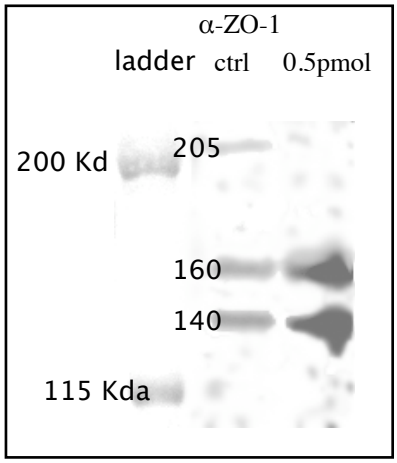


D

| Protein | Predicted length | Mass (Kd) |
|---|---|---|
| ZO-1.1 | 1612-1692 | 180-188 |
| ZO-1.2 | 1463-1555 | 165-173 |
| ZO-2.1 | 1108-1223 | 125-135 |
| ZO-2.2 | 1071-1179 | 120-132 |

Fig. 4.3. Redundancy in function of the ZO-1 family of proteins

A,B). Projections of ZO-1 expression in the hindbrain of 30hpf control and 0.5pmol ZO- 1.1 MO injected fish. ZO expression appears to persist and the hindbrain appears normal.
C). Western blot analysis of control and 0.5pmol ZO-1 morpholino injected fish shows that the αZO-1 antibody detects 3 proteins with masses of 205Kd, 160 Kd and 140Kd. Translation of the 205Kd protein is prevented by the morpholino.
D). Based upon their predicted masses, amino acid length and sequences, it appears that the three bands belong to ZO-1.1, ZO-1.2 and ZO-2.1 (Kiener et al., 2007). There is a large discrepancy between predicted masses and their actual masses, indicating that the predicted masses are innacurate.
Scale bar: 25μm

# *Discussion*

## Apical end feet sizes are partly controlled by the Notch signalling pathway

I have ruled out the possibility that the size differences are due to variable rates of proliferation along the anterior posterior axis (Guthrie et al., 1991) because inhibition of proliferation from tailbud to 30hpf had no effect upon the distribution of AEF sizes. Through manipulating the Notch signalling pathway I have demonstrated that Notch signalling plays a role in dictating AEF size. The Notch signalling pathway is an important mediator of boundary formation in dorso-ventral compartmentation in *Drosophila* imaginal wing discs (Micchelli and Blair, 1999) and in rhombomere boundary formation and maintenance (Amoyel et al., 2005; Cheng et al., 2004) so I took two approaches to disrupt Notch signalling and examined the effect on patterning of AEF in the hindbrain: Knockdown of *lfng* by morpholino injection and *hdac-1* mutant zebrafish.

### Hdac-1 regulates AEF size

I examined *hdac-1*$^{-/-}$ zebrafish, rather than more severe mutants, such as *mindbomb* because severe reduction of Notch signalling causes nearly all progenitors to differentiate early (Itoh et al., 2003) and so would not be appropriate. *hdac-1*$^{-/-}$ mutant zebrafish have overactive Notch signalling and the segmental arrangement of GFAP expressing progenitors and neurons was disrupted, without any severe anatomical defects (Cunliffe, 2004). Fourth ventricles were smaller and more cylindrical in most mutants and AEF size distribution was remarkably different from wildtype fish. There were only 2 statistically different tiers of neuroepithelial cells, rather than 4 in wildtype fish. The size of peri-boundary AEF was the same in both conditions, while *hdac*$^{-/-}$ boundary cells were smaller than non boundary cells and rhombomere centre cells were larger than their wild type equivalents. Therefore segmental AEF size differences are diminished in *hdac-1* mutants and they all approach peri-boundary AEF size. *Hdac-1*$^{-/-}$ mutants gain glial cells, that express GFAP, at the expense of neurons, which appear less concentrated at boundaries and in the centre of rhombomeres (Cunliffe, 2004). This loss of segmental organisation is also apparent in the pattern of GFAP expressing glial fibres; they spread throughout the entire length of each rhombomere in *hdac1*$^{-/-}$ fish (Cunliffe, 2004), instead of only populating peri-boundary regions (Trevarrow et al., 1990). Therefore there is a correlation between segmental arrangement of cell types and

segmental patterning of the apical surface, both of which are dependent upon Notch signalling.

**Lfng does not affect AEF size**

I have used *lfng* knockdown to generate a moderate reduction in Notch signalling and examined their ventricular surfaces with ZO-1 staining to determine if hindbrain epithelial patterning was disrupted. *Lfng* is a member of the Fringe family of proteins that modulate Notch activation (Bruckner et al., 2000; Moloney et al., 2000; Munro and Freeman, 2000). It is expressed in rhombomeres 2 and 4 in the zebrafish hindbrain (Prince et al., 2001). Zebrafish injected with a morpholino against *lfng* have a mild phenotype characterised by an over production of neurons at the expense of progenitors (Nikalaou et al. 2009). *Lfng* knockdown injection failed to induce any changes in AEF patterning in the hindbrain. There was a slight increase in average size, but this affected all tiers equally. This increased size may have resulted from increased neurogenesis that occurs when *lfng* is knocked down because progenitor number would have been reduced compared with wt, while the ventricular surface area did not appear to change extensively. Therefore each AEF could be larger to fill the space. The unchanged distribution of AEF sizes was not surprising since segmentation was normal in embryos with *lfng* knocked down embryos at 28hpf and the neurogenic phenotype is mild (Nikalaou et al. 2009). Perhaps the ZO-1 labelling pattern will appear different in older fish, when the number of neural progenitors is decreased in embryos with *lfng* knocked down (Nikalaou et al., 2009).

It is surprising that boundary position and shape are normal in fish with *lfng* knocked down. Since the edge of *fng* expression determines where the dorso-ventral boundary forms in the *Drosophila* wing disc (Panin et al., 1997; Rauskolb et al., 1999) and that *lfng* is expressed in alternating rhombomeres in the zebrafish (Prince et al., 2001), it would be reasonable to assume that boundary formation should be disrupted in fish with *lfng* knocked down. There may have been enough residual Lfng protein to prevent a phenotype or compensation by other Fringe proteins could preserve boundary formation in zebrafish. *Rfng* is expressed in boundary cells (Cheng et al., 2004) and so it could ensure boundary formation proceeds in the absence of *Lfng*. When expressed along the anterior posterior border of wing imaginal discs, mouse *lfng* had no effect upon Wg expression (i.e. boundary position), while expression of *dfng,* mouse *mfng* and mouse *rfng* did have effects (Johnston et al., 1997). So Lfng may be a less potent modulator of Notch activity and mediator of boundary formation than the other vertebrate Fringes.

**Boundary cells do not require *hdac-1* or *lfng* to form**

It is interesting that despite changing the size of boundary AEF and affecting the linearity of the interface between rhombomeres, alteration of Notch activity did not fully prevent boundary AEF from becoming enlarged. So it is tempting to conclude that Notch signalling and Lfng activity are expendable for boundary formation. Complete inhibition of Notch signalling was not possible because gross anatomical aberrations in the *mindbomb* mutant result in disrupted ventricle opening (Bingham et al., 2003; Schier et al., 1996) so visualising the ventricular surface is not possible. The boundary marker *foxb1.2* can be detected (albeit disrupted and at lower levels) in *mindbomb* mutants at 24hpf and segmental expression of EphA4 is relatively normal, but then disappears as the ventricular zone is lost (Cheng et al., 2004), which implies that boundary formation is not wholly dependent on Notch signalling in the zebrafish. Since there is widespread intermingling of dorsal and ventral cells in *notch*$^{-/-}$ imaginal discs (Micchelli and Blair, 1999), the vertebrate hindbrain must employ other mechanisms to prevent mixing of different segments.

## Wnt signalling as a possible signal to pattern hindbrain AEF

The graded arrangement of AEF suggests that there is a graded signal instructing the neuroepithelial cells on how large their AEF should be. *Wnt1, wnt3a, wnt8b,* and *wnt10b* are expressed at rhombomere boundaries (Riley et al., 2004) and they have been shown to be important both in ensuring that boundary specific genes (e.g. *rfng* and *foxb1.2)* are restricted to boundaries and also in the expression of proneural genes (Amoyel et al., 2005). It is also requires normal Notch signalling at rhombomere boundaries in order to be expressed (Cheng et al., 2004) and over expression of *wnt1* in *mindbomb* mutants partially rescued boundary cell loss (Riley et al., 2004) . Therefore the Wnt signalling pathway is a suitable candidate for the graded signal that may pattern apical arrangement in the hindbrain.

## Eph-Ephrin signalling as a future experimental direction

Since Eph-Ephrin interactions are important for segregation of alternate rhombomeres (Xu et al., 1995; Xu et al., 1999), they could protect the hindbrain from extensive disruption in zebrafish with deficient Notch signalling. It will be interesting to discover how the arrangement of AEF is altered in zebrafish with disrupted rhombomere segregation from lacking one or more Eph or Ephrin. Studies have shown that EphrinB1 interacts with Par6 and that over expression of, or knock down of EphrinB1 disrupts both tight junction formation and cell-cell adhesion (Jones et al., 1998; Lee et al., 2008). Therefore the Eph-Ephrin interactions at rhombomere boundaries could influence junctional composition and AEF sizes at boundaries. However results of these experiments may need to be treated with caution because manipulating Eph-Ephrin signalling could alter the ability of neuroepithelial cells to form or maintain intercellular junctions. The interaction of Ephrins with polarity proteins could therefore affect apical end feet size independently of rhombomere segregation.

## Redundancy in the Zonula Occludens family

A surprising and disappointing finding was a morpholino against ZO-1 did not produce a phenotype and immunofluorescence for ZO-1 protein persisted and. Injections of large masses of the morpholino to the point of poisoning the embryo could also not eliminate immunolabelling (data not shown). Western blots with the ZO-1 antibody produced many bands, only one of which was eliminated. The morpholino sensitive band disappeared at morpholino concentrations that did not generate a phenotype. This confusing result was explained by the publication of predicted gene sequences for 5 ZO proteins in the zebrafish: ZO-1.1, ZO-1.2, ZO-2.1, ZO-2.2 and ZO-3 (Kiener et al., 2007). Blasting the antigen used to create the ZO-1 antibody showed that there is a high probability that the antibody can bind to ZO-1.1, ZO-1.2, and ZO-2.1 and based upon their predicted molecular weights and gene sequences, the morpholino may knock down expression of only ZO-1.1. mRNA for all 4 of these ZOs is present in the neural tube during development. Their sequence similarities and a lack of discernable phenotype in ZO-1 deficient zebrafish strongly suggest they play redundant roles in development. Further knock down of other ZO proteins alongside ZO-1.1 is needed to address the role that ZOs play in brain morphogenesis, however since ZO proteins are expressed in the EVL throughout the first 12 hours of development, they could be essential for

maintaining the integrity of the early embryo and so may prohibit their knock-down by injection at the 1 cell stage.

In summary, the arrangement of AEF sizes within the zebrafish hindbrain is partially dependent upon the Notch signalling pathway. Increased Notch signalling in *hdac-1* mutants caused AEF sizes to change towards peri-boundary size, while decreased Notch signalling in embryos deficient for *lfng*, did not affect AEF patterning, but did cause a general increase in AEF size.

# Chapter 5:
# Linear arrangements of enlarged apical end feet in other CNS boundaries

## *Introduction*

Rhombomeres are unequivocally regarded as neuromeres: subdivisions that behave as developmental compartments. Features that are used to define compartments include morphology, borders of gene expression, lineage restriction, apically displaced S phase nuclei and axon tract position. Other brain regions have these properties suggesting they also contain neuromeres. However, which regions of the forebrain are separate compartments is currently unclear (fig. 1.3). The prosomeric model originally divided the forebrain into 6 domains called prosomeres based upon gene expression patterns and morphology (Puelles and Rubenstein, 1993; Rubenstein et al., 1994). The telencephalon contained three prosomeres (P4-6) and the diencephalon the other three (P1-3) (Puelles and Rubenstein, 1993; Rubenstein et al., 1994). Since lineage restriction is not complete in the telencephalic segments, whether they are true compartments has been questioned (Szele and Cepko, 1998).

Lineage tracing in chick diencephalon agreed that the diencephalic subdivisions were prosomeres (Figdor and Stern, 1993). However dividing the diencephalon into 3 compartments may have been premature, because the hypothalamus was excluded from P1-3. Instead it was placed in P5 along with rostral telencephalic structures (Puelles and Rubenstein, 1993). Since there is lineage restriction within the hypothalamus, it may be another diencephalic compartment (Golden and Cepko, 1996). It has also been argued that, based upon scanning EM, axon tract location, gene expression and lineage restriction, the chick synencephalon can be divided into two, to create a further addition to the potential number of diencephalic prosomeres (Figdor and Stern, 1993). The zona limitans intrathalamica (ZLI) was originally suggested to be the border between D1/ D2 (dorsal and ventral thalamus), because D1 expresses d*lx2* and s*ix3* while D2 expresses *gbx2* and *irx3* (Kiecker and Lumsden, 2005; Larsen et al., 2001). Strong *Hes1* expression in the mouse ZLI indicates heightened Notch signalling, a property common to the dorso-ventral boundary in *Drosophila* imaginal discs (de Celis and Garcia-Bellido, 1994) and hindbrain boundaries (Cheng et al., 2004). Further work has suggested that the ZLI is also a compartment since it is many cells wide in the ventral

neural tube (Scholpp et al., 2006; Zeltser et al., 2001), a lineage restricted zone (Zeltser et al., 2001) and is flanked by *lfng* expressing domains at both its anterior and posterior borders (Zeltser et al., 2001). Therefore there is a total of 6 potential neuromeres in the vertebrate diencephalon.

Whether this is true is unclear because detection of some compartment borders has not been reproducible (Larsen et al., 2001). The subdivision of the synencephalon into two has been contested, since other researchers could not find any boundary characteristics within it until late neurogenesis, when it had a boundary-like morphology, but not lineage restriction (Larsen et al., 2001). Likewise, experimenters were unable to see a morphological boundary, or lineage restriction between the edge of D1 and the telencephalon (Larsen et al., 2001). The developmental stage at which each prosomere becomes visible and disappears varies from one compartment to the next (Figdor and Stern, 1993; Larsen et al., 2001), further complicating their characterisation. Therefore it is unclear at the present how the diencephalon is subdivided into prosomeres.

There is also conflicting evidence regarding whether the midbrain hindbrain boundary (MHB) is a boundary, compartment, or a mixture of the two. Lineage restriction between r1 and the midbrain has been found in some contexts (Langenberg and Brand, 2005; Millet et al., 1996; Zervas et al., 2004), but not others (e.g. Jungbluth et al., 2001) and in some cases the MHB itself has been shown to be a lineage restricted zone (Zervas et al., 2004).

I have demonstrated that rhombomere boundaries are characterised by a unique epithelial organisation - enlarged apical end feet organised in two rows, one belonging to the anterior rhombomere and one to the posterior rhombomere, with a linear interface between the rows. The two boundary properties may be a common feature of CNS boundaries, so I used the pattern of ZO-1 expression at the ventricular surface as an objective means to locate other CNS regions with boundary-like characteristics. I provide evidence to support the prosomeric theory of brain compartmentation as boundary characteristics in the apical arrangement of the neuroepithelium were present at all proposed prosomere borders and discovered a novel subdivision of the midbrain.

## *Results*

### The zona limitans intrathalamica is a hybrid boundary/compartment

The zona limitans intrathalamica (ZLI) is situated at the border between the ventral and dorsal thalami. Defining the ZLI as either a boundary or a separate compartment has been source of debate (Figdor and Stern, 1993; Larsen et al., 2001). The size of the AEF within and around the ZLI were measured to determine if the ZLI possessed the same epithelial properties as seen in rhombomere boundaries - enlarged AEFs and linear interfaces with surrounding tissue – as a test to determine if it can be classed as a boundary or a compartment.

**Evidence in support of the ZLI being a boundary**

A transgenic zebrafish line that expresses GFP in Sonic Hedgehog (Shh) expressing cells (Neumann and Nuesslein-Volhard, 2000) was used to visualise the ZLI, since ZLI cells expresses Shh. Embryos were co-immunolabeled for GFP and ZO-1, then dissected so that the ventricular surface of the diencephalon could be imaged with a confocal microscope (fig. 5.1A,B).

The average size of AEF in cells expressing GFP was 8.4±4.3$\mu m^2$, 40% larger than the 5.0±3.6$\mu m^2$ in cells not expressing GFP ($P<0.001$ student's t-test, n=639, 1680 respectively, N=3 embryos. Fig. 5.1D). The interface between AEF expressing GFP and AEF not expressing GFP (the edge of the ZLI) was also linear in some areas, but in others a linear interface was not clear (fig. 5.1A,B). Both of these observations support the argument that the ZLI is a boundary.

**Evidence for the ZLI being a compartment**

The dorsal half of the ZLI is one or two cells thick along the anterior posterior axis, suggesting that the ZLI is not large enough to be a compartment. In the ventral half, the ZLI is larger in size along the anterior posterior axis, so it appears to be too large to be a boundary and may be a compartment. The GFP expressing ZLI cells were divided into up to 8 tiers with AEF at the edge of the ShhGFP expressing zone (prospective boundary cells) coloured red, prospective peri-boundary AEF were coloured green and so on. (fig. 5.1C). Prospective boundary cells were 13% larger in size than other Shh:GFP expressing AEF: 9.2 ±5.2µm2, compared with 8.1± 5.2$\mu m^2$ (n = 190, 449 respectively, fig. 5.1E). Cells outside the ZLI that did not express GFP were also subdivided into tiers. The AEF touching GFP expressing AEF (potential boundary cells)

were labelled mauve (fig. 5.1C), prospective peri-boundary cells labelled green etc. (fig. 5.1C). The mean AEF area of these prospective boundary cells were 6.8±4.2μm2 (n=214), 46% larger than the mean AEF size of the other GFP negative cells, which were on average 4.6±3.5μm2 ($P<0.001$, student's t-test, n=1466).

Comparing each GFP expressing tier with its equivalent GFP negative tier revealed that from tiers 1-6, GFP expressing, ZLI AEF were larger than the equivalent tiers of GFP negative AEF ($P<0.007$). This was not the case for tiers 7 and 8, where there was no significant difference between GFP expressing and non-expressing cells ($P>0.07$).

The distribution of AEF sizes within the ZLI was similar to the distribution of sizes in the hindbrain, since AEF appeared to decrease in size with increasing distance from the edge of the ZLI. Unlike in the hindbrain a linear fit best represented the data, rather than an exponential decay (fig. 5.1E,F).

The equation for the line of best fit for GFP expressing cells is:

AEF = 9.97 – 0.55 x tier number

And the equation for the line of best fit for cells not expressing GFP is:

AEF= 6.54 – 0.38 x tier number

The linear regression confirms that AEF size decreases with increasing distance from the interface between ZLI and non-ZLI cells. The decrease appears more pronounced within the ZLI than outside the ZLI, however the difference in slope is not significantly different ($P=0.09$). This result supports the argument that the ZLI is a compartment in its own right, since the same graded decrease in AEF size occurs on each side of rhombomere boundaries.

Fig. 5.1. Apical end feet (AEF) sizes in and around the zona limitans intrathalamica (ZLI)

A,B). ZLI cells expressing Shh:GFP (green) and ZO-1 (red) immunolabelling reveal enlarged AEF in the ZLI. There is a linear arrangement of AEF in some places around the edge of the ZLI, marked by brackets.

C). AEF were divided into tiers based upon their position with respect to the interface between GFP expressing (GFP+) and non-expressing cells (GFP-). GFP+ cells at the interface are coloured red and GFP- cells at the interface coloured purple.

D). Comparison of mean AEF size between GFP+ and GFP- cells. AEF were 40% larger ($P<0.01$) in GFP+ cells than in GFP- cells.

E,F). Plots of GFP+ (E) and GFP- (F) AEF sizes. Largest AEF are located at the interface between GFP+ and GFP- AEF size decreased in a linear fashion both away from and into the ZLI. GFP+ AEF within tiers 1 - 6 are larger in size than GFP- AEF from the same tier ($P<0.05$). Tiers 7 and 8 are not statistically different.

Scale bars: 25$\mu$m.

vt: ventral thalamus, dt: dorsal thalamus, ZLI: zona limitans intrathalamica, a: anterior, p: posterior, d: dorsal, v: ventral.

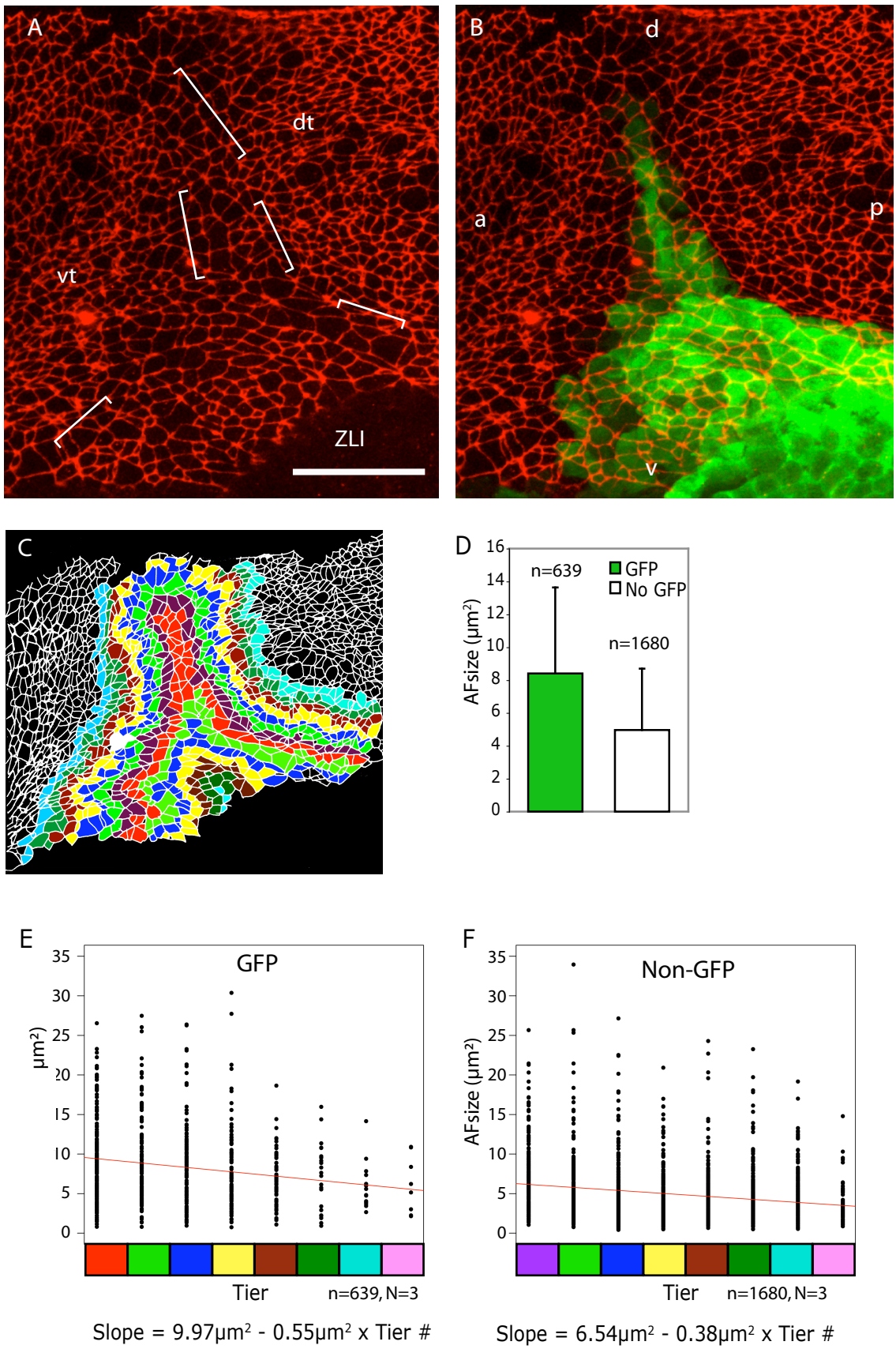


Fig. 5.1. Apical end feet (AEF) sizes in and around the Zona Limitans Intrathalamica (ZLI)

The ZLI has properties of both a boundary and a compartment. It appears to be a boundary because ZLI AEF are, on average, larger in size than non-ZLI cells, there is a linear interface between the ZLI and the surrounding dorsal and ventral thalami and in the dorsal half of the neural tube it is only 1-2 cells thick. It appears to be a compartment because in the wider ventral half of the neural tube it is too wide to appear to be a boundary and there is a graded distribution of AEF sizes with the largest AEF at the interfaces of the ZLI with the dorsal and ventral thalami and the smallest in the centre of the ZLI. It is therefore possible to define the ZLI as a hybrid boundary/compartment according to these epithelial characteristics. This is a significant discovery because it confirms that linearity and increased AEF at the interface between different populations of cells and a graded distribution of AEF sizes are common features of CNS boundaries and compartments and so these three properties may be useful, objective means to demarcate boundaries between different sub-regions of the CNS.

#### ZO-1 labelling reveals further CNS boundaries

To test if there are other areas in the CNS that display boundary characteristics in their AEF size arrangement, ZO-1 immunolabelling of the midbrain and diencephalon ventricular surface was examined after dissection to reveal the ventricular surface. At 30 hpf, 3 zones with boundary characteristics at the midbrain were seen (fig. 5.2, 5.3 and 5.4). The most striking boundary was the midbrain hindbrain boundary (MHB), seen in 4/4 embryos, which in some places had two rows of enlarged AEF running across it, while in other places the arrangement of AEF was less obviously 2 rows (fig. 5.4G,H). Whilst the AEF were enlarged, the interface between them was not linear to the same degree as hindbrain boundaries. It is positioned close to the anterior edge of the infolding of the neural tube and so may mark the edge of Otx2 expression. There were also two rows of linearly arranged, enlarged AEF in a position corresponding to the midbrain/diencephalon boundary (fig. 5.2, 5.3). This was seen in 3/3 embryos, however it could not be traced fully to the dorsal edge of the midbrain in one of the embryos. One further boundary-like stripe was also seen in the middle of the midbrain in 3/3 embryos. Again it appeared incomplete in one embryo (fig. 5.2, 5.3).

There were at least 6 diencephalic boundaries (fig. 5.1). Four are clearly identifiable as the diencephalon/midbrain boundary, the ZLI (7/7 embryos), the ventral thalamus/ hypothalamus boundary (2/2 embryos) and the diencephalon/telencephalon boundary (2/2 embryos). The other two were ambiguous. Two lie caudal to the ZLI so may

correspond to the synencephalon/parencephalon (thalamus) boundary (5/6 embryos) and to the boundary within the synencephalon (3/3 embryos, fig. 5.2, 5.3, 5.4A-F)).

The floor plate also has boundary characteristics, with enlarged AEF and a liner interface with non-floor plate cells in the hindbrain (fig. 5.4I).

There is discrepancy in the N numbers for each area with boundary characteristics because I did not attempt to visualise all boundary regions in each dissection and in some cases damage to the tissue destroyed the boundary region.

These observations support the prosomeric theory of the neuroepithelium, where it is not just the hindbrain that is subdivided into segments, however, co-immunolabelling ZO-1 with antibodies against the segmental proteins that pattern the midbrain are needed to confirm that these boundary-like arrangements lie at patterning gene expression borders and so can be considered true boundaries.

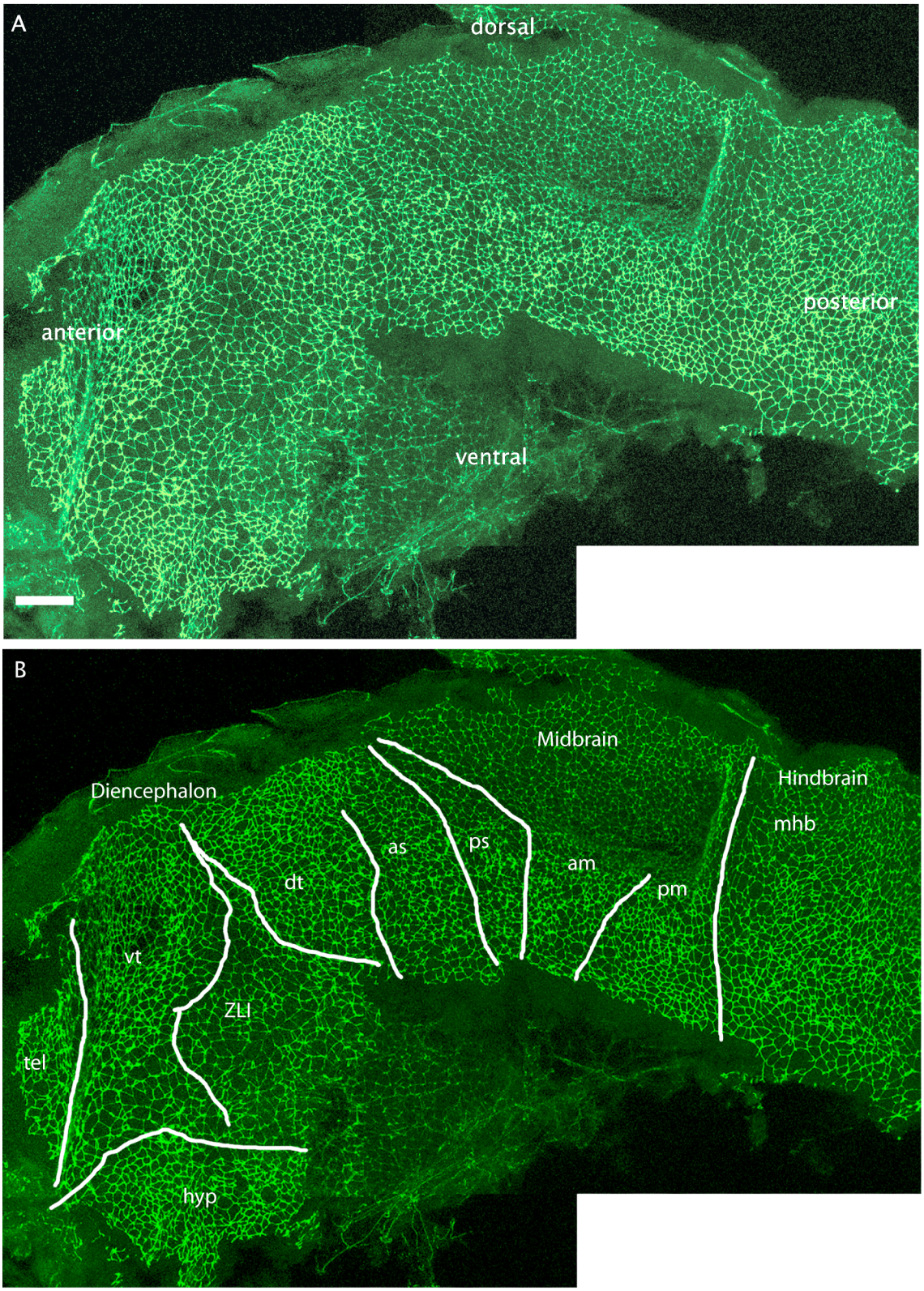


Fig. 5.2. Boundaries in the midbrain and diencephalon
A,B) Projection of a confocal stack of half a dissected zebrafish forebrain labelled for ZO-1 expression to visualise the ventricular surface of the diencephalon, midbrain and part of the telencephalon. Regions with boundary characteristics are visible by their enlarged apical end feet and linear arrangement. They have been marked in white to aid recognition (B). Scale: 25µm
tel:telencephalon, hyp: hypothalamus, vt:ventral thalamus, dt: dorsal thalamus, as: anterior synencephalon, ps: posterior synencephalon, am: anterior midbrain, pm: posterior midbrain, mhb: midbrain hindbrain boundary. Anterior is left, dorsal is up.

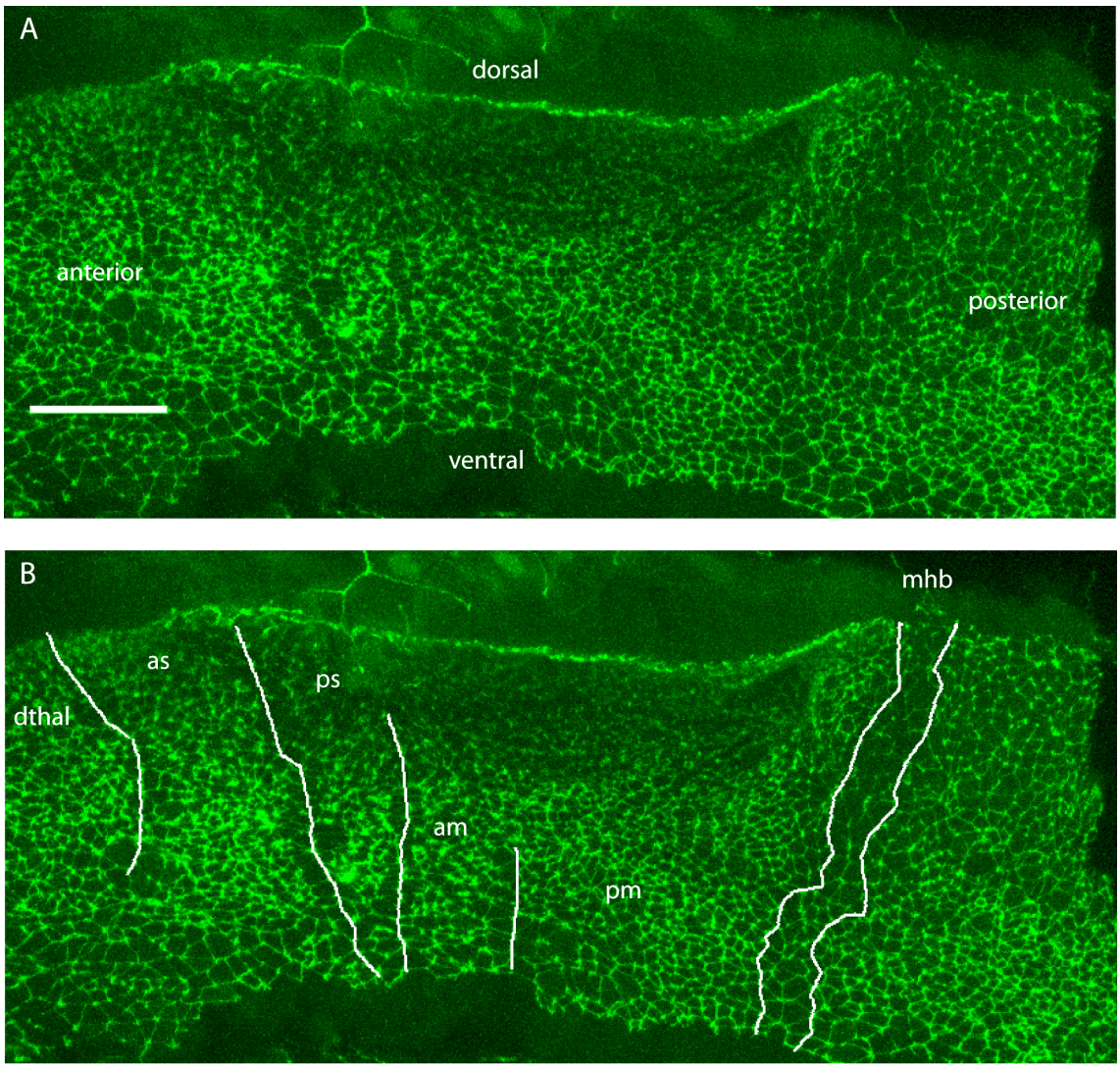


Fig. 5.3. Midbrain and diencephalic boundaries 2
A,B) Projection of a confocal stack of half a dissected zebrafish forebrain labelled for ZO-1 expression to visualise the ventricular surface of the midbrain and part of the diencephalon. Enlarged AEF are arranged in rows in positions corresponding to proposed compartment boundaries and have been marked to aid recognition (B). The boundaries are located in the same places as in the previous figure and include the midbrain-hindbrain boundary, a boundary within the midbrain, the midbrain-diencephalic boundary, mid synencephalon boundary and the synencephalon-dorsal thalamus boundary.
Scale: 50µm
As: anterior synencephalon, am: anterior midbrain, dthal: dorsal thalamus, MHB: midbrain - hindbrain boundary, pm: posterior midbrain, ps: posterior synencephalon. Anterior is left, dorsal is up.

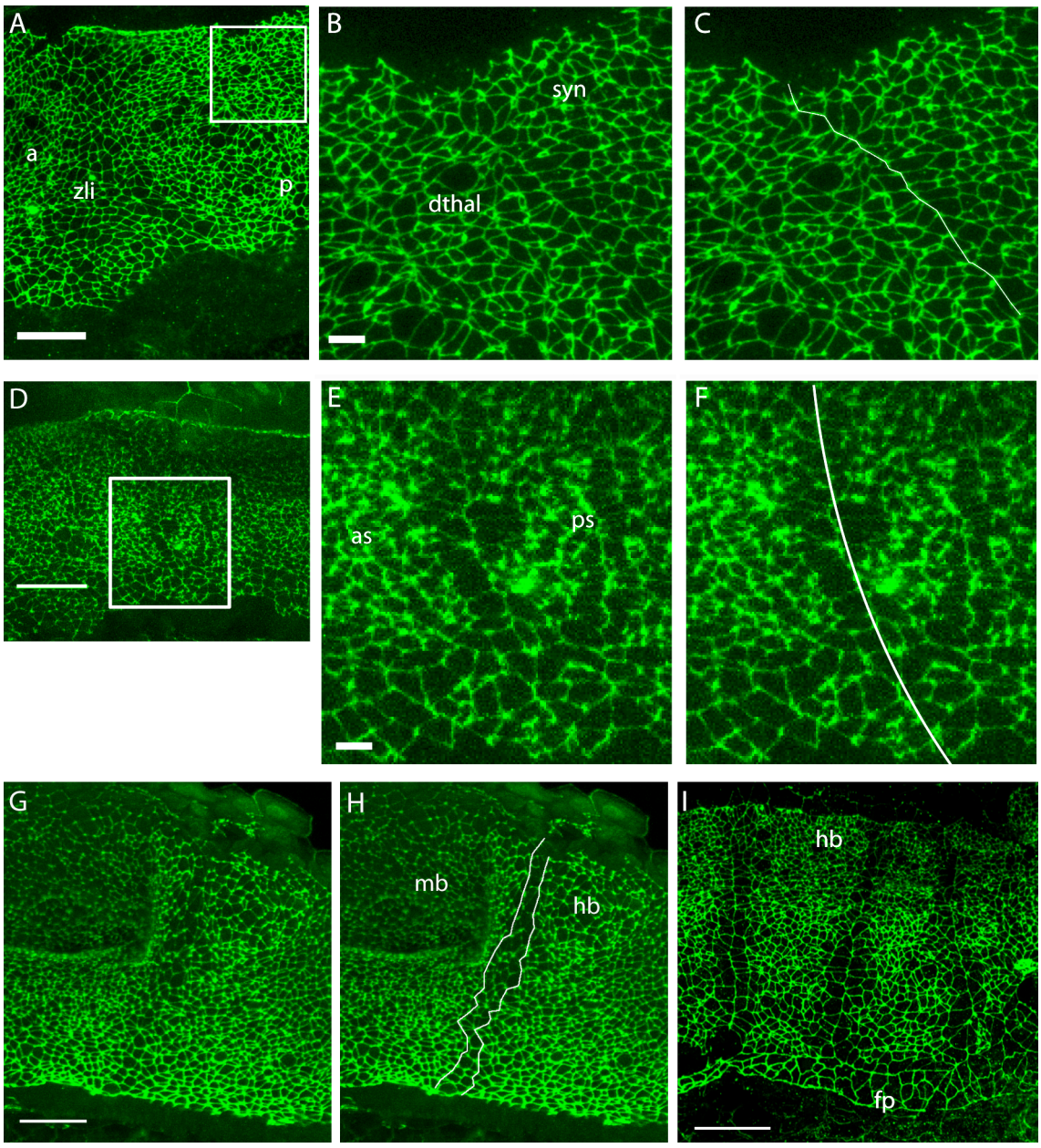


Fig. 5.4. High magnification views of CNS boundaries
A-C). Posterior to the ZLI lies the proposed boundary between the dorsal thalamus and anterior synencephalon (pretectum). B and C are magnifications of the box in A that show AEF are enlarged and arranged in two rows reminiscent of rhombomere boundaries. The proposed boundary has been marked in white to aid recognition (C).
D-F). The synencephalon (pretectum) is subdivided into two by a boundary-like region that also has the apical arrangemet seen in rhombomere boundaries. E and F are enlargements of the box in D. The proposed boundary has been marked in white to aid recognition (F).
G,H). Enlarged AEF are also a feature of the anterior border of the midbrain-hindbrain boundary, marked in white (H).
I). Floor plate AEF are enlarged and have a linear border with the ventral hindbrain.
Scale: A,D,G,H,I: 50µm. B,C,E,F: 10µm.
a: anterior, p: posterior, zli: zona limitans intrathalamica, dthal: dorsal thalamus, syn: synencephalon, as: anterior synencephalon, ps: posterior synencephalon, mb: midbrain, hb: hindbrain, fp: floor plate

## *Discussion*

### The zona limitans intrathalamica as a hybrid boundary / compartment or an extension of the floor plate

There has been uncertainty regarding whether the ZLI is a boundary or a compartment because different studies found it to have different properties. It is regarded as a border between D1 and D2 (dorsal and ventral thalamus) since S phase nuclei lie closer to the apical surface in the ZLI than in neighbouring areas, boundary markers are present within it (Larsen et al., 2001). There is also alternating expression of AchE and of PNA binding in D1-D4 that would be disrupted if the ZLI is a compartment (Figdor and Stern. 1993). The ZLI also has important functions in patterning the thalamus by secreting Shh (Scholpp et al. 2005). Therefore it has boundary properties. On the other hand, it is a lineage restricted zone and is an island of *lfng* non expressing cells (Zeltser et al. 2001). At stages 12-13 in chick embryos this *lfng* free zone covers 1/3 of the diencephalon, suggesting that the ZLI begins as a large compartment then shrinks in size as it matures. The ZLI should have a boundary at both its anterior and posterior edges because *lfng* is expressed at both of these edges, but not inside the ZLI. This is because the edge of *fng* expression demarcates the dorso-ventral boundary in *Drosophila* wing discs (Irvine and Wieschaus, 1994) and *lfng* is expressed in alternating rhombomeres, marking their boundaries (Johnston et al., 1997; Prince et al., 2001). This gives it compartment properties. In the dorsal half of the neural tube the ZLI is narrow and so appears similar to rhombomere boundaries, however it appears more like a compartment in the ventral half of the neural tube because it is many cells wide. It could therefore be a hybrid boundary/compartment.

My investigation into the properties of the zona limitans intrathalamica (ZLI) suggests that it is a hybrid boundary-compartment since it has properties of both. It has properties of a boundary since its AEF are considerably larger than non-ZLI AEF, while other properties are more ambiguous: there is often a linear arrangement of enlarged AEF at its edge. In the dorsal half of the neural tube its small size makes this arrangement appear boundary-like. Ventrally the ZLI widens and the boundary splits into two, one at the anterior edge and the other at the posterior edge of the ZLI. There were two rows of enlarged AEF, one inside and the other outside the ZLI in much the same arrangement as between adjacent rhombomeres and there was a graded decrease in AEF size both into and away from the ZLI. It could therefore be a triangular compartment.

There is another possibility regarding the categorisation of the ZLI. The ZLI and floor plate both express Shh. Unlike the hindbrain, I could not find a clear boundary that demarcated where the floor plate ended and the ZLI began. Therefore it is possible that the ZLI is actually an extension of the floor plate that has invaded the thalamus. I have shown in the hindbrain that the floor plate is separated from the rest of the CNS by a linear boundary and that floor plate AEF are larger than non-floor plate AEF. It is a lineage restricted zone (Fraser et al., 1990) and there is also extensive literature detailing how the floor plate patterns the neural tube (Ericson et al., 1995). All of these features it shares in common with the ZLI.

## Using ZO expression to find other CNS boundaries

Enlarged contacts with the ventricular surface have previously been found in scanning electron micrographs of chick rhombomere boundaries (Ojeda et al. 1998). At the dorsoventral border in *Drosophila* imaginal wing discs the apical surface of boundary cells is not larger than non-boundary cells, however dorsal and ventral boundary cells are arranged in two clear lines (Major & Irvine. 2005). Therefore epithelial modification and arrangement of boundary cells may be conserved across species. So enlarged AEF and linear arrangements of AEF may be objective markers of segment boundaries and these properties can be used to identify other CNS compartment boundaries.

Aside from rhombomeres and the ZLI, the most striking boundary was a stripe of large AEF running the length of the midbrain hindbrain boundary (MHB). Much like the ZLI there is argument over if the MHB is a compartment or a boundary (e.g. Langenberg and Brand, 2005; Millet et al., 1996; Zervas et al., 2004). My data shows boundary characteristics that lie approximately 1/3 away from the anterior edge of the infolding of the neural tube at the MHB. This may coincide with the posterior edge of Otx2 expression, which is also a lineage restriction point and marks the anterior edge of the MHB, but will need to be confirmed with a co-immunolabelling of ZO-1 and Otx2 (fig. 1.4) (Langenberg and Brand, 2005). I found no evidence for a boundary at the posterior edge of the MHB, but the complicated folding of the neural tube may have prevented its detection.

Another clear boundary separated the midbrain from the diencephalon. This has been categorised as a boundary in terms of morphology, lineage restriction, gene expression and nuclei position (Figdor and Stern, 1993; Rubenstein et al., 1994) and so I can confirm unequivocally that this also has epithelial characteristics of a boundary. There

are two boundaries within the diencephalon posterior to the ZLI, which could mark the border between first, the synencephalon (pretectum)/dorsal thalamus and second, the mid-synencephalon division proposed by Figdor and Stern (Figdor and Stern, 1993).

In the prosomeric model proposed by Pueles and Rubenstien the hypothalamus is included in P5, a group that includes telencephalic structures such as the neocortex and medial and lateral ganglionic eminences (Bulfone et al., 1993; Puelles and Rubenstein, 1993; Rubenstein et al., 1994). My data do not support this grouping since the boundary at the edge of the hypothalamus isolates it from all other segments.

The synencephalon/dorsal thalamus boundary is transient in chick embryos and in one study did not act as a lineage restriction site, while it did in another (Figdor and Stern, 1993; Larsen et al., 2001). The same two studies disagree over the existence of the mid-synencephalon boundary. Figdor and Stern located it based upon gene expression, morphology and lineage restriction, while Larsen et al. could find none of these attributes, nor did they see other characteristics of boundaries, such as a wider apical spread of S-phase nuclei. My results support the existence of both the synencephalon/dorsal thalamus boundary and the mid-synencephalon boundaries at 30hpf in the zebrafish. Therefore my results suggest the diencephalon is divided into 6, not 4 (Figdor and Stern, 1993) or 3 (Larsen et al., 2001; Puelles and Rubenstein, 1993) parts, being the hypothalamus, ventral thalamus, ZLI, dorsal thalamus, anterior and posterior synencephalon.

Finally I found a novel boundary in the midbrain, suggesting that there are at least 2 compartments in this brain region. This is a novel finding with respect to neuromeres as the midbrain is classed as a single segment in the neuromeric model (Bulfone et al., 1993; Rubenstein et al., 1994).

In summary the zebrafish ventricular surface is patterned in a way to suggest that the prosomeric theory is correct. Dye transfer experiments at the ZLI, the border between the dorsal and ventral thalamus confirm there is indeed a functional boundary between these two neuromeres. This correlation between enlarged AEF and reduced dye transfer occurs at both hindbrain boundaries and the ZLI, supporting the hypothesis that AEF with boundary characteristics are compartment boundaries.

# Chapter 6:
# Boundaries inhibit communication between adjacent segments

## *Introduction*

Gap junctions are vertebrate channels that electrically and chemically couple cells (Dermietzel, 1998). They are predominantly located at the intercellular junctions of epithelial cells (Dermietzel, 1998; Giepmans, 2004). A single gap junction channel is composed of two docked connexons. Connexons are transmembrane hexamers composed of Connexins, which assemble into a barrel formation with a central pore (fig. 1.6A)(Unwin and Zampighi, 1980).

Neural progenitors are extensively coupled by functional gap junctions in chick hindbrain, mouse and rat cortex (Bittman et al., 2002; Lo Turco and Kriegstein, 1991; Martinez et al., 1992) in a cell cycle dependent manner (Bittman et al., 1997). Gap junction communication within the VZ encourages proliferation and coordinates the developmental programs of coupled cells. For example, anti Connexinx43 gel decreased proliferation of mouse retinal progenitors (Tibber et al., 2007) and gap junction blockade significantly reduced proliferation in embryonic mouse cortex (Bittman et al., 1997). Cx43 is over-expressed in E18 albino rat retinas, which along with a lack of pigmentation also over-proliferate in a gap junction dependent manner (Tibber et al., 2007).

Borders between epithelial compartments have reduced gap junction connectivity, a phenomenon that is evolutionarily conserved. This has been found in neuroepithelial cells of chick rhombomeres, in the epidermis of larvae of the milkweed bug *Oncopeltus fasciatus*, epithelial cells in maggots of the blowfly *Calliphora erythrocephala* and *Drosophila* (fig. 1.6B,C)(Martinez et al., 1992; Ruangvoravat and Lo, 1992; Warner and Lawrence, 1982). This spatial regulation of intercellular communication may be developmentally significant, because, first, gap junctional communication is important for coordinating proliferation and second, rhombomere boundaries appear capable of preventing the ectopic induction of patterning genes. For example, transplantation of *en2* expressing quail midbrain structures into the embryonic chick hindbrain resulted in induction of *en2* in the host, but only up to rhombomere boundaries (Martinez et al., 1995). It has not been directly confirmed that this induction was via gap junctions,

though. Reduced intercellular communication between rhombomeres has not yet been tested in other vertebrates. Since *cx43.4* mRNA is expressed in rhombomere centres but not boundaries in zebrafish hindbrain (Thisse, 2001), intercellular communication via gap junctions may also be inhibited across zebrafish rhombomere boundaries (fig. 1.6.D). Other CNS compartment boundaries have also not been probed to see if intercellular communication is reduced across them. The zona limitans intrathalamica (ZLI) is a boundary that separates the dorsal and ventral thalamus (Figdor and Stern, 1993), so it will be interesting to discover if gap junction connectivity across the ZLI is reduced.

Calcium signalling has been shown to be important for progenitor cell division/proliferation (Weissman et al., 2004) and differentiation into neurons (Gu and Spitzer, 1995). Progenitors spontaneously generate calcium transients during neurogenesis in rodents, rabbits, *Xenopus,* chick and zebrafish (e.g. Gu and Spitzer, 1997; Owens and Kriegstein, 1998; Syed et al., 2004; Zimprich et al., 1998). Calcium activity in neighbouring cells is coordinated because intercellular calcium waves that require functional gap junctions and/or connexon hemichannels, have been observed in the VZ of rodent cortical slices and in retinas of chick and rabbits (Owens et al., 2000; 1998; Pearson et al., 2004; Syed et al., 2004; Weissman et al., 2004). Since gap junction communication appears to be segmentally regulated, then intercellular calcium activity may be too. To date, segmental restriction of calcium activity in the vertebrate CNS has not been studied. Also, in zebrafish, intercellular calcium waves have not been resolved at single cell level, either because of sparse labelling techniques (Ashworth and Bolsover, 2002), or poor spatio-temporal resolution of the calcium imaging technique (Creton et al., 1998; Webb and Miller, 2003b).

To assess if gap junction communication is segmentally regulated in the zebrafish, I injected gap junction permeable calcein AM into the hindbrain and dorsal thalamus. Rhombomere boundaries and the ZLI both inhibited dye transfer, confirming that zebrafish CNS boundaries do prevent intercellular communication. To address if intercellular calcium waves are segmentally regulated in the neuroepithelium I recorded spontaneous calcium activity and attempted to induce calcium waves artificially. Neither spontaneous nor induced calcium waves occurred, suggesting that the zebrafish hindbrain is not competent to produce calcium waves.

## *Results*

### Reduced gap junction communication across rhombomere boundaries

To test if gap junction coupling is reduced across rhombomere boundaries, the transgenic fish Tg:(PGFP5.3) (Picker et al., 2002), which expresses GFP in rhombomeres 1, 3 and 5 was used. In these embryos it is possible to determine the exact location of the interface between two rhombomeres in living embryos. A gap junction and cell permeable dye, calcein AM was injected directly into the centre of rhombomeres. Once it enters a cell, the dye is cleaved by endogenous esterases and it becomes cell impermeant. However at all times it can pass through gap junctions. I found that the dye spread from the injection site and into the neuroepithelial cells within the targeted rhombomere. There appeared to be little dye transfer into the neighbouring rhombomeres (fig. 6.1A). To quantify the dye transfer, the fluorescence intensity of the dye was measured and plotted. The merged fluorescence image of calcein AM and PGFP5.3 were used to accurately locate the position of the boundaries (fig. 6.1B). To detect with greater ease the location where dye transfer was inhibited, the fluorescence data were processed to find the change in fluorescence intensity per micron (fig. 6.1C). The peak rates of change in fluorescence (i.e. where dye transfer stopped) occurred at rhombomere boundaries in 22/24 occasions ($P<0.05$, $N=17$, fig. 6.1D).

### Decreased coupling between boundary and non-boundary cells

Overloading the brain and spinal cord with calcein AM produced another noteworthy observation. Injection of large volumes of calcein AM into the central lumen of the spinal cord labelled all CNS progenitors, but boundary cells appeared to preferentially labelled with dye. I found 56 clusters of dye-bright cells in 20 embryos. Boundary cells comprised 82% (46/56, $P=0$ student's t test) of these dye-bright clusters (fig. 6.1E,F). This indicates that calcein sometimes does not equilibrate between boundary cells and neighbouring non-boundary cells within a single rhombomere.

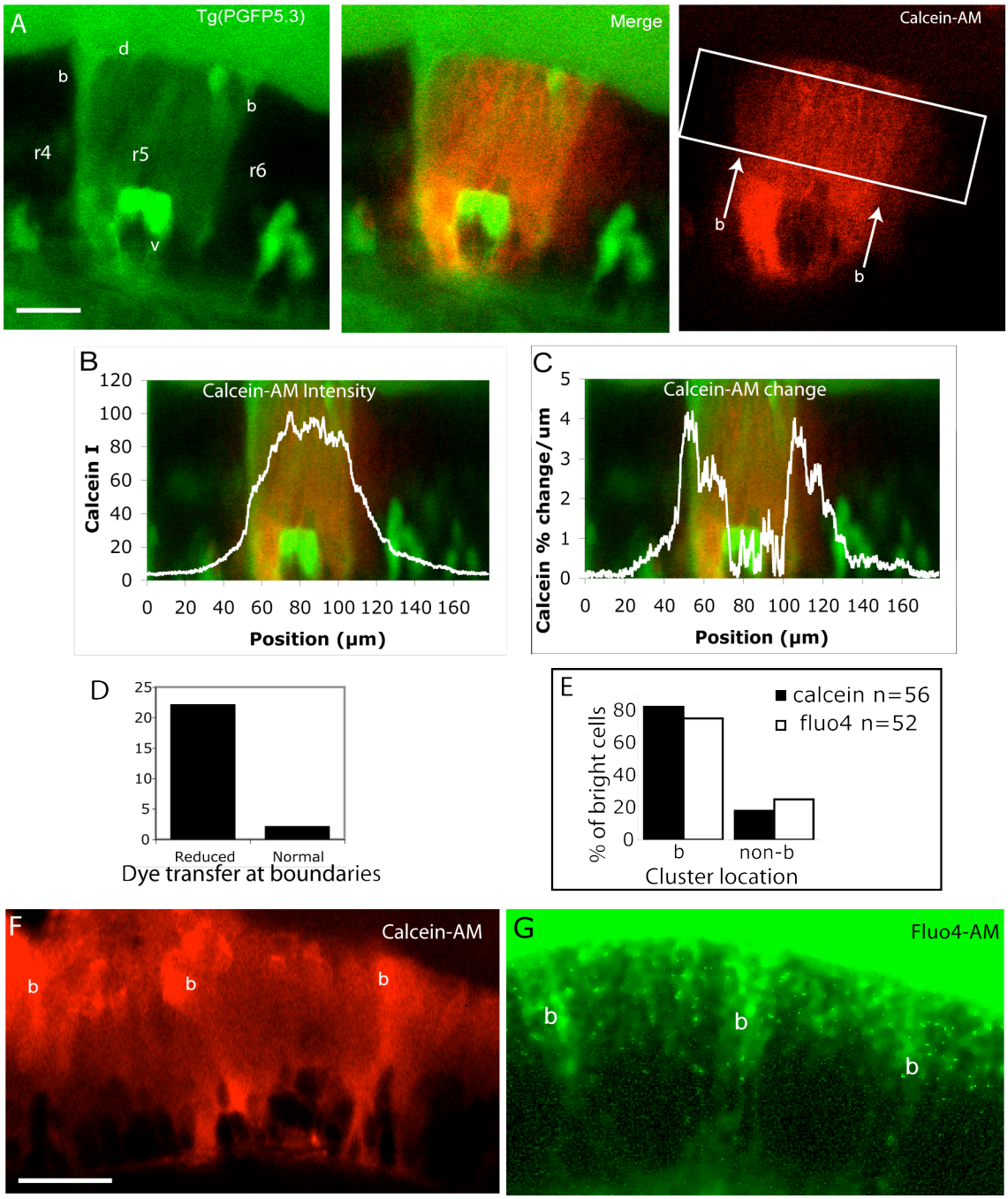


Fig. 6.1. Gap junction communication is reduced at rhombomere boundaries
A). Single confocal section of a lateral view of rhombomeres 4-6 (r4-6) in Tg:(PGFP5.3) fish. R5 is green. Fish were injected with 20-50nl calcein AM (red) into r5. Little or no calcein AM diffused into adjacent rhombomeres. Fluorescence measurements made in white box.
B,C). Calcein fluorescence intensity was measured across the injected rhombomere (B) and converted into % change per micron (C). The trace is underlayed by the fluorescence image to depict the location of rhombomere boundaries. The 2 peak rates of change occur at boundaries, indicating that gap junction connectivity is reduced at rhombomere boundaries.
D). Connectivity was reduced across 19/23 (83%) rhombomere boundaries (N=16, $P<0.001$).
E). Bright clusters were located at boundaries in 46/56 (82%) cases when calcien AM was injected (N=20) and 39/52 (75%) cases when Fluo 4 AM was injected (N=18).
F,G). Single confocal slices in lateral view, showing that injection of large volumes of Calcein AM (E) and Fluo 4 AM (F) into the spinal cord caused rhombomere boundary cells to become more heavily labelled than non boundary cells.
Scale bars: 25µm.
b and arrows: rhombomere boundaries. d: dorsal, v: ventral. Anterior is left. Dorsal is up.

Thus connectivity may be reduced between boundary and non-boundary cells, which is similar to the situation in chick rhombomeres, where injected small molecular weight dyes did not diffuse from boundary cells into non-boundary cells (Martinez et al., 1992). Injection of a different AM dye, Fluo4 AM also preferentially labelled boundary cells (fig. 6.2G). In 18 embryos Fluo4-AM labelled 52 bright cell clusters and 39 (75%, P=0, Student's t test) of these clusters were boundary cells (fig. 6.2E). There is increased extracellular space surrounding rhombomere boundary cells (Heyman et al., 1993), which may have facilitated dye loading into progenitors.

In conclusion these results demonstrate primarily reduced gap junction connectivity between neighbouring rhombomeres. Second, non boundary cells within a rhombomere are coupled the more strongly to other non boundary cells than to boundary cells. These results also suggest that the intercellular diffusion of calcein AM can be used to assay for compartment boundaries elsewhere in the CNS.

## Dye transfer does not occur between progenitors and neurons

The above result suggests that gap junction connectivity is reduced across zebrafish rhombomere boundaries, however it was necessary to confirm that dye transfer occurred through gap junctions and not by another mechanism. To confirm that calcein is transferred between cells coupled with functional gap junctions and not via another route, I tested if dye transfer occurred between two populations of cells known not to be coupled via gap junctions. Differentiated neurons are not coupled to neuroepithelial cells (Bittman et al., 2004; Noctor et al., 2001; Weissman et al., 2004) so I examined whether injecting calcein AM into the neuroepithelium also labelled neurons. Neurons are readily identified in the transgenic line tg(HuC:GFP) (Park et al., 2000) in which GFP is expressed in all neurons (fig. 6.2B). A large volume of calcein AM was pressure injected into the central lumen of either the rostral spinal cord or into the caudal hindbrain. This labelled most hindbrain neuroepithelial cells intensely, while no $GFP^+$ neurons became co-labelled with dye (fig. 6.2A,C,D). This confirms calcein transfer does not occur between uncoupled cells and so confirms that it passes through gap junctions when injected into zebrafish hindbrains.

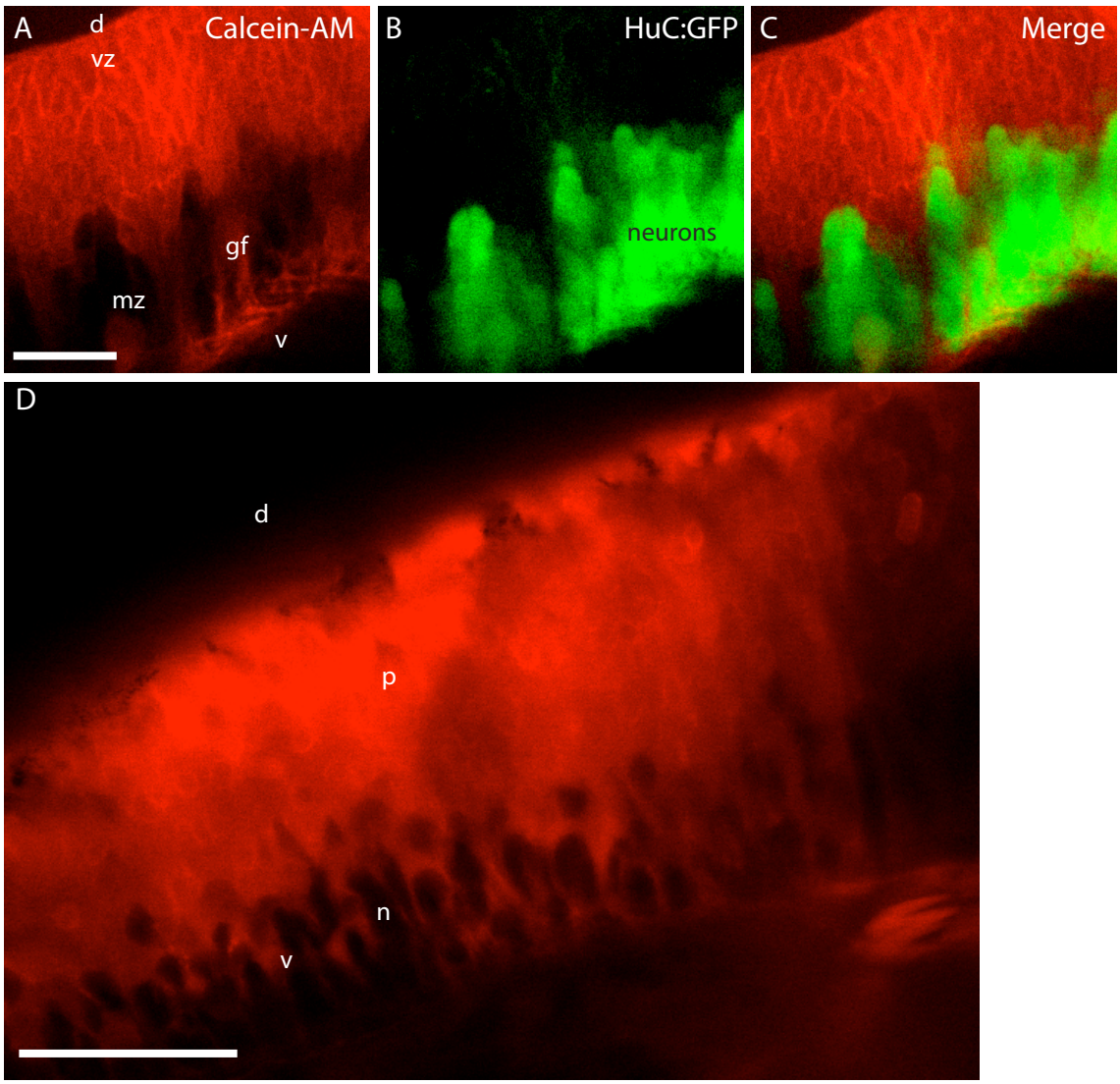


Fig. 6.2. Neurons and progenitors are not coupled by gap junctions
A). Parasagital confocal section of a 30hpf hindbrain, showing how heavy loading of calcein-AM, injected into the spinal cord labels all hindbrain progenitor cells. The mantle zone glial fibres, belonging to progenitors.
B). The transgenic zebrafish Tg(HuC:GFP) expresses GFP in postmitotic neurons located in the mantle zone.
C). There is minimal overlap of GFP and calcein fluorescence demonstrating that calcein-AM cannot diffuse from progenitors into neurons and that the two populations are not coupled to each other by gap junctions.
D). Lateral view of the hindbrain labelled with calcein AM. Note the close association between calcein-AM loaded progenitor processes and the silhouettes of un-labelled neurons.
Scale: 50µm vz: ventricular zone, ma: mantle zone, gf: glial fibre, d: dorsal, v: ventral, p: progenitor, n: neuron.

## The zona limitans intrathalamica inhibits intercellular communication

In the previous chapter I have shown that the arrangement of apical end feet in and around the zona limitans intrathalamica is similar to rhombomere boundaries. To further examine if the ZLI is a boundary I tested if, like rhombomere boundaries, the ZLI prevented the exchange of small molecular weight dyes between cells on either side of it. Calcein-AM was pressure injected into the dorsal thalamus of tg(Shh:GFP) transgenic zebrafish embryos near to the ZLI. As in the hindbrain, the dye spread outwards from the site of injection, but a decrease in fluorescence intensity was apparent at the GFP expressing ZLI cells, indicating that little dye had diffused across the ZLI into the ventral thalamus (fig. 6.3A). The fluorescence intensity of calcein AM was measured and converted into percent change in fluorescence intensity per micron (fig. 6.3B,C). Peak changes in fluorescence occurred at the ZLI in 14/15 embryos ($P<0.001$, fig. 6.3.D). This result demonstrates that small molecular weight molecules are not easily transferred between the dorsal thalamus and ventral thalamus, suggesting that they are separate developmental compartments. This finding further supports the hypothesis that the ZLI functions as a boundary region that separates these two regions of the CNS and so it may serve as a restriction site to developmental signals.

## Calcium activity during neurogenesis includes transients but not intercellular calcium waves

Recent studies of calcium activity in slice cultures of embryonic rat cortex have found coordinated intercellular calcium activity within groups of up to 35 neuroepithelial cells (Owens et al., 2000; 1998; Weissman et al., 2004). I reasoned that if a similar process occurs in the zebrafish hindbrain, then reduced gap junction connectivity at rhombomere boundaries may prevent calcium signalling between rhombomeres. Therefore I developed a calcium imaging technique that enabled me to monitor calcium activity in all VZ cells *in vivo*. Zebrafish embryos were injected with 2ng calcium green dextran at the 1 cell stage to ubiquitously label the hindbrain VZ.

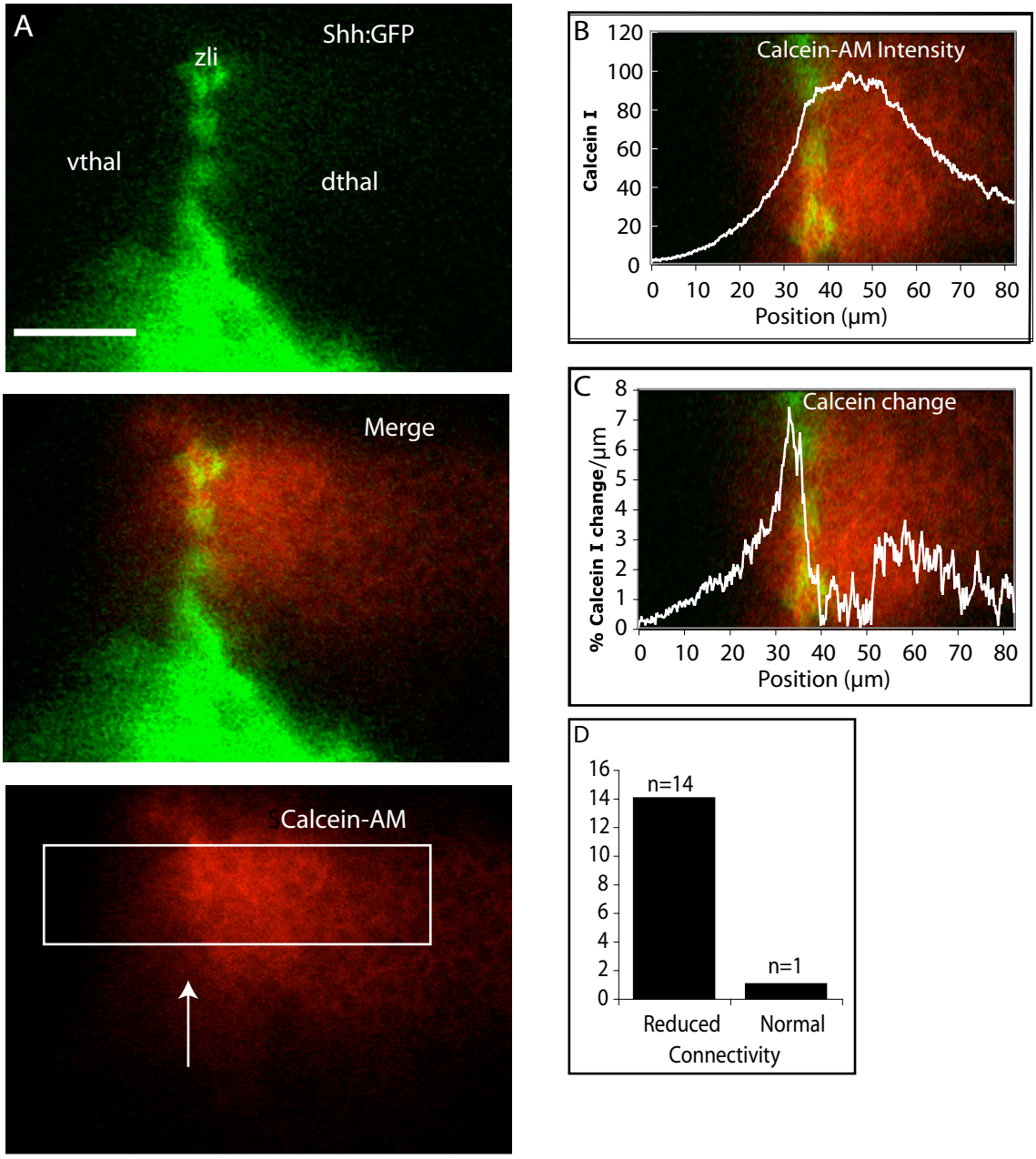


Fig. 6.3. Gap junctional communication is reduced at the Zona Limitans Intrathalamica.
A). Single optical section depicting the Zona Limitans Intrathalamica (ZLI) at 30hpf using the Tg(Shh:GFP) zebrafish line. Calcein AM was injected into the dorsal thalamus. Diffusion of Calcein AM from the dorsal thalamus into the ventral thalamus was minimal. The white box demarcates the region that was measured (B,C).
B). Calcein fluorescence intensity was measured across the ZLI.
C). Calcein fluorescence intensity was converted into % change per μm. The peak rate of change occured at the ZLI, indicating that gap junction connectivity is decreased.
D). 14/15 injected embryos exhibited decreased connectivity.
Scale bar: 25μm. vthal: ventral thalamus, dthal: dorsal thalamus, zli: zona limitans intrathalamica, arrow: ZLI position

I recorded calcium activity from 24-30hpf zebrafish hindbrains, mounted in dorsal view and a 15µm depth (3 slices at 7.5µm spacing) was sampled at 5s intervals (N=30 embryos). Calcium transients were defined as an increase in fluorescence intensity of the calcium indicator that exceeded a threshold, followed by a return to the baseline level of fluorescence. Thresholds were set for each time-lapse individually, as the percentage change that best differentiated between noise fluctuations and true calcium activity (see methods).

Surprisingly, no calcium activity was seen in 14 embryos (total imaging time, 167min). This paucity of activity may be a true reflection of endogenous calcium activity, or could be a result of calcium indicator toxicity or poor detection sensitivity. For further analysis only time-lapses with at least one calcium transient were included (N=16 embryos, total imaging time 482 minutes). Individual time-lapses varied in their duration, between 5-120min, however there was no correlation between time-lapse length and the number of transients produced. For example in a 120min time-lapse, covering 180µm of ventricular length, 5 active cells each produced a single transient (0.02 transients/min/100µm), while a 30min time-lapse covering 280µm of ventricular length contained 26 transients generated by 19 cells (0.3 transients/min/100µm). Calcium transients occurred either in single cells, pairs of touching cells or in groups of three cells, in accordance with the small, non-wave transients seen in rodent cortical slices (Owens et al., 2000; 1998; Weissman et al., 2004) (fig. 6.4A,B and supplementary movies 1 and 2). The majority of VZ cells were inactive for the duration of the time-lapses and large intercellular calcium waves were never seen. A total of 118 active cells produced 149 calcium transients in 482min imaging. Transient frequency was therefore 0.15 transients/minute/100µm of ventricular surface (measured anterior-posterior). Transient duration lasted between 1 time-point (less than 5s) and 12 time points (60s). Average transient duration was 27.7 ± 12.9 s (n=48). Of the 118 active cells, 78 (69%) generated single cell transients, there were 17 pairs of cells, 16 of which were co-active and the other pair had wave-like activity (27%), since each cell produced a transient in consecutive time-points. There were two groups of 3 cells with coordinated calcium activity (5%). These were composed of a coactive pair and a neighbouring cell that produced a transient in the subsequent time point (fig. 6.4C). Therefore coordinated calcium activity was not a common occurrence.

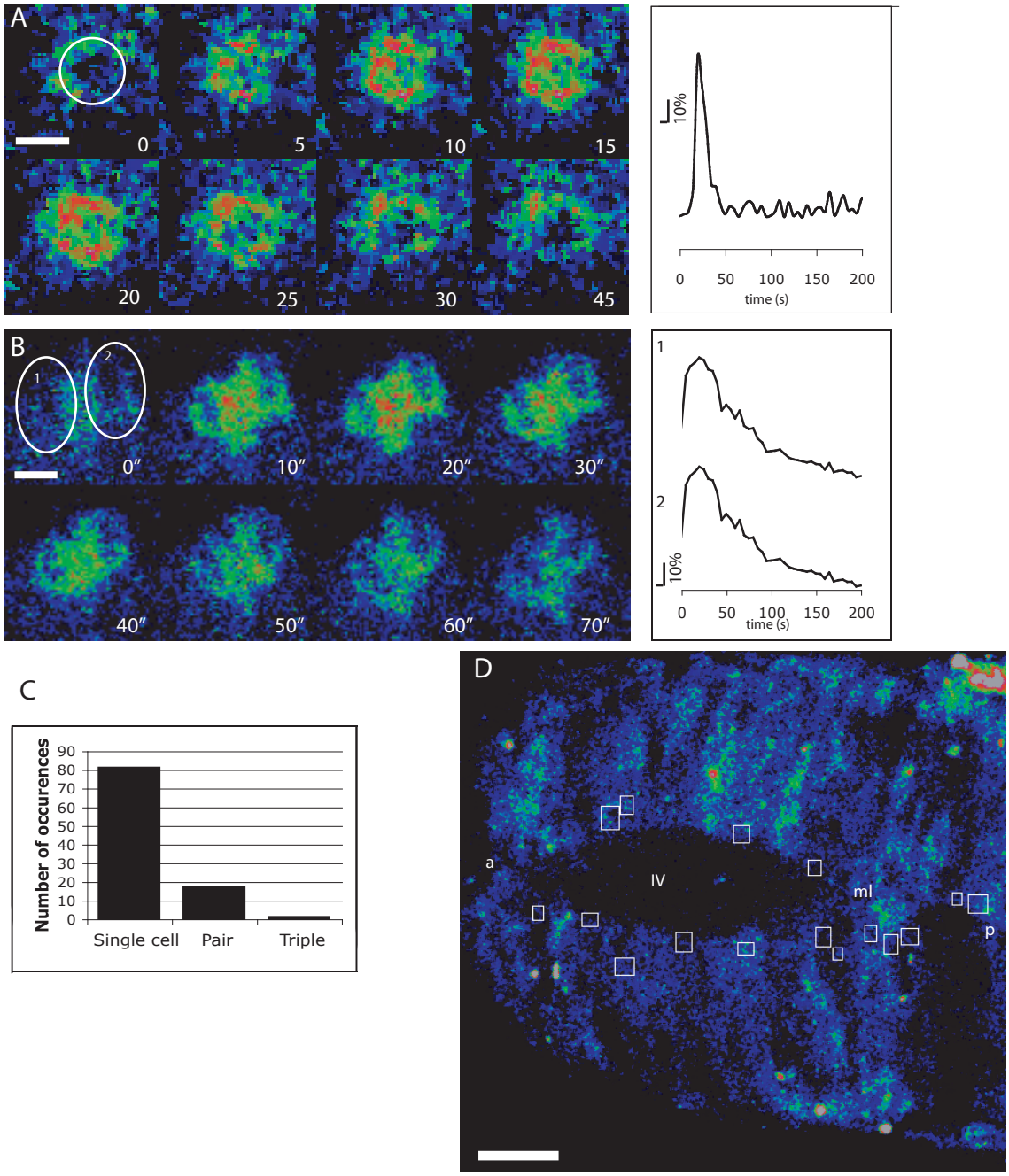


Fig. 6.4. Calcium transients during neurogenesis

A,B). Frames from a timelapse of calcium activity in calcium green dextran injected 24-30 hpf zebrafish embryo. A single hindbrain VZ cell (A) and a coactive pair (B) produce calcium transients (Supplementary movies 1 & 2). Traces show the change in fluorescence intensity within the cells.

C). The majority of transients were produced by a single cell (78/118). Coordinated pairs of cells were far fewer in number (17/118) and two instances of three coordinated cells were observed.

D). Dorsal view of a zebrafish hindbrain labelled with calcium green dextran. White boxes depict locations of calcium transients. Most are located at the IV ventricle (Supplementary movie 3).

Scale A,B: 5µm, C: 25µm

IV: 4th ventricle, a: anterior, p: posterior, ml: midline.

In conclusion, single cells and coactive pairs of cells produce calcium transients at low frequency during early neurogenesis. No large intercellular waves were detected in the intact zebrafish CNS, unlike in slices of rodent cortex where waves of up to 35 cell diameters were commonly found (Weissman et al., 2004).

## Calcium activity may be regulated by the cell cycle

The majority of cell bodies with calcium activity were touching the ventricular surface (97/118 cells), suggesting that calcium activity is related to cell division (fig. 6.4D and supplementary movie 3). All 16 coactive pairs were touching the ventricular surface. In 3 of these cases it was possible to observe a cell division followed by the daughter pairs producing simultaneous calcium transients (supplementary movie 4). These patterns of activity were also observed in the rodent neocortex and are probably daughter pairs of recently divided cells (Owens and Kriegstein, 1998). The majority of transients were produced by cells touching the IV ventricle, therefore calcium activity appears to be cell cycle dependent and is heightened during mitosis.

## Photo-uncaging calcium chelators does not induce calcium waves

The lack of detectable coordinated, and low frequency of calcium activity within progenitors during early zebrafish neurogenesis prevented me from determining if rhombomere boundaries restrict calcium ion exchange between rhombomeres. It was necessary to then develop a method to artificially induce intracellular calcium transients in order to address if the tissue is both competent to allow the spread of intercellular calcium ions and if $Ca^{2+}$ can or cannot pass between cells residing in different rhombomeres.

To induce calcium transients optically, zebrafish zygotes were injected with calcium green dextran and mCherry mRNA to visualise cell membranes. At 24-30hpf embryos were pressure injected with NP-EGTA AM, a cell permeant, and photolabile calcium chelator into the central lumen of the spinal cord. Pulses of UV laser light were applied to target cells to selectively uncage $Ca^{2+}$ within a targeted cell. Fluorescence intensity changes of calcium green dextran were measured by time-lapse confocal microscopy to determine the spread of calcium activity.

I found that in embryos loaded with NP-EGTA and calcium green dextran, the maximal level of fluorescence intensity occurred in the time point immediately after the UV pulse. Fluorescence intensity always increased in the targeted region. Fluorescence intensity increase in cells outside the UV targeted region occurred in 36/38 experiments

(95%, fig. 6.5A). Responses in neighbouring cells were normalised to the targeted cell's response. The average fluorescence increase in cells touching the targeted cell was 41 ±31% (n=135). Fluorescence increase in cells that were 1 cell removed from the targeted cell was 12 ±20% (n=72) and in cells two cells removed it was 9 ±15% (n=30) (fig. 6.5A,C). The increase in fluorescence intensity in cells outside the targeted region was always maximal in the time-point immediately following the uncaging step and subsequently faded to baseline.

Previous reports of intercellular calcium waves in the VZ described propagating calcium activity with the following properties: first the magnitude of the calcium increase in each cell was similar to the magnitude of the calcium increase in the trigger cell and second cells distant from the trigger cell reached maximum fluorescence intensity many seconds after the trigger cell (Owens and Kriegstein, 1998; Pearson et al., 2004; Weissman et al., 2004). I never observed this type of activity, so uncaging NP-EGTA did not elicit propagating intercellular calcium waves.

My results suggest that uncaged calcium diffused from the target cell into its neighbours; however it could also be an indication that the UV laser actually uncaged NP-EGTA from a larger area than the targeted region. I tested this possibility next.

## Kaede photo-conversion compared with NP-EGTA uncaging reveals intercellular calcium spread does not occur

To determine if the observed spread of calcium was caused by intercellular communication, or by the confocal laser uncaging calcium beyond the targeted region, I also injected control embryos with mRNA encoding Kaede, a photo switchable fluorescent protein (Ando et al., 2002). Before switching, Kaede has an absorption and emission spectrum similar to GFP. After a targeted UV pulse, the protein's spectral properties more closely resemble RFP. Kaede has a molecular weight that exceeds the maximum size of gap junction permeable molecules and so it should only switch directly under the UV laser with no possibility of intercellular transfer. Any photo-conversion of Kaede that occurred beyond the UV laser target showed the true extent of laser activation and photo-conversion.

Photoconverting Kaede yielded equivalent results to NP-EGTA (N=8, fig. 6.5B). Photo-conversion was normalised against the target cell's response. Cells adjacent to the targeted cell converted 47 ±44% compared to the target cell (n=30). Cells one removed from the target cell converted 15 ±12% of the target cells' response (n=33) and cells 2

removed from the target cell uncaged 11 ±10% of the target response (n=10) (fig. 6.5C). None of these results is significantly different from NP-EGTA photo-uncaging (1: P=0.18, 2: P=0.56, 3: P=.72, student's T test). This result strongly suggests that calcium activity induced by photo-uncaging NP-EGTA did not spread beyond the uncaged cell through gap junctions.

It is possible that a low level of calcium ion diffusion was masked by the uncaging outside the targeted cell. For example, intracellular injection of gap junction permeable dyes into rodent VZ produced radially arranged clusters of cells (Lo Turco and Kriegstein, 1991), suggesting that apico-basal (ab) connectivity is greater than rostro-caudal (rc) coupling. I therefore divided cells into groups according to their location: along the rc axis or ab axis. While fluorescence change in cells 1 cell removed from the targeted cell along the ab axis was larger than the rc change (11 ±12%,n=59 vs. 23 ±23% n=22, P=0.01) (fig. 6.5D,E); no other measurements of ab or rc changes in calcium levels were significantly different and no calcium measurements were significantly different from equivalent Kaede photoconversions.

In conclusion, this result demonstrates that I have developed a reliable method to induce focal increases in calcium concentrations in small groups of cells *in vivo* that can be used to test a tissue's ability to propagate intercellular calcium waves. However, it was not possible to induce calcium waves in the hindbrain VZ by photo-uncaging caged calcium compounds. This finding, along with the observations of spontaneous calcium activity in the hindbrain suggests that calcium activity is minimal during early neurogenesis and there are no large intercellular calcium waves. Since it was not possible to induce waves artificially, the neuroepithelium may not be competent to propagate them.

**Fig. 6.5. Photo-uncaging calcium fails to induce intercellular waves**

A). Calcium green dextran and mCherry labelled hindbrain loaded with NP-EGTA AM (colourless). Images have been processed to only display green signal where increased calcium green dextran occurred. Photouncaging NP-EGTA AM in a single cell results in strong intracellular elevation of calcium, but minimal diffusion of calcium ions into neighbouring cells.

B). Hindbrain expressing Kaede. Targeted photoconversion of Kaede in a single cell results in conversion of Kaede in neighbouring cells. Kaede is not gap junction permeable, suggesting that the increase in intracellular calcium in non-targeted cells is artifactual.

C,D,E). Mean responses to either calcium uncaging or Kaede photoconversion, normalised to the targeted cell. Analysed cells include the targeted cells, cells adjacent to, one removed and two removed from the targeted cell and include all cells (C), cells positioned rostro-caudal (D) and apico-basal (E) to the targeted cell. There is no difference in response to calcium uncaging or Kaede photo-conversion. Therefore calcium uncaged from NP-EGTA did not diffuse from the targeted cell into neighbours via gap junctions in any direction.

Scale bar: 10μm.

a: apical. b: basal Arrow: uncaged calcium/converted Kaede outside the targeted region

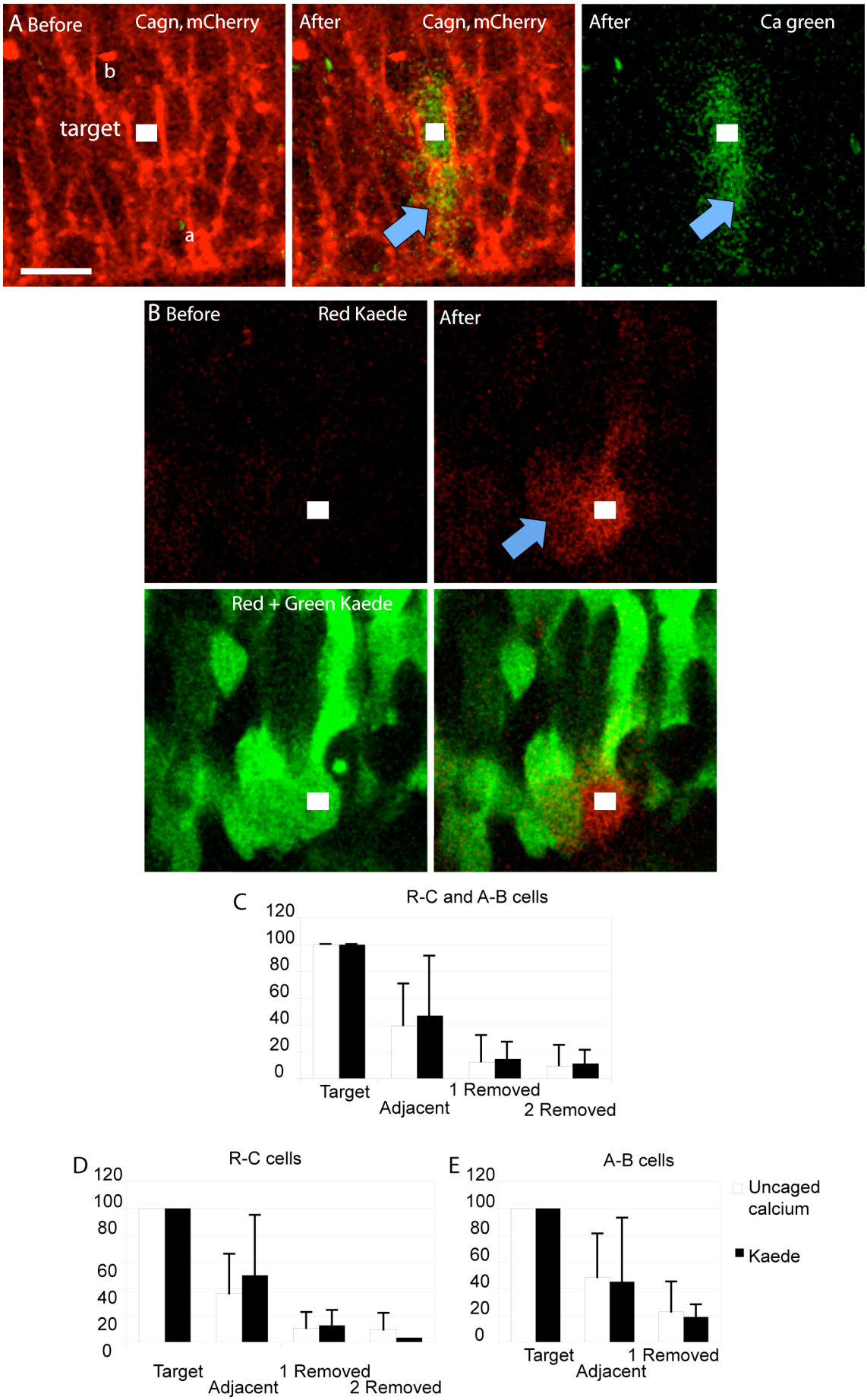


Fig. 6.5. Photo-uncaging calcium fails to induce intercellular waves

## Gap junction coupling in the hindbrain VZ demarcates developmental compartments

I have attempted to analyse whether cell-cell communication is reduced at rhombomere and other CNS boundaries in the zebrafish and to determine if this could be a barrier to intercellular calcium activity. My results show the former is true, but have been unable to assess the latter because intercellular calcium activity appears not to be detectable in the zebrafish hindbrain.

## Gap junction based communication is reduced at CNS boundaries

Calcein-AM injection into the centre of rhombomeres labelled cells in the injected rhombomere, while little dye crossed boundaries into adjacent rhombomeres, confirming data from chick embryos, where gap junction permeable dyes fail to cross rhombomere boundaries (Martinez et al., 1992). If the site of injection was moved to the dorsal thalamus, a similar labelling pattern occurred, since little dye diffused across the ZLI into the ventral thalamus. Therefore interrupted gap junction coupling is a common feature of at least two CNS boundaries.

In a previous study of gap junction communication at rhombomere boundaries, when dye was injected specifically into boundary cells no diffusion into neighbouring cells occurred (Martinez et al., 1992), while I always saw labelled boundary cells when I injected non-boundary cells. I did however find that boundary cells were more intensely labelled than non-boundary cells when I attempted to label the entire VZ by injecting large volumes of calcein AM. Therefore calcein did not evenly diffuse from boundary cells into the rest of the rhombomere. Taken together the chick boundary cell labelling and my results suggest that there is non-symmetrical coupling between boundary cells and non-boundary cells. Asymmetrical gap junctional coupling has been described *in vitro* (Dermietzel et al., 2000) and between pyramidal neurons and astrocytes in early postnatal rat pup cortex (Bittman et al., 2002), and is attributed to differences in the composition of connexons between the coupled cells. Accordingly, *cx43.4* is not expressed in rhombomere boundaries, but is present in non-boundary cells (Thisse, 2001); therefore the composition, gating and conductance of connexons in boundary cells may be different from the connexons in non-boundary cells and could underlie the asymmetry of dye transfer. The reason why AM dyes preferentially labelled boundary cells in this manner is not known, but may be due to the increased extracellular space

surrounding boundary cells (Heyman et al., 1993). This could lead to improved dye access compared with the more tightly packed non-boundary cells.

Reduced dye transfer across zebrafish rhombomere boundaries adds further weight to the neuromeric theory, as it supports the view that morphologically distinct brain areas are separate developmental compartments. It was not possible to address the mechanism by which gap junction communication is down regulated at zebrafish CNS boundaries, yet I suggest that the down regulation of *cx43.4* mRNA at the boundaries could be, at least in part, responsible for this phenomenon. Experimentally induced expression of Cx43.4 in rhombomere boundaries, followed by dye injection experiments could shed further light on this issue.

## Is cx43.4 down-regulation at rhombomere boundaries essential to reduce communication between compartments?

Cell-cell affinities differ between rhombomeres in chick and zebrafish (Guthrie et al., 1993; Wizenmann and Lumsden, 1997; Xu et al., 1999) and between the ZLI and thalamus (Zeltser et al., 2001). However it may not simply be that reduced gap junction communication between compartments is caused by affinity differences that inhibit connexon docking. This is because heterogeneous populations of cells are capable of forming functional gap junctions. Clusters of coupled spinal neural progenitors express different homeodomain transcription factors. Likewise, lateral horn motoneurons contain $Isl1^{+}$ and $Isl1^{-}$ cells (Bittman et al., 2004). This may be due to some cells in the cluster being either too mature or immature to express the appropriate proteins, but it does suggest that phenotypically heterogeneous populations of progenitors or neurons can couple. Along a similar vein in newborn rat cortex, pyramidal neurons coupled to interneurons and to astrocytes have been detected (Bittman et al., 2002) and retinal ganglion cells are coupled to amacrine cells in the retina (Roerig and Feller, 2000). Since cells with different identities and functions can form functional gap junctions, it may be possible that cells in neighbouring rhombomeres or ZLI and thalamic cells would also form functional gap junctions if they were not separated from each other by 2 rows of boundary cells that do not express *cx43.4* mRNA. It would be interesting to test for intercellular dye transfer in zebrafish hindbrains that lack boundary cells, without disrupting segmental organisation to test this hypothesis. At present a mutant fish of this kind does not exist, however in the future a method to eliminate boundary cells without disrupting hindbrain segmentation may be discovered. At present the best option would be to knock down Eph-Ephrin interactions as this eliminates rhombomere

boundaries with the least severe disruption of segmentation compared with other methods (Cooke et al., 2005; Xu et al., 1995).

## The ZLI: boundary or compartment revisited

I found that gap junction communication was reduced between the dorsal and ventral thalamus, indicating that the ZLI acts as a barrier to diffusion of small molecular weight signals between them. It has been proposed that the ZLI is either a boundary (Figdor and Stern, 1993; Puelles and Rubenstein, 1993) or a compartment (Zeltser et al., 2001). My dye injection results agree that there is a boundary between the dorsal and ventral thalamus, because reduced intercellular communication is an evolutionarily conserved feature of compartment borders (Martinez et al., 1992; Ruangvoravat and Lo, 1992; Warner and Lawrence, 1982). I did not address if the ventral ZLI (where it is many cells wide) had anterior and posterior communication boundaries and would therefore be a compartment. It would be interesting to repeat the experiment, but target the ZLI itself to see if dye can or cannot pass between the ZLI and the thalamus to obtain further evidence regarding whether it is a boundary, compartment or both.

What can be concluded is that a proposed forebrain compartment border (Figdor and Stern, 1993; Puelles and Rubenstein, 1993) has both an apical surface with boundary characteristics (chapter 5) and acts as a barrier to intercellular communication. This finding supports my proposal that regions of the CNS with enlarged AEF and increased linearity of the interfaces between AEF are compartment boundaries.

## Increased coupling within the zebrafish VZ compared with rodent cortex

In both the hindbrain and the thalamus, calcein AM injection labelled large numbers of cells. This may not seem entirely consistent with previous studies of coupling between neural progenitors in rodent cortices. The difference in labelling may be due to the technique employed to label the cells, or species differences.

Intracellular injection of gap junction permeable dyes into the rodent ventricular zone labelled radial clusters of cells ranging in size from 15-25 cells (Bittman et al., 1997; Lo Turco and Kriegstein, 1991), while ballistic delivery of gap junction permeable dye soaked beads into the mouse ventricular zone also labelled radial clusters of 2-12 cells (Bittman et al., 2004). Since less dye was delivered by the ballistic approach compared

to intracellular injection, differences in observed cluster size may be the product of technical differences, rather than true differences in connectivity.

I injected a larger amount of dye than other studies. Since calcein AM is cell permeant, I could inject it into the extracellular space and so was not restricted to the same degree in the amount of dye I could inject. I also waited at least 1hr before imaging the injected fish. In this way it was possible to label all connected progenitors, regardless of their distance from the injection site. Single cell injection of gap junction permeable dyes could be carried out in zebrafish VZ to see if small, radial clusters of progenitors become labelled.

The other explanation is that there are coupling differences between fish and mammals. The pattern of connectivity does not fit with the suggested idea that larger organisms will contain larger clusters (Bittman et al., 1997) because zebrafish exhibit the largest clusters and are the smallest organism. Alternatively, zebrafish neuroepithelial cells may be more extensively coupled than mammalian neuroepithelial cells because of the speed at which zebrafish develop. There is a strong positive correlation between expression levels of gap junctions and the rate at which a tissue proliferates. For example Cx43 is expressed at higher levels in the hyperproliferating albino mouse retina than in wt retina (Tibber et al., 2007) and gap junction blockade reduces the number of neocortical progenitors that enter mitosis (Bittman et al., 1997). Therefore it is logical to predict that the rapidly growing and proliferating zebrafish brain should contain extensively coupled progenitor cells.

It is also possible that developmental stage my influence connectivity, since the size of clustered rat neural progenitors decreases with increasing age (Lo Turco and Kriegstein, 1991). My experiments took place at developmentally earlier times than the rodent studies (early vs mid neurogenesis). Therefore more extensive coupling may have resulted from the neuroepithelium being less mature. To address if coupling difference arose as a result of developmental stage, older zebrafish could be injected with calcein AM and the size of dye labelled clusters measured.

## Intercellular calcium waves do not occur in the zebrafish VZ

Due to the extensive coupling of zebrafish hindbrain VZ cells and the segmental regulation of dye transfer, I investigated if intercellular calcium activity is segmentally regulated during neurogenesis. The rationale behind this investigation is that Connexin dependent intercellular calcium waves have been observed in neuroepithelial cells in rat cortical slices during neurogenesis (Owens et al., 2000; Owens and Kriegstein, 1998; Weissman et al., 2004) and in the VZ of the chick retina (Pearson et al., 2004). The most important difference between the calcium activity seen in the zebrafish neuroepithelium and rodent cortical slices was the lack of large intercellular waves. I saw no intercellular calcium waves in the zebrafish hindbrain VZ that were larger than 3 cells and was unable to induce calcium waves using caged calcium compounds. Two studies by the Kreigstein laboratory recorded waves spreading between up to 35 cells. There is however conflicting data regarding cortical VZ calcium waves. In their first study it was not possible to quantify the frequency of calcium waves, but the waves they did observe passed between 14-16 cells (Owens and Kriegstein, 1998). In a more recent study the waves spread in up to 35 cells at a frequency of 1.1 waves/min/mm in E16 rat cortical slices (Weissman et al., 2004).

There are five possible reasons for the discrepancy between their results and mine:

***1. Calcium indicator choice***

I used calcium green dextran in my calcium imaging experiments, where the Kreigstein laboratory used fluo3. Calcium green dextran has a Kd of 260nmol while Fluo3 has a Kd of 390nmol, so their calcium binding properties are similar. Fluo3 does however have a much wider dynamic range than calcium green dextran (in the region of 10x wider range), so it may be more effective at detecting small changes in calcium concentration. However Weissman and colleagues reported fluorescence changes in excess of 50% and up to 150%, which should also be detectable with calcium green dextran (Weissman et al., 2004). I was also able to record calcium waves during the blastula period of zebrafish development using calcium green dextran (chapter 7). Therefore calcium green dextran is capable of detecting calcium waves in the zebrafish embryo.

2. Delivery method

In the rodent studies, cortical slices or slabs were placed in a solution containing a cell permeant calcium indicator 1-3 hours before imaging (Owens et al., 2000; Owens and Kriegstein, 1998; Weissman et al., 2004). It was not possible to do this with zebrafish embryos as attempts to load cell permeant calcium indicators into 24-30 hpf zebrafish hindbrains yielded few successes (data not shown). Instead embryos were loaded with calcium green dextran, a cell impermeant indicator at the 1 cell stage. Calcium green dextran is BATPA based. BAPTA based calcium indicators buffer intracellular calcium, reducing the frequency and amplitude of calcium transients in zebrafish embryos (Ashworth et al., 2001; Chang and Lu, 2000; Webb et al., 1997) and can prevent cell division and disrupt the normal developmental program. Therefore to avoid disturbing development I injected very low concentrations of calcium green dextran. By 24hpf, the signal produced by this low concentration of calcium indicator was extremely weak and so small fluctuations in calcium levels, which could have included intercellular calcium waves, may have been occluded by noise in the recording.

***3. Organism size***

It has been proposed that intercellular calcium signals function to coordinate development (Webb and Miller, 2006; Weissman et al., 2004) and that the complexity of calcium signals mirrors the complexity of the embryo/tissue (Gu and Spitzer, 1997; Owens and Kriegstein, 1998; Webb and Miller, 2006). An organism such as the zebrafish with a simple brain may not require large calcium waves to correctly control neurogenesis.

***4. Physical damage***

There are reports detailing how physical damage stimulates calcium waves in a variety of tissues, which include the chick cochlear and rabbit trachea (Gale et al., 2004; Sanderson et al., 1990), thus some of the activity seen in mouse cortical slices may be in response to the removal and slicing of the brain. Since it is possible to visualise the zebrafish brain non-invasively, this physical damage was avoided and so, damage responsive calcium waves did not occur. In agreement with this proposal, in experiments not included in this thesis, I attempted to monitor calcium activity using Fluo4-AM injected directly into the hindbrain. In most cases where I observed calcium activity, neuroepithelial cells became highly active, then died shortly afterwards.

To address this issue further, it may be necessary to physically damage a zebrafish brain, or to make slice preparations, to see if there is a resulting increase in calcium activity that mirrors the activity seen in embryonic mouse cortex.

***5. Endogenous calcium buffering***

Calcium activity in the zebrafish VZ did not include spontaneous or stimulated propagated calcium waves and passive diffusion of calcium ions between cells seen after uncaging NP-EGTA did not occur either. Calcein-AM injection into the zebrafish VZ showed that progenitors are extensively coupled by gap junctions. Cx43.4 is expressed in the hindbrain VZ and is permeable to calcium ions (Desplantez et al., 2003; Thisse, 2001). Therefore it is logical to predict that calcium ions should be able to pass from one neuroepithelial cell to the next through gap junctions. It is unlikely that uncaging calcium caused gap junctions between the targeted cell and its neighbours to close because the time-course of junction closure in response to changes in calcium concentration is in the minute range (reviewed in Evans et al., 2006), while the uncaging step lasted roughly 1s. If hindbrain gap junctions are composed of heteromeric connexons, their gating properties may be different compared to Cx43.4 homomeric gap junctions and may not allow the passage of calcium ions.

Another plausible explanation is that the hindbrain may prevent intercellular calcium exchange with endogenous calcium buffers. Therefore the zebrafish neuroepithelium may not be competent to allow calcium to transfer between many cells. If this is the case, this situation is remarkably different from the rodent cortex, which is competent to produce them (Weissman et al., 2004).

Since I have demonstrated that the hindbrain neuroepithelium is interconnected by gap junctions, different second messengers other than calcium ions may be utilised in intercellular signalling. In many cell types intracellular calcium concentrations are tightly regulated, so IP3 and/or ATP is used as the second messenger that makes calcium waves propagate (reviewed in Giaume and Venance, 1998). Therefore these signalling molecules may be able to pass between zebrafish neuroepithelial cells via gap junctions and could provoke calcium waves. While I have not detected large intercellular calcium waves, it is premature to claim that calcium waves do not and cannot occur during zebrafish neurogenesis without further experimentation. To do so would be to fall into the trap of researchers such as Whittaker & Patel, who state that:

"Strictly speaking, something that cannot be detected does not exist" (Whitaker and Patel, 1990). Further work with other calcium indicators, development of a reliable

method to deliver calcium indicator just prior to imaging rather than the day before, or use of caged IP3 to stimulate calcium waves may produce fruitful answers.

## Non-wave like calcium activity may be related to the cell cycle

While trying to record intercellular calcium waves in the zebrafish hindbrain I observed two patterns of calcium activity in progenitors: single cell transients and paired cell transients lasting approximately 27s. The majority of single cell transients were located close to the IV ventricle, while all paired cell transients occurred in cell bodies touching the IV ventricle. Since this is the location where cells divide, it appeared that these were paired daughter cells. In 3 cases I was able to observe the calcium activity in a dividing cell and synchronous calcium activity in the two daughters following division. These patterns of activity are in agreement with the activity of progenitor cells in embryonic rat cortex. The frequency of calcium transients was much lower in the zebrafish compared with the rat slices. In a 20min period of imaging, over 80% of rat VZ cells generated transients, while the percentage of active cells in the fish was too low to quantify directly. While different from the rat, this result does agree with published data on the calcium activity of VZ progenitor cells during zebrafish neurogenesis, where infrequent VZ calcium transients were also observed. In some time-lapses, activity was very infrequent, while it was more frequent in others. While I could not provide evidence for this, these differences in activity may reflect fluctuations in calcium activity that are linked to the cell cycle, with high activity occurring when many cells are in mitosis and low activity when few cells are dividing. Extended duration time-lapses that last many cell cycles could reveal if this hypothesis is correct.

## Kaede photo-conversion occurred outside the targeted cell

Some cells that did not fall directly under the UV laser line showed increased calcium concentrations, however this also happened in cells loaded with Kaede which is not permeant to gap junctions. The spreading of Kaede in this manner could be caused by the architecture of the neuroepithelium and/or by the cone of laser light that is created by a single photon confocal microscope. Tissue both above and below the focal plane of the laser was stimulated because a single photon laser beam is not confined to a single focal plane. Neuroepithelial cells are not shaped exactly like radial glia in the zebrafish CNS during the phase of neurogenesis. Instead of having a cell body and two long thin processes (one apical, one basal), zebrafish neuroepithelial cells have more complicated membrane architecture (fig. 6.6). Therefore a cell that appeared to be horizontal to the

targeted cell might have had lamelepoid processes entwining the targeted cell, either above or below it, resulting in being hit with the laser. There is also the possibility that the lasers targeting was inaccurate, stimulating a wider field than was selected.

In conclusion, the zebrafish VZ displays strong dye coupling between neural progenitors, suggesting it is heavily interconnected by gap junctions. Reduced dye transfer between adjacent rhombomeres is most likely due to reduced gap junction expression at rhombomere boundaries. Boundary cells create buffer zones that prevent intercellular communication between adjacent compartments. Calcium activity is low during early neurogenesis and appears to be linked to the cell cycle. Finally, the zebrafish VZ appears not to be competent to transmit intercellular calcium waves.

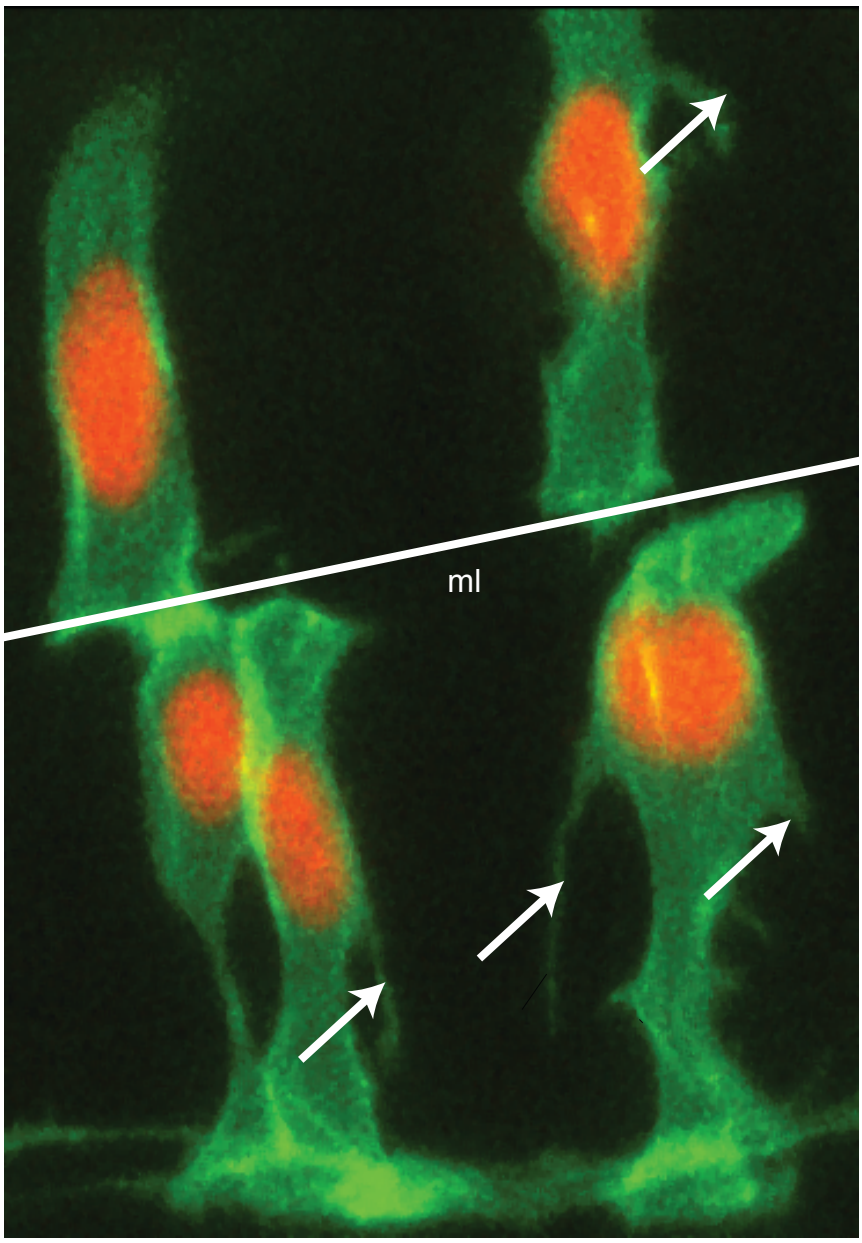


(Paula Alexandre)

Fig. 6.6. Complex morphology of zebrafish neuroepithelial cells. Zebrafish neurepithelial cells labelled with mGFP and H2B RFP. Cells are bipolar ancontact the apical and basal surfaces of the CNS. Their apical and basal processesllamelopoid, large and irregular and have filopoid secondary processes. Scale bar: 10μm. ml: midline, arrows: filopods

# Chapter 7:
# Intercellular Junctions are required to coordinate embryonic development

## *Introduction*

The blastula stage is the simplest developmental stage when intercellular communication through gap junctions occurs (Webb and Miller, 2003a). In zebrafish, the blastula stage commences at the end of the 64 cell stage and lasts for 3-4 cell cycles, until the 512-1024 stage, when epiboly commences (fig.1.7A) (Kane and Kimmel, 1993; Kimmel et al., 1995). Two important developments occur in the blastula period: superficial cells flatten and become an epithelium called the enveloping layer (EVL) and deep cells touching the yolk form the yolk syncytial layer (YSL) (Kimmel and Law, 1985a; Kimmel and Law, 1985b).

During the first 4 hours of development, mitoses in the zebrafish embryo occur synchronously as their cell cycles are aligned. Mitoses become less synchronous during divisions 5-10, which includes the blastula period. Blastomeres divide in a wave starting at the animal pole and ending at the blastoderm marginal. This pattern of division has been termed 'metasynchronous' (Kimmel et al., 1995). This coordinated pattern of cell divisions suggests that there is an organising factor that instructs each blastomere when it may divide. It is unclear what this factor is. Gene expression is uniform, as is the concentration of intracellular calcium (reviewed in Webb and Miller, 2006) and IP3 (Reinhard et al., 1995). Since cell cycles in the zebrafish blastocyst are spatio-temporally regulated, blastomeres may use gap junction communication to coordinate their cell cycles. Functional gap junctions are expressed in blastulas of all vertebrates, including human, mouse, zebrafish and bovine embryos (Essner et al., 1996; Guthrie, 1984; Hardy et al., 1996; Lo and Gilula, 1979a; Lo and Gilula, 1979b; Wrenzycki et al., 1996). Gap junctions may encourage blastomere proliferation because the proliferative advantage of normal blastomeres over UV irradiated blastomeres is abolished by gap junction inhibitors (Vance and Wiley, 1999), however it has not been demonstrated if gap junction communication is required to coordinate zebrafish division waves.

Current knowledge of the requirement for gap junction communication during the blastula period is difficult to interpret. For example, inhibition of gap junction function in *Xenopus* embryos at the 1 or 2 cell stage resulted in developmental arrest before

gastrulation (Warner et al., 1984), while total blockade of gap junction channels in mouse blastocysts, using 18 α-glycyrrhetinic acid (AGA) did not disrupt blastula development (Vance and Wiley, 1999). Individual *connexins* are expendable during the blastula stage, since genetic ablation of single *connexin* genes did not significantly disrupt mouse or zebrafish blastula development (De Sousa et al., 1997; Gong et al., 1997; Guldenagel et al., 2001; Houghton, 2005; Houghton et al., 1999; Iovine et al., 2005; Kumai et al., 2000; Nelles et al., 1996; Plum et al., 2001; Simon et al., 1997; Simon et al., 1998). This lack of disruption may be due to redundancy in function within the *connexin* gene family.

Calcium ions can pass through gap junctions and coordinate cellular processes in a variety of developmental contexts, including cytokinesis (Fluck et al., 1991) and controlling proliferation (Weissman et al., 2004); therefore calcium signalling may be an important coordinator of cell division waves in the blastocyst. However, calcium activity during the blastula period of development, especially in zebrafish, is less well understood than gap junction function. No cell cycle dependent or pan-embryonic patterns of activity have been reported in the zebrafish blastocyst, but calcium spikes and small waves consisting of up to 5 cells were observed (Creton et al., 1998; Reinhard et al., 1995) (fig. 1.7B). However the dependence of these calcium events on gap junction communication has not been addressed. In *Xenopus* blastocysts calcium levels are cell cycle dependent, but there is debate over when calcium levels are high (Grandin and Charbonneau, 1991; Keating et al., 1994; Kubota et al., 1993). Based upon comparisons between calcium oscillations in single blastomeres and the entire blastocyst, it has been proposed that oscillations occur in a wave (Keating et al., 1994). However a direct observation of calcium activity in all blastomeres individually is required to confirm if this is the case.

In an attempt to clarify what role gap junctions play in the blastula stage of development, I used cell division waves as an assay for cellular coordination. Through inhibiting gap junction communication I disrupted the spatio-temporal pattern of cell division waves, demonstrating that gap junctions are required to organise the behaviour of groups of cells. I have also improved upon our knowledge of calcium activity during the blastula period, finding that gap junction dependent cyclical changes in calcium activity occur throughout the blastula stage.

## *Results*

### Quantification of metasynchronous divisions in blastocysts

Before it was possible to assess the requirement for gap junction communication in the control of coordinated cell division in zebrafish blastocysts, I first quantified how metasynchronous divisions occurred in untreated embryos. Time-lapse movies of tg(H2A:GFP) zebrafish were recorded from the $7^{th}$ to $11^{th}$ waves of cell division. To quantitatively assess cell division waves, the 3D locations of mitotic nuclei were recorded. The origin of the division wave was considered as either the site of the first mitosis, or as the midpoint between mitotic nuclei in situations where two or more mitoses were seen in the first frame of the division wave. In 4 control embryos divisions were metasynchronous during the $7^{th}$-$10^{th}$ cell cycles (fig. 7.1C). The mean distance from the division wave origin increased as the division wave progressed, during the $7^{th}$-$10^{th}$ waves of mitoses (fig. 7.1A,B and supplementary movie 5). This pattern broke down in the $11^{th}$ round of division, during the mid-blastula transition. From the total of 15 division waves observed, the increase in mean distance (slope) from the point of wave origin was statistically significant in 14 cases (fig. 7.1D, 7.3A),

The duration of division waves (time between the first and last mitosis) increased from 3.2 ± 1.3 min during the $7^{th}$ cycle to 15.9 ± 6.4 min at the end of the $10^{th}$ (n=3, 4, 4, 4 respectively), which demonstrates the gradual loss of cell division timing synchrony during the blastula stage (fig. 7.2D). This was reflected by a decrease in the length of time between the last division of one wave and the first division of the next wave. In detail, the time interval between last and first mitoses decreased by 20%, from 20.0 min to 16.0 ± 2.5 min from cell cycle 7-10 (n=1, 4, 4, 4 respectively), reflecting reducing synchrony of mitoses, rather than a decrease in interphase length in individual cells (fig. 7.2D). Cell cycle length, measured as the time between the first mitosis of each division wave, increased by 45% between the $7^{th}$ and $10^{th}$ waves of mitosis, from 22.0 min to 31.9±7.5 min (n=1, 4, 4, 4 respectively) (fig. 7.2D).

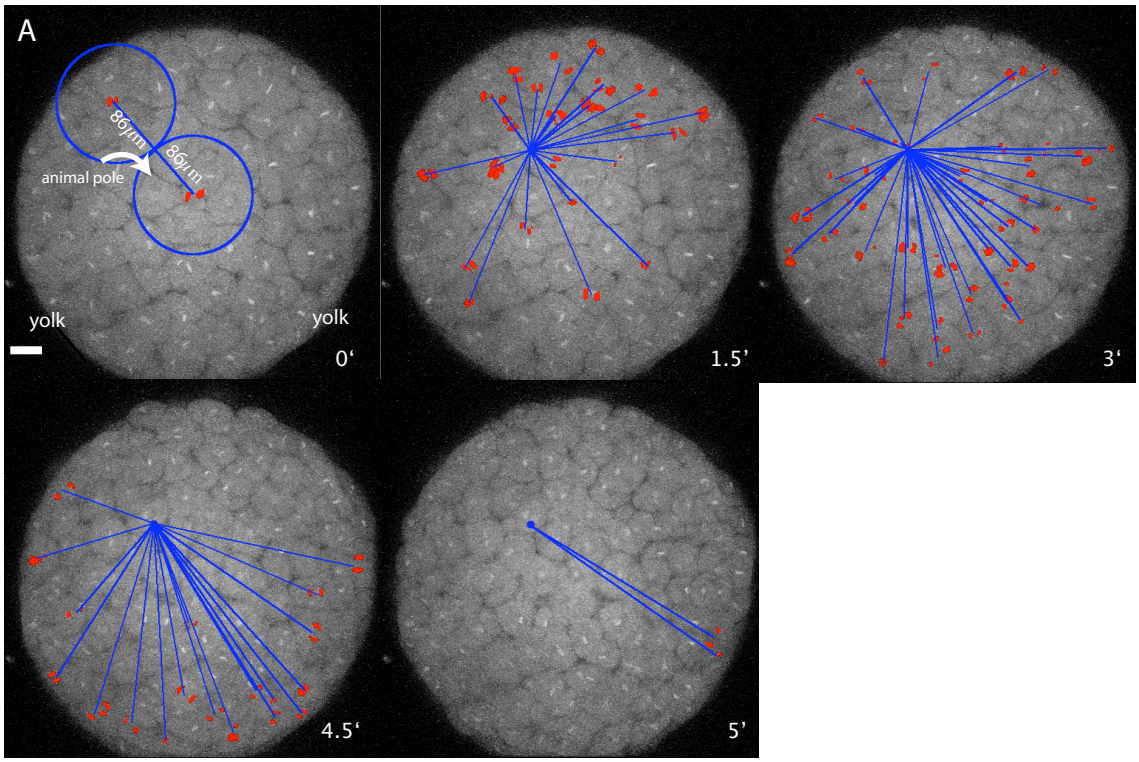


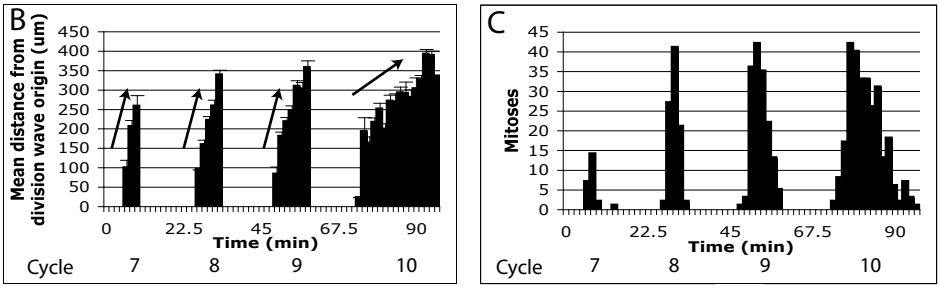


D

| Cell cycle | Wave duration | N | Time (min) Interval | N | Cycle length | N |
|---|---|---|---|---|---|---|
| 7 | 3.2 ± 1.3 | 3 | 20.0 | 1 | 22.0 | 1 |
| 8 | 5.1 ± 1.0 | 4 | 17.5 ± 0.9 | 4 | 22.8 ± 1.0 | 4 |
| 9 | 9.4 ± 2.6 | 4 | 16.8 ± 1.9 | 4 | 26.1 ± 3.3 | 4 |
| 10 | 15.9 ± 6.4 | 4 | 16.0 ± 2.5 | 4 | 31.9 ± 7.5 | 4 |
| 11 | 26.3 ± 7.4 | 2 | 15.0 ± 4.2 | 2 | 41.3 ± 3.2 | 2 |

Fig. 7.1. Blastomere cell divisions occur in waves originating at the animal pole
A). Zebrafish blastocyst expressing H2B-RFP in nuclei, during its 8th mitosis, viewed from the animal pole. Images are projections taken at 1.5 min intervals. Sister nuclei are pseudocoloured red in the first frame post nuclear fission. The midpoint between mitotic nuclei at the first timepoint in the division wave is the point of origin. The distance between mitotic nuclei and the point of origin was measured for later timepoints. Divisions progress in a wave from the animal pole towards the vegetal pole (Supplementary movie 5).
B). Mean distance between dividing nuclei and the point of origin increased in each division wave during cycles 7-10, as seen by the height of bars increasing at each timepoint.
C). A count of mitoses during the blastula stage of embryogenesis demonstrates cell cycles are metasychronous: mitoses are aligned, however they are not perfecly synchronous.
D). During early development the cell cycle lengthens from 22 ±1min during the 7th cell cycle to 41.3 ±3.2min in the 11th cell cycle. The duration of each division wave also increased with each successive cell cycle, from 3.2 ±1.3min to 26.3 ±7.4min indicating that cell cycle alignment decreases with each successive cell cycle. The interval between last mitosis of one wave and the first mitosis of the next, decreased from 20.0min to 15.0 ±4.2min during this time period, reflecting the loss of cell cycle synchronicity.
N= Number of embryos.
Scale bar: 50µm

## Gap junction communication is required to coordinate cell divisions in the blastocyst

To assess if gap junctions are required to coordinate metasynchronous divisions in the blastocyst, gap junction function was inhibited with 100µM FFA, a reversible inhibitor of gap junction communication (reviewed in Evans et al., 2006). FFA was added to embryos 30min prior to imaging to allow the drug to penetrate the blastocyst.

In FFA treated embryos divisions were still metasynchronous, however there was a less coordinated pattern to mitoses than in control embryos (fig. 7.2A,B,C and Supplementary Movie 6). First, the initial mitosis was not necessarily located at the animal pole and second, the mean distance of subsequent mitoses from the point of the division wave origin did not increase as the division wave progressed (N=4), indicating that the spatio-temporal organisation of mitoses had become disrupted (fig. 7.2A,B,C). Of the 16 rounds of division analysed, 11 had disrupted division waves since they did not produce statistically significant positive slopes (fig. 7.3B). There is, therefore a remarkable reduction in the coordination of cell divisions in gap junction inhibited embryos.

## Gap junction blockade does not affect the cell cycle or proliferation

It was possible that gap junction blockade disrupted cell cycles in the blastocyst, which then resulted in disruption to the division waves. To determine if this was the case, the duration of each round of division, the length of time between division waves and of the entire cell cycle were compared between control and FFA treated embryos. The duration of division waves in each cell cycle was not significantly different between control and 100µM FFA treated embryos. ($P>0.67$ for each division wave) (fig 7.3C). The duration of division waves increased from 3.1 ± 1.0 min at the end of the $7^{th}$ cell cycle to 16.8 ± 8.2 min at the end of the $10^{th}$ cell cycle in FFA treated embryos (N=4 for each division wave). In FFA treated embryos, the interval between division waves decreased by 22%, from 18.0 to 14.0 ± 1.4min (fig. 7.3D). Again there was no significant difference between the intervals between division waves compared with control blastocysts ($P>0.1$ for all cell cycles, N= 1, 4, 4, 4, 4 for cycles 7-10 respectively). As in control blastocysts, there was also an equivalent increase in cell cycle length in embryos treated with 100µM FFA.

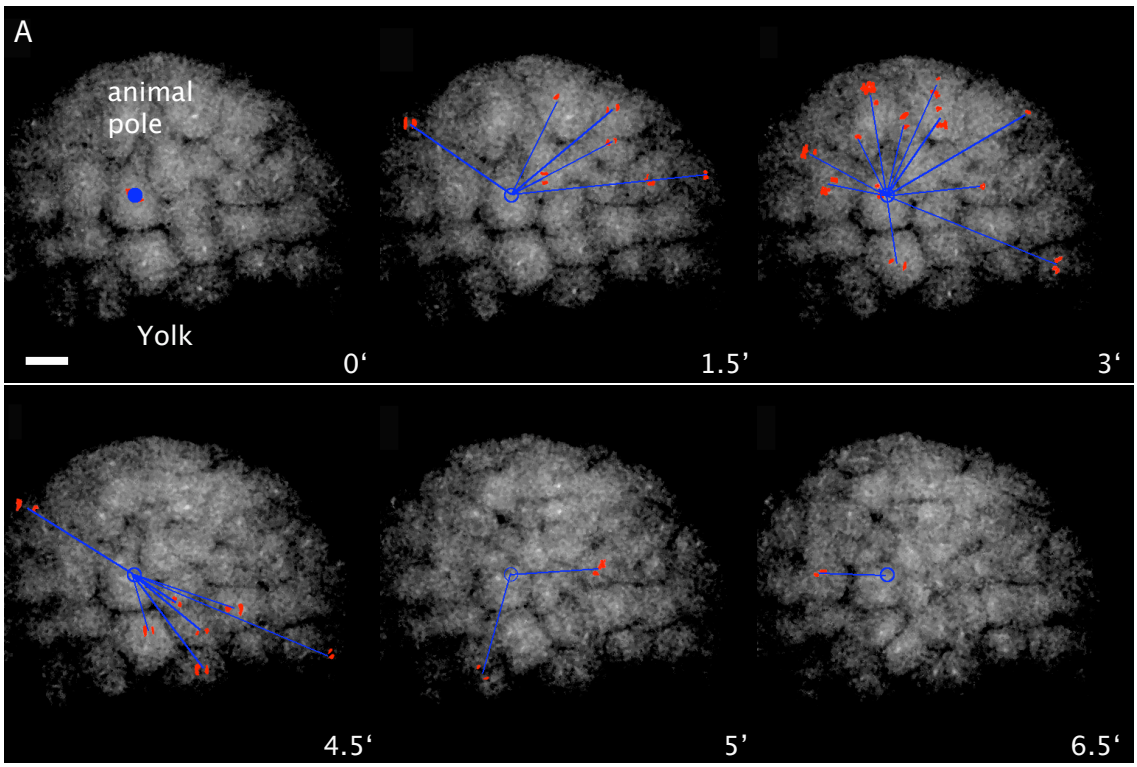


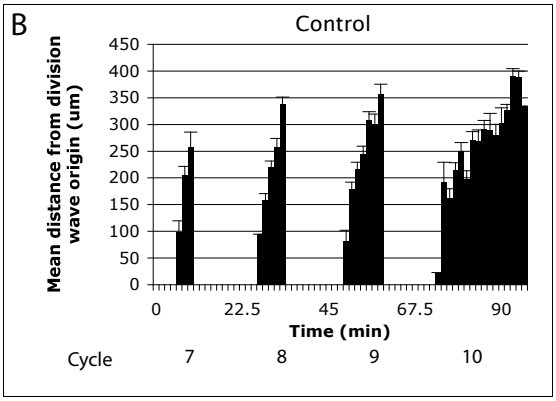


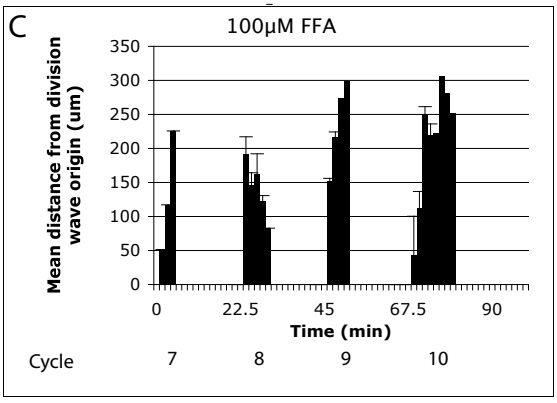


Fig. 7.2. Gap Junction Blockade with FFA disrupts blastocyst cell division waves
A). Projections of single time points during the 8th wave of cell division in a zebrafish blastocyst expressing H2B-RFP in nuclei, treated with 100µm FFA to abolish gap junctional communication. Dividing nuclei are marked in red and the origin of division is marked by a blue circle, which unlike control embryos is not located at the animal pole. The distance between each mitotic body and the division origin were measured (blue lines) (Supplementary movie 6).
B). The mean distance from the division wave origin increases with time in control embryos.
C). The relationship between distance from the division wave origin and time is disrupted in FFA treated embryos, as can be seen in this example from cell cycles 7-10, because mean distance from the division wave origin does not increase during division wave 8 and does not increase beyond the second timepoint in division wave 10 .
Scale bar: 50µm

Cell cycle length increased by 46% over cell cycles 7-10 in FFA treated embryos, which was not significantly different from wildtype (21.0 min to 30.8 ± 6.8 min, P> 0.3 for all cell cycles N= 1, 4, 4, 4 for cycles 7-10 respectively) (fig. 7.3E).

These results suggest that blockade of gap junction communication between blastomeres disrupts their ability to coordinate their pattern of mitosis. Rather than a wave of cell divisions originating at the animal pole and spreading towards the vegetal pole, divisions become less coordinated and more randomized. This occurs without significantly affecting the cell cycle, or the metasynchronous timing of cell divisions, further strengthening the argument that the loss of the pattern of division is due to lost intercellular communication, rather than a more pervasive disruption of blastomere cell biology.

## Calcium activity is correlated with metasynchronous divisions during the blastula period

Previous studies have suggested that connexon mediated intercellular $Ca^{2+}$ ion exchange is important for proliferation (Weissman et al. 2004, Bittman et al. 1997), so $Ca^{2+}$ is a likely candidate for the factor that coordinates the metasynchronous, animal to vegetal division wave during the blastomere stage. To elucidate if intercellular calcium communication plays a role in coordinating blastomere divisions, I characterized the patterns of $Ca^{2+}$ activity during this time period. Zebrafish zygotes were injected with 2ng calcium green dextran 10kD and imaged at 5s intervals during the blastula period and then gap junction communication was inhibited with FFA to determine if gap junction communication was required for blastocyst calcium activity.

**Fig. 7.3. Gap junction blockade disrupts division wave patterns but does not affect cell cycle length or the length of cell cycle phases**

A). Graphs showing blastula stage divisions in 4 control embryos. Division waves show increasing distance from the division wave origin in 14/15 rounds of division.

B). Graphs from 4 100μM FFA treated blastocysts. In 11/16 rounds of division there was not a statistically significant increase in distance from the division wave origin. Therefore division waves were disrupted.

C). Comparison of division wave duration between FFA treated and control blastocysts. The duration of each wave increased from 3.1±1.0min to16.8 ±8.2min in successive cell cycles, but there was no difference between control and FFA treated embryos (P> 0.9, 0.7, 0.6 and 0.8 for the 7th, 8th, 9th and 10th waves of mitoses respectively).

D). The interval between division waves (time between the final mitosis in the previous cell cycle and the first mitosis in the current cycle) decreased from 18.0min to 14.0 ±1.4min in successive cell cycles. Again there were no significant differences between conditions (P> 0.6, 0.1 and 0.1 for the 8th, 9th and 10th cell cycles).

E) Cell cycle length increased from 21.0 to 30.8 ±6.8min in both conditions, but there is no significant difference between conditions (P>0.9, 0.3, 0.8 for cycles 8, 9 and 10 respectively, student's t test).

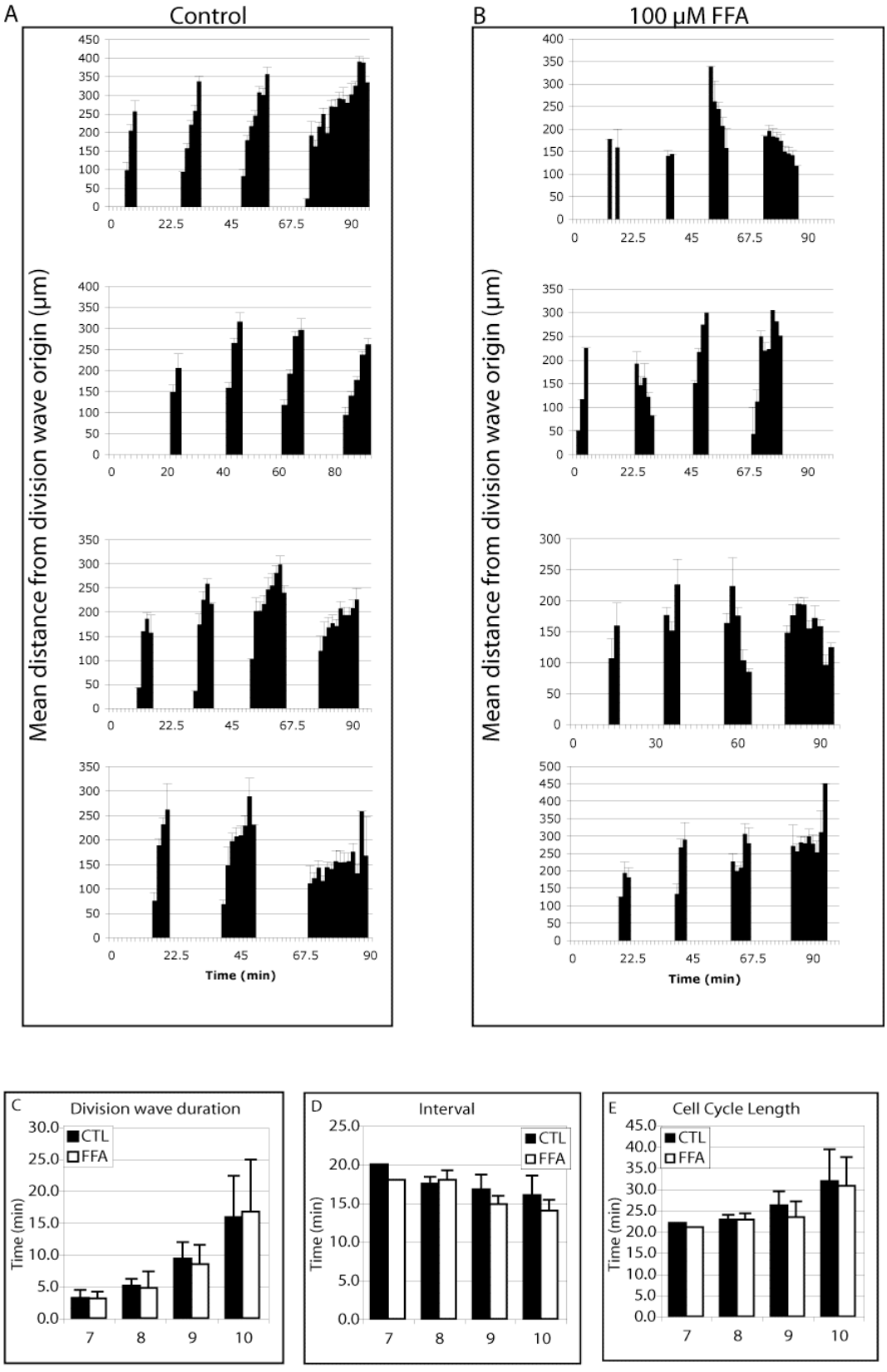


Fig. 7.3. Gap junction blockade disrupts division wave patterns but does not affect cell cycle length or the length of cell cycle phases

Recording calcium transients across the animal surface reveals cyclical calcium activity
Acquiring calcium green dextran fluorescence data from the animal surface of the blastocyst every 5s for 2 hours produced data sets in excess of 3GB. These large data sets and the exponential growth of the number of cells (cell number doubling every 15-25 min), made analysis of the calcium activity in all cells incredibly difficult and time consuming. Two techniques were used to simplify the analysis method:

1. To reduce the size of the data set, a maximum projection was analysed, rather than the entire stack of images at each time-point. This is acceptable because the surface blastomeres were the most fluorescent and the vast majority of calcium transients detected at the surface of the blastocyst (fig. 7.9).
2. Mean fluorescence intensity measurements were recorded from a grid of 50µm x 50µm regions of interest (ROI). This size was chosen, as it was approximately the size of cells during the 8$^{th}$ and 9th cell cycles. The caveat to this method is that at earlier stages, each cell may have been covered by more than one ROI, thus a single transient may have been counted more than once. Likewise at later stages when cells were smaller in size, each ROI covered more than one cell, meaning that the mean intensity within each ROI increased to a lesser extent when a single cell produced a transient. So the grid analysis method became less sensitive at later stages and may have missed some of the calcium transients. Calcium transients were counted in each ROI by recording the change in mean fluorescence intensity over time. Increases in fluorescence intensity were scored as calcium transients if they exceeded a threshold that was set for each time-lapse individually (see methods).

I found that the duration of individual calcium transients ranged from one time point to 6 time points. Imaging at 5s intervals allows measurement of calcium transient duration to the nearest 5s, therefore transient duration lasted from less than 5s, to at least 25s. The median duration was 15-20s (4 time points). Observing calcium activity over the entire animal surface of zebrafish embryos revealed that there were periods of time when few calcium transients occurred and other periods of time in which there were many.

**Fig. 7.4. Blastocyst calcium activity is correlated with cell division**

A). Calcium green dextran fluorescence intensity was recorded from the animal surface of a zebrafish blastocyst at 5s invervals. The embryo was divided into 50 x 50μm squares, which is approximately the size of a blastomere in the 8th and 9th cell cycles. The frequency of calcium transients within each square were counted at 1min intervals. This representative trace shows that activity varied from 0 transients/min to 41 transients/min. Variation was cyclical. Periods of high activity occurred following the onset of each division wave (the first sign of cytokinesis in the first cell to divide), which are marked as squares. Periods of inactivity preceded the onset of division (Supplementary movie 7).

B). Higher resolution recording of calcium activity from the cortex of a single blastomere. It divides at time 0. Transients occur throughout the cell cycle. Note minimal activity 4 minutes prior to division. This is conserved between blastomeres (Supplementary movie 8)

C). Transients per minute when cell cycles are aligned, so that each blastomere starts cytokinesis at time 0. As in A, cells are relatively inactive immediately prior to cytokinesis. There is a burst of activity 7-5 minutes prior to cytokinesis of (1.2 transients/cell), that is not apparent in A, where cell cycles are not perfectly aligned (n=31 cells, N=2 embryos).

D.) Percentage of active cells in 2 minute periods in the 31 individual blastomeres from C. 27/31 (87%) blastomeres produce one or more calcium transient between 7-5 minutes prior to division, contributing to the burst of activity that can be seen in C, but not A. The proportion of active cells decreases to 28% over the following 6 minutes, then increases again as cytokinesis began, however the percentage of active cells never exceeds 60%.

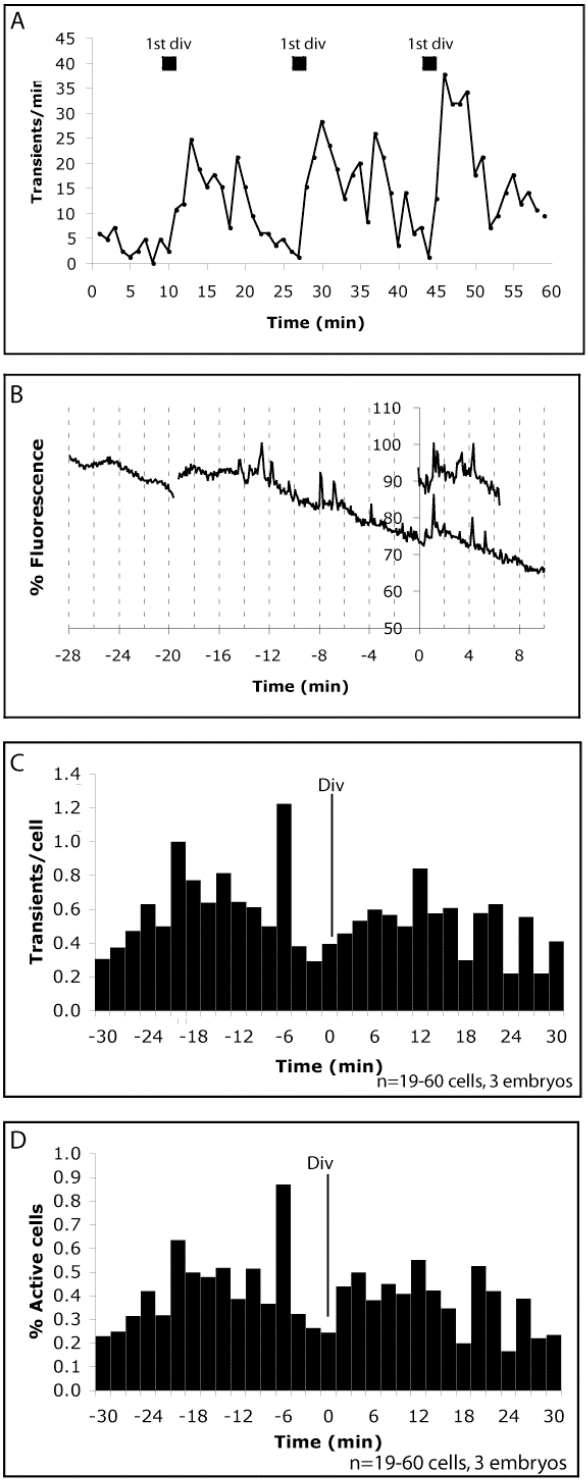


Fig. 7.4. Blastocyst calcium activity is correlated with cell division

The animal surface is approximately 200,000μm$^2$ and so the following data will be presented as the number of events over this area that occurred each minute. The minimum number of transients per minute was 0 and the maximum was 40 (fig. 7.4A). Changes in activity were cyclical and had a period of approximately 20min, which is equivalent to a single cell cycle (N=3).

Since cell cycles are metasynchronous during the blastula stage, the periodicity of calcium activity suggested that calcium transients are in some way connected with the cell cycle. This was indeed the case. The first visible signs of cytokinesis preceded periods of increased calcium activity by 2.6 ± 1.4 min (fig. 7.4A and supplementary movie 7), n=9 cell cycles). The cell cycle stage with the lowest transient frequency immediately preceded mitosis.

**High resolution imaging of individual blastomeres reveals two periods of increased calcium activity in the cell cycle**

While close to synchronous, blastomere cell cycles are not perfectly aligned. The time difference between first and last mitoses of a wave of division ranged from 3.2 ± 13min in the 7$^{th}$ cell cycle to 15.9 ± 6.4 min in the 10$^{th}$. Therefore calcium transients that occur during events at specific points of the cell cycle did not occur simultaneously. To assess with greater accuracy at what point in the cell cycle calcium transients occur, it was necessary to measure calcium activity in single blastomeres and correlate the activity with the time they divided.

Blastomeres where division was clearly visible were selected and the timing of their calcium transients was recorded. The recorded calcium activity of a representative blastomere is shown in fig. 7.4B and supplementary movie 8. Calcium transients in a single blastomere appear not to have a pattern, except for few calcium transients in the 5 minutes prior to cell division (N=3 embryos, 34 blastomeres). The calcium activity from 34 blastomeres was pooled into 2 minute periods, to build up a picture of how calcium activity varies between 30 min prior to division until 30 min after division. It was not possible to follow all cells for the entire hour, due to cell rearrangements that obscured the location of some of the cells. Therefore the number of cells contributing to date in fig. 7.4C and D varies with time. Prior to division, the maximum number of blastomeres recorded from was 34 and the minimum number was 22. After cytokinesis the maximum number of cells being recorded from was 60 and the minimum was 19.

I found that transient frequency, was similar in the aligned cells when compared with the calcium activity recorded from the entire animal surface (fig. 7.4 A,C). The two

periods of lowest calcium activity were between 5-3 minutes and 3-1 minutes before division, with transient frequencies of 0.4 transients/cell and 0.3 transients/cell respectively. This was followed by a steady increase in transient frequency that peaked 5-7 minutes after division with 0.6 transients/cell. A striking finding was the appearance of a burst of activity in the 7-5 minutes prior to cytokinesis, with 1.2 transients/cell (n=31). To determine if this new peak of calcium activity was the result of many cells producing transients (i.e. a marker of a cell cycle related event), or conversely, caused by a few cells becoming highly active (and therefore not being a reliable marker of a cell cycle dependent event), blastomeres were scored as either active (1 or more transient) or inactive (no transients) over 2 minute periods (fig. 7.4D). 87% (27/31) of the cells were active 5-7 minutes prior to cytokinesis and the percentage of active cells did not exceed 65% at any other time-point. This indicates that the peak of calcium activity that preceded cytokinesis may well be a cell cycle related event that produces a transient elevation of intracellular calcium. The proportion of active cells 1-3 min after the onset of cytokinesis) was 44% (26/59) and 3-5 minutes after cytokinesis was 50% (30/60) (fig. 7.4D). In agreement with the movies made of transient frequency, cells were least active 5-3 minutes prior to and 3-1 minutes prior to cytokinesis, with 32% (11/34) and 26% (9/34) active respectively (fig. 7.4D).

In summary this data demonstrates an elevated probability of calcium activity 7-5 minutes prior to cytokinesis and a significantly decreased probability of calcium activity 5-1 minutes prior to cytokinesis.

## Intercellular calcium waves occur over two timescales in blastocysts

To assess if there was a spatial pattern to the calcium transients generated during the blastula stage that might correlate with spatial patterns of division, the coordinates of each calcium transient generated by 3 blastocysts were recorded. Each blastomere was assigned an ROI that was moved each frame to ensure it matched the cell's position despite cell movement and drift (fig. 7.5A). The data is represented as the number of events per cell per minute. In control conditions, calcium activity was followed in 101 cells for 154 minutes. This produced a total cell time of 3145min.

I often found coordinated bursts of calcium activity. They usually consisted of a calcium transient initiating in one blastomere, then propagating into adjacent blastomeres in subsequent time points (fig. 7.5B,C and supplementary movie 9a,b). The frequency of these calcium waves was 0.05 ± 0.01 waves/cell min (fig7.5.D. n= 128

waves, N=3 embryos). The number of cells contributing to an individual wave varied from 2-11 (fig. 7.7B) and the average number of cells in a wave was 3-4. The distribution of wave sizes were as follows: 2 cells: 33% (49/150); 3 cells: 28% (42/150); 4 cells: 15% (23/150), and 5 or more cells: 24% (36/128). The mean distance of the calcium waves was 75 ± 40 μm and mean duration was 18 ± 9s. Wave propagation speed was 8.8 ± 3.6 μm/s (n=128 waves), suggesting they are too fast to be the slow waves (1μ/s) and slightly too slow to be the fast waves (10-30μm/s), described by previous authors (Jaffe, 1999). The frequency of calcium transients that occurred independently of calcium waves was 0.17 ± 0.04/ cell min (n= 1017 transients).

To test if there were also patterns of calcium activity that occurred over longer timescales, all calcium events in 30s bins were integrated. The resulting images showed what appeared to be a calcium wave that swept from the animal pole towards the vegetal pole during division waves (fig. 7.6 and supplementary movie 10). From the 10 division waves analysed in this manner 5/10 were accompanied by a wave that propagated across the entire animal surface of the blastocyst, with average propagation speed of 1.6 ± .08 μm/s. The other 5/10 showed no discernable pattern to their calcium activity when integrated over 30s.

These results suggest that intercellular calcium waves may occur on two different timescales, illustrating that calcium activity is coordinated in the blastocyst. Since this coordinated activity also oscillates during the cell cycle, it is possible that the spatio-temporal coordination of cell divisions in the blastocyst is in some way related to calcium activity.

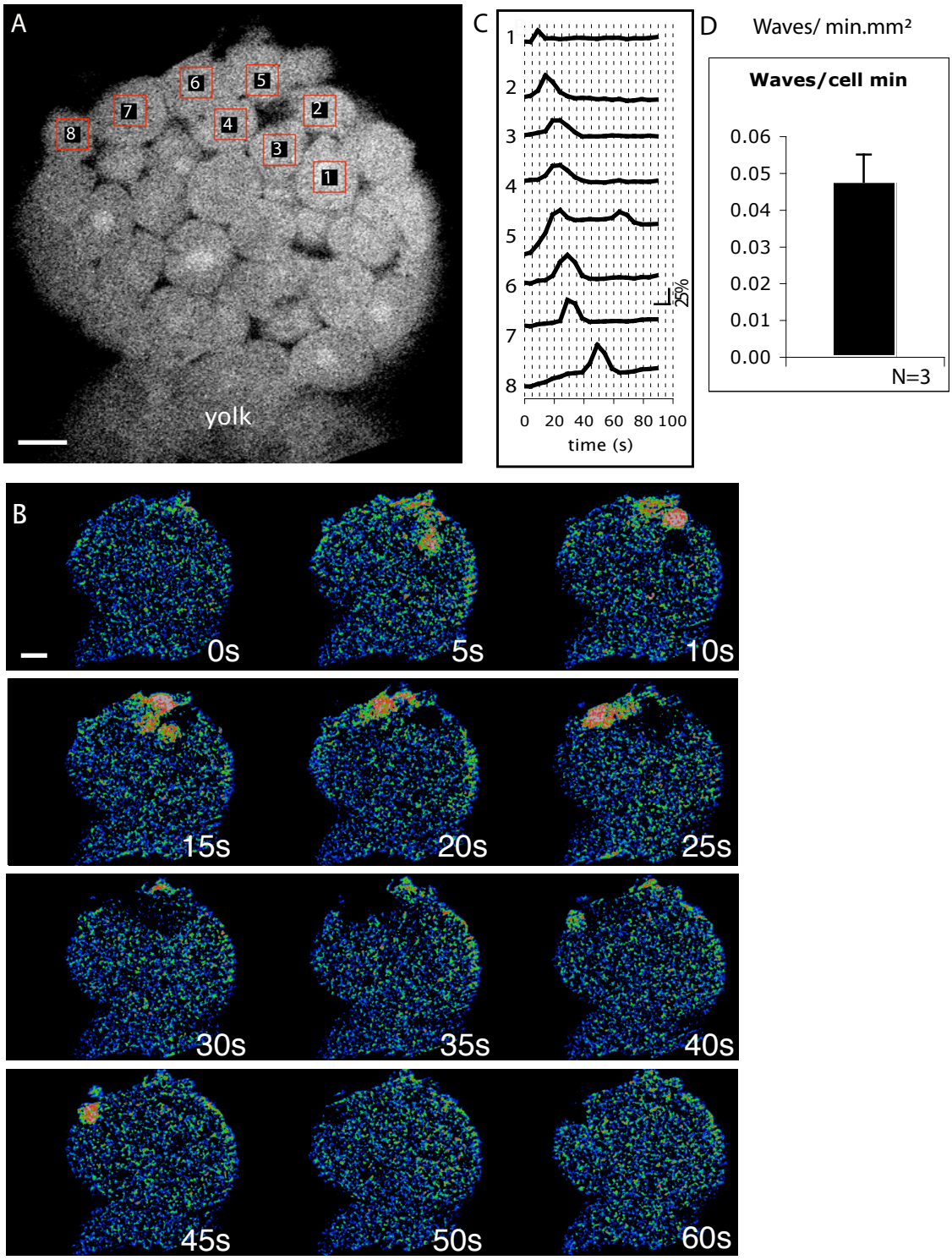


Fig. 7.5. Spontaneous calcium waves propagate across the surface of zebrafish blastocysts
A). Single confocal section of a 4hpf blastocyst labelled with calcium green dextran (10k). Cells that produced calcium transients are highlighted and numbered.
B). Pseudocoloured frames from a timelapse to show only increases in fluorescence/calcium concentration. Regions of increased calcium activity become red/white. Areas with low activity are blue or green.The wave initiates in cell 1 and then propagates into 7 more cells, all of which were superficial. The example wave duration was 30s. Average wave duration was 18 ±9s (Supplementary movie 9).
C). Intensity-time graphs of the 8 cells that produced calcium trasients during the wave. Transient duration ranged between 15-30s.
D). The frequency of intercellular calcium waves (2.5-5hpf) across superficial cells was 0.05/cell min.
Scale bars: 50µm

**Fig. 7.6. Animal to vegetal calcium waves during blastocyst division waves**

A). Projection of a blastocyst undergoing its 9th wave of cell division labelled with calcium green dextran. Red arrows mark the progression of a slow calcium wave that initiates at the animal pole and propagates towards the vegetal pole.

B). Pseudcoloured images to show only increases in fluorescence intensity. Each timepoint is an integration of the increase in fluorescence intensity over a 30s time period (images were acquired at 5s intervals). A calcium wave initiates at the animal pole and propagates towards the vegetal pole. White arrows: wave initiation point and end point (Supplementary movie 10).

Scale bars: 100$\mu$m

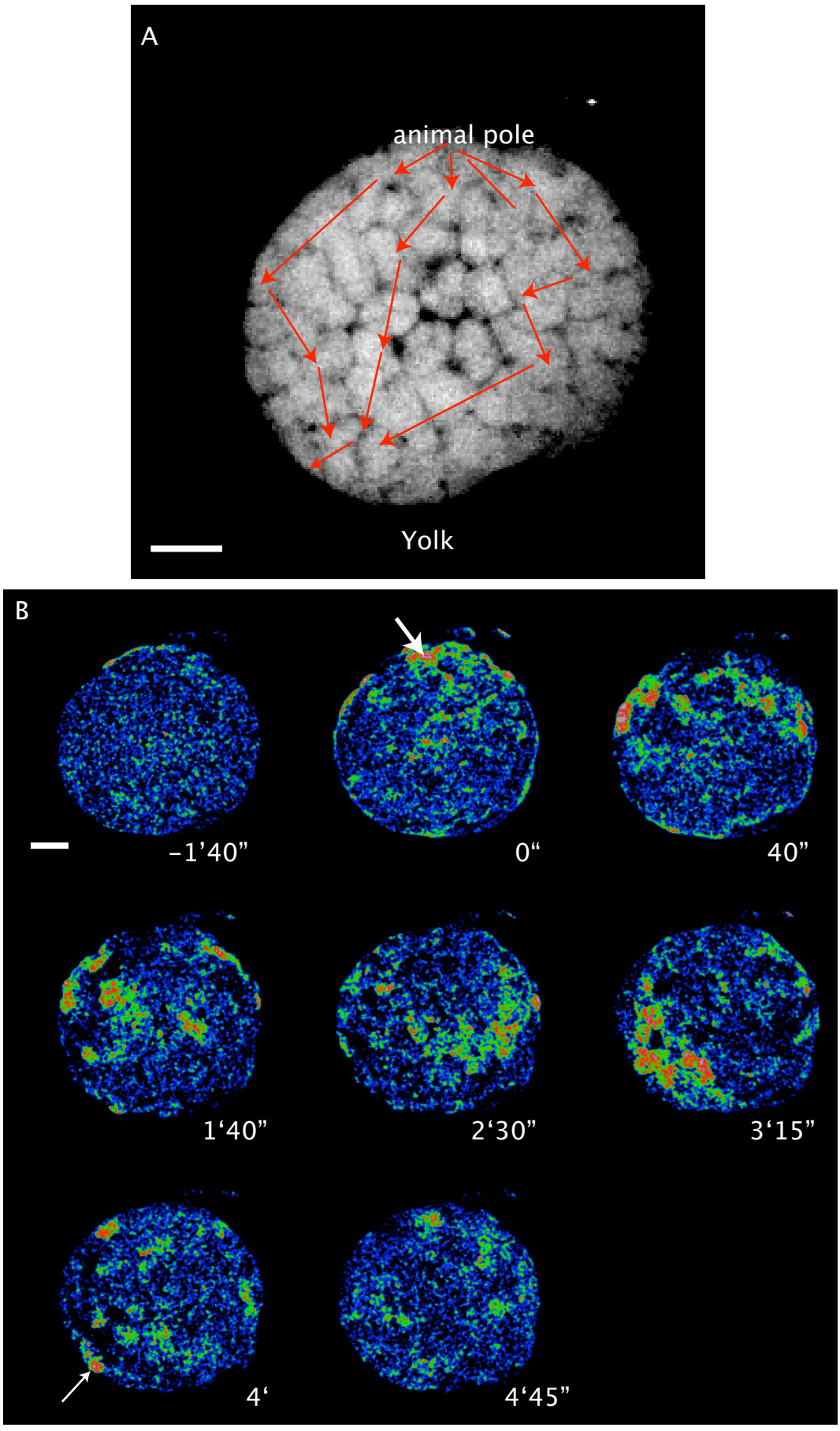


Fig. 7.6. Animal to vegetal calcium waves during blastocyst division waves

## Coordinated calcium activity depends upon gap junction communication

To assess if gap junction communication is required for coordinated, intercellular calcium activity to occur in the blastocyst, blastocysts were immersed in 100μM FFA to block gap junction communication and the calcium activity was recorded.

My results show gap junction mediated intercellular communication is a requirement for the generation of calcium waves, because FFA severely reduced calcium wave frequency by 80%, from 0.05 ± 0.01 waves/cell min to 0.01 ± 0.01 waves/cell min ($P<0.04$ n= 16 waves, N=2 embryos) (fig. 7.7A and supplementary movie 11). The size of each calcium wave was also reduced in FFA treated embryos, as the average number of cells per wave decreased from 3-4 to 2-3. In detail, the percentages of each size cell wave changed from: 2 cells from 33% to 44% (7/16), 3 cells from 28% to 44% (7/16), 4 cells from 15% to 13% (2/16) and 5+ cells from 24% to 0 % (fig. 7.7B). As well as a decrease in both number and size when gap junction communication was inhibited, the frequency of individual calcium transients (those occurring independently of calcium waves) also decreased by 90%, from 0.17 ± 0.04 transients/ cell min to 0.02 ± 0.04 transients/ cell min (fig. 7.7C, $P<0.02$, ctrl:n=1017 transients, N=3 embryos FFA:n=130 transients, N= 2 embryos). This was a surprising result because individual transients were predicted to remain equal in both conditions as it was assumed single calcium transients were produced in a cell autonomous manner. The reason for this is not known, however it may be possible that intercellular communication, or connexon hemichannel function is required for cells to become primed to generate calcium transients.

These results demonstrate that inhibition of gap junction communication with FFA severely reduces both the number of calcium waves and calcium transients, suggesting that gap junction communication is required for the generation of calcium activity at this developmental stage. Since gap junction inhibition also disrupts the spatio-temporal regulation of mitotic waves during the blastula period, this result is consistent with a role for intercellular calcium communication in the coordination of cell divisions.

A

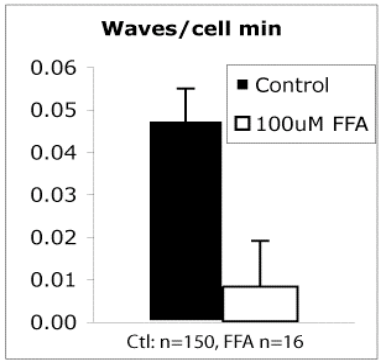


B

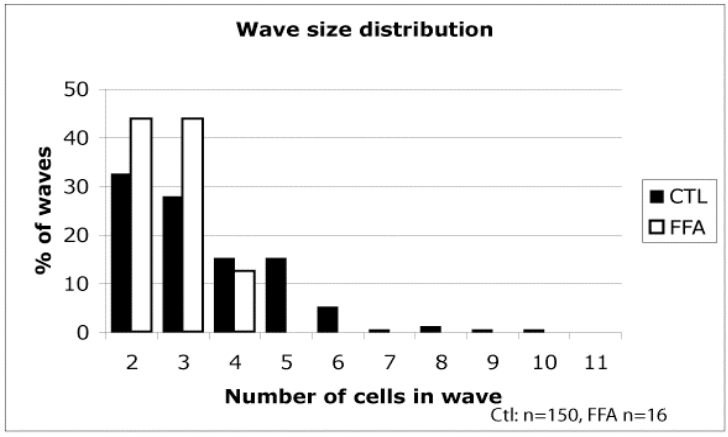


C

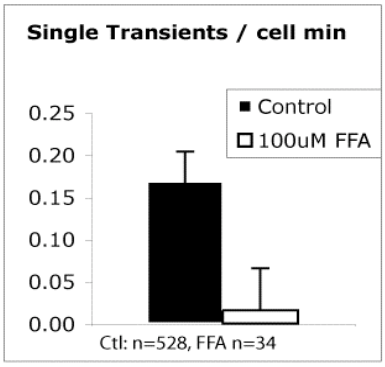


Fig. 7.7. Gap junction blockade reduces calcium waves and transients in blastocysts
A). The frequency of calcium waves in zebrafish blastomeres loaded with calcium green dextran decreased from 0.05 ± 0.01/cell min to 0.01 ± 0.01/cell min on addition of 100μM FFA (P>0.04 student's t-test, N=3 and 2 embryos, ctl and FFA respectively. Supplementary movie 11).
B). The number of cells contributing to each calcium wave also decreased in FFA treated embryos. No waves exceding 4 cells occurred in FFA treated embryos (n=16 waves, N=2 embryos), when 24% did in control blastocysts (n=150 waves, N=3 embryos).
C). The number of non-wave calcium transients were recorded. This too displayed a dramatic decrease, from 0.17 ± 0.04 to 0.02 ± .003 transients/cell min in FFA treated embryos (P<0.02. student's t-test).

## Subcellular calcium transients suggest that calcium ions do not freely diffuse within cells early in development

Previous studies of calcium activity in the blastula period zebrafish development have claimed that since free diffusion of calcium ions occurs through blastomeres, calcium transients can be detected at any location within the cell (Reinhard et al. 1995). However, since localised calcium transients have been found at the cleavage furrow (e.g. Fluck et al. 1991), I examined calcium activity in more detail in the blastula and pre blastula stages to determine if sub cellular transients could be detected.

During the 7$^{th}$ cell cycle, which is the end of the cleavage period I detected calcium transients at the contact points between cells. These contact point transients were the most common type of calcium event during the late cleavage period, since they made up 69% of the calcium activity (83/120 transients, N=2). They often oscillated between the contacting cells in a wave-like manner. (fig. 7.8 and supplementary movie 12). At this period of development, whole cell calcium transients were less common and made up the other 31% of transients (37/120%, N=2) of the instances. Subsequent to the 7$^{th}$ cell division calcium transients appeared to occur within entire cells, however recording the fluorescence intensity of the calcium indicator at different levels through individual cells revealed that the majority of calcium activity is localised within the cell cortex (fig. 7.9 and supplementary movie 13). Transients were detected when recording from the cortex, while fluorescence measurements taken 10 and 20µm deeper failed to detect any transients (n= 90 cells, N=3 embryos). This suggests that the calcium transients may be playing a role in membrane remodelling, leading to cell movement and or cytokinesis. It also means that when imaging the blastocyst, recordings had to be made from the surface of the blastomeres, otherwise the transients they produced were not detected. Since the embryo is close to spherical at this developmental stage, a large depth of tissue had to be recorded from in order to maximise the number of cells that could be recorded from with any degree of confidence. Also, in agreement with previous work (Reinhard et al., 1995), there was no discernable calcium activity within cells located deep within the blastocyst (data not shown, N=6).

**Fig. 7.8. Subcellular calcium transients in contact points between pre-blastula stage cells**

A). Single confocal sections from a time-lapse of a cleavage stage zebrafish embryo loaded with calcium green dextran. Two touching blastomeres are labelled (b). Calcium transients occur at the contact point between two cells. Arrows mark transients. Numbered boxes show where fluorescence measurements were made (Supplementary movie 13).

B). Traces of % change in fluorescence intensity from 2 regions in each cell. The two regions distant from the contact point (1,4) are less active than the two regions on either side of the contact point (2,3), indicating that the transients are local to the contact point.

C). Schematic of a cleavage stage zebrafish embryo. The red box depicts the region displayed in A. (Kimmel et al., 1995).

Scale bar: 25$\mu$m.

b: blastomere

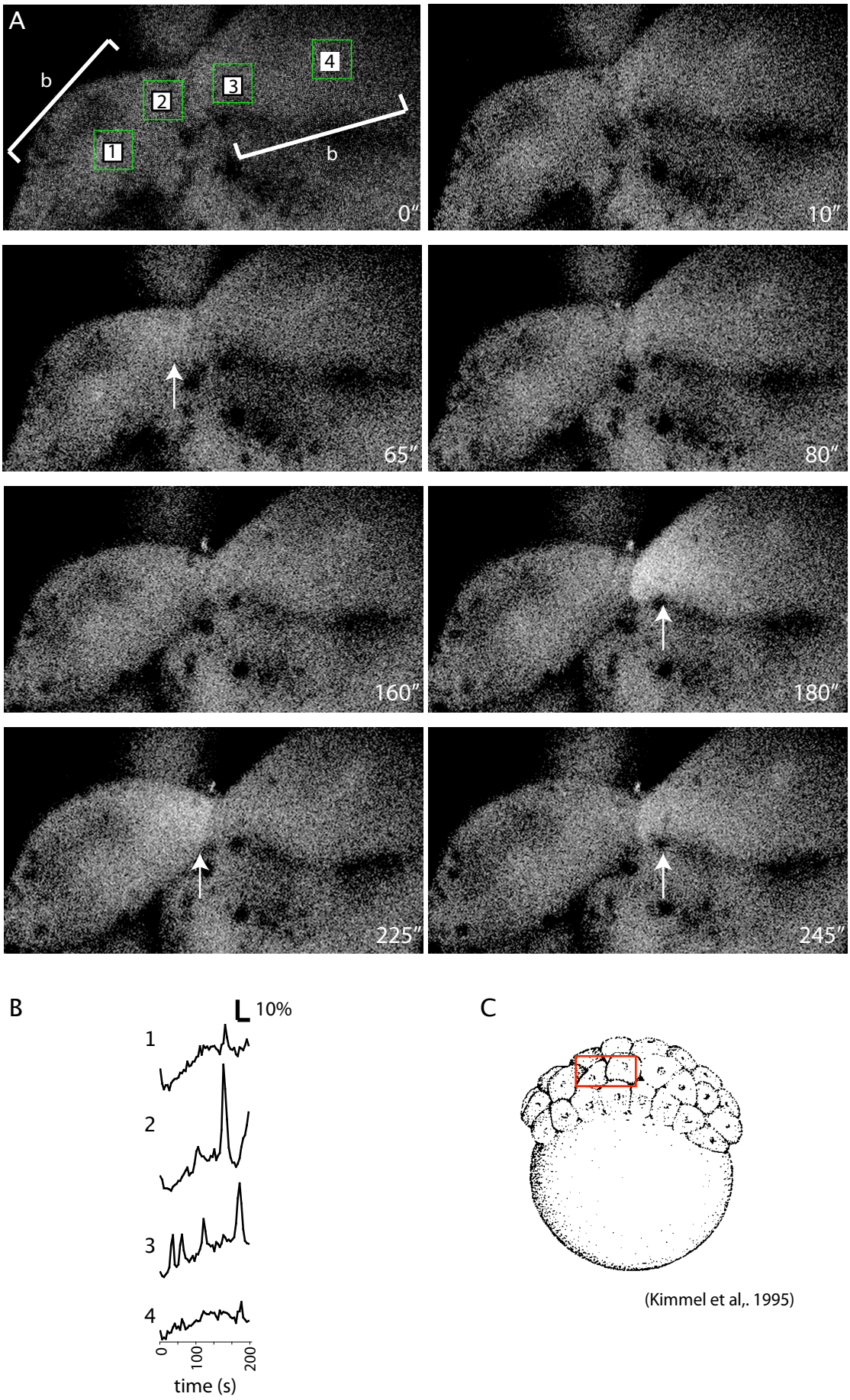


(Kimmel et al,. 1995)

Fig. 7.8. Subcellular calcium transients in contact points between pre-blastula stage cells

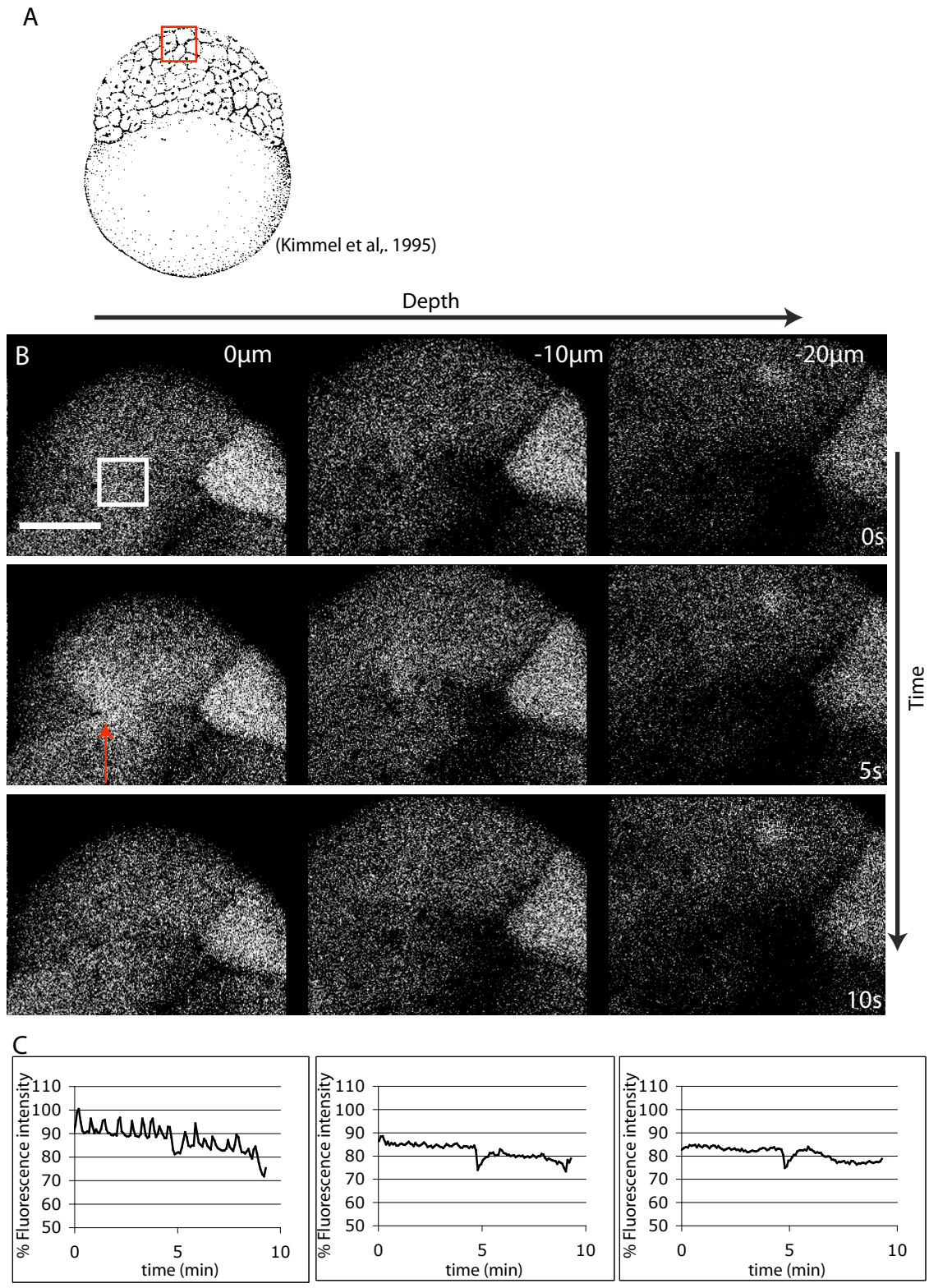


Fig. 7.9. Blastomere calcium transients are restricted to the cell cortex
A). Schematic of a 256 cell stage blastocyst. The red box depicts the region displayed in B. (Kimmel et al,. 1995).
B). Single optical slices from a timelapse recording of a calcium green dextran labelled zebrafish. Fluorescence intensity was measured from the region in the white box at 3 depths. A transient, marked with a red arrow, is clearly visible in the superficial slice. The transient is less apparent 10µm deep and is not detectable 20µm deep (Supplementary movie 13).
C). Fluorescence intensity graphs over a 10min period show tonic activity in the superficial slice and recordings from deep in the cell miss the transients.
Scale bar: 25µm

# *Discussion*

## Cell division wave coordination requires intercellular communication

To determine the role of gap junction communication in coordinating the cell cycles in zebrafish blastocysts I blocked gap junction communication with the reversible connexon pore inhibitor flufenamic acid (FFA). This disrupted the tightly coordinated order of cell divisions that normally occur in an animal to vegetal wave in normal embryos without other effects on cell division (Kimmel et al., 1995). This result suggests that the precise timing and spatial organisation of blastomere cell cycles is dependent on intercellular communication via gap junctions, or through unopposed connexin hemichannels.

Previous attempts to disrupt gap junction communication produced a different phenotype. Injection of antibodies that block gap junction channels into single blastomeres of compacted, 8 cell stage mouse embryos resulted in the injected cells being extruded from the blastocyst and not taking any further part in embryonic development (Becker et al., 1995; Lee et al., 1987). Extrusion did not occur in FFA treated blastocysts in my experiments, however injection of anti-connexin antibodies depleted the size of gap junctions assembled at cell interfaces (Lee et al., 1987). Gap junctions have been shown to be important mediators of cell-cell adhesion independently of channel function (Elias et al., 2007), therefore de-adhesion of antibody injected blastomeres, rather than blocked channel function may have been the cause of their extrusion.

To date, the requirement for gap junction communication between blastomeres has not been elucidated. Currently, all known *connexin* mutants appear to complete the blastula stage of development without severe defects, however most of the studies were focused on later developmental stages, so may have missed mild defects (Houghton, 2005). Attempts to block gap junction communication globally have also not produced fruitful insights into connexin function. When irradiated and normal mouse blastomeres were aggregated, the normal cells proliferated faster and in a gap junction dependent manner, since 18a-glycyrrhetinic acid (AGA) treatment abolished this advantage (Vance and Wiley, 1999). The requirement for gap junction communication in blastomere proliferation is not essential because total blockade of gap junction channels in rodent blastocysts with AGA failed to cause a phenotype (Houghton et al., 2002). It is unclear

if this treatment affected later stages of development and since the study did not observe individual cell behaviour, if AGA disrupted cell division patterns, they were missed. (Houghton et al., 2002). Therefore my study is one of the first (if not the first) study to provide direct evidence that gap junction communication is employed by the early embryo to coordinate the spatio-temporal pattern of cell division.

This result must be treated with caution because developmental defects caused by FFA (which is a reversible inhibitor of gap junctions) treating embryos were irreversible, with most embryos not surviving 24 hours and the rest exhibiting severe developmental defects. This result can be interpreted in three ways. First: residual FFA remained in the embryos despite washing, which is possible since FFA is difficult to remove from tissues (Pan et al., 2007). Second: coordinating cell division during the blastula stage is essential for later development. Third: experimental concentrations of FFA are toxic. Aside from a lack of calcium activity and loss of division coordination, the inhibited embryos appeared to be normal at the end of my period of analysis. Cell cycles were not perturbed; cells divided metasynchronously for the duration of calcium imaging and their nuclei appeared normal in both appearance and behaviour. Likewise there was no effect on the duration of the cell cycle or on the duration of individual phases of the cell cycle. This suggests that any toxic effects of FFA must occur at later stages of development. Another fact that must be considered is that FFA has been shown to block non-specific cation channels (Gogelein and Pfannmuller, 1989). and so its effect upon cell division waves and calcium activity could possibly be due, in part, to effects other than gap junction blockade. To control for potential non-specific and toxic effects of FFA, the experiment should be repeated using a different chemical to inhibit gap junction communication to see if the same result can be achieved. If this turns out to be true, this result strongly suggests that intercellular signalling is required to determine the spatio-temporal organisation of cell division in the blastocyst.

## Spatio temporal patterns of calcium activity suggest a role in coordinating metasynchronous cell division

I have demonstrated for the first time that during the blastula stage calcium activity has both spatial and temporal patterns. Calcium activity is cyclical and organised into intercellular calcium waves. Taking these observations into account with the finding that gap junction inhibition disrupts both calcium wave generation and coordinated cell division, suggests that calcium activity may regulate cell division in the blastocyst:

**Calcium activity oscillates during the cell cycle**

It has previously been suggested that calcium levels oscillate throughout the *Xenopus* cell cycle (Grandin and Charbonneau, 1991; Keating et al., 1994; Kubota et al., 1993), yet these methods either averaged the calcium levels throughout the entire embryo by the use of calcium sensitive microelectrodes, or could only record calcium activity from small numbers of cells because aequorin was injected into individual blastomeres.

By injecting calcium green dextran into zebrafish zygotes and using acquisition speeds rapid enough to visualise the entire animal surface of the blastocysts every 5 seconds, I was able to record cyclical calcium activity during the blastula period of development. Calcium activity was closely tied to the cell cycle. Low activity immediately preceded the onset of division while high activity occurred following the onset of division. This agrees with the work of Kubota, who observed increased levels of calcium following the appearance of the cleavage furrow in dividing *Xenopus* cells (Kubota et al., 1993). My results demonstrate that the cyclical calcium levels are in fact produced by a cell cycle dependent change in the frequency of calcium spikes and wave production, rather than a simple increase in basal levels of intracellular calcium, which was unclear in previous studies (Grandin and Charbonneau, 1991; Keating et al., 1994; Kubota et al., 1993). I cannot be certain what function these calcium transients have, but they may be involved in chromasome separation (Whitaker and Patel, 1990), cleavage (Fluck et al., 1991) or in coordinating the behaviour of neighbouring blastomeres (my results).

In previous studies of calcium activity in the zebrafish blastocyst, there were either few transients seen (Leclerc et al., 2000) or no reported patterns to the cells producing calcium transients. Cells with high and low transient frequency were observed at all times during previous movies (Reinhard et al., 1995), or the methodology was not sensitive enough to resolve single cell calcium activity (Creton et al., 1998). In the former, a nuclear calcium indicator was used, which would have missed many calcium transients that were localised to the cortices of the blastomeres. Also, dissolution of the nuclear envelope precedes cytokinesis, so it was not possible to record calcium activity during cytokinesis, which was the time at which I observed the highest frequency of calcium transients.

**Aligning cell cycles revealed a calcium transient 7-5 minutes before cell division**

High resolution imaging of small numbers of blastomeres yielded similar but subtly different results than when the entire animal surface of the blastocyst was imaged. I measured the fluorescence intensity of single cells and then aligned their cell cycles during analysis in order to observe if calcium transients occurred at specific points in the cell cycle. The period of lowest transient frequency occurred prior to cytokinesis and a long period of high activity followed the onset of cytokinesis. However there was also a burst of calcium activity 7-5 mins prior to cytokinesis in 90% of the blastomeres that was not apparent in the unaligned, whole blastocyst movies. When recording calcium transients across the entire animal surface of the blastocyst, the cell cycles of each blastomere were not aligned perfectly, so at any given time point, different blastomeres were in different phases of the cell cycle. For example, the length of time between the first and last mitoses of each round of division ranged from 3.2 (±1.3) min during the $7^{th}$ cycle to 15.9 ±6.5 min in the $10^{th}$, therefore calcium events that occurred at certain times in the cell cycle were dispersed through the population of blastomeres by equivalent periods of time. This is the reason why the peak of calcium activity that occurred in 90% of blastomeres 7-5 mins prior to cell division was not detected when the unaligned calcium activity from the animal surface of the blastocyst was imaged. Since 90% of all blastomeres generated calcium transients in this time period, there may have been an important calcium dependent cellular event occurring. Two possible candidates are nuclear envelope breakdown, or G1-S phase transition, both of which are accompanied by calcium transients in zebrafish and sea urchin (Berridge, 1995; Creton et al., 1998; Poenie et al., 1985; Whitaker, 2008).

During no time periods following the onset of cytokinesis were such a high proportion of blastomeres active, despite there being a prolonged period of high calcium activity in this time period. This suggests either that calcium transients following cytokinesis, while occurring frequently, are not as tightly linked with the cell cycle as the calcium transients before cytokinesis, or that the cell cycles themselves de-align. The latter may be the case because the pool of aligned blastomeres contained cells in the $8^{th}$, $9^{th}$ and $10^{th}$ cell cycles, which have different cell cycle lengths. Therefore transients that occur at set points in the cell cycle may not have been in register, despite alignment of cytokinesis.

**Intercellular calcium waves indicate cell-cell coupling in the blastocyst**

Intercellular calcium exchange has been reported in zebrafish blastocysts previously (Reinhard et al., 1995) and my results confirm that this is the case. I observed 8.8 μm/s calcium waves that propagated between clusters of blastomeres up to 11 cells in size. While the previous report observed coordinated patterns of calcium activity, the number of cells seen contributing to a single wave did not exceed 5. The time taken for the waves to spread through these 5 cells was 5s, whereas I observed the time-course of calcium wave propagation to be 1-2 cells per 5s. Therefore it seems that Reinhard missed the waves of longer duration and size. Again this is probably due to the use of a nuclear localised calcium indicator for the reasons stated above. Regardless of this difference, both studies confirm that intercellular calcium activity occurs during the blastula stage of development. One might argue that the increased frequency of calcium activity I observed was a product of physical damage to the blastocyst. However blastocysts were not removed from their chorions before imaging and so were subject to minimal disturbances.

When viewed at 5s intervals, global calcium waves could not be detected. Individual transients and intercellular waves spreading between up to 11 cells were seen. This is in agreement with a previous study of zebrafish blastocysts (Reinhard et al., 1995). Global calcium waves appear to occur over longer time durations (30s range), which will be discussed later.

**Are metasynchronous cell divisions coordinated by intercellular calcium exchange?**

I have demonstrated that there is a correlation between coordination of cell division and calcium activity in blastocysts. Cell divisions are metasynchronous and occur in an animal to vegetal wave, while calcium activity is tied closely to the cell cycle and is composed of individual transients and intercellular calcium waves.

Inhibiting gap junction communication with FFA both disrupted the pattern of cell divisions and also severely reduced the frequency and size of calcium waves and transients. It has not been possible to test if calcium activity is directly linked with the organisation of cell divisions. It may be possible that calcium activity is not the cause of the division waves occurring in an animal to vegetal direction because individual cells had a very high chance of generating transients 7-5 min prior to cytokinesis, but no pan-embryonic coordinated patterns of calcium activity were seen before the division waves started. The large calcium waves seen in the integrated 30s movies and the increased

activity seen at 5s intervals actually occurred *after* the onset of cytokinesis. Thus calcium cannot be the instruction that causes animal pole cells to divide first. I propose that calcium signalling is an *effector* of division coordination - the final step in a long process of communication that determines the order in which cells divide. It is also not possible to differentiate between the two possible mechanisms of calcium wave propagation that could be occurring in blastocysts. The first possibility is for calcium itself to spread in a wave from one cell to the next. The other is for a signalling molecule that causes intracellular calcium levels to increase to be the factor that is exchanged by cells. In support of the latter, calcium ions are heavily buffered by endogenous molecules and so may not be able to spread extensively between cells (Giaume and Venance, 1998).

IP3 or ATP may actually be the signalling molecules that cause the propagating increase in calcium concentration because it diffuses between cells more readily than calcium ions and have been shown to be important in cell cycle regulation, cytokinesis and in calcium wave propagation in tissues that include neuronal precursors, astrocytes and lung epithelium (Berridge et al., 2000; Giaume and Venance, 1998; Weissman et al., 2004; Whitaker, 2008). These molecules then interact with IP3 receptors on the ER to release calcium into the cytoplasm, or on P2Y receptors on the cell surface, which via a signalling cascade cause an increase in IP3 production and ultimately an increase in cytosolic calcium. In agreement with this hypothesis, IP3 concentrations increase steadily from the 32 cell stage onwards in zebrafish, when the blastocyst forms and intercellular communication becomes apparent (Reinhard et al., 1995).

I have developed a technique to experimentally manipulate calcium levels that may be able to address what role calcium and IP3 have in determining the order that cells divide in the blastocyst. I have demonstrated that it is possible to photo uncage calcium from NP-EGTA in intact blastocysts, but this method failed to generate regular calcium waves (Data not shown).

Calcium ions are highly buffered by cells, so perhaps its intercellular spread is prevented. It is technically possible to inject caged IP3 and photo uncage it during the blastula stage and this results in an increase in intracellular free calcium in the target cell (Ashworth et al., 2007). IP3 can be injected at the 1 cell stage, then vegetal blastomeres repeatedly exposed to UV. This will cause increased IP3 and calcium levels in the target cell and also, possibly cause intercellular calcium waves to be initiated. If this experiment results in a reversal or disruption of the cell division wave, it will

confirm that intercellular communication is required to coordinate cell division in the blastocyst.

## Why does FFA inhibit single cell activity?

Bathing blastocysts in FFA inhibited single cell transients as well as intercellular calcium waves. This seems strange because one might expect single cell transients to occur in a cell autonomous manner. In accordance with this, in chick neural retina waves, but not transients, are reduced when gap junction inhibitors are used (Pearson et al., 2004). A recent study has shown that FFA can disrupt normal regulation of intracellular calcium concentrations independent of gap junction inhibition (Gardam et al., 2008), suggesting that the loss of calcium transients I observed in the presence of FFA may not be the result of connexon channel blockade. On the other hand, calcium induced ATP release via connexon hemichannels has been shown to generate calcium transients in a cell autonomous manner, while blockade of connexon pores abolished this signalling loop (reviewed in Evans et al., 2006). Therefore the single cell transients I observed in blastocysts may be produced by autocrine signalling. To confirm if this is the case, an ATP antagonist, such as suramin should be applied to the embryo medium and its effect on calcium signalling be recorded. Secondly the effect of other gap junction inhibitors such as AGA or carbenoxalone can be used to confirm if the results obtained with FFA are caused by inhibition of connexon pore function.

## Integrating calcium activity: waves or artefacts?

Slow and ultraslow calcium waves that propagate at velocities less than 2μm/s have been observed or proposed to occur in a variety of developmental contexts, including cleavage furrow extension (0.2μm/s), convergent extension (0.05μm/s) and somitogenesis (0.07μm/s) in zebrafish embryos (Creton et al., 1998; Webb et al., 1997).

From my data, slow calcium waves were not visible in time-lapses of zebrafish blastocysts when time points were spaced 5s apart, but did become apparent when 6 frame averages were created from the data to generate 30s integrated periods of calcium activity. During cell division waves, when integrated over 30s periods, calcium activity appeared in the form of pan-embryonic slow calcium waves that swept from the animal pole towards the vegetal pole at a rate of 1.6μm/s. Interpreting the data in this manner potentially supports the, until now, unsupported hypothesis that calcium activity occurs in waves during the blastula period (Keating et al., 1994). However, since these slow calcium waves were not clear when the time-lapses were viewed at 5s intervals, this

interpretation may not be accurate. In time-lapses viewed at 5s intervals there were spatial and temporal gaps in calcium activity that caused me to believe I was observing many separate, small calcium waves rather than few large ones. A perhaps fundamental problem is that, when seen at 5s intervals some calcium waves actually propagated *towards* the animal pole. Integration of these vegetal to animal calcium into 30s pools makes the cells appear to be active simultaneously and so occludes true calcium activity.

One depressing possibility is that the animal to vegetal calcium 'wave' may simply be an illustration of the increased number of calcium spikes produced by mitotic cells. Since cell divisions occur in a wave, increased calcium spike production could also follow this pattern without calcium ions being propagated. If this is the case pooling activity over 30s may only create the *illusion* of a wave. The studies of slow and ultraslow calcium waves in early development utilised aequorin to visualise calcium activity (Creton et al., 1998; Webb et al., 1997). The use of aequorin prevents fast image acquisition, so they used acquisition rates of, at best, 1 frame every 30s. The detection mechanism pools the number of photons produced over this time period. Thus the calcium waves they detected may actually be an integrated count of calcium transients rather than a propagating wave. Such a loss of temporal resolution when using aequorin has been reported previously: during the period following the first cell division, a series of calcium transients were detected with fluorescent indicator calcium green dextran (Chang and Lu, 2000). When visualised with aequorin at slow acquisition rates, these calcium transients could not be resolved. Instead, calcium activity appeared to be a steady increase in calcium concentration (Fluck et al., 1991; Webb et al., 1997). In fact this principle of temporal integration has been exploited to reconstruct the action potential frequency within olfactory bulb neurons from their patterns of calcium activity (Yaksi and Friedrich, 2006).

Therefore claims that slow and ultraslow calcium waves propagate through large areas of embryonic tissue during early development, based on calcium activity integrated over extended time periods, must be treated with caution as they integration may not truly reflect the calcium activity of the tissue under examination.

## Novel observations of subcellular calcium activity

Previous knowledge of calcium activity in the cleavage stage of teleost development consisted of only 4 calcium transients associated with cell division: the cleavage positioning, elongating and deepening signals and a post division calcium spike (Chang and Lu, 2000; Chang and Meng, 1995; Fluck et al., 1991; Webb et al., 1997). While in the blastula stage, transients with no spatial or temporal pattern and small, 5 cell calcium waves have been reported (Reinhard et al., 1995). I can now confirm that these transients exist and add a few new findings to this list. The duration of individual transients I observed is similar in length to those previously reported in zebrafish blastocysts and is indicative that IP3 signalling mediates their generation (Reinhard et al., 1995). Also in accordance with previous work is the lack of observed calcium activity in deep cells in the blastocyst. From my study it was not clear if this was caused by a true lack of activity in deep cells or by an inability to detect deep activity, however previous work suggests that it is a true observation and not caused by technical difficulties (Reinhard et al., 1995).

The first new observation was that within the outer cells, calcium activity is restricted to their cortices, suggesting that they mediate cell membrane rearrangements. The second new observation was of calcium transients at the contact points of cleavage stage cells. The purpose of these cell-cell contact localised calcium transients is unclear, however it has been shown that mechanical stretching of cell membranes can stimulate calcium activity (Lee et al., 1999), thus these small scale calcium waves may have been caused by mechanical stress and could be required to maintain cell-cell contacts. Since at this point in development the embryo lacks a tough outer layer of cells (either an EVL or epidermis) these cell-cell contacts may be important in ensuring that cells do not dissociate.

Except for the work of Chang and Reinhard (Chang and Lu, 2000; Chang and Meng, 1995; Reinhard et al., 1995), many of the previous studies of cleavage stage zebrafish embryos was carried out using aequorin, which does not have the temporal or spatial resolution to see such subcellular calcium activity (Fluck et al., 1991; Webb et al., 1997). Chang and others did in fact use the same calcium indicator for their experiments as I did, however they did not study calcium activity beyond the 4 cell stage, while Reinhard used a nuclear localised calcium indicator (Reinhard et al., 1995). While she claimed that there is free diffusion of calcium ions from cytoplasm to nucleus and thus did not miss any calcium activity, I have demonstrated that calcium transients are most

prevalent at the cortices of the outer blastomeres and that little activity could be recorded from the central cytoplasm. Therefore it seems unlikely that nucleus localised calcium indicators can detect all calcium activity. In support of this argument, Reinhard and colleagues failed to detect the cleavage furrow related transients that have been detected in both medaka and zebrafish using aequorin (Fluck et al., 1991; Webb et al., 1997) and also in the zebrafish with calcium green dextran (Chang and Meng, 1995).

In summary, this discussion illustrates the care needed to interpret calcium activity data and emphasizes the importance of understanding the temporal limitations of some detection methods (aequorin), the need to analyse the whole cell (cytoplasm and nucleus) and the need to question whether spreading intercellular calcium activity is a driver or a consequence of cell activities such as mitosis.

# Concluding Remarks

Intercellular junctions are essential for embryonic development as they ensure the structural integrity of the embryo is maintained and provide an intercellular signalling system that allows the development of cells, compartments and tissues to be coordinated. Through studying intercellular junctions in zebrafish neurogenesis and at the blastula stage, I have discovered novel characteristics and found new roles for intercellular junctions.

Through looking at ZO-1 expression in the hindbrain I have confirmed that, like with chick (Guthrie et al., 1991; Ojeda and Piedra, 1998), zebrafish hindbrain boundary cells have enlarged apical end feet (AEF) compared with non-boundary cells, accompanied by junctional domains with larger perimeters. The interrhombic interfaces, as visualised with ZO-1, are also often linear. These two properties gave me an objective means to seek out other regions of the neuroepithelium with boundary characteristics. I explored anterior brain regions that have previously been suggested to be compartmental borders, including the ZLI, MHB and floor plate (Figdor and Stern, 1993; Fraser et al., 1990; Rubenstein et al., 1994). All proposed compartment borders (plus a novel border in the midbrain), display AEF modifications in common with rhombomere boundaries, which suggests that the proposed compartment borders are indeed boundaries. It also strongly suggests that examining epithelial arrangement is a valid approach to understanding compartmentation.

A striking feature of the epithelial organisation in the embryonic zebrafish hindbrain was a graded change in AEF size. Large end feet were in boundaries and small end feet in the centre of rhombomeres. Since cell fate choices and cell identity have been shown to be related to intercellular junctions at the apical surface (Mirzadeh et al., 2008; Rasin et al., 2007), I explored whether altering the spatial regulation of neurogenesis, through manipulating Notch signalling, also altered the size distribution of AEF in the hindbrain. I reduced Notch signalling by using embryos with *lfng* knocked down and increased Notch signalling by using *hdac-1*$^{-/-}$ mutant zebrafish. The size of AEF were altered in both situations, however only in *hdac-1*$^{-/-}$ was the graded size distribution of apical end feet disrupted. AEF sizes were more uniform than wt, which accurately reflects the changes in cellular arrangement seen in *hdac-1*$^{-/-}$ hindbrain (Cunliffe, 2004). Knockdown of *lfng* does not significantly alter segmental patterning at the stage I examined (Nikolaou et al., 2009). Taken together, these results support the hypothesis

that the graded arrangement of AEF in the hindbrain is linked to the segmental organisation of boundary and non-boundary progenitor cells, and neurons in the hindbrain.

Rhombomere boundary AEF were largest in all situations and in *hdac-1*$^{-/-}$ hindbrains the interface between rhombomeres appeared to be more linear than in wildtype embryos, indicating that the integrity of interrhombic interfaces was not reduced. This probably means that boundary formation was not affected in either treatment and that boundary cells may be resistant to disrupting the Notch signalling pathway. It will be interesting to learn if AEF are enlarged in embryos were boundary formation does not happen. Eliminating antagonistic Eph-Ephrin signalling at interrhombic interfaces caused mixing of cells from different rhombomeres, close to their interface, and loss of boundary cell specific gene expression (Cooke et al., 2005; Xu et al., 1995). It would be interesting to learn if expanded AEF at boundaries are also lost in zebrafish lacking one or more Eph or Ephrin.

Another interesting avenue that could be explored to better understand the relationship between epithelial organisation, and neurogenesis would be to asses the role that the Wnt signalling pathway plays in determining AEF size. Various *wnts* are expressed in zebrafish rhombomere boundaries and there is a growing body of evidence that they are required to ensure proper development of boundary cells (Amoyel et al., 2005; Riley et al., 2004). Secreted Wnts also pattern the surrounding rhombomeres by encouraging neuronal differentiation (Amoyel et al., 2005). Therefore AEF size distribution may also be dependent upon Wnt expression at, and signalling from rhombomere boundaries.

A common feature of many epithelial compartment borders is restricted intercellular exchange of gap junction permeable dyes (Martinez et al., 1992; Warner and Lawrence, 1982). By bulk loading the gap junction permeable dye calcein AM into zebrafish hindbrain and thalamus, I have shown this is conserved in fish and also in other anterior compartment boundaries (the ZLI). Intercellular communication through gap junctions appears to be remarkably different in the zebrafish neuroepithelium compared with the rodent cortex, since all cells within a rhombomere were found to be coupled, while radially arranged clusters of up to 25 cells were seen in rat neuroepithelium (Lo Turco and Kriegstein, 1991). This discrepancy may be due to differences in experimental technique, interspecies differences in connectivity, or in the stage of neurogenesis chosen for study. Intracellular injection of dye was used in the rodent studies (Lo Turco and Kriegstein, 1991), so single cell injection could be carried out in the zebrafish to

confirm if radial VZ clusters also exist in the fish (but this has proved to be technically very challenging).

The finding that dye transfer between CNS compartments occurs in the zebrafish suggests that intercellular communication between compartments is reduced and that, in terms of gap junction communication, each compartment is an autonomous unit.

Gap junction dependent intercellular calcium waves have been observed in mammalian and avian neuroepithelium (Owens and Kriegstein, 1998; Pearson et al., 2004; Syed et al., 2004; Weissman et al., 2004). Previous zebrafish studies neurogenesis used sparse labelling techniques because of the severe toxicity of fluorescent calcium indicators (Ashworth and Bolsover, 2002). Therefore I developed a technique to ubiquitously label the hindbrain VZ with minimal toxic effects. I examined if intercellular calcium waves were segmentally regulated because of reduced gap junction coupling between rhombomeres. Surprisingly, the zebrafish neuroepithelium may not be competent to exchange calcium ions because I saw no endogenous intercellular calcium waves and attempts to optically induce intercellular waves using caged calcium compounds also failed. Further investigation is necessary to either confirm or refute this possibility. First, a different calcium indicator can be employed to address the possibility that the indicator I used (calcium green dextran) was not sensitive enough to detect calcium waves during neurogenesis. Second, caged IP3, when uncaged, induces increases in intracellular calcium concentrations (Ashworth et al., 2007). Therefore uncaging IP3 in the hindbrain should be done to test if calcium waves can be induced by a less direct mechanism. Third, it is possible that physical damage to the neuroepithelium resulted in damage responsive calcium waves in the mammalian studies, since all were carried out on dissected tissue (Owens and Kriegstein, 1998; Pearson et al., 2004; Syed et al., 2004; Weissman et al., 2004). To confirm if this is the case, calcium imaging of slice explants of zebrafish neuroepithelium should be carried out.

Aside from searching for intercellular calcium waves in the hindbrain VZ, I also observed low frequency calcium activity in single cells and pairs of cells, the majority of which had cell bodies in contact with the IV ventricle. In a few cases it was possible to confirm that co-active pairs of cells were recently divided sisters. Similar patterns of activity have been observed in the rodent cortex (Owens and Kriegstein, 1998), suggesting that calcium activity may be linked to the cell cycle and is high at M phase. In some experiments I observed many active cells, while I saw few or none in other experiments. While I do not have direct evidence for this, I propose that these

differences reflect cell cycle dependent oscillations in calcium activity. By this I mean that in a given area of neuroepithelium, cell cycles are partially aligned. When most cells are in interphase there is little calcium activity, but when a group of cells enter M phase, calcium activity increases. Long duration timelapses that cover many cell cycles are required to test this hypothesis.

The lack of intercellular calcium activity during neurogenesis and technical difficulties obtaining decent recordings with acceptable signal to noise ratios *in vivo* lead me to explore calcium activity in the blastocyst, since this is the first, and hence least complicated, developmental stage when intercellular communication via gap junctions occurs (Webb and Miller, 2003). I adapted established calcium imaging techniques to record calcium activity through large depths of focus, which enabled me to record across the surface of a whole blastocyst hemisphere. I found that the frequency of calcium transients oscillates during the cell cycle. Relative inactivity precedes mitosis and relative high activity follows mitosis. High resolution imaging of individual blastomeres produced similar results as observing the entire population of blastomeres, with one exception: there was a nearly perfect probability that blastomeres produce 1 or more calcium transient 7-5 minutes before cytokinesis. This event may be nuclear envelope breakdown or G1-S phase transition (Berridge, 1995; Creton et al., 1998; Poenie et al., 1985; Whitaker, 2008). Blastocyst calcium activity consisted of single cell transients and intercellular calcium waves that propagated through up to 11 cells. I saw no spatial pattern to these calcium waves as they travelled in all directions. Mitoses occur in an animal to vegetal wave in the zebrafish blastocyst (Kimmel et al., 1995) (Keller et al., 2008) and since calcium activity is cell cycle dependent, animal blastomeres increased calcium transient frequency before vegetal blastomeres. When I pooled all calcium activity over 30s periods, this animal to vegetal progression of increased calcium activity appeared to be a calcium wave. This finding casts doubt over earlier studies of embryonic calcium activity that used aequorin, which has low temporal resolution, to see slow calcium waves during morphogenetic events, including somite segmentation (e.g. Creton et al., 1998). What appeared to be calcium waves in these studies may actually have been sequential increases in the frequency of calcium activity.

Through inhibition of Connexons with FFA, I found that not only is intercellular calcium activity dependent upon gap junctions, but also individual calcium transients. This suggests that calcium activity required autocrine signalling via Connexon

hemichannels (Evans et al., 2006). A caveat is that FFA may have had off-target and/or toxic effects, such as inhibition of non-specific cation channels {Gogelein, 1989 #463}, so the reduction in calcium activity may have been caused by disruption of other cellular machinery on top of Connexons. Repetition of the experiment with a different gap junction antagonist is required to confirm this result with certainty.

I also discovered that a FFA sensitive process (most likely gap junction) function is required to coordinate the animal to vegetal waves of mitosis during the blastula period, since application of FFA to blastocysts disrupted the pattern of mitoses in most division waves. Again, as with the effect of FFA on calcium activity, another gap junction antagonist should be used to ensure the mechanism of disruption was via gap junction/Connexon hemichannel inhibition.

The requirement for gap junctions/Connexon hemichannels for mitotic waves, and for cell cycle oscillations in calcium activity, implies that the two processes are in some way linked. I do not believe that calcium activity triggers cell division waves, because increased activity occurs approximately 2 minutes after the onset of the wave. However it is possible that at least some of the spatiotemporal coordination of the divisions is mediated by calcium signalling. An interesting study would be to find a method to artificially stimulate calcium waves in the blastocyst to see if the pattern of cell division can be disrupted. I was unsuccessful in using caged calcium compounds to do this (data not included in this thesis), however caged IP3 can be used as a substitute because uncaging it induces calcium transients in early embryos (Ashworth et al., 2007). It remains to be seen if this will cause intercellular waves though.

To conclude, intercellular junctions play diverse roles in embryonic development. Studying their arrangement and function has provided insight into the relationship between epithelial arrangement and neurogenesis in the hindbrain, and between intercellular communication and cellular behaviour in the blastocyst.

# Supplementary Movies

**1). Calcium activity in a single neuroepithelial cell**

Excerpt from a confocal time-lapse of calcium activity in the 24-30 hpf zebrafish VZ loaded with calcium green dextran and pseudo-coloured to highlight changes in fluorescence intensity. Blue indicates low intensity, red indicates high intensity. A single cell, located adjacent to the IV ventricle produces a calcium transient that lasts 25s.

Time between frames: 5s

**2). Calcium activity in a pair of coactive neuroepithelial cells**

A pair of neuroepithelial cells located adjacent to the IV ventricle from the same time-lapse as supplementary movie 1. The pair of cells simultaneously generate a calcium transient lasting 50s.

Time between frames: 5s

**3).Calcium transients occur in cell bodies near the IV ventricle**

Extended focus of 15µm of 24-30hpf Zebrafish hindbrain loaded with calcium green dextran. Images are pseudo-coloured to highlight changes in fluorescence intensity. The embryo is mounted in a near-dorsal view, anterior to the left. The IV ventricle is the dark space in the centre of the image. The majority of calcium transients occur in cell bodies touching the ventricular surface. Time between frames: 5s

**4). Coactive, postmitotic neuroepithelial pair**

A VZ neuroepithelial cell labelled with calcium green dextran (top) and H2B-RFP (bottom). The nucleus divides during the time-lapse. After sister nuclear separate, the daughter cells simultaneously produce two calcium transients.

Time between frames: calcium green dextran: 5s, H2B-RFP:30s

**5). Blastocyst mitotic waves**

Extended focus time-lapse of a zebrafish blastocyst expressing H2B-RFP during cell cycles 8-10. A shows the raw data. In B, each mitotic nucleus is marked with a red circle in the first frame where two sister nuclei are visible. Division waves initiate at the animal pole (top) and sweep to the vegetal pole (bottom).

Time between frames: 2min

**6). Gap junction blockade disrupts mitotic waves**

Extended focus time-lapse of a zebrafish blastocyst expressing H2B-RFP during cell cycles 8-9 and bathed in 100μM FFA. The animal pole is at the top of the image. A shows the raw data. In B, each mitotic nucleus is marked with a red circle in the first frame where two sister nuclei are visible. Divisions are metasynchronous but the spatial pattern is disorganised, showing that gap junction communication is required for division wave coordination.

Time between frames: 1.5min

**7). Calcium activity oscillates during the blastocyst cell cycle**

Extended focus of a blastocyst loaded with calcium green dextran during the $8^{th}$ cell cycle. Initially calcium transient frequency is quite low with some transients and intercellular calcium waves. Immediately prior to the onset of the division wave, calcium activity decreases. After the onset of the division wave calcium transient frequency increases and intercellular calcium waves become more prevalent. Cells at the animal pole increase transient frequency first, then increased activity sweeps from the animal pole to the vegetal pole. Intercellular calcium waves occur in all directions, including towards the animal pole.

Time between frames: 5s

**8). Calcium activity drops before mitosis**

Single confocal slice of a blastomere undergoing cytokinesis. Note that it produces two calcium transients 7 minutes before division. It then produces few transients until the onset of cytokinesis. Daughter cells simultaneously generate a calcium transient 1min after cytokinesis begins, reminiscent of co-active cells in the VZ of 24-30hpf embryos.

Time between frames: 5s

**9). Blastocyst intercellular calcium wave**

Single confocal slice of a calcium green dextran loaded blastocyst coloured in greyscale (a) or pseudo-coloured and processed to only show increase in fluorescence intensity (b). The animal pole is at the top, vegetal pole at the bottom. A calcium wave initiates in a superficial blastomere and propagates through 7 neighbouring superficial blastomeres across the animal pole.

Time between frames: 5s

**10). Calcium activity integrated over 30s reveals animal to vegetal calcium waves**

Extended focus projection of a zebrafish blastocyst beginning its $9^{th}$ wave of mitoses. Images have been processed to show only increases in calcium activity and have been integrated over 30s time periods. A wave of increased calcium activity initiates at the animal pole (top) and meanders over the surface of the embryo towards the vegetal pole (bottom).

Time between frames: 5s

**11). Gap junction blockade inhibits calcium activity**

Extended focus through the superficial 30µm of a calcium green dextran loaded blastocyst bathed in 100µM FFA. Calcium transient frequency is low, suggesting that blocking gap junction connectivity inhibits calcium transient and intercellular wave production.

Time between frames: 5s

**12). Subcellular calcium transients in cell-cell contact points**

Single confocal slice of a calcium green dextran loaded cleavage stage embryo. Calcium transients occur at the contact point of two neighbouring cells and appear to propagate between them. Increased fluorescence intensity does not occur in deeper regions of the cells.

Time between frames: 5s

**13). Subcellular calcium transients at the cell surface of a blastomere**

Three confocal slices at 10µm spacing, of zebrafish blastomeres loaded with a calcium green dextran. Calcium transients are clearly visible in the superficial slice, less visible in the middle slice, and absent from the deep slice.

Time between frames: 5s

## Acknowledgements

First of all big thanks have to go to Jon for letting me run wild with an ambitious and risky project, for giving me the freedom to experiment without consideration of cost and for the critical look at my work that has kept it (almost) grounded.

Thanks to David Becker for his invaluable advice on gap junctions and the open door to the drugs cabinet. Thanks to Masa T for his tutorage in molecular witchcraft and for his patience with me regularly invading his lab. To Alexander Reugels for his immense skills in gene splicing. Together we designed the perfect fusion protein…that didn't bloody work! Thanks Daniel Ciantar for your Java skills that turned impossible analysis into fabulous calcium waves. Thanks to Eric Blanc for help with statistics.

Thanks to all the kind and helpful folk in the UCL and KCL fish facilities who've looked after the fish and kept them healthy.

And then to the fabulous Clarke lab: Claudio, Gemma Paula, Una and the departed Marcel (proud Brit). Thanks for the support, the humour, the gallons of tea, and for teaching me all the useful sciency things, like *in situs* and, immunos.

It's been a rocky road of hope, fear, excitement, victory, failure and excessive sweating.

Now I'm off for a badger hunt.

# References


Aaku-Saraste, E., Hellwig, A. and Huttner, W. B. (1996). Loss of occludin and functional tight junctions, but not ZO-1, during neural tube closure--remodeling of the neuroepithelium prior to neurogenesis. Dev Biol 180, 664-79.

Amoyel, M., Cheng, Y. C., Jiang, Y. J. and Wilkinson, D. G. (2005). Wnt1 regulates neurogenesis and mediates lateral inhibition of boundary cell specification in the zebrafish hindbrain. Development 132, 775-85.

Ando, R., Hama, H., Yamamoto-Hino, M., Mizuno, H. and Miyawaki, A. (2002). An optical marker based on the UV-induced green-to-red photoconversion of a fluorescent protein. Proc Natl Acad Sci U S A 99, 12651-6.

Appel, B. and Eisen, J. S. (1998). Regulation of neuronal specification in the zebrafish spinal cord by Delta function. Development 125, 371-80.

Ashworth, R. and Bolsover, S. R. (2002). Spontaneous activity-independent intracellular calcium signals in the developing spinal cord of the zebrafish embryo. Brain Res Dev Brain Res 139, 131-7.

Ashworth, R., Devogelaere, B., Fabes, J., Tunwell, R. E., Koh, K. R., De Smedt, H. and Patel, S. (2007). Molecular and functional characterization of inositol trisphosphate receptors during early zebrafish development. J Biol Chem 282, 13984-93.

Ashworth, R., Zimprich, F. and Bolsover, S. R. (2001). Buffering intracellular calcium disrupts motoneuron development in intact zebrafish embryos. Brain Res Dev Brain Res 129, 169-79.

Baek, J. H., Hatakeyama, J., Sakamoto, S., Ohtsuka, T. and Kageyama, R. (2006). Persistent and high levels of Hes1 expression regulate boundary formation in the developing central nervous system. Development 133, 2467-76.

Bailey, A. M. and Posakony, J. W. (1995). Suppressor of hairless directly activates transcription of enhancer of split complex genes in response to Notch receptor activity. Genes Dev 9, 2609-22.

Bazzoni, G. (2003). The JAM family of junctional adhesion molecules. Curr Opin Cell Biol 15, 525-30.

Becker, D. L., Evans, W. H., Green, C. R. and Warner, A. (1995). Functional analysis of amino acid sequences in connexin43 involved in intercellular communication through gap junctions. J Cell Sci 108 ( Pt 4), 1455-67.

Berridge, M. J. (1995). Calcium signalling and cell proliferation. Bioessays 17, 491-500.

Berridge, M. J., Lipp, P. and Bootman, M. D. (2000). The versatility and universality of calcium signalling. Nat Rev Mol Cell Biol 1, 11-21.

Bettenhausen, B., Hrabe de Angelis, M., Simon, D., Guenet, J. L. and Gossler, A. (1995). Transient and restricted expression during mouse embryogenesis of Dll1, a murine gene closely related to Drosophila Delta. Development 121, 2407-18.

Bevans, C. G., Kordel, M., Rhee, S. K. and Harris, A. L. (1998). Isoform composition of connexin channels determines selectivity among second messengers and uncharged molecules. J Biol Chem 273, 2808-16.

Bierkamp, C. and Campos-Ortega, J. A. (1993). A zebrafish homologue of the Drosophila neurogenic gene Notch and its pattern of transcription during early embryogenesis. Mech Dev 43, 87-100.

Bingham, S., Chaudhari, S., Vanderlaan, G., Itoh, M., Chitnis, A. and Chandrasekhar, A. (2003). Neurogenic phenotype of mind bomb mutants leads to severe patterning defects in the zebrafish hindbrain. Dev Dyn 228, 451-63.

Birgbauer, E. and Fraser, S. E. (1994). Violation of cell lineage restriction compartments in the chick hindbrain. Development 120, 1347-56.

Bittman, K., Becker, D. L., Cicirata, F. and Parnavelas, J. G. (2002). Connexin expression in homotypic and heterotypic cell coupling in the developing cerebral cortex. J Comp Neurol 443, 201-12.

Bittman, K., Owens, D. F., Kriegstein, A. R. and LoTurco, J. J. (1997). Cell coupling and uncoupling in the ventricular zone of developing neocortex. J Neurosci 17, 7037-44.

Bittman, K. S., Panzer, J. A. and Balice-Gordon, R. J. (2004). Patterns of cell-cell coupling in embryonic spinal cord studied via ballistic delivery of gap-junction-permeable dyes. J Comp Neurol 477, 273-85.

Brower, D. L. (1985). The sequential compartmentalization of Drosophila segments revisited. Cell 41, 361-4.

Bruckner, K., Perez, L., Clausen, H. and Cohen, S. (2000). Glycosyltransferase activity of Fringe modulates Notch-Delta interactions. Nature 406, 411-5.

Brunmeir, R., Lagger, S. and Seiser, C. (2009). Histone deacetylase HDAC1/HDAC2-controlled embryonic development and cell differentiation. Int J Dev Biol 53, 275-89.

Bruzzone, R. and Dermietzel, R. (2006). Structure and function of gap junctions in the developing brain. Cell Tissue Res 326, 239-48.

Buehr, M., Lee, S., McLaren, A. and Warner, A. (1987). Reduced gap junctional communication is associated with the lethal condition characteristic of DDK mouse eggs fertilized by foreign sperm. Development 101, 449-59.

Bulfone, A., Puelles, L., Porteus, M. H., Frohman, M. A., Martin, G. R. and Rubenstein, J. L. (1993). Spatially restricted expression of Dlx-1, Dlx-2 (Tes-1), Gbx-2, and Wnt-3 in the embryonic day 12.5 mouse forebrain defines potential transverse and longitudinal segmental boundaries. J Neurosci 13, 3155-72.

Cai, L., Hayes, N. L. and Nowakowski, R. S. (1997). Synchrony of clonal cell proliferation and contiguity of clonally related cells: production of mosaicism in the ventricular zone of developing mouse neocortex. J Neurosci 17, 2088-100.

Chang, D. C. and Lu, P. (2000). Multiple types of calcium signals are associated with cell division in zebrafish embryo. Microsc Res Tech 49, 111-22.

Chang, D. C. and Meng, C. (1995). A localized elevation of cytosolic free calcium is associated with cytokinesis in the zebrafish embryo. J Cell Biol 131, 1539-45.

Chang, Q., Gonzalez, M., Pinter, M. J. and Balice-Gordon, R. J. (1999). Gap junctional coupling and patterns of connexin expression among neonatal rat lumbar spinal motor neurons. J Neurosci 19, 10813-28.

Chatterjee, B., Chin, A. J., Valdimarsson, G., Finis, C., Sonntag, J. M., Choi, B. Y., Tao, L., Balasubramanian, K., Bell, C., Krufka, A. et al. (2005). Developmental regulation and expression of the zebrafish connexin43 gene. Dev Dyn 233, 890-906.

Cheng, Y. C., Amoyel, M., Qiu, X., Jiang, Y. J., Xu, Q. and Wilkinson, D. G. (2004). Notch activation regulates the segregation and differentiation of rhombomere boundary cells in the zebrafish hindbrain. Dev Cell 6, 539-50.

Chitnis, A., Henrique, D., Lewis, J., Ish-Horowicz, D. and Kintner, C. (1995). Primary neurogenesis in Xenopus embryos regulated by a homologue of the Drosophila neurogenic gene Delta. Nature 375, 761-6.

Chitnis, A. B. (1995). The role of Notch in lateral inhibition and cell fate specification. Mol Cell Neurosci 6, 311-21.

Clarke, D. J., Johnson, R. T. and Downes, C. S. (1993). Topoisomerase II inhibition prevents anaphase chromatid segregation in mammalian cells independently of the generation of DNA strand breaks. J Cell Sci 105 ( Pt 2), 563-9.

Coffman, C., Harris, W. and Kintner, C. (1990). Xotch, the Xenopus homolog of Drosophila notch. Science 249, 1438-41.

Coffman, C. R., Skoglund, P., Harris, W. A. and Kintner, C. R. (1993). Expression of an extracellular deletion of Xotch diverts cell fate in Xenopus embryos. Cell 73, 659-71.

Cohen, B., Bashirullah, A., Dagnino, L., Campbell, C., Fisher, W. W., Leow, C. C., Whiting, E., Ryan, D., Zinyk, D., Boulianne, G. et al. (1997). Fringe boundaries coincide with Notch-dependent patterning centres in mammals and alter Notch-dependent development in Drosophila. Nat Genet 16, 283-8.

Colas, J. F. and Schoenwolf, G. C. (2001). Towards a cellular and molecular understanding of neurulation. Dev Dyn 221, 117-45.

Connors, B. W., Benardo, L. S. and Prince, D. A. (1983). Coupling between neurons of the developing rat neocortex. J Neurosci 3, 773-82.

Cooke, J., Moens, C., Roth, L., Durbin, L., Shiomi, K., Brennan, C., Kimmel, C., Wilson, S. and Holder, N. (2001). Eph signalling functions downstream of Val to regulate cell sorting and boundary formation in the caudal hindbrain. Development 128, 571-80.

Cooke, J. E., Kemp, H. A. and Moens, C. B. (2005). EphA4 is required for cell adhesion and rhombomere-boundary formation in the zebrafish. Curr Biol 15, 536-42.

Cooke, J. E. and Moens, C. B. (2002). Boundary formation in the hindbrain: Eph only it were simple. Trends Neurosci 25, 260-7.

Cordes, S. P. and Barsh, G. S. (1994). The mouse segmentation gene kr encodes a novel basic domain-leucine zipper transcription factor. Cell 79, 1025-34.

Creton, R. (2004). The calcium pump of the endoplasmic reticulum plays a role in midline signaling during early zebrafish development. Brain Res Dev Brain Res 151, 33-41.

Creton, R., Speksnijder, J. E. and Jaffe, L. F. (1998). Patterns of free calcium in zebrafish embryos. J Cell Sci 111 ( Pt 12), 1613-22.

Cunliffe, V. T. (2004). Histone deacetylase 1 is required to repress Notch target gene expression during zebrafish neurogenesis and to maintain the production of motoneurones in response to hedgehog signalling. Development 131, 2983-95.

Davy, A., Bush, J. O. and Soriano, P. (2006). Inhibition of gap junction communication at ectopic Eph/ephrin boundaries underlies craniofrontonasal syndrome. PLoS Biol 4, e315.

de Celis, J. F. and Garcia-Bellido, A. (1994). Roles of the Notch gene in Drosophila wing morphogenesis. Mech Dev 46, 109-22.

de Celis, J. F., Garcia-Bellido, A. and Bray, S. J. (1996). Activation and function of Notch at the dorsal-ventral boundary of the wing imaginal disc. Development 122, 359-69.

de la Pompa, J. L., Wakeham, A., Correia, K. M., Samper, E., Brown, S., Aguilera, R. J., Nakano, T., Honjo, T., Mak, T. W., Rossant, J. et al. (1997). Conservation of the Notch signalling pathway in mammalian neurogenesis. Development 124, 1139-48.

De Sousa, P. A., Juneja, S. C., Caveney, S., Houghton, F. D., Davies, T. C., Reaume, A. G., Rossant, J. and Kidder, G. M. (1997). Normal development of preimplantation mouse embryos deficient in gap junctional coupling. J Cell Sci 110 ( Pt 15), 1751-8.

Dermietzel, R. (1998). Diversification of gap junction proteins (connexins) in the central nervous system and the concept of functional compartments. Cell Biol Int 22, 719-30.

Dermietzel, R., Kremer, M., Paputsoglu, G., Stang, A., Skerrett, I. M., Gomes, D., Srinivas, M., Janssen-Bienhold, U., Weiler, R., Nicholson, B. J. et al. (2000). Molecular and functional diversity of neural connexins in the retina. J Neurosci 20, 8331-43.

Desplantez, T., Marics, I., Jarry-Guichard, T., Veteikis, R., Briand, J. P., Weingart, R. and Gros, D. (2003). Characterization of zebrafish Cx43.4 connexin and its channels. Exp Physiol 88, 681-90.

Durston, A. J., Timmermans, J. P., Hage, W. J., Hendriks, H. F., de Vries, N. J., Heideveld, M. and Nieuwkoop, P. D. (1989). Retinoic acid causes an anteroposterior transformation in the developing central nervous system. Nature 340, 140-4.

Eastman, S. D., Chen, T. H., Falk, M. M., Mendelson, T. C. and Iovine, M. K. (2006). Phylogenetic analysis of three complete gap junction gene families reveals lineage-specific duplications and highly supported gene classes. Genomics 87, 265-74.

Elfgang, C., Eckert, R., Lichtenberg-Frate, H., Butterweck, A., Traub, O., Klein, R. A., Hulser, D. F. and Willecke, K. (1995). Specific permeability and selective formation of gap junction channels in connexin-transfected HeLa cells. J Cell Biol 129, 805-17.

Elias, L. A., Wang, D. D. and Kriegstein, A. R. (2007). Gap junction adhesion is necessary for radial migration in the neocortex. Nature 448, 901-7.

Ericson, J., Muhr, J., Jessell, T. M. and Edlund, T. (1995). Sonic hedgehog: a common signal for ventral patterning along the rostrocaudal axis of the neural tube. Int J Dev Biol 39, 809-16.

Essner, J. J., Laing, J. G., Beyer, E. C., Johnson, R. G. and Hackett, P. B., Jr. (1996). Expression of zebrafish connexin43.4 in the notochord and tail bud of wild-type and mutant no tail embryos. Dev Biol 177, 449-62.

Evans, W. H., De Vuyst, E. and Leybaert, L. (2006). The gap junction cellular internet: connexin hemichannels enter the signalling limelight. Biochem J 397, 1-14.

Fanning, A. S., Jameson, B. J., Jesaitis, L. A. and Anderson, J. M. (1998). The tight junction protein ZO-1 establishes a link between the transmembrane protein occludin and the actin cytoskeleton. J Biol Chem 273, 29745-53.

Figdor, M. C. and Stern, C. D. (1993). Segmental organization of embryonic diencephalon. Nature 363, 630-4.

Fishell, G., Mason, C. A. and Hatten, M. E. (1993). Dispersion of neural progenitors within the germinal zones of the forebrain. Nature 362, 636-8.

Fluck, R. A., Miller, A. L. and Jaffe, L. F. (1991). Slow calcium waves accompany cytokinesis in medaka fish eggs. J Cell Biol 115, 1259-65.

Foe, V. E. (1989). Mitotic domains reveal early commitment of cells in Drosophila embryos. Development 107, 1-22.

Fraser, S., Keynes, R. and Lumsden, A. (1990). Segmentation in the chick embryo hindbrain is defined by cell lineage restrictions. Nature 344, 431-5.

Frohman, M. A., Martin, G. R., Cordes, S. P., Halamek, L. P. and Barsh, G. S. (1993). Altered rhombomere-specific gene expression and hyoid bone differentiation in the mouse segmentation mutant, kreisler (kr). Development 117, 925-36.

Furuse, M., Fujita, K., Hiiragi, T., Fujimoto, K. and Tsukita, S. (1998). Claudin-1 and -2: novel integral membrane proteins localizing at tight junctions with no sequence similarity to occludin. J Cell Biol 141, 1539-50.

Furuse, M., Hirase, T., Itoh, M., Nagafuchi, A., Yonemura, S. and Tsukita, S. (1993). Occludin: a novel integral membrane protein localizing at tight junctions. J Cell Biol 123, 1777-88.

Furuse, M., Itoh, M., Hirase, T., Nagafuchi, A., Yonemura, S. and Tsukita, S. (1994). Direct association of occludin with ZO-1 and its possible involvement in the localization of occludin at tight junctions. J Cell Biol 127, 1617-26.

Gale, J. E., Piazza, V., Ciubotaru, C. D. and Mammano, F. (2004). A mechanism for sensing noise damage in the inner ear. Curr Biol 14, 526-9.

Garcia-Bellido, A., Ripoll, P. and Morata, G. (1973). Developmental compartmentalisation of the wing disk of Drosophila. Nat New Biol 245, 251-3.

Garcia-Lopez, R., Vieira, C., Echevarria, D. and Martinez, S. (2004). Fate map of the diencephalon and the zona limitans at the 10-somites stage in chick embryos. Dev Biol 268, 514-30.

Gardam, K. E., Geiger, J. E., Hickey, C. M., Hung, A. Y. and Magoski, N. S. (2008). Flufenamic acid affects multiple currents and causes intracellular Ca2+ release in Aplysia bag cell neurons. J Neurophysiol 100, 38-49.

Geldmacher-Voss, B., Reugels, A. M., Pauls, S. and Campos-Ortega, J. A. (2003). A 90-degree rotation of the mitotic spindle changes the orientation of mitoses of zebrafish neuroepithelial cells. Development 130, 3767-80.

Giaume, C. and Venance, L. (1998). Intercellular calcium signaling and gap junctional communication in astrocytes. Glia 24, 50-64.

Giepmans, B. N. (2004). Gap junctions and connexin-interacting proteins. Cardiovasc Res 62, 233-45.

Gogelein, H. and Pfannmuller, B. (1989). The nonselective cation channel in the basolateral membrane of rat exocrine pancreas. Inhibition by 3',5-dichlorodiphenylamine-2-carboxylic acid (DCDPC) and activation by stilbene disulfonates. Pflugers Arch 413, 287-98.

Golden, J. A. and Cepko, C. L. (1996). Clones in the chick diencephalon contain multiple cell types and siblings are widely dispersed. Development 122, 65-78.

Golling, G., Amsterdam, A., Sun, Z., Antonelli, M., Maldonado, E., Chen, W., Burgess, S., Haldi, M., Artzt, K., Farrington, S. et al. (2002). Insertional mutagenesis in zebrafish rapidly identifies genes essential for early vertebrate development. Nat Genet 31, 135-40.

Grandin, N. and Charbonneau, M. (1991). Intracellular free calcium oscillates during cell division of Xenopus embryos. J Cell Biol 112, 711-8.

Grapin-Botton, A., Bonnin, M. A., McNaughton, L. A., Krumlauf, R. and Le Douarin, N. M. (1995). Plasticity of transposed rhombomeres: Hox gene induction is correlated with phenotypic modifications. Development 121, 2707-21.

Gu, X. and Spitzer, N. C. (1995). Distinct aspects of neuronal differentiation encoded by frequency of spontaneous Ca2+ transients. Nature 375, 784-7.

Gu, X. and Spitzer, N. C. (1997). Breaking the code: regulation of neuronal differentiation by spontaneous calcium transients. Dev Neurosci 19, 33-41.

Gumbiner, B. M. (2005). Regulation of cadherin-mediated adhesion in morphogenesis. Nat Rev Mol Cell Biol 6, 622-34.

Guthrie, S., Butcher, M. and Lumsden, A. (1991). Patterns of cell division and interkinetic nuclear migration in the chick embryo hindbrain. J Neurobiol 22, 742-54.

Guthrie, S. and Lumsden, A. (1991). Formation and regeneration of rhombomere boundaries in the developing chick hindbrain. Development 112, 221-9.

Guthrie, S., Muchamore, I., Kuroiwa, A., Marshall, H., Krumlauf, R. and Lumsden, A. (1992). Neuroectodermal autonomy of Hox-2.9 expression revealed by rhombomere transpositions. Nature 356, 157-9.

Guthrie, S., Turin, L. and Warner, A. (1988). Patterns of junctional communication during development of the early amphibian embryo. Development 103, 769-83.

Guthrie, S. C. (1984). Patterns of junctional communication in the early amphibian embryo. Nature 311, 149-51.

Hanneman, E., Trevarrow, B., Metcalfe, W. K., Kimmel, C. B. and Westerfield, M. (1988). Segmental pattern of development of the hindbrain and spinal cord of the zebrafish embryo. Development 103, 49-58.

Hardy, K., Warner, A., Winston, R. M. and Becker, D. L. (1996). Expression of intercellular junctions during preimplantation development of the human embryo. Mol Hum Reprod 2, 621-32.

Haskins, J., Gu, L., Wittchen, E. S., Hibbard, J. and Stevenson, B. R. (1998). ZO-3, a novel member of the MAGUK protein family found at the tight junction, interacts with ZO-1 and occludin. J Cell Biol 141, 199-208.

Henrique, D., Adam, J., Myat, A., Chitnis, A., Lewis, J. and Ish-Horowicz, D. (1995). Expression of a Delta homologue in prospective neurons in the chick. Nature 375, 787-90.

Henrique, D., Hirsinger, E., Adam, J., Le Roux, I., Pourquie, O., Ish-Horowicz, D. and Lewis, J. (1997). Maintenance of neuroepithelial progenitor cells by Delta-Notch signalling in the embryonic chick retina. Curr Biol 7, 661-70.

Heyman, I., Faissner, A. and Lumsden, A. (1995). Cell and matrix specialisations of rhombomere boundaries. Dev Dyn 204, 301-15.

Heyman, I., Kent, A. and Lumsden, A. (1993). Cellular morphology and extracellular space at rhombomere boundaries in the chick embryo hindbrain. Dev Dyn 198, 241-53.

Higashijima, S., Hotta, Y. and Okamoto, H. (2000). Visualization of cranial motor neurons in live transgenic zebrafish expressing green fluorescent protein under the control of the islet-1 promoter/enhancer. J Neurosci 20, 206-18.

Hong, E. and Brewster, R. (2006). N-cadherin is required for the polarized cell behaviors that drive neurulation in the zebrafish. Development 133, 3895-905.

Houghton, F. D. (2005). Role of gap junctions during early embryo development. Reproduction 129, 129-35.

Houghton, F. D., Barr, K. J., Walter, G., Gabriel, H. D., Grummer, R., Traub, O., Leese, H. J., Winterhager, E. and Kidder, G. M. (2002). Functional significance of gap junctional coupling in preimplantation development. Biol Reprod 66, 1403-12.

Hueber, S. D. and Lohmann, I. (2008). Shaping segments: Hox gene function in the genomic age. Bioessays 30, 965-79.

Ingham, P. W. and Martinez Arias, A. (1992). Boundaries and fields in early embryos. Cell 68, 221-35.

Irvine, K. D. and Wieschaus, E. (1994). fringe, a Boundary-specific signaling molecule, mediates interactions between dorsal and ventral cells during Drosophila wing development. Cell 79, 595-606.

Irving, C., Nieto, M. A., DasGupta, R., Charnay, P. and Wilkinson, D. G. (1996). Progressive spatial restriction of Sek-1 and Krox-20 gene expression during hindbrain segmentation. Dev Biol 173, 26-38.

Itasaki, N., Sharpe, J., Morrison, A. and Krumlauf, R. (1996). Reprogramming Hox expression in the vertebrate hindbrain: influence of paraxial mesoderm and rhombomere transposition. Neuron 16, 487-500.

Itoh, M., Furuse, M., Morita, K., Kubota, K., Saitou, M. and Tsukita, S. (1999). Direct binding of three tight junction-associated MAGUKs, ZO-1, ZO-2, and ZO-3, with the COOH termini of claudins. J Cell Biol 147, 1351-63.

Itoh, M., Kim, C. H., Palardy, G., Oda, T., Jiang, Y. J., Maust, D., Yeo, S. Y., Lorick, K., Wright, G. J., Ariza-McNaughton, L. et al. (2003). Mind bomb is a ubiquitin ligase that is essential for efficient activation of Notch signaling by Delta. Dev Cell 4, 67-82.

Itoh, M., Nagafuchi, A., Moroi, S. and Tsukita, S. (1997). Involvement of ZO-1 in cadherin-based cell adhesion through its direct binding to alpha catenin and actin filaments. J Cell Biol 138, 181-92.

Itoh, M., Nagafuchi, A., Yonemura, S., Kitani-Yasuda, T. and Tsukita, S. (1993). The 220-kD protein colocalizing with cadherins in non-epithelial cells is identical to ZO-1, a tight junction-

associated protein in epithelial cells: cDNA cloning and immunoelectron microscopy. J Cell Biol 121, 491-502.

Itoh, M., Sasaki, H., Furuse, M., Ozaki, H., Kita, T. and Tsukita, S. (2001). Junctional adhesion molecule (JAM) binds to PAR-3: a possible mechanism for the recruitment of PAR-3 to tight junctions. J Cell Biol 154, 491-7.

Jaffe, L. F. (1999). Organization of early development by calcium patterns. Bioessays 21, 657-67.

Janssen-Bienhold, U., Dermietzel, R. and Weiler, R. (1998). Distribution of connexin43 immunoreactivity in the retinas of different vertebrates. J Comp Neurol 396, 310-21.

Jesaitis, L. A. and Goodenough, D. A. (1994). Molecular characterization and tissue distribution of ZO-2, a tight junction protein homologous to ZO-1 and the Drosophila discs-large tumor suppressor protein. J Cell Biol 124, 949-61.

Johnston, S. H., Rauskolb, C., Wilson, R., Prabhakaran, B., Irvine, K. D. and Vogt, T. F. (1997). A family of mammalian Fringe genes implicated in boundary determination and the Notch pathway. Development 124, 2245-54.

Jones, T. L., Chong, L. D., Kim, J., Xu, R. H., Kung, H. F. and Daar, I. O. (1998). Loss of cell adhesion in Xenopus laevis embryos mediated by the cytoplasmic domain of XLerk, an erythropoietin-producing hepatocellular ligand. Proc Natl Acad Sci U S A 95, 576-81.

Jungbluth, S., Larsen, C., Wizenmann, A. and Lumsden, A. (2001). Cell mixing between the embryonic midbrain and hindbrain. Curr Biol 11, 204-7.

Jungbluth, S., Willecke, K. and Champagnat, J. (2002). Segment-specific expression of connexin31 in the embryonic hindbrain is regulated by Krox20. Dev Dyn 223, 544-51.

Ke, Z., Kondrichin, I., Gong, Z. and Korzh, V. (2008). Combined activity of the two Gli2 genes of zebrafish play a major role in Hedgehog signaling during zebrafish neurodevelopment. Mol Cell Neurosci 37, 388-401.

Keating, T. J., Cork, R. J. and Robinson, K. R. (1994). Intracellular free calcium oscillations in normal and cleavage-blocked embryos and artificially activated eggs of Xenopus laevis. J Cell Sci 107 ( Pt 8), 2229-37.

Keller, P. J., Schmidt, A. D., Wittbrodt, J. and Stelzer, E. H. (2008). Reconstruction of zebrafish early embryonic development by scanned light sheet microscopy. Science 322, 1065-9.

Kiecker, C. and Lumsden, A. (2005). Compartments and their boundaries in vertebrate brain development. Nat Rev Neurosci 6, 553-64.

Kiener, T. K., Sleptsova-Friedrich, I. and Hunziker, W. (2007). Identification, tissue distribution and developmental expression of tjp1/zo-1, tjp2/zo-2 and tjp3/zo-3 in the zebrafish, Danio rerio. Gene Expr Patterns 7, 767-76.

Kimmel, C. B., Ballard, W. W., Kimmel, S. R., Ullmann, B. and Schilling, T. F. (1995). Stages of embryonic development of the zebrafish. Dev Dyn 203, 253-310.

Kimmel, C. B. and Law, R. D. (1985a). Cell lineage of zebrafish blastomeres. I. Cleavage pattern and cytoplasmic bridges between cells. Dev Biol 108, 78-85.

Kimmel, C. B. and Law, R. D. (1985b). Cell lineage of zebrafish blastomeres. II. Formation of the yolk syncytial layer. Dev Biol 108, 86-93.

Kimmel, C. B. and Law, R. D. (1985c). Cell lineage of zebrafish blastomeres. III. Clonal analyses of the blastula and gastrula stages. Dev Biol 108, 94-101.

Komuro, H. and Rakic, P. (1996). Intracellular Ca2+ fluctuations modulate the rate of neuronal migration. Neuron 17, 275-85.

Kopan, R., Nye, J. S. and Weintraub, H. (1994). The intracellular domain of mouse Notch: a constitutively activated repressor of myogenesis directed at the basic helix-loop-helix region of MyoD. Development 120, 2385-96.

Kreiling, J. A., Balantac, Z. L., Crawford, A. R., Ren, Y., Toure, J., Zchut, S., Kochilas, L. and Creton, R. (2008). Suppression of the endoplasmic reticulum calcium pump during zebrafish gastrulation affects left-right asymmetry of the heart and brain. Mech Dev 125, 396-410.

Kubota, H. Y., Yoshimoto, Y. and Hiramoto, Y. (1993). Oscillation of intracellular free calcium in cleaving and cleavage-arrested embryos of Xenopus laevis. Dev Biol 160, 512-8.

Kuratani, S. C. and Eichele, G. (1993). Rhombomere transplantation repatterns the segmental organization of cranial nerves and reveals cell-autonomous expression of a homeodomain protein. Development 117, 105-17.

Landesman, Y., Goodenough, D. A. and Paul, D. L. (2000). Gap junctional communication in the early Xenopus embryo. J Cell Biol 150, 929-36.

Landesman, Y., Postma, F. R., Goodenough, D. A. and Paul, D. L. (2003). Multiple connexins contribute to intercellular communication in the Xenopus embryo. J Cell Sci 116, 29-38.

Langenberg, T. and Brand, M. (2005). Lineage restriction maintains a stable organizer cell population at the zebrafish midbrain-hindbrain boundary. Development 132, 3209-16.

Lardelli, M., Dahlstrand, J. and Lendahl, U. (1994). The novel Notch homologue mouse Notch 3 lacks specific epidermal growth factor-repeats and is expressed in proliferating neuroepithelium. Mech Dev 46, 123-36.

Lardelli, M. and Lendahl, U. (1993). Motch A and motch B--two mouse Notch homologues coexpressed in a wide variety of tissues. Exp Cell Res 204, 364-72.

Lardelli, M., Williams, R., Mitsiadis, T. and Lendahl, U. (1996). Expression of the Notch 3 intracellular domain in mouse central nervous system progenitor cells is lethal and leads to disturbed neural tube development. Mech Dev 59, 177-90.

Larsen, C. W., Zeltser, L. M. and Lumsden, A. (2001). Boundary formation and compartition in the avian diencephalon. J Neurosci 21, 4699-711.

Larsson, C., Lardelli, M., White, I. and Lendahl, U. (1994). The human NOTCH1, 2, and 3 genes are located at chromosome positions 9q34, 1p13-p11, and 19p13.2-p13.1 in regions of neoplasia-associated translocation. Genomics 24, 253-8.

Lawrence, P. A. and Morata, G. (1994). Homeobox genes: their function in Drosophila segmentation and pattern formation. Cell 78, 181-9.

Leclerc, C., Becker, D., Buehr, M. and Warner, A. (1994). Low intracellular pH is involved in the early embryonic death of DDK mouse eggs fertilized by alien sperm. Dev Dyn 200, 257-67.

Leclerc, C., Daguzan, C., Nicolas, M. T., Chabret, C., Duprat, A. M. and Moreau, M. (1997). L-type calcium channel activation controls the in vivo transduction of the neuralizing signal in the amphibian embryos. Mech Dev 64, 105-10.

Leclerc, C., Webb, S. E., Daguzan, C., Moreau, M. and Miller, A. L. (2000). Imaging patterns of calcium transients during neural induction in Xenopus laevis embryos. J Cell Sci 113 Pt 19, 3519-29.

Lee, H. S., Nishanian, T. G., Mood, K., Bong, Y. S. and Daar, I. O. (2008). EphrinB1 controls cell-cell junctions through the Par polarity complex. Nat Cell Biol 10, 979-86.

Lee, J., Ishihara, A., Oxford, G., Johnson, B. and Jacobson, K. (1999). Regulation of cell movement is mediated by stretch-activated calcium channels. Nature 400, 382-6.

Lee, S., Gilula, N. B. and Warner, A. E. (1987). Gap junctional communication and compaction during preimplantation stages of mouse development. Cell 51, 851-60.

Levin, M. and Mercola, M. (1998). Gap junctions are involved in the early generation of left-right asymmetry. Dev Biol 203, 90-105.

Levin, M. and Mercola, M. (1999). Gap junction-mediated transfer of left-right patterning signals in the early chick blastoderm is upstream of Shh asymmetry in the node. Development 126, 4703-14.

Levitt, P. and Rakic, P. (1980). Immunoperoxidase localization of glial fibrillary acidic protein in radial glial cells and astrocytes of the developing rhesus monkey brain. J Comp Neurol 193, 815-40.

Lin, J. H., Takano, T., Arcuino, G., Wang, X., Hu, F., Darzynkiewicz, Z., Nunes, M., Goldman, S. A. and Nedergaard, M. (2007). Purinergic signaling regulates neural progenitor cell expansion and neurogenesis. Dev Biol 302, 356-66.

Lo, C. W. and Gilula, N. B. (1979a). Gap junctional communication in the post-implantation mouse embryo. Cell 18, 411-22.

Lo, C. W. and Gilula, N. B. (1979b). Gap junctional communication in the preimplantation mouse embryo. Cell 18, 399-409.

Lo Turco, J. J. and Kriegstein, A. R. (1991). Clusters of coupled neuroblasts in embryonic neocortex. Science 252, 563-6.

Lumsden, A. and Keynes, R. (1989). Segmental patterns of neuronal development in the chick hindbrain. Nature 337, 424-8.

Major, R. J. and Irvine, K. D. (2005). Influence of Notch on dorsoventral compartmentalization and actin organization in the Drosophila wing. Development 132, 3823-33.

Major, R. J. and Irvine, K. D. (2006). Localization and requirement for Myosin II at the dorsal-ventral compartment boundary of the Drosophila wing. Dev Dyn 235, 3051-8.

Malatesta, P., Hartfuss, E. and Gotz, M. (2000). Isolation of radial glial cells by fluorescent-activated cell sorting reveals a neuronal lineage. Development 127, 5253-63.

Mann, B., Gelos, M., Siedow, A., Hanski, M. L., Gratchev, A., Ilyas, M., Bodmer, W. F., Moyer, M. P., Riecken, E. O., Buhr, H. J. et al. (1999). Target genes of beta-catenin-T cell-factor/lymphoid-enhancer-factor signaling in human colorectal carcinomas. Proc Natl Acad Sci U S A 96, 1603-8.

Martin-Padura, I., Lostaglio, S., Schneemann, M., Williams, L., Romano, M., Fruscella, P., Panzeri, C., Stoppacciaro, A., Ruco, L., Villa, A. et al. (1998). Junctional adhesion molecule, a novel member of the immunoglobulin superfamily that distributes at intercellular junctions and modulates monocyte transmigration. J Cell Biol 142, 117-27.

Martinez, S., Geijo, E., Sanchez-Vives, M. V., Puelles, L. and Gallego, R. (1992). Reduced junctional permeability at interrhombomeric boundaries. Development 116, 1069-76.

Martinez, S., Marin, F., Nieto, M. A. and Puelles, L. (1995). Induction of ectopic engrailed expression and fate change in avian rhombomeres: intersegmental boundaries as barriers. Mech Dev 51, 289-303.

McLachlan, E., White, T. W., Ugonabo, C., Olson, C., Nagy, J. I. and Valdimarsson, G. (2003). Zebrafish Cx35: cloning and characterization of a gap junction gene highly expressed in the retina. J Neurosci Res 73, 753-64.

Mellitzer, G., Xu, Q. and Wilkinson, D. G. (1999). Eph receptors and ephrins restrict cell intermingling and communication. Nature 400, 77-81.

Micchelli, C. A. and Blair, S. S. (1999). Dorsoventral lineage restriction in wing imaginal discs requires Notch. Nature 401, 473-6.

Millet, S., Bloch-Gallego, E., Simeone, A. and Alvarado-Mallart, R. M. (1996). The caudal limit of Otx2 gene expression as a marker of the midbrain/hindbrain boundary: a study using in situ hybridisation and chick/quail homotopic grafts. Development 122, 3785-97.

Mirzadeh, Z., Merkle, F. T., Soriano-Navarro, M., Garcia-Verdugo, J. M. and Alvarez-Buylla, A. (2008). Neural stem cells confer unique pinwheel architecture to the ventricular surface in neurogenic regions of the adult brain. Cell Stem Cell 3, 265-78.

Moens, C. B. and Prince, V. E. (2002). Constructing the hindbrain: insights from the zebrafish. Dev Dyn 224, 1-17.

Molenaar, M., van de Wetering, M., Oosterwegel, M., Peterson-Maduro, J., Godsave, S., Korinek, V., Roose, J., Destree, O. and Clevers, H. (1996). XTcf-3 transcription factor mediates beta-catenin-induced axis formation in Xenopus embryos. Cell 86, 391-9.

Moloney, D. J., Panin, V. M., Johnston, S. H., Chen, J., Shao, L., Wilson, R., Wang, Y., Stanley, P., Irvine, K. D., Haltiwanger, R. S. et al. (2000). Fringe is a glycosyltransferase that modifies Notch. Nature 406, 369-75.

Moreau, M., Leclerc, C., Gualandris-Parisot, L. and Duprat, A. M. (1994). Increased internal Ca2+ mediates neural induction in the amphibian embryo. Proc Natl Acad Sci U S A 91, 12639-43.

Morin, P. J., Sparks, A. B., Korinek, V., Barker, N., Clevers, H., Vogelstein, B. and Kinzler, K. W. (1997). Activation of beta-catenin-Tcf signaling in colon cancer by mutations in beta-catenin or APC. Science 275, 1787-90.

Muders, K., Fischera, A. and Bluma, M. (2006). Gap junctions mediate asymmetric gene expression in rabbit embryos Dev Biol 295, 2.

Munro, S. and Freeman, M. (2000). The notch signalling regulator fringe acts in the Golgi apparatus and requires the glycosyltransferase signature motif DXD. Curr Biol 10, 813-20.

Myat, A., Henrique, D., Ish-Horowicz, D. and Lewis, J. (1996). A chick homologue of Serrate and its relationship with Notch and Delta homologues during central neurogenesis. Dev Biol 174, 233-47.

Nadarajah, B., Jones, A. M., Evans, W. H. and Parnavelas, J. G. (1997). Differential expression of connexins during neocortical development and neuronal circuit formation. J Neurosci 17, 3096-111.

Nagajski, D. J., Guthrie, S., Ford, C. C. and Warner, A. E. (1989). The correlation between patterns of dye transfer through gap junctions and future developmental fate in Xenopus: the consequences of u.v. irradiation and lithium treatment. Development 105, 6.

Nakamoto, A. and Nagy, L. M. (2006). Gap junctions are required for activation of the 3D organizer in Ilyanassa. Dev Biol, 11.

Neumann, C. J. and Nuesslein-Volhard, C. (2000). Patterning of the zebrafish retina by a wave of sonic hedgehog activity. Science 289, 2137-9.

Nikolaou, N., Watanabe-Asaka, T., Gerety, S., Distel, M., Koster, R. W. and Wilkinson, D. G. (2009). Lunatic fringe promotes the lateral inhibition of neurogenesis. Development 136, 2523-33.

Nittenberg, R., Patel, K., Joshi, Y., Krumlauf, R., Wilkinson, D. G., Brickell, P. M., Tickle, C. and Clarke, J. D. (1997). Cell movements, neuronal organisation and gene expression in hindbrains lacking morphological boundaries. Development 124, 2297-306.

Noctor, S. C., Flint, A. C., Weissman, T. A., Dammerman, R. S. and Kriegstein, A. R. (2001). Neurons derived from radial glial cells establish radial units in neocortex. Nature 409, 714-20.

Ogawa, H., Oyamada, M., Mori, T., Mori, M. and Shimizu, H. (2000). Relationship of gap junction formation to phosphorylation of connexin43 in mouse preimplantation embryos. Mol Reprod Dev 55, 393-8.

Ohno, S. (2001). Intercellular junctions and cellular polarity: the PAR-aPKC complex, a conserved core cassette playing fundamental roles in cell polarity. Curr Opin Cell Biol 13, 641-8.

Ojeda, J. L. and Piedra, S. (1998). Supraependymal cells and fibers during the early stages of chick rhombencephalic development. Anat Embryol (Berl) 198, 237-44.

Olson, D., Christian, J. and Moon, R. (1991). Effect of wnt-1 and related proteins on gap junctional communication in Xenopus embryos. Science 252, 1173-1176.

Owens, D. F., Flint, A. C., Dammerman, R. S. and Kriegstein, A. R. (2000). Calcium dynamics of neocortical ventricular zone cells. Dev Neurosci 22, 25-33.

Owens, D. F. and Kriegstein, A. R. (1998). Patterns of intracellular calcium fluctuation in precursor cells of the neocortical ventricular zone. J Neurosci 18, 5374-88.

Pan, F., Mills, S. L. and Massey, S. C. (2007). Screening of gap junction antagonists on dye coupling in the rabbit retina. Vis Neurosci 24, 609-18.

Panin, V. M., Papayannopoulos, V., Wilson, R. and Irvine, K. D. (1997). Fringe modulates Notch-ligand interactions. Nature 387, 908-12.

Park, H. C., Kim, C. H., Bae, Y. K., Yeo, S. Y., Kim, S. H., Hong, S. K., Shin, J., Yoo, K. W., Hibi, M., Hirano, T. et al. (2000). Analysis of upstream elements in the HuC promoter leads to the establishment of transgenic zebrafish with fluorescent neurons. Dev Biol 227, 279-93.

Pearson, R. A., Catsicas, M., Becker, D. L., Bayley, P., Luneborg, N. L. and Mobbs, P. (2004). Ca(2+) signalling and gap junction coupling within and between pigment epithelium and neural retina in the developing chick. Eur J Neurosci 19, 2435-45.

Pearson, R. A., Dale, N., Llaudet, E. and Mobbs, P. (2005). ATP released via gap junction hemichannels from the pigment epithelium regulates neural retinal progenitor proliferation. Neuron 46, 731-44.

Peinado, A., Yuste, R. and Katz, L. C. (1993). Extensive dye coupling between rat neocortical neurons during the period of circuit formation. Neuron 10, 103-14.

Picker, A., Scholpp, S., Bohli, H., Takeda, H. and Brand, M. (2002). A novel positive transcriptional feedback loop in midbrain-hindbrain boundary development is revealed through analysis of the zebrafish pax2.1 promoter in transgenic lines. Development 129, 3227-39.

Poenie, M., Alderton, J., Tsien, R. Y. and Steinhardt, R. A. (1985). Changes of free calcium levels with stages of the cell division cycle. Nature 315, 147-9.

Prince, V. E., Holley, S. A., Bally-Cuif, L., Prabhakaran, B., Oates, A. C., Ho, R. K. and Vogt, T. F. (2001). Zebrafish lunatic fringe demarcates segmental boundaries. Mech Dev 105, 175-80.

Puelles, L. and Rubenstein, J. L. (1993). Expression patterns of homeobox and other putative regulatory genes in the embryonic mouse forebrain suggest a neuromeric organization. Trends Neurosci 16, 472-9.

Puelles, L. and Rubenstein, J. L. (2003). Forebrain gene expression domains and the evolving prosomeric model. Trends Neurosci 26, 469-76.

Rakic, P. (1972). Mode of cell migration to the superficial layers of fetal monkey neocortex. J Comp Neurol 145, 61-83.

Rasin, M. R., Gazula, V. R., Breunig, J. J., Kwan, K. Y., Johnson, M. B., Liu-Chen, S., Li, H. S., Jan, L. Y., Jan, Y. N., Rakic, P. et al. (2007). Numb and Numbl are required for maintenance of cadherin-based adhesion and polarity of neural progenitors. Nat Neurosci 10, 819-27.

Rauskolb, C., Correia, T. and Irvine, K. D. (1999). Fringe-dependent separation of dorsal and ventral cells in the Drosophila wing. Nature 401, 476-80.

Reichert, M., Muller, T. and Hunziker, W. (2000). The PDZ domains of zonula occludens-1 induce an epithelial to mesenchymal transition of Madin-Darby canine kidney I cells. Evidence for a role of beta-catenin/Tcf/Lef signaling. J Biol Chem 275, 9492-500.

Reinhard, E., Yokoe, H., Niebling, K. R., Allbritton, N. L., Kuhn, M. A. and Meyer, T. (1995). Localized calcium signals in early zebrafish development. Dev Biol 170, 50-61.

Riley, B. B., Chiang, M. Y., Storch, E. M., Heck, R., Buckles, G. R. and Lekven, A. C. (2004). Rhombomere boundaries are Wnt signaling centers that regulate metameric patterning in the zebrafish hindbrain. Dev Dyn 231, 278-91.

Roerig, B. and Feller, M. B. (2000). Neurotransmitters and gap junctions in developing neural circuits. Brain Res Brain Res Rev 32, 86-114.

Rubenstein, J. L., Martinez, S., Shimamura, K. and Puelles, L. (1994). The embryonic vertebrate forebrain: the prosomeric model. Science 266, 578-80.

Rulifson, E. J. and Blair, S. S. (1995). Notch regulates wingless expression and is not required for reception of the paracrine wingless signal during wing margin neurogenesis in Drosophila. Development 121, 2813-24.

Saez, J. C., Retamal, M. A., Basilio, D., Bukauskas, F. F. and Bennett, M. V. (2005). Connexin-based gap junction hemichannels: gating mechanisms. Biochim Biophys Acta 1711, 215-24.

Sanderson, M. J., Charles, A. C. and Dirksen, E. R. (1990). Mechanical stimulation and intercellular communication increases intracellular Ca2+ in epithelial cells. Cell Regul 1, 585-96.

Sauer, M. E. and Chittenden, A. C. (1959). Deoxyribonucleic acid content of cell nuclei in the neural tube of the chick embryo: evidence for intermitotic migration of nuclei. Exp Cell Res 16, 1-6.

Schier, A. F., Neuhauss, S. C., Harvey, M., Malicki, J., Solnica-Krezel, L., Stainier, D. Y., Zwartkruis, F., Abdelilah, S., Stemple, D. L., Rangini, Z. et al. (1996). Mutations affecting the development of the embryonic zebrafish brain. Development 123, 165-78.

Scholpp, S., Wolf, O., Brand, M. and Lumsden, A. (2006). Hedgehog signalling from the zona limitans intrathalamica orchestrates patterning of the zebrafish diencephalon. Development 133, 855-64.

Shibata, T., Yamada, K., Watanabe, M., Ikenaka, K., Wada, K., Tanaka, K. and Inoue, Y. (1997). Glutamate transporter GLAST is expressed in the radial glia-astrocyte lineage of developing mouse spinal cord. J Neurosci 17, 9212-9.

Shields, C. R., Klooster, J., Claassen, Y., Ul-Hussain, M., Zoidl, G., Dermietzel, R. and Kamermans, M. (2007). Retinal horizontal cell-specific promoter activity and protein expression of zebrafish connexin 52.6 and connexin 55.5. J Comp Neurol 501, 765-79.

Shimoyama, Y., Nagafuchi, A., Fujita, S., Gotoh, M., Takeichi, M., Tsukita, S. and Hirohashi, S. (1992). Cadherin dysfunction in a human cancer cell line: possible involvement of loss of alpha-catenin expression in reduced cell-cell adhesiveness. Cancer Res 52, 5770-4.

Spitzer, N. C. and Gu, X. (1997). Purposeful patterns of spontaneous calcium transients in embryonic spinal neurons. Semin Cell Dev Biol 8, 13-9.

Spitzer, N. C., Olson, E. and Gu, X. (1995). Spontaneous calcium transients regulate neuronal plasticity in developing neurons. J Neurobiol 26, 316-24.

Stevenson, B. R., Siliciano, J. D., Mooseker, M. S. and Goodenough, D. A. (1986). Identification of ZO-1: a high molecular weight polypeptide associated with the tight junction (zonula occludens) in a variety of epithelia. J Cell Biol 103, 755-66.

Studer, M., Lumsden, A., Ariza-McNaughton, L., Bradley, A. and Krumlauf, R. (1996). Altered segmental identity and abnormal migration of motor neurons in mice lacking Hoxb-1. Nature 384, 630-4.

Suzuki, A. and Ohno, S. (2006). The PAR-aPKC system: lessons in polarity. J Cell Sci 119, 979-87.

Syed, M. M., Lee, S., He, S. and Zhou, Z. J. (2004). Spontaneous waves in the ventricular zone of developing mammalian retina. J Neurophysiol 91, 1999-2009.

Szele, F. G. and Cepko, C. L. (1998). The dispersion of clonally related cells in the developing chick telencephalon. Dev Biol 195, 100-13.

Tawk, M., Araya, C., Lyons, D. A., Reugels, A. M., Girdler, G. C., Bayley, P. R., Hyde, D. R., Tada, M. and Clarke, J. D. (2007). A mirror-symmetric cell division that orchestrates neuroepithelial morphogenesis. Nature 446, 797-800.

Thisse, B., Pflumio, S., Fürthauer, M., Loppin, B., Heyer, V., Degrave, A., Woehl, R., Lux, A., Steffan, T., Charbonnier, X.Q. and Thisse, C. (2001). Expression of the zebrafish genome during embryogenesis. ZFIN Direct Data Submission (***http://zfin.org)***. .

Thomas, B. J., Gunning, D. A., Cho, J. and Zipursky, L. (1994). Cell cycle progression in the developing Drosophila eye: roughex encodes a novel protein required for the establishment of G1. Cell 77, 1003-14.

Tibber, M. S., Becker, D. and Jeffery, G. (2007). Levels of transient gap junctions between the retinal pigment epithelium and the neuroblastic retina are influenced by catecholamines and correlate with patterns of cell production. J Comp Neurol 503, 128-34.

Trevarrow, B., Marks, D. L. and Kimmel, C. B. (1990). Organization of hindbrain segments in the zebrafish embryo. Neuron 4, 669-79.

Umeda, K., Matsui, T., Nakayama, M., Furuse, K., Sasaki, H., Furuse, M. and Tsukita, S. (2004). Establishment and characterization of cultured epithelial cells lacking expression of ZO-1. J Biol Chem 279, 44785-94.

Unwin, P. N. and Zampighi, G. (1980). Structure of the junction between communicating cells. Nature 283, 545-9.

Vance, M. M. and Wiley, L. M. (1999). Gap junction intercellular communication mediates the competitive cell proliferation disadvantage of irradiated mouse preimplantation embryos in aggregation chimeras. Radiat Res 152, 544-51.

Voigt, T. (1989). Development of glial cells in the cerebral wall of ferrets: direct tracing of their transformation from radial glia into astrocytes. J Comp Neurol 289, 74-88.

von Trotha, J. W., Campos-Ortega, J. A. and Reugels, A. M. (2006). Apical localization of ASIP/PAR-3:EGFP in zebrafish neuroepithelial cells involves the oligomerization domain CR1, the PDZ domains, and the C-terminal portion of the protein. Dev Dyn 235, 967-77.

Wallingford, J. B., Ewald, A. J., Harland, R. M. and Fraser, S. E. (2001). Calcium signaling during convergent extension in Xenopus. Curr Biol 11, 652-61.

Warner, A. E. (1987). The use of antibodies to gap junction protein to explore the role of gap junctional communication during development. Ciba Found Symp 125, 154-67.

Warner, A. E., Guthrie, S. C. and Gilula, N. B. (1984). Antibodies to gap-junctional protein selectively disrupt junctional communication in the early amphibian embryo. Nature 311, 127-31.

Warner, A. E. and Lawrence, P. A. (1982). Permeability of gap junctions at the segmental border in insect epidermis. Cell 28, 243-52.

Waskiewicz, A. J., Rikhof, H. A. and Moens, C. B. (2002). Eliminating zebrafish pbx proteins reveals a hindbrain ground state. Dev Cell 3, 723-33.

Webb, S. E., Lee, K. W., Karplus, E. and Miller, A. L. (1997). Localized calcium transients accompany furrow positioning, propagation, and deepening during the early cleavage period of zebrafish embryos. Dev Biol 192, 78-92.

Webb, S. E. and Miller, A. L. (2003a). Calcium signalling during embryonic development. Nat Rev Mol Cell Biol 4, 539-51.

Webb, S. E. and Miller, A. L. (2003b). Imaging intercellular calcium waves during late epiboly in intact zebrafish embryos. Zygote 11, 175-82.

Webb, S. E. and Miller, A. L. (2006). Ca2+ signaling and early embryonic patterning during the blastula and gastrula periods of zebrafish and Xenopus development. Biochim Biophys Acta 1763, 1192-208.

Wei, X., Cheng, Y., Luo, Y., Shi, X., Nelson, S. and Hyde, D. R. (2004). The zebrafish Pard3 ortholog is required for separation of the eye fields and retinal lamination. Dev Biol 269, 286-301.

Weinmaster, G., Roberts, V. J. and Lemke, G. (1991). A homolog of Drosophila Notch expressed during mammalian development. Development 113, 199-205.

Weissman, T. A., Riquelme, P. A., Ivic, L., Flint, A. C. and Kriegstein, A. R. (2004). Calcium waves propagate through radial glial cells and modulate proliferation in the developing neocortex. Neuron 43, 647-61.

Whitaker, M. (2008). Calcium signalling in early embryos. Philos Trans R Soc Lond B Biol Sci 363, 1401-18.

Whitaker, M. and Patel, R. (1990). Calcium and cell cycle control. Development 108, 525-42.

Wilkinson, D. G., Bhatt, S., Chavrier, P., Bravo, R. and Charnay, P. (1989a). Segment-specific expression of a zinc-finger gene in the developing nervous system of the mouse. Nature 337, 461-4.

Wilkinson, D. G., Bhatt, S., Cook, M., Boncinelli, E. and Krumlauf, R. (1989b). Segmental expression of Hox-2 homoeobox-containing genes in the developing mouse hindbrain. Nature 341, 405-9.

Williams, B. P. and Price, J. (1995). Evidence for multiple precursor cell types in the embryonic rat cerebral cortex. Neuron 14, 1181-8.

Williams, J. A., Paddock, S. W. and Carroll, S. B. (1993). Pattern formation in a secondary field: a hierarchy of regulatory genes subdivides the developing Drosophila wing disc into discrete subregions. Development 117, 571-84.

Willott, E., Balda, M. S., Fanning, A. S., Jameson, B., Van Itallie, C. and Anderson, J. M. (1993). The tight junction protein ZO-1 is homologous to the Drosophila discs-large tumor suppressor protein of septate junctions. Proc Natl Acad Sci U S A 90, 7834-8.

Wittchen, E. S., Haskins, J. and Stevenson, B. R. (1999). Protein interactions at the tight junction. Actin has multiple binding partners, and ZO-1 forms independent complexes with ZO-2 and ZO-3. J Biol Chem 274, 35179-85.

Wizenmann, A. and Lumsden, A. (1997). Segregation of rhombomeres by differential chemoaffinity. Mol Cell Neurosci 9, 448-59.

Wrenzycki, C., Herrmann, D., Carnwath, J. W. and Niemann, H. (1996). Expression of the gap junction gene connexin43 (Cx43) in preimplantation bovine embryos derived in vitro or in vivo. J Reprod Fertil 108, 17-24.

Xu, Q., Alldus, G., Holder, N. and Wilkinson, D. G. (1995). Expression of truncated Sek-1 receptor tyrosine kinase disrupts the segmental restriction of gene expression in the Xenopus and zebrafish hindbrain. Development 121, 4005-16.

Xu, Q., Mellitzer, G., Robinson, V. and Wilkinson, D. G. (1999). In vivo cell sorting in complementary segmental domains mediated by Eph receptors and ephrins. Nature 399, 267-71.

Yaksi, E. and Friedrich, R. W. (2006). Reconstruction of firing rate changes across neuronal populations by temporally deconvolved Ca2+ imaging. Nat Methods 3, 377-83.

Yoon, K. and Gaiano, N. (2005). Notch signaling in the mammalian central nervous system: insights from mouse mutants. Nat Neurosci 8, 709-15.

Yuste, R., Nelson, D. A., Rubin, W. W. and Katz, L. C. (1995). Neuronal domains in developing neocortex: mechanisms of coactivation. Neuron 14, 7-17.

Yuste, R., Peinado, A. and Katz, L. C. (1992). Neuronal domains in developing neocortex. Science 257, 665-9.

Zeltser, L. M., Larsen, C. W. and Lumsden, A. (2001). A new developmental compartment in the forebrain regulated by Lunatic fringe. Nat Neurosci 4, 683-4.

Zervas, M., Millet, S., Ahn, S. and Joyner, A. L. (2004). Cell behaviors and genetic lineages of the mesencephalon and rhombomere 1. Neuron 43, 345-57.

Zheng-Fischhofer, Q., Kibschull, M., Schnichels, M., Kretz, M., Petrasch-Parwez, E., Strotmann, J., Reucher, H., Lynn, B. D., Nagy, J. I., Lye, S. J. et al. (2007). Characterization of connexin31.1-deficient mice reveals impaired placental development. Dev Biol 312, 258-71.

Zimmerman, K., Shih, J., Bars, J., Collazo, A. and Anderson, D. J. (1993). XASH-3, a novel Xenopus achaete-scute homolog, provides an early marker of planar neural induction and position along the mediolateral axis of the neural plate. Development 119, 221-32.

Zimprich, F., Ashworth, R. and Bolsover, S. (1998). Real-time measurements of calcium dynamics in neurons developing in situ within zebrafish embryos. Pflugers Arch 436, 489-93.